Analysis of Surface Air Temperature Anomalies

Masatsugu Wakaura

Doctor of Philosophy

(in Statistical Science)

Department of Statistical Science
School of Multidisciplinary Science
The Graduate University for Advanced Studies

2006
(School Year)

This work was carried out under the supervision of

Professor Yosihiko Ogata

Abstract

This study is analysis of anomalies of surface air temperature in Japan. The surface air temperature anomalies relative to the seasonal variations are of our great concern from a long-term forecasting viewpoint. The result of the analysis presents us the useful knowledge not only for the climatic analysis but also for the prediction and the weather risk management.

In this paper, to begin with, we investigate seasonal periodicities of the time series and show that the surface air temperature has the intense seasonality and there are seasonal periodicities in not only the mean but also the variance. Under the strategy of detection of the yearly distinctive variablities that is the object of the prediction, the means and variances of the deterministic seasonal periodicities are removed from the original temperature data and the residuals are defined as the anomalies.

The low-pass filtered anomalies represent the yearly distinctive variablities quantitatively and analysis of the monthly divided dataset suggests seasonality in the anomalies. Then a particular parametric form for a nonstationary autoregressive (AR) model is considered to analyze seasonality in the anomalies and the new knowledge is shown. The model shows that there are seasonal changes in the autocorrelation of surface air temperature and the daily power spectrum transformed from the coeffients of the model clarifies the seasonal feature. Applying the model to the high-pass filtered datasets clarifies the influence of the Japan Current on the seasonality and it is expected that the long-term prediction might be improved by taking the effect from the Japan Current as an exogenous factor. On the other hand, applying the model to the pricing of the weather derivatives shows that we cannot neglect the seasonality in the valuation of the weather risk in the future.

Furthermore, the model is extended multivariate model. In analysis using the noise contribution, the relation and causality between stations is shown and the structure of the surface air temperature in Japan is explained. The daily noise contribution estimated from the multivariate model can quantitatively grasp the clearly seasonal change and the propagation of the causality, and suggests that there are the local teleconnections between stations. The knowledge will also be import factors for the prediction.

Acknowledgement

First, I am greatly indebted to my advisor, Prof. Yosihiko Ogata, for his continuous support in the Ph.D. program. He was always there to listen and to give advice. He taught me not only theory and skills of statistical science but also the attitude of research.

A special thanks goes to my co-advisor, Prof. Yoshiyasu Tamura who gave me valuable advices through the Ph.D. program and suggestions on the study.

Additional thanks to Prof. Tohru Ozaki who taught me the context of time series theory, this is, the seasonal model, the noise contribution and the causality.

I would like to thank Mrs. Akiko Kutsuna who was the secretary of the Institute of Statistical Mathematics. I was able to research without a procedural nuisance by her support.

I would also like to thank all the reviewers for their valuable comments.

Last, but not least, I would like to extend my gratitude to my family: my wife, daughter and son. They give me the great support mentally.

Contents

List of Figures

List of Tables

Chapter 1

Introduction

1.1 Temperature and society

Weather gives great influence to human activities. Even in everyday life, we can find out various scenes; if it rains, we have to prepare an umbrella, if it is cold, we should wear an overcoat, and if a storm comes over, we must be careful to disasters. Furthermore in economic activities, the change in weather can be accompanied with profit and loss; in construction industry, a long rain causes a delay of term of construction works, a cool summer and a warm winter have an influence on sales of seasonal goods and the growth of farm products, and the ski resort business depends upon a snowfall. 1998's announcement of the American Department of Commerce reports that it is said weather influences on businesses of about 11% of the GNP in the USA (Hijikata 2000), and the GDP of winter season from 1995 until 1996 in the UK was pulled down by the influence of weather (Hijikata 2000).

In weather variables, air temperature can frequently affects decision making in management of corporations. For example, because the average temperature of summer greatly influences the sales of an air conditioner, the manager of maker needs to consider it as for the production plan, and the manager of dealer needs to consider it as for the stock plan. We can confirm such a decision making in other seasons and in the other industries; the clothing, the beer, the electric power and the fuel. For the decision making, the prediction, especially the long-range prediction of the period more than from three until six months, of air temperature can be an important information.

However, the long-range prediction of enough precision to make a decision in management of corporations cannot be realized at present. In the next section, we consider the *dynamical forecast model* used as technique of long-range forecast at present, and discuss the difficult of the prediction.

1.2 Dynamical forecast models

The core method of the weather forecast at present is the *numerical weather prediction*. In the numerical weather prediction model, the state of the atmosphere on the imaginary space divided into a three-dimensional grid with discrete cells is computed forward in time using mathematical equations that describe the physics and dynamics of the atmosphere. Since the numerical weather prediction model uses the equations of fluid dynamics to estimate future states, it is called the *dynamical forecast model*. However, because the equations of fluid dynamics in the dynamical forecast model are nonlinear, the errors in initial values will inevitably grow with time (Lorenz 1963). The increase of the errors is called *chaos*, therefore the precision of a prediction decreases with time as these errors increase. It is impossible to definitively predict the state of the atmosphere more than approximately 10 days in advance, owing to the chaotic nature (Wikipedia), this is, we cannot utilize the dynamical forecast model for long-range forecast more than a month.

For the limit of the definitive prediction, a method of *Ensemble forecasting* has appeared from the view of the prediction of the predictive precision (Iwasaki and Kuma (1999)). It is a method to run the multiple dynamical forecast models using initial values with a little errors to reflect the uncertainty in the initial state of the atmosphere, since initial errors due to the errors of observations and insufficient sampling. Each forecast of the multiple models is called the *ensemble member*. The errors growth depending upon the evolution of the atmospheric state in each ensemble member, and the spread of the forecast between the ensemble members represents the degree of the predictive precision. When the spread is low, the ensemble members are in relatively high agreement and the forecast confidence is high. Conversely, when the spread is large, the ensemble members diverge and poor forecast confidence (Japan Meteorological Agency (2000)). The spread can be considered a probability distribution, therefore, ensemble forecasting realizes the stochastic prediction by definitive dynamical forecast models and has enabled long-range forecast.

Ensemble forecasting is utilized in one-week and one-month forecasts of the Japan Meteorological Agency (JMA), at present. Three-months forecasts and seasonal forecasts of JMA, however, are provided not only by ensemble forecasting, this is, dynamical forecasting, but also by statistical methods (Japan Meteorological Agency (1999)). Moreover even in one-week and one-month forecasts, it seems that the precision of forecasts using ensemble forecasting is not so good.

The reason can be considered as follows. Ensemble forecasting is considered under the assumption of the *perfect model* that can perfectly reproduce the state of the atmosphere (Japan Meteorological Agency (2000)). Though, from the assumption that a model is complete, the errors of ensemble forecasting consider only initial errors, this is, the errors of observations and insufficient sampling, it is impossible that a model is complete. If the individual equation of fluid dynamics to explain the behavior of atmosphere makes clear, the model may not express a system that they were connected with each other complicatedly. That is to say that the inferior precision results from technically incomplete model (Palmer (1999) and Harrison et al. (1999)). We must recognize the climatic system is complicated and the complete comprehension of the system is impossible, therefore the difficulty of the long-term prediction of weather events and vatiables emerges.

1.3 Approach of statistical models

If definitive dynamical forecast models aim at stchastic output such as ensemble forecasting, applying stchastic processes to weather variables such as temperature processes seems spontaneous idea for the expression and the prediction of the behavior (for example, Hasselmamm (1976) , Dobrovolski (1999) and Imkeller and Storch(2001)). Then, stchastic processes can be represented by statistical time series models and the approach of statistical model that let data speak to data emerges as an effective method to obtain new knowledge for the long-range prediction. It seems that inductive statistical approach is effective, because a system of the atmosphere is complicated and the mechanism is not elucidated completely. It is expected that the problem of the long-range prediction advances toward solution not only by deductive dynamical approach but also by inductive statistical approach.

This paper is a study on analysis of temperature processes using statistical models. The purpose of statistical modeling and analysis of temperature processes is as follows. The first is to research the possibility of the stchastic long-range prediction using statistical models; searching preceding indices and correlative systems by multiple modeling and analysis. The second is to detect new climatical knowridge by making clear the qualitative relations between maltiple variables. The third is to consider the application to the risk management by identifing the stchastic behavior.

In particular, third issue is a subject of research that recently has come to be argued

actively with the appearance of a financial instrument called weather derivatives. Weather derivatives are contingent claims, which are written on the index of weather variables and used to hedge the profit fluctuation risk caused by the fluctuation of weather variables. For the pricing and application of weather derivatives, the modeling of weather variables, the method of the management of the weather fluctuation risk and so on are argued in the research area (Dischel (1998), Dornier and Queruel (2000), Zeng (2000), Wakaura (2005) and Wakaura (2006)). This paper is also given a great motive for study from the argument.

1.4 Precedent studies on modeling temperature processes

Some weather variables and climatic variables have been researched as stchastic processes, and time series models such as the auto-regressive model (AR model) have been applied to them. For example, Storch and Zwiers (1999) consider examples of applications of the AR model. Zwiers and Storch (1990) applied various time series models to the Sea Surface Temperature (SST) index of the Southern Oscillation. Stephenson et al. (2000) applied the AR model and a fractional differenced AR model to the North Atlantic Oscillation.

As for surface air temperature (SAT), especially daily mean surface air temperature, the features have been investigated in the research area of finance from necessity to evaluate the prospective variability of air temperature in the pricing of weather derivatives mentioned in previous section. Moreno (2000) applied the AR model to Paris-Orly daily average temperatures. Cao and Wei (2000) points out the seasonality of the variances in the daily surface air temperature of USA. Torro et al. (2001) discuss the modeling of the seasonally periodic variances and the conditional heteroskedasticity in daily surface air temperature of Spain. Caballero et al. (2002) applied the fractional ARIMA model and points out the seasonality in the autocorrelation of surface air temperature data in USA, and Jewson and Caballero (2003) discusses the seasonal changes of the autocorrelation.

The precedent studies make clear that surface air temperature processes are non-stationary processes; seasonal periodicity in the mean and variance, conditional heteroskedasticity and long memory. This paper focuses seasonal periodicities which surface air temperature processes possess, and intend to obtain their new knowledge.

1.5 Outline of this paper

The outline of this paper is as follows. In Chapter 2, we survey the daily mean surface temperature data in Japan and the existence of seasonality is shown. The seasonal ajustment is argued and the anomaly of the surface air temperature (the daily mean surface tenperature data in Japan) in this paper is defined in Chapter 3. The property of the anomaly, this is, the yearly distinctive variablities and the autocorrelation are shown in Chapter 4. In Chapter 5, the existence of seasonality of the autocorrelation is shown and a particular parametric form for a nonstationary autoregressive (AR) model is considered to quantify the anomalies. Furthermore, the model is extended to a multiple model and the relation between stations is considered using the noise contribution (Akaike, 1968) in Chapter 6. The concluding remarks are provided in Chapter 7.

Chapter 2

Data

2.1 The SYNOP data and the aerological data of Japan

Japan consists of large and small islands located from northeast to southwest over a long distance. Therefore, the difference of observed surface air temperature is large between the northern and the southern areas in the Japan islands. Japan has various climatic characters and clear four seasons, and is influenced by warm and cold currents, as well as having some unique geographical features.

In this paper we use the surface synoptic observations (SYNOP data) of Japan compiled by the Japan Meteorological Agency (JMA) as the daily mean surface air temperature data, and if necessary, we use also the aerological data of Japan compiled by the JMA as the upper atmospheric data. We will analyze the SYNOP data for the 40 years period from 1961 through 2000. The whole data size is 14600 days for each station, omitting February 29 in the leap years. The number of the total observation stations is 137. Table 2.1 provides the location of the stations in the latitude and longitude, where “WMO code” refers to the code of the World Meteorological Organization. The locations of the stations are indicated in Figure 2.1.

Figure 2.2 shows the daily changes of the mean surface air temperature at the Sapporo station (the WMO code 47412), the Sendai station (the WMO code 47590), the Wajima station (the WMO code 47600), the Tokyo station (the WMO code 47662), the Osaka station (the WMO code 47772), the Fukuoka station (the WMO code 47807), the Kochi station (the WMO code 47893) and the Naha station (the WMO code 47936) for a given 10 year period from 1991 until 2000. The horizontal axis represents the date for 10 years, and the vertical axis represents the values of the mean surface air temperature. From this we can confirm an apparently regular seasonal periodicity in all stations. Figure 2.3 shows the periodogram and power spectrum of the same stations of Figure 2.2, where the power spectrum was estimated by the AR model (see Chapter 4). The

horizontal axis represents the frequency in logarithmic scale, where “y” represents the frequency corresponding to a year, and the vertical axis represents values in logarithmic scale. In each panel, the black points and lines represent periodogram, and the red solid line represents the estimated power spectrum. We can confirm that the period of a year is exceptional in their stations.

Figure 2.4 shows the daily standard deviations obtained within a one-year period at the same stations of Figure 2.2. The horizontal axis represents the date within a one-year period, and the vertical axis represents the values of the daily standard deviations. As Cao and Wei (2000) and Torro et al. (2001) pointed out, this clearly indicates the seasonality of the variances.

On the other hand, the outline of the aerological data that will be analyzed secondarily is as follows. The aerological data is observed by a rawinsonde at twice a day; 9:00 and 21:00 JST (Japan Standard Time), and the atmospheric pressure, the air temperature, the humidity, the wind (the direction and the speed) are obtained by the observation. There are 17 aerological observatories in Japan, Table 2 .2 and Figure 2.5 show the location of them. We will analyze the data for the 10-year period from 1991 through 2000. The whole data size is 3650 days for each station, omitting February 29 in the leap years.

We will argue the seasonal adjustment on the basis of the above-mentioned property in the next chapter.

Table 2.1. The location of the stations (the surface synoptic observations) in the latitude and longitude, where “WMO code” means the code of the World Meteorological Organization.

WMO code	Station Name	Latitude(N)	Longitude(E)	WMO code	Station Name	Latitude(N)	Longitude(E)
47401	Wakkanai	45 ° 24.8'	141 ° 41.0'	47402	Kitamiesashi	44 ° 56.3'	142 ° 35.4'
47404	Haboro	44 ° 21.7'	141 ° 42.3'	47405	Omu	44 ° 34.7'	142 ° 58.1'
47406	Rumoi	43 ° 56.6'	141 ° 38.2'	47407	Asahikawa	43 ° 46.2'	142 ° 22.4'
47409	Abashiri	44 ° 01.0'	144 ° 17.0'	47411	Otaru	43 ° 10.8'	141 ° 01.2'
47412	Sapporo	43 ° 03.4'	141 ° 19.9'	47413	Iwamizawa	43 ° 12.6'	141 ° 47.3'
47417	Obihiro	42 ° 55.1'	143 ° 12.9'	47418	Kushiro	42 ° 59.0'	144 ° 22.8'
47420	Nemuro	43 ° 19.7'	145 ° 35.4'	47421	Suttsu	42 ° 47.5'	140 ° 13.6'
47423	Muroran	42 ° 18.6'	140 ° 58.9'	47424	Tomakomai	42 ° 37.2'	141 ° 33.0'
47426	Urakawa	42 ° 09.5'	142 ° 46.8'	47428	Esashi	41 ° 51.9'	140 ° 07.7'
47430	Hakodate	41 ° 48.8'	140 ° 45.4'	47433	Kutchan	42 ° 53.9'	140 ° 45.7'
47435	Mombetsu	44 ° 20.6'	143 ° 21.6'	47440	Hiroo	42 ° 17.5'	143 ° 19.2'
47520	Shinjo	38 ° 45.2'	140 ° 18.9'	47570	Wakamatsu	37 ° 29.1'	139 ° 54.8'
47574	Fukaura	40 ° 38.6'	139 ° 56.2'	47575	Aomori	40 ° 49.1'	140 ° 46.3'
47576	Mutsu	41 ° 16.9'	141 ° 12.9'	47581	Hachinohe	40 ° 31.5'	141 ° 31.5'
47582	Akita	39 ° 42.9'	140 ° 06.2'	47584	Morioka	39 ° 41.7'	141 ° 10.1'
47585	Miyako	39 ° 38.7'	141 ° 58.1'	47587	Sakata	38 ° 54.3'	139 ° 50.8'
47588	Yamagata	38 ° 15.2'	140 ° 20.9'	47590	Sendai	38 ° 15.5'	140 ° 54.0'
47592	Ishinomaki	38 ° 25.5'	141 ° 18.2'	47595	Fukushima	37 ° 45.4'	140 ° 28.5'
47597	Shirakawa	37 ° 07.7'	140 ° 13.2'	47600	Wajima	37 ° 23.4'	136 ° 53.9'
47602	Aikawa	38 ° 01.5'	138 ° 14.5'	47604	Niigata	37 ° 54.5'	139 ° 03.0'
47605	Kanazawa	36 ° 35.2'	136 ° 38.3'	47606	Fushiki	36 ° 47.3'	137 ° 03.4'
47607	Toyama	36 ° 42.4'	137 ° 12.3'	47610	Nagano	36 ° 39.6'	138 ° 11.7'
47612	Takada	37 ° 06.2'	138 ° 15.0'	47615	Utsunomiya	36 ° 32.8'	139 ° 52.3'
47616	Fukui	36 ° 03.2'	136 ° 13.6'	47617	Takayama	36 ° 09.2'	137 ° 15.4'
47618	Matsumoto	36 ° 14.6'	137 ° 58.4'	47620	Suwa	36 ° 02.6'	138 ° 06.7'
47624	Maebashi	36 ° 24.1'	139 ° 03.8'	47626	Kumagaya	36 ° 08.8'	139 ° 23.0'
47629	Mito	36 ° 22.6'	140 ° 28.2'	47631	Tsuruga	35 ° 39.0'	136 ° 03.9'
47632	Gifu	35 ° 23.8'	136 ° 45.9'	47636	Nagoya	35 ° 09.9'	136 ° 58.1'
47637	Iida	35 ° 30.6'	137 ° 50.3'	47638	Kofu	35 ° 39.8'	138 ° 33.4'
47640	Kawaguchiko	35 ° 29.8'	138 ° 45.8'	47641	Chichibu	35 ° 59.2'	139 ° 04.6'
47648	Choshi	35 ° 44.2'	140 ° 51.6'	47649	Ueno	34 ° 45.5'	136 ° 08.7'
47651	Tsu	34 ° 43.8'	136 ° 31.3'	47653	Irako	34 ° 37.5'	137 ° 05.8'
47654	Hamamatsu	34 ° 42.4'	137 ° 43.4'	47655	Omaezaki	34 ° 36.1'	138 ° 12.9'
47656	Shizuoka	34 ° 58.3'	138 ° 24.4'	47657	Mishima	35 ° 06.7'	138 ° 55.8'
47662	Tokyo	35 ° 41.2'	139 ° 45.8'	47663	Owase	34 ° 03.9'	136 ° 11.7'

WMO code	Station Name	Latitude(N)	Longitude(E)	WMO code	Station Name	Latitude(N)	Longitude(E)
47666	Irozaki	34 ° 36.0'	138 ° 50.8'	47668	Ajiro	35 ° 02.6'	139 ° 05.7'
47670	Yokohama	35 ° 26.2'	139 ° 39.3'	47674	Katsuura	35 ° 08.8'	140 ° 18.9'
47675	Oshima	34 ° 44.8'	139 ° 21.9'	47678	Hachijojima	33 ° 06.1'	139 ° 47.3'
47690	Nikko	36 ° 44.1'	139 ° 30.2'	47740	Saigo	36 ° 12.1'	133 ° 20.2'
47741	Matsue	35 ° 27.2'	133 ° 04.1'	47742	Sakai	35 ° 32.5'	133 ° 14.2'
47744	Yonago	35 ° 25.9'	133 ° 20.5'	47746	Tottori	35 ° 29.1'	134 ° 14.4'
47747	Toyooka	35 ° 32.0'	134 ° 49.5'	47750	Maizuru	35 ° 26.8'	135 ° 19.2'
47754	Hagi	34 ° 24.7'	131 ° 23.6'	47755	Hamada	34 ° 53.6'	132 ° 04.4'
47756	Tsuyama	35 ° 03.7'	134 ° 00.7'	47759	Kyoto	35 ° 00.7'	135 ° 44.1'
47761	Hikone	35 ° 16.4'	136 ° 14.8'	47762	Shimonoseki	33 ° 56.7'	130 ° 55.7'
47765	Hiroshima	34 ° 23.7'	132 ° 27.9'	47766	Kure	34 ° 14.3'	132 ° 33.2'
47768	Okayama	34 ° 39.4'	133 ° 55.1'	47769	Himeji	34 ° 50.2'	134 ° 40.5'
47770	Kobe	34 ° 41.6'	135 ° 12.9'	47772	Osaka	34 ° 40.7'	135 ° 31.3'
47776	Sumoto	34 ° 20.1'	134 ° 54.4'	47777	Wakayama	34 ° 13.6'	135 ° 10.0'
47778	Shionomisaki	33 ° 26.9'	135 ° 45.8'	47780	Nara	34 ° 41.4'	135 ° 49.8'
47800	Izuhara	34 ° 11.7'	129 ° 17.6'	47805	Hirado	33 ° 21.4'	129 ° 33.2'
47807	Fukuoka	33 ° 34.8'	130 ° 22.6'	47809	Iizuka	33 ° 39.0'	130 ° 41.7'
47812	Sasebo	33 ° 09.1'	129 ° 44.1'	47813	Saga	33 ° 15.8'	130 ° 18.4'
47814	Hita	33 ° 19.1'	130 ° 55.9'	47815	Oita	33 ° 13.9'	131 ° 37.2'
47817	Nagasaki	32 ° 43.8'	129 ° 52.2'	47819	Kumamoto	32 ° 48.6'	130 ° 42.6'
47821	Asosan	32 ° 52.6'	131 ° 04.5'	47823	Akune	32 ° 01.5'	130 ° 12.2'
47824	Hitoyoshi	32 ° 12.9'	130 ° 45.4'	47827	Kagoshima	31 ° 33.1'	130 ° 33.1'
47829	Miyakonojo	31 ° 43.6'	131 ° 05.0'	47830	Miyazaki	31 ° 56.1'	131 ° 25.0'
47831	Makurazaki	31 ° 16.1'	130 ° 17.7'	47835	Aburatsu	31 ° 34.5'	131 ° 24.6'
47836	Yakushima	30 ° 22.7'	130 ° 39.7'	47837	Tanegashima	30 ° 44.1'	130 ° 59.6'
47838	Ushibuka	32 ° 11.7'	130 ° 01.7'	47887	Matsuyama	33 ° 50.4'	132 ° 46.8'
47890	Tadotsu	34 ° 16.4'	133 ° 45.3'	47891	Takamatsu	34 ° 18.8'	134 ° 03.4'
47892	Uwajima	33 ° 13.4'	132 ° 33.3'	47893	Kochi	33 ° 33.9'	133 ° 33.1'
47895	Tokushima	34 ° 03.9'	134 ° 34.6'	47897	Sukumo	32 ° 55.1'	132 ° 41.8'
47898	Shimizu	32 ° 43.1'	133 ° 00.7'	47899	Murotomisaki	33 ° 14.9'	134 ° 10.8'
47909	Naze	28 ° 22.6'	129 ° 29.9'	47912	Yonagunijima	24 ° 27.7'	123 ° 00.6'
47918	Ishigakijima	24 ° 19.9'	124 ° 09.8'	47927	Miyakojima	24 ° 47.4'	125 ° 16.7'
47929	Kumejima	26 ° 20.1'	126 ° 48.3'	47936	Naha	26 ° 12.2'	127 ° 41.3'
47945	Minamidaitojima	25 ° 49.7'	131 ° 13.5'				

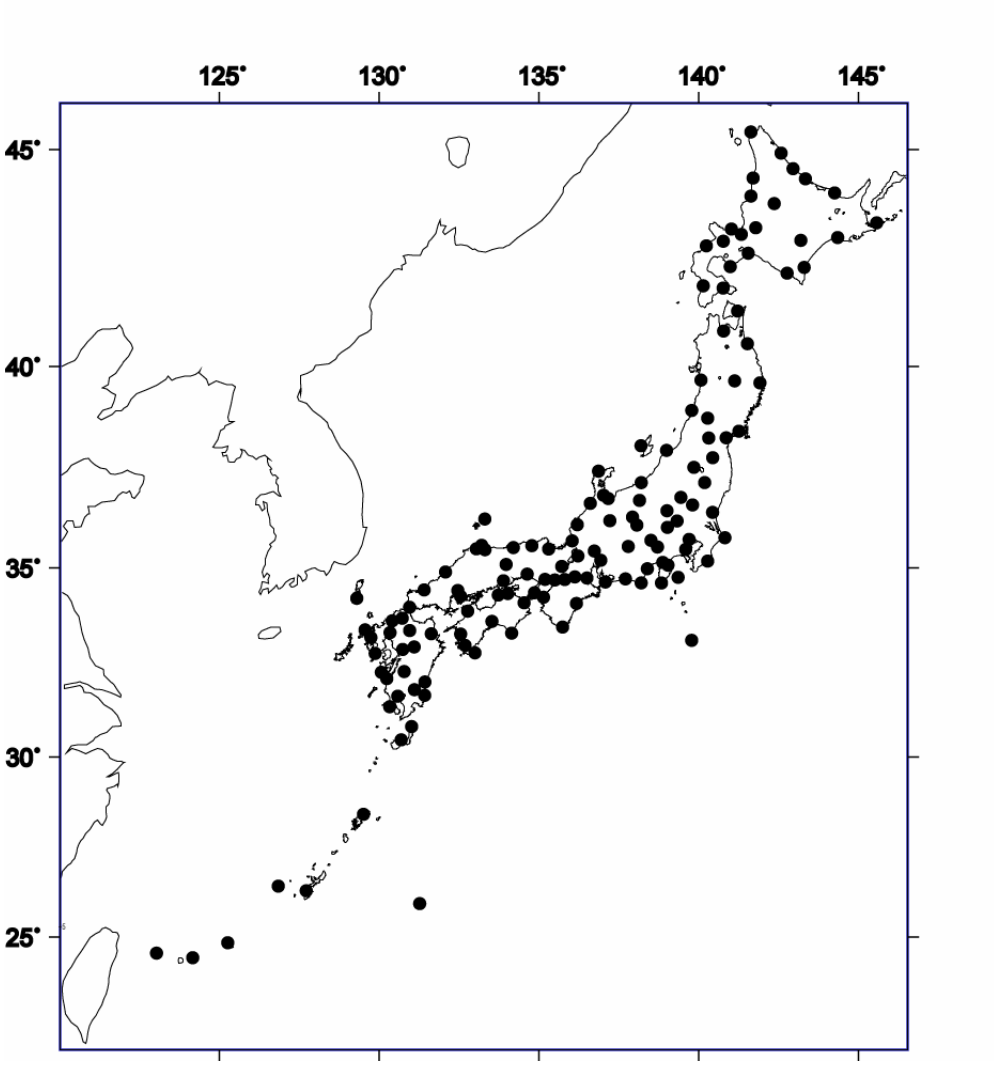

Figure 2.1. The locations of the stations (the surface synoptic observations).

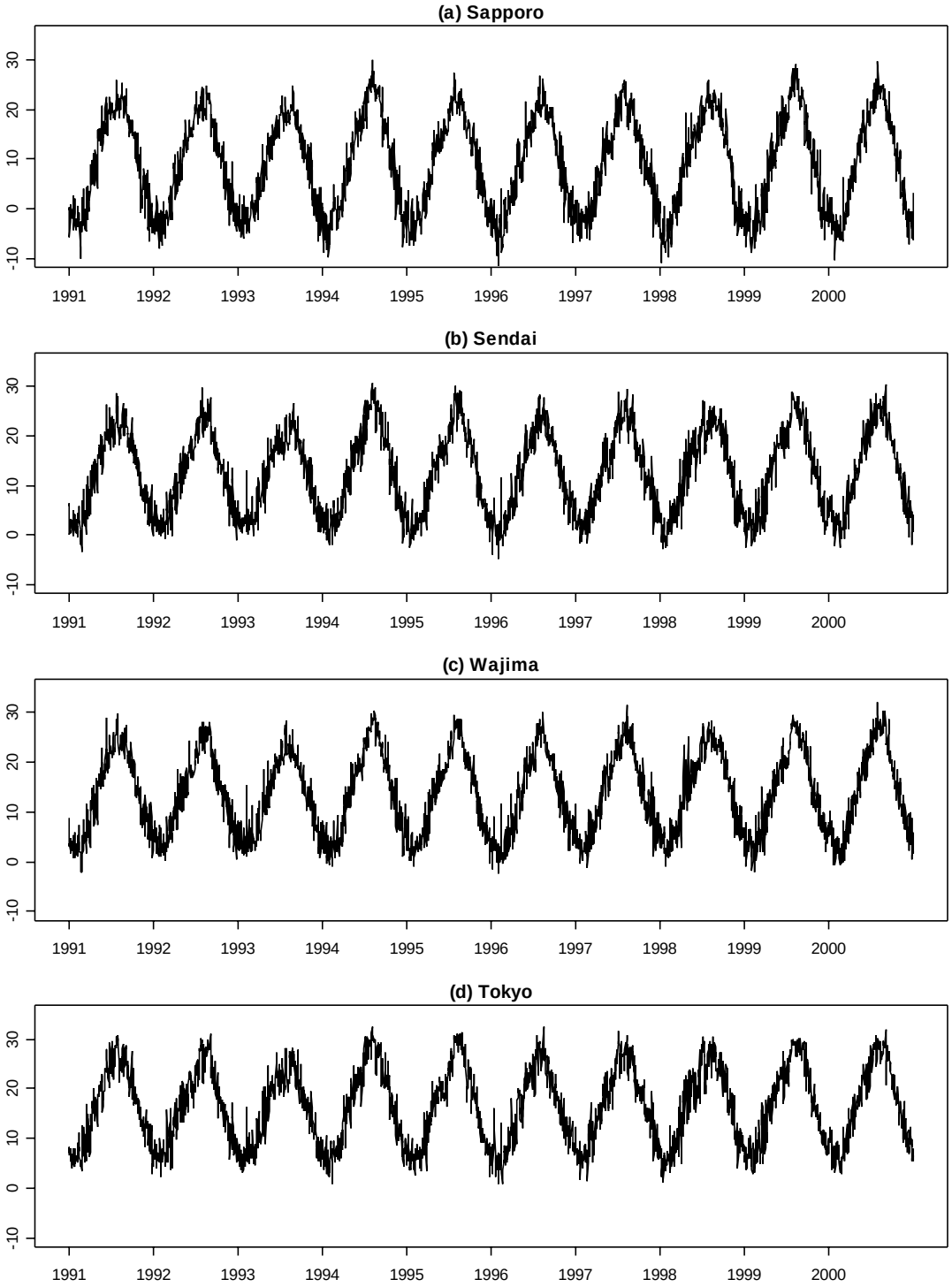

Figure 2.2 - 1. The daily changes of the mean surface air temperature for a given 10 year period from 1991 until 2000; (a) the Sapporo station (the WMO code 47412), (b) the Sendai station (the WMO code 47590), (c) the Wajima station (the WMO code 47600), (d) the Tokyo station (the WMO code 47662). The horizontal axis represents the date for 10 years, and the vertical axis represents the values of the mean surface air temperature.

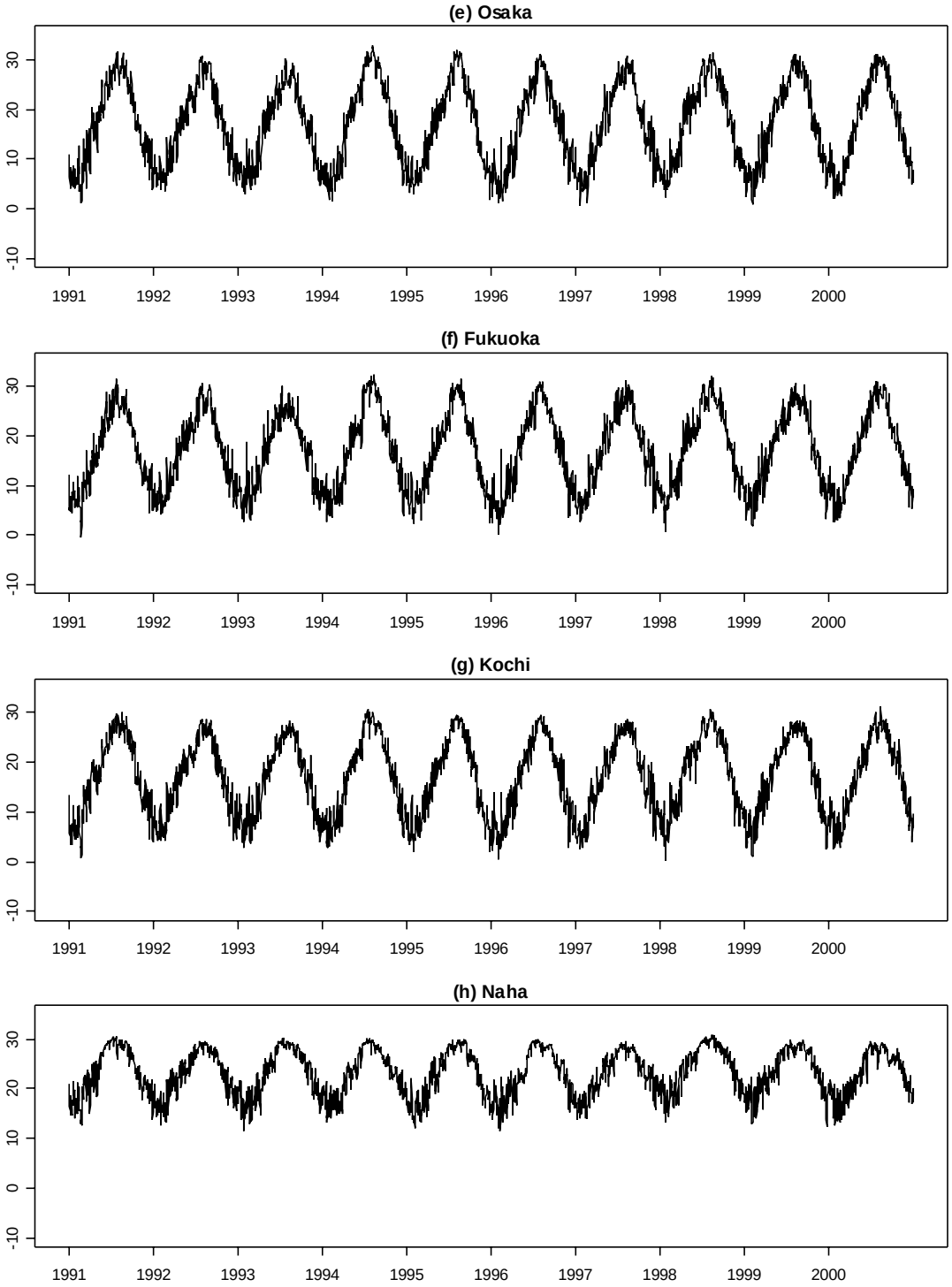

Figure 2.2 - 2. The daily changes of the mean surface air temperature for a given 10 year period from 1991 until 2000; (e) the Osaka station (the WMO code 47772), (f) the Fukuoka station (the WMO code 47807), (g) the Kochi station (the WMO code 47893), (h) the Naha station (the WMO code 47936). The horizontal axis represents the date for 10 years, and the vertical axis represents the values of the mean surface air temperature.

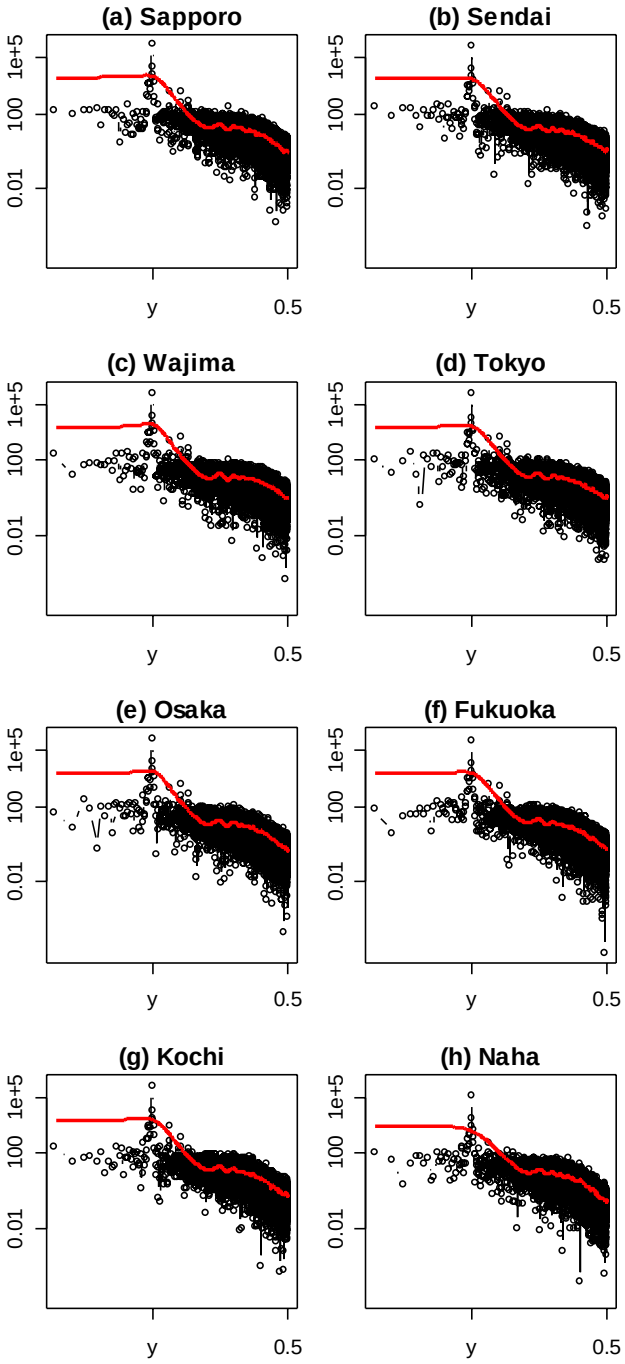

Figure 2.3. The periodogram and estimated power spectrum of the same stations of Figure 2.2. The horizontal axis represents the frequency in logarithmic scale, where "y" represents the frequency corresponding to a year, and the vertical axis represents values in a logarithmic scale. The black points and lines represent the periodogram, and the red solid line represents the power spectrum.

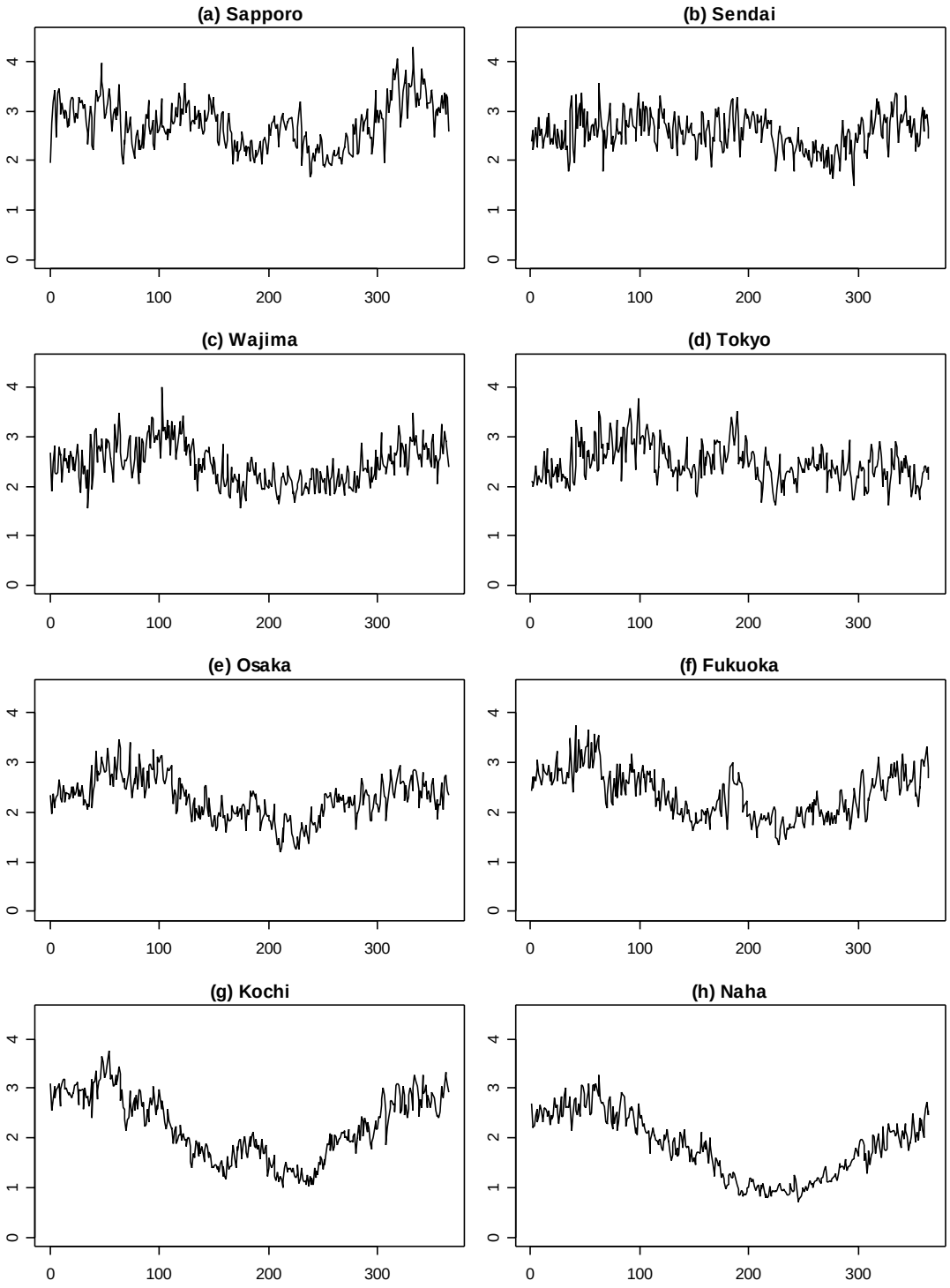

Figure 2.4. The daily standard deviations obtained within a one year period at the same stations of Figure 2.2. The horizontal axis represents the date within a one year period, and the vertical axis represents the values of the daily standard deviations.

Table 2.2. The location of the aerological observatories in the latitude and longitude, where “WMO code” refers to the code of the World Meteorological Organization.

WMO code	Station Name	Latitude(N)	Longitude(E)
47401	Wakkanai	45° 25’	141° 41’
47412	Sapporo	43° 3’	141° 20’
47420	Nemuro	43° 20’	145° 35’
47582	Akita	39° 43’	140° 6’
47590	Sendai	38° 16’	140° 54’
47600	Wajima	37° 23’	136° 54’
47646	Tateno	36° 3’	140° 8’
47678	Hachijojima	33° 7’	139° 47’
47744	Yonago	35° 26’	133° 21’
47778	Shionomisaki	33° 27’	135° 46’
47807	Fukuoka	33° 35’	130° 23’
47827	Kagoshima	31° 33’	130° 33’
47909	Naze	28° 23’	129° 33’
47918	Ishigakijima	24° 20’	124° 10’
47936	Naha	26° 12’	127° 41’
47945	Minamidaitojima	25° 50’	131° 14’
47971	Chichijima	27° 5’	142° 11’

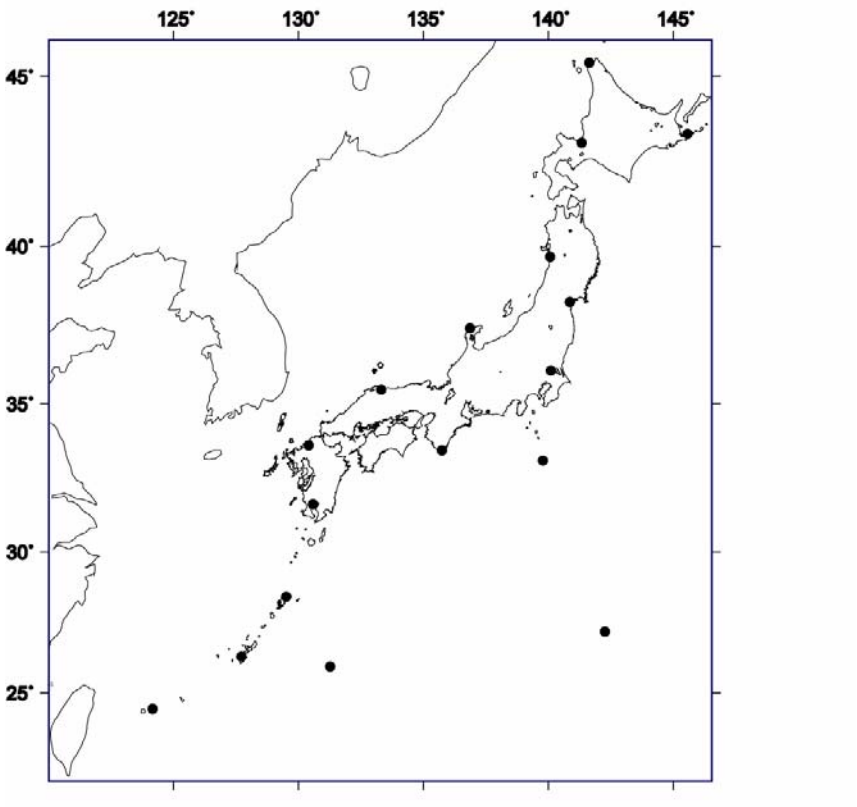

Figure 2.5. The locations of the aerological observatories.

2.2 Survey of the seasonal trend of the surface air temperature

Wakaura(2004) argue the concise non-parametric method for the seasonal adjustment. In this section, through the presentation of the method, we will briefly survey the seasonal trend of the daily mean surface air temperature data in advance of the argument of the seasonal adjustment in the Chapter 3.

There are some methods as for the seasonal adjustment using the non-parametric method or regression, for example, Cleveland et al. (1990) propose a seasonal trend decomposition procedure based on Loess. Wakaura (2004) propose two phases method using smoothing spline in order to estimate the seasonality of the variance; in the first phase, for a seasonal trend decomposition of the mean, an additive model using smoothing spline is applied, then in the second phase, for a seasonal trend decomposition of the variance, the residuals removed the estimated trend in first phase are squared, and, under assumption that the squared residuals follow a gamma distribution, the generalized additive model (Hastie and Tibshirani(1990)) with a log-link function using smoothing spline is applied to the squared residuals.

In Wakaura (2004), the model is applied to the SYNOP data for the 30 year period from 1971 through 2000 omitting February 29 in the leap years, this is, let $\{T_n\ ;\ n=1, 2, \cdots, N\ ;\ N=10950\}$ be the original daily mean surface temperature data,

$$T_n = \mu_n + \varepsilon_n ,$$

$$\mu_n = s_\mu^{(1)}(n) + s_\mu^{(2)}(\sin(2\pi n/365 - \pi/2)) + s_\mu^{(3)}(\cos(2\pi n/365 - \pi/2)), \qquad (2.1)$$

,where ε_n is the residuals for μ_n and $s_\mu^{(1)}(\cdot)$, $s_\mu^{(2)}(\cdot)$, $s_\mu^{(3)}(\cdot)$ are smoothing spline functions. The first term represents the long term trend, and the second and third term represents the seasonal trend. The smoothing splines are fitted by minimizing the penalized residual sum of squares

$$PRSS = \sum_{n=1}^{N}\left(T_n - \sum_{i}^{3} s_\mu^{(i)}(X_i(n))\right)^2 + \sum_{i}^{3}\lambda_i \int_{-\infty}^{\infty}\left(\frac{\partial^2 s_\mu^{(i)}(x_i)}{\partial x_i^2}\right)^2 dx_i , \qquad (2.2)$$

where $X_1(n) = n$, $X_2(n) = \sin(2\pi n/365 - \pi/2)$, $X_3(n) = \cos(2\pi n/365 - \pi/2)$, and $\lambda_i\ (i=1,2,3)$ is the smoothing parameter. As a practical matter, $s_\mu^{(i)}(\cdot)\ (i=1,2,3)$ are

represented by the linear combination of (N + 2) B-splines, and are fitted by the backfitting algorithm (for example, Chambers and Hastie (1991)). Then let $\mathbf{S}_{\mu}^{(i)}\ (i=1,2,3)$ be smoothing matrices for $s_{\mu}^{(i)}(\cdot)$, $\mathbf{S}_{\mu}^{(i)}$ depend on each λ_i, and tr($\mathbf{S}_{\mu}^{(i)}$) −1 is called the *equivalent degrees of freedom* and represent the degree of smoothing. Each equivalent degrees of freedom of the fitted smoothing spline functions is 4. Figure 2.6 plots the estimated values of the daily mean surface temperature data of the Tokyo station, where the top panel represents the estimates of $s_{\mu}^{(1)}(n)$, the middle panel represents the estimates of $s_{\mu}^{(2)}(\sin(2\pi n/365-\pi/2))$, the bottom panel represents $s_{\mu}^{(3)}(\cos(2\pi n/365-\pi/2))$ and broken lines represent 95% confidence interval.

In the next phase, for a seasonal trend decomposition of the variance, to the residuals removed the estimated $\hat{\mu}$, this is, $e_n = T_n - \hat{\mu}_n$, assuming the squared residuals follow a gamma distribution the generalized additive model based on smoothing spline with a log-link function is applied

$$\upsilon_n^2 = E[e_n^2],$$

$$\log \upsilon_n^2 = s_{\upsilon}^{(1)}(n) + s_{\upsilon}^{(2)}(\sin(2\pi n/365-\pi/2)) + s_{\upsilon}^{(3)}(\cos(2\pi n/365-\pi/2)), \qquad (2.3)$$

where, $s_{\upsilon}^{(1)}(\cdot)$, $s_{\upsilon}^{(2)}(\cdot)$, $s_{\upsilon}^{(3)}(\cdot)$ are smoothing spline functions. The first term represents the long term trend, and the second and third term represents the seasonal trend. The smoothing splines are fitted by maximizing the penalized likelihood instead of minimizing the penalized residual sum of squares, because of assuming the squared residuals follow a gamma distribution. As a practical matter, $s_{\upsilon}^{(i)}(\cdot)\ (i=1,2,3)$ is fitted by the local-scoring algorithm with the working response and the weight correspond to assuming distribution and a link function. Each equivalent degrees of freedom of the fitted smoothing spline functions is 4. Figure 2.7 plots the estimated values of the daily mean surface temperature data of the Tokyo station, where the top panel represents the estimates of $s_{\upsilon}^{(1)}(n)$, the middle panel represents the estimates of $s_{\upsilon}^{(2)}(\sin(2\pi n/365-\pi/2))$, the bottom panel represents $s_{\upsilon}^{(3)}(\cos(2\pi n/365-\pi/2))$ and broken lines represent 95% confidence interval. Figure 2.8 plots the estimated mean and variance within a year in the Tokyo station. We can recognize the seasonal trend of the mean and variance.

Figure 2.9 plots the long term trend and the seasonal trend of the estimated mean and variance in other several stations. We can recognize the long term and the seasonal trend of the mean and variance according to areas. In particular, we can recognize some

patterns with peaks in the seasonality of the variance.

The aerological temperature data at the 850hpa and 500hpa isobaric surface for the 10 year period from 1991 through 2000 is also analyzed in Wakaura(2004). Figure 2.10 and Figure 2.11 plot the long term trend and the seasonal trend of the estimated mean and variance of the aerological temperature data in some observatories. Figure 2.10 is at the 850hpa isobaric surface and Figure 2.11 is at the 500hpa isobaric surface. Though we can recognize the long term and the seasonal trend of the mean and variance, the patterns of the seasonality of the variance are uniform and it is suggested that the variety of the seasonality of the variance is proper to surface.

(a) $s_{\mu}^{(1)}(n)$

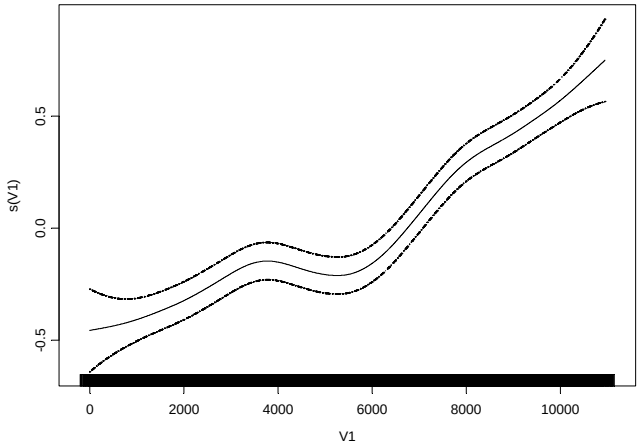

(b) $s_{\mu}^{(2)}(\sin(2\pi n/365-\pi/2))$

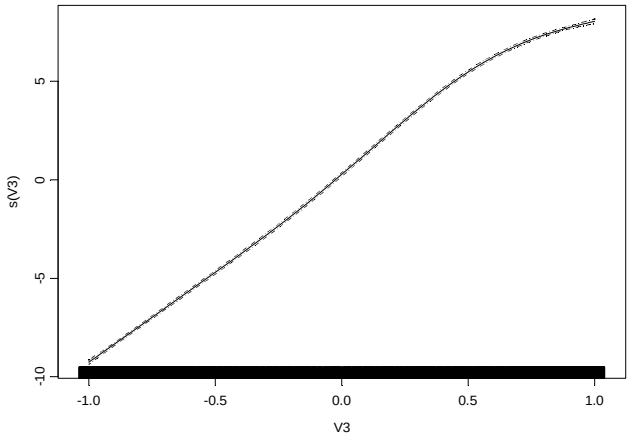

(c) $s_{\mu}^{(3)}(\cos(2\pi n/365-\pi/2))$

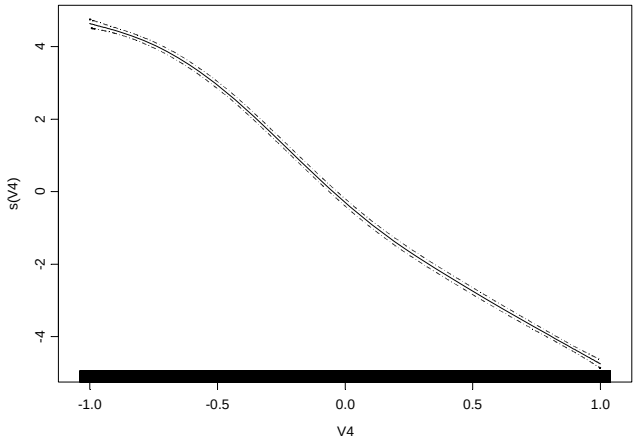

Figure 2.6. The estimated values of smoothing spline functions of μ_n (the data is the Tokyo station), where broken lines represent 95% confidence interval.

(a) $s_{\sigma}^{(1)}(n)$

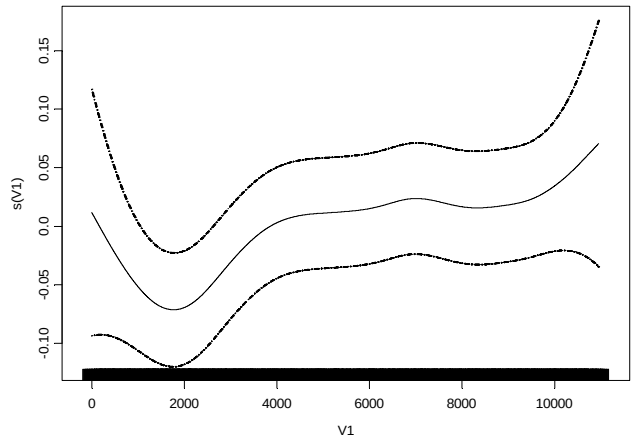

(b) $s_{\sigma}^{(2)}(\sin(2\pi m/365-\pi/2))$

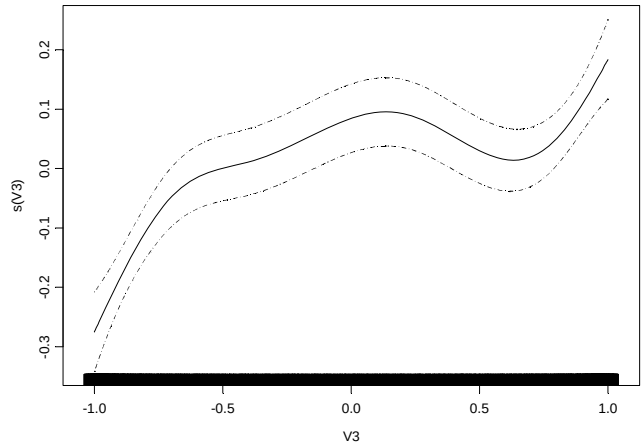

(c) $s_{\sigma}^{(3)}(\cos(2\pi m/365-\pi/2))$

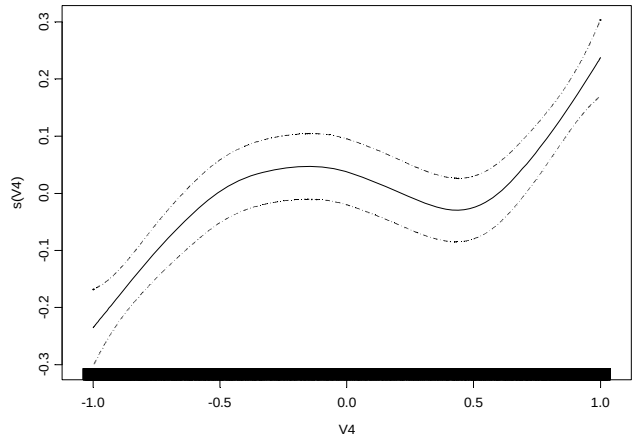

Figure 2.7. The estimated values of smoothing spline functions of σ_n^2 (the data is the Tokyo station), where broken lines represent 95% confidence interval.

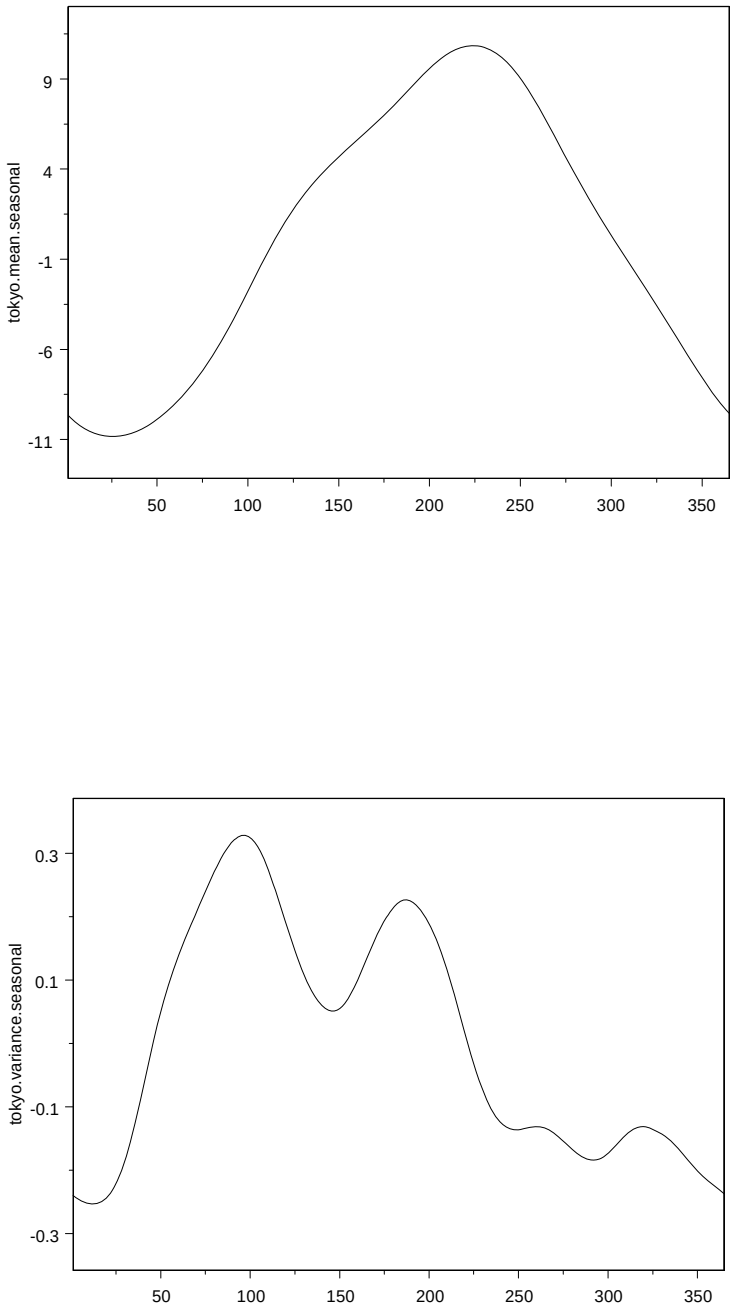

Figure 2.8. The estimated mean and variance within a year in the Tokyo station. the top panel is the mean and the bottom panel is the variance.

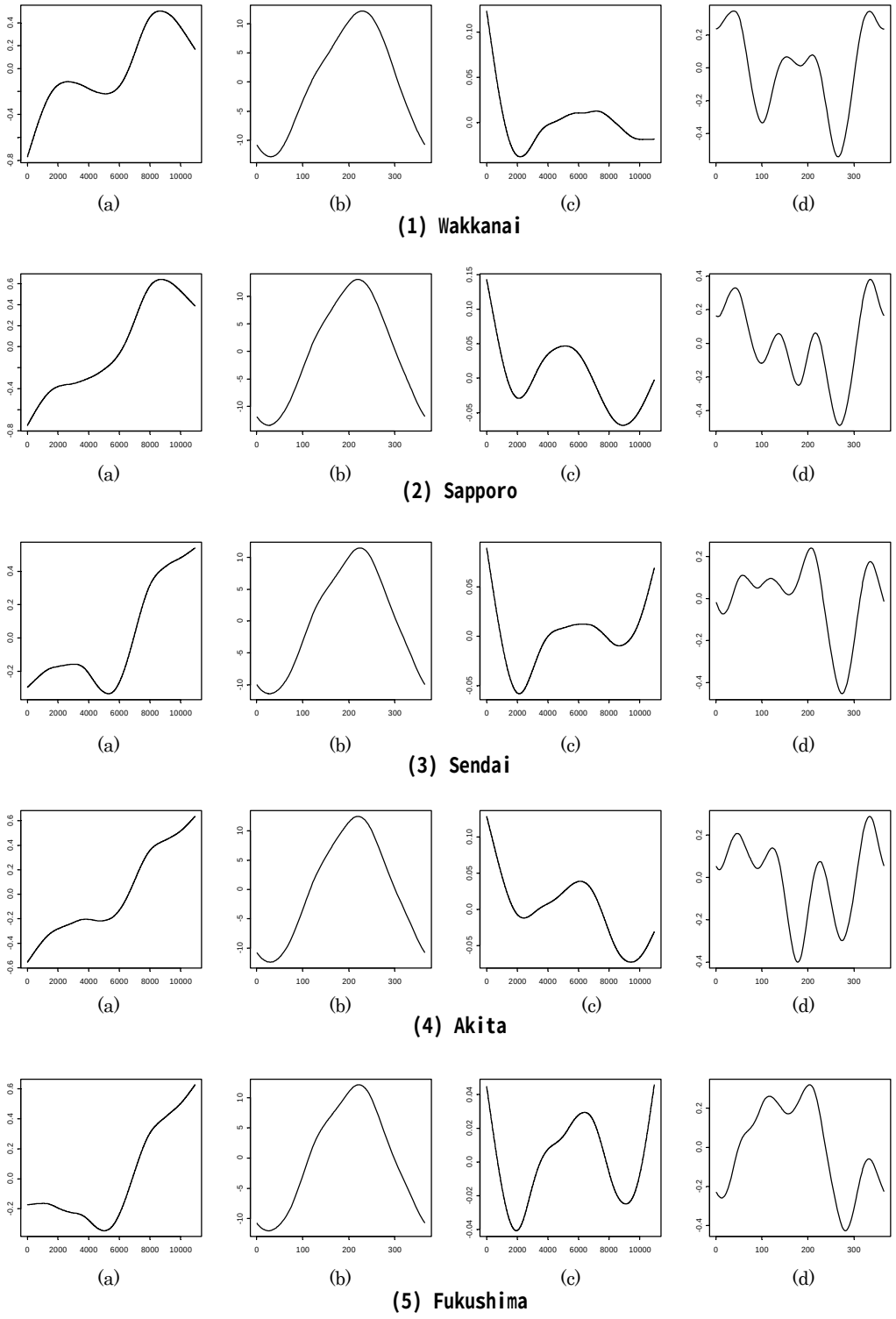

Figure 2.9-1. The long term trend and the seasonal trend of the estimated mean and variance in typical stations. The panel (a) and (c) are the long term trend of the mean and variance and the panel (b) and (d) are the seasonal trend of the mean and variance respectively.

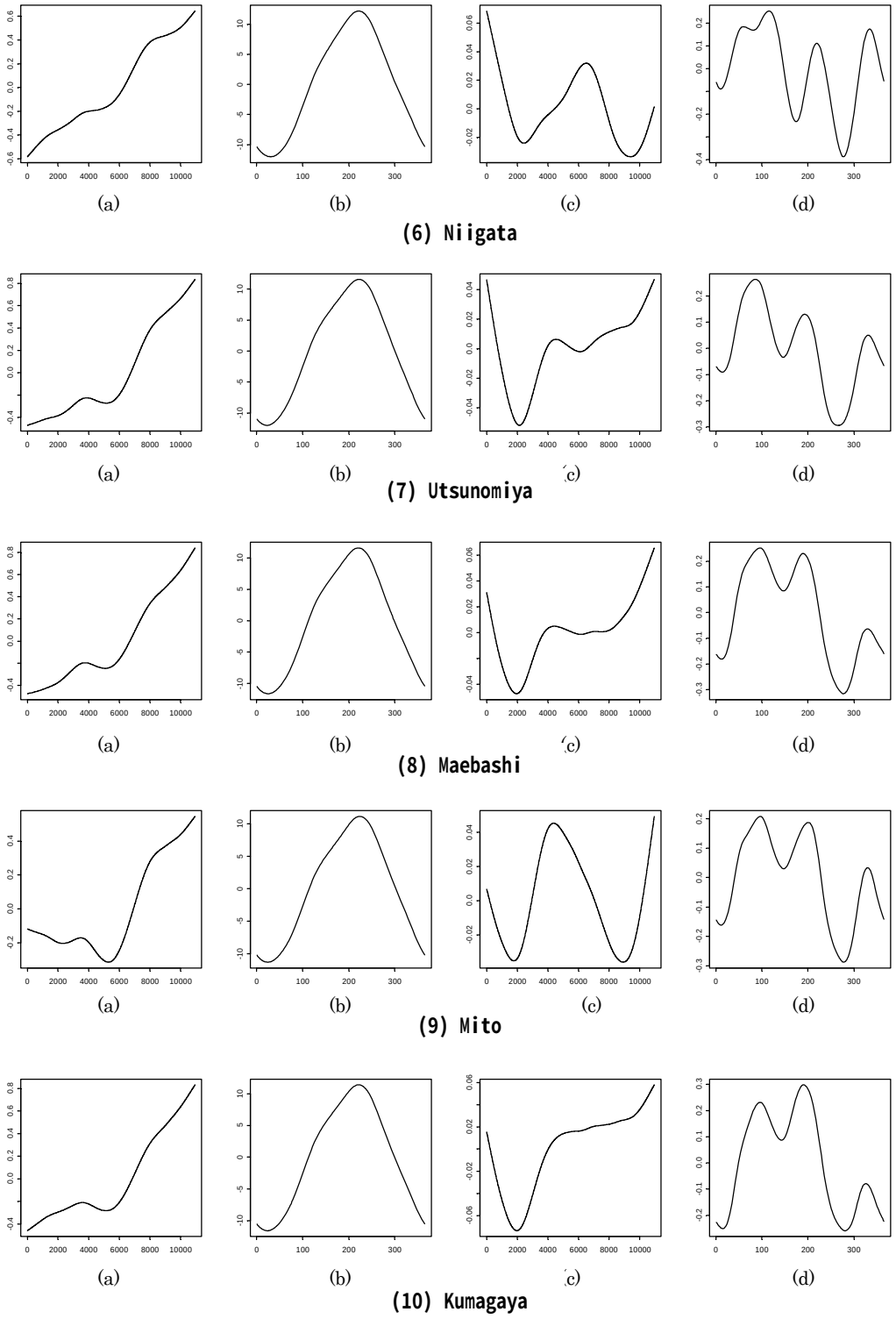

Figure 2.9-2. The long term trend and the seasonal trend of the estimated mean and variance in typical stations. The panel (a) and (c) are the long term trend of the mean and variance and the panel (b) and (d) are the seasonal trend of the mean and variance respectively.

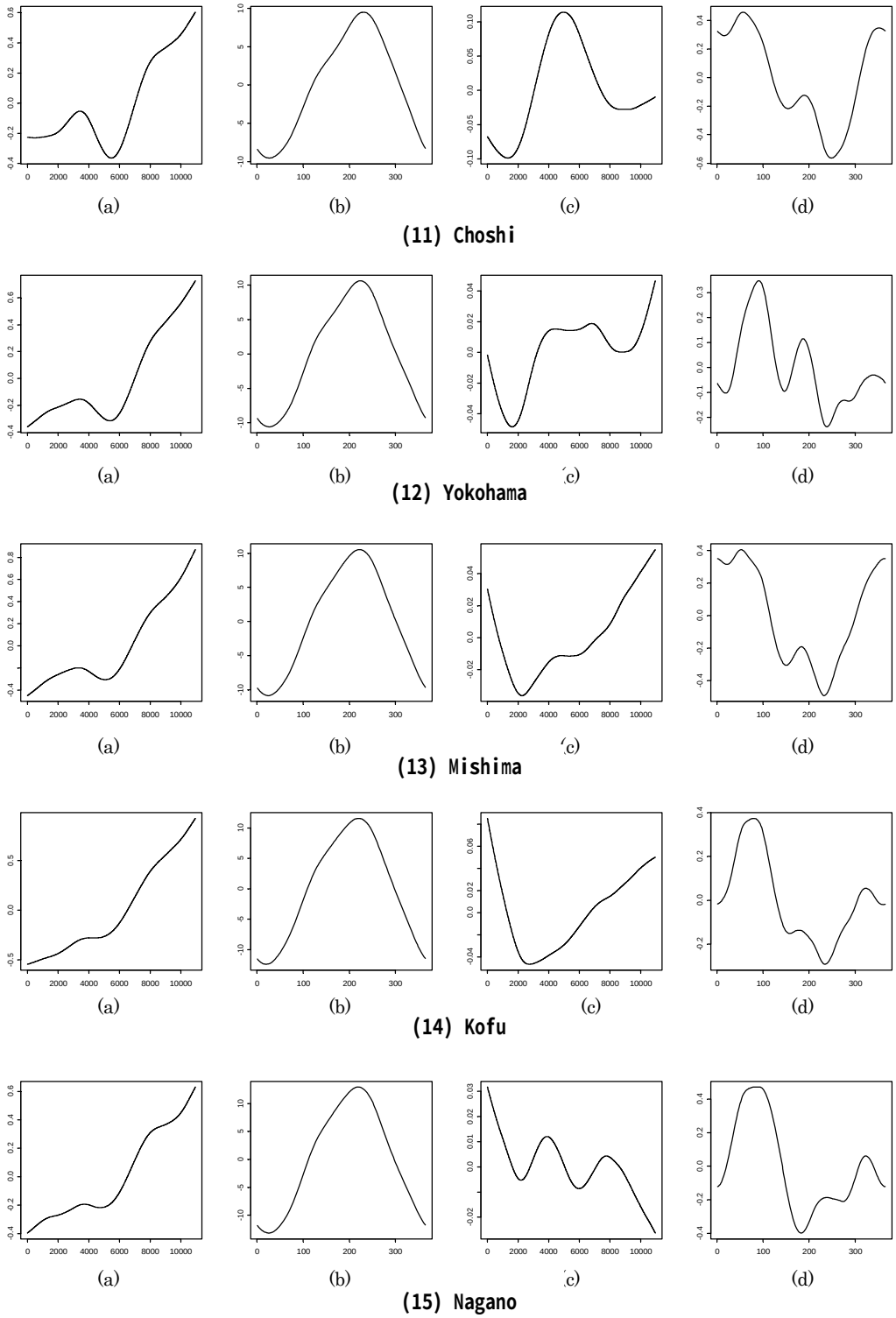

Figure 2.9-3. The long term trend and the seasonal trend of the estimated mean and variance in typical stations. The panel (a) and (c) are the long term trend of the mean and variance and the panel (b) and (d) are the seasonal trend of the mean and variance respectively.

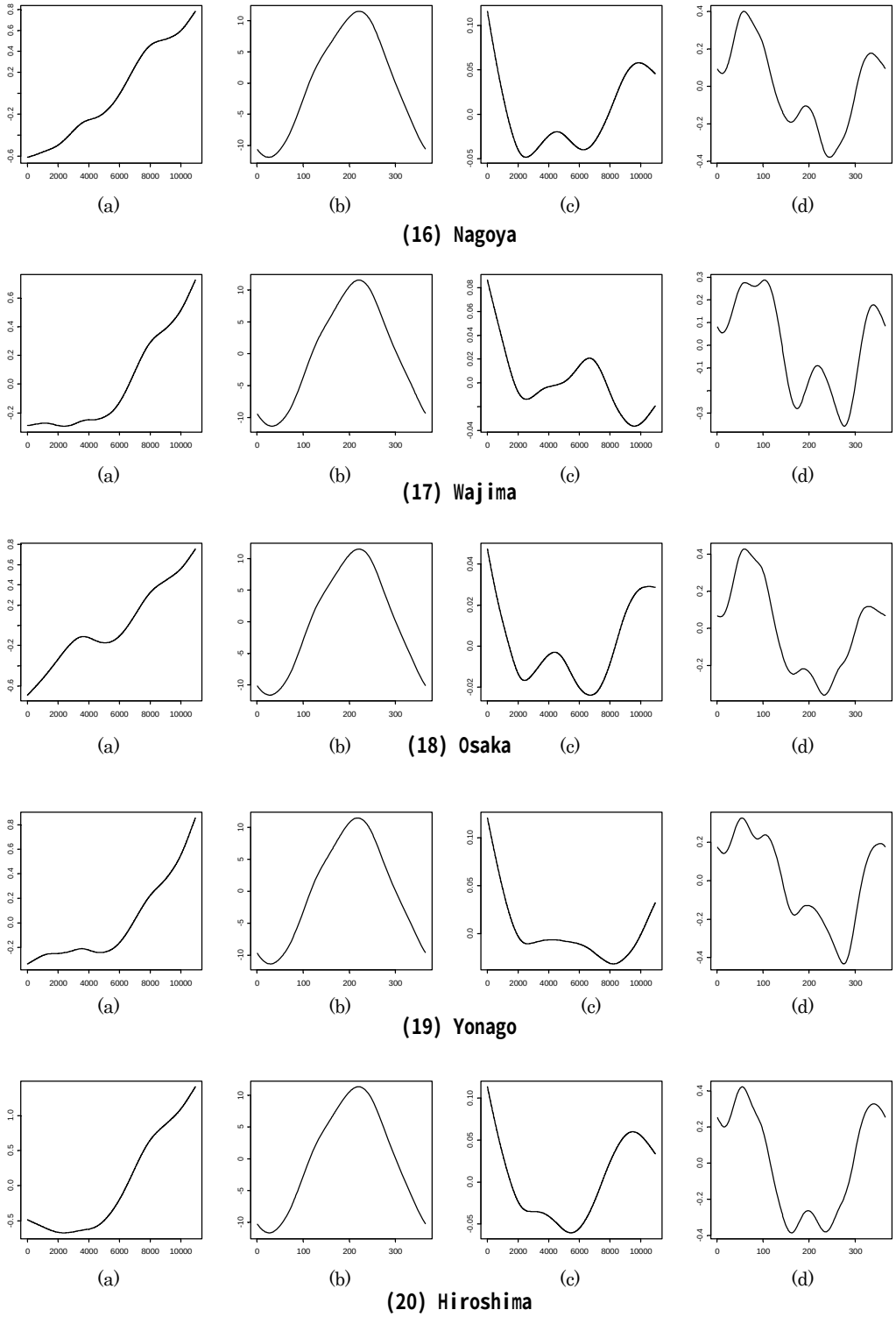

Figure 2.9-4. The long term trend and the seasonal trend of the estimated mean and variance in typical stations. The panel (a) and (c) are the long term trend of the mean and variance and the panel (b) and (d) are the seasonal trend of the mean and variance respectively.

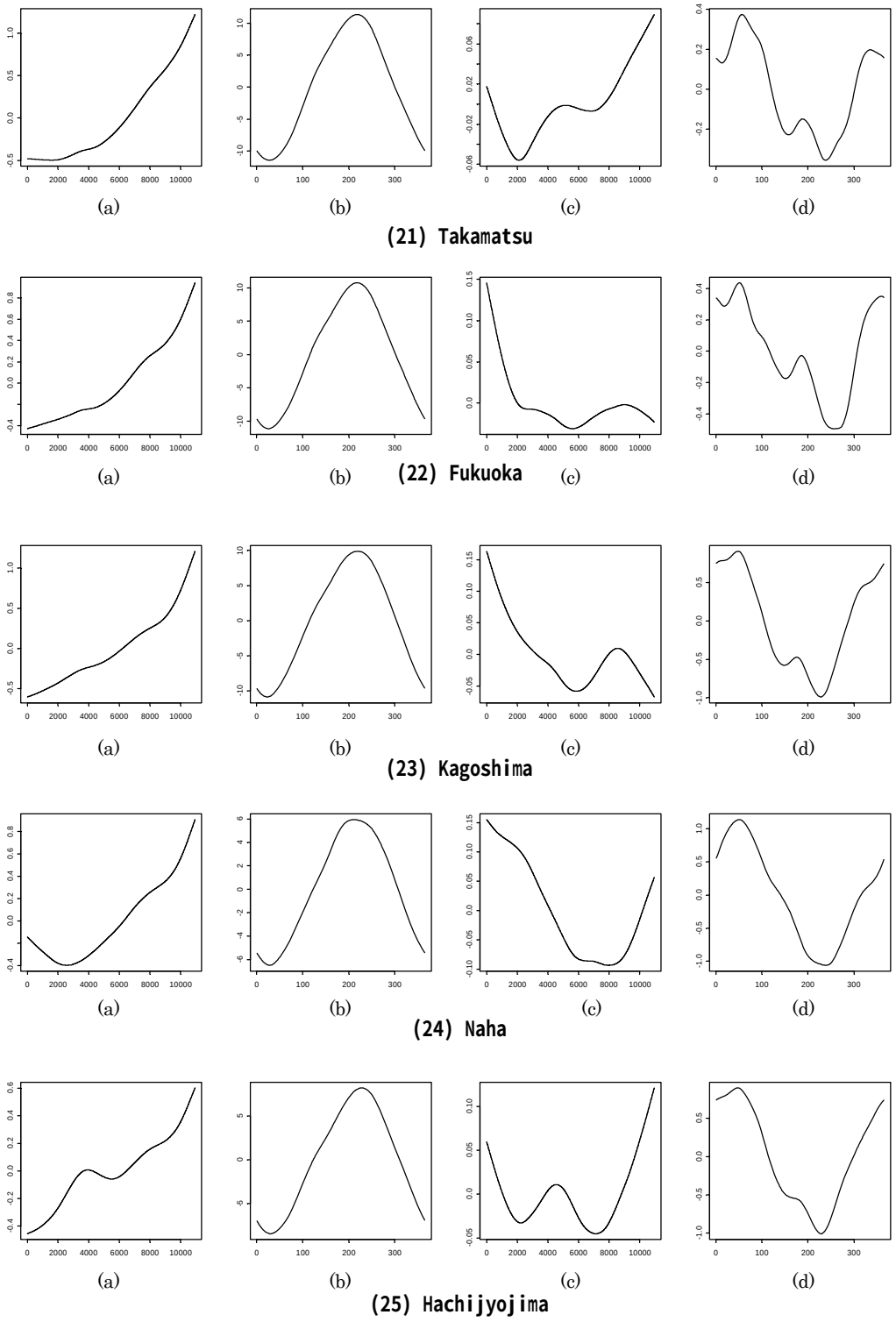

Figure 2.9-5. The long term trend and the seasonal trend of the estimated mean and variance in typical stations. The panel (a) and (c) are the long term trend of the mean and variance and the panel (b) and (d) are the seasonal trend of the mean and variance respectively.

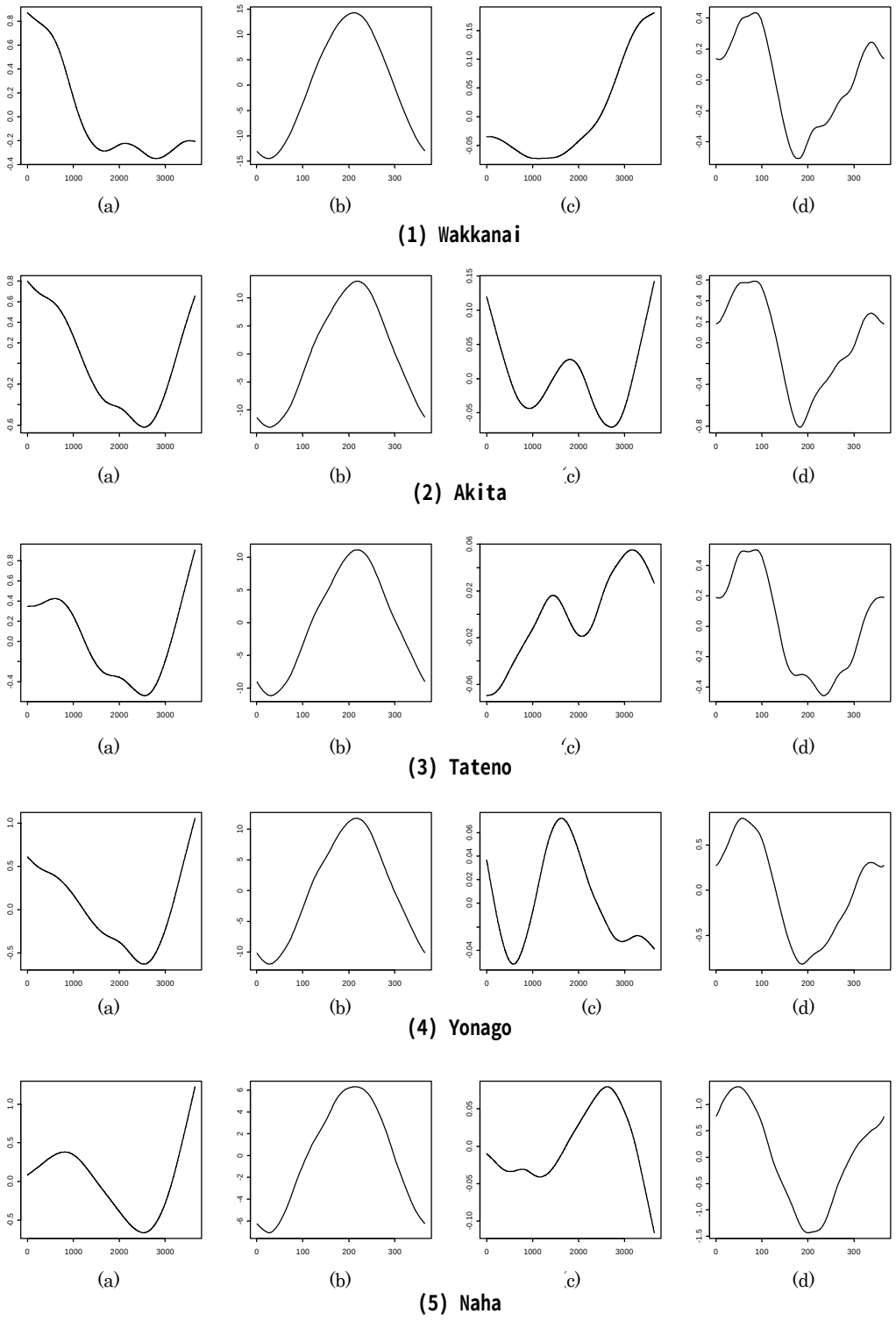

Figure 2.10. The long term trend and the seasonal trend of the estimated mean and variance of the aerological temperature data at the 850hpa isobaric surface. The panel (a) and (c) are the long term trend of the mean and variance and the panel (b) and (d) are the seasonal trend of the mean and variance respectively.

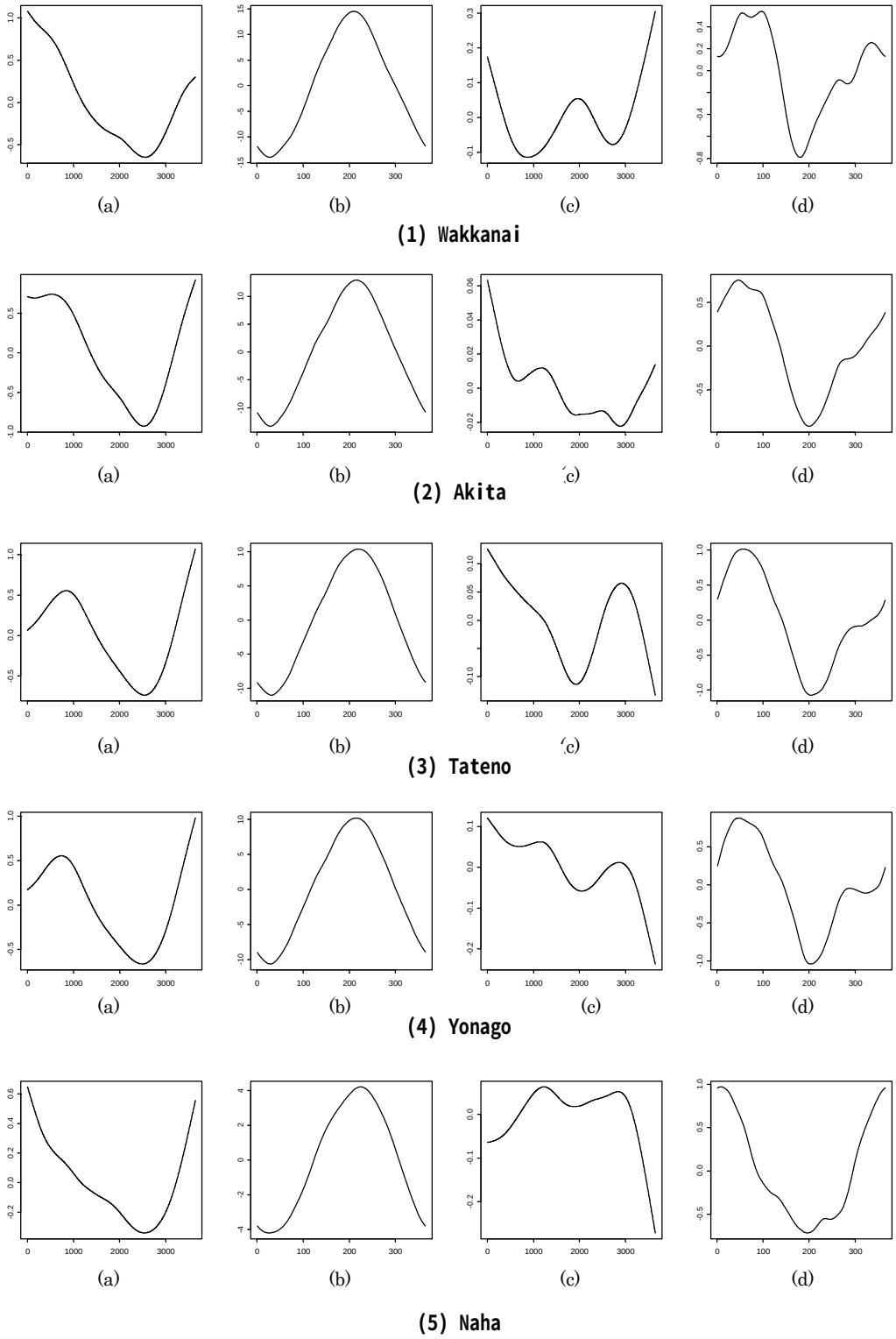

Figure 2.11. The long term trend and the seasonal trend of the estimated mean and variance of the aerological temperature data at the 500hpa isobaric surface. The panel (a) and (c) are the long term trend of the mean and variance and the panel (b) and (d) are the seasonal trend of the mean and variance respectively.

Chapter 3

Seasonal adjustment

In this paper, we would like to investigate air temperature anomalies. The seasonal periodicities of the daily means are removed from the raw data and then the seasonal periodicities of the variances are standardized. There are some methods in the seasonal adjustment; the running mean (Shiskin et al. (1967)), fitting polynomial, analysis of the seasonal AR model (Zwiers and Storch (1990)), the ARIMA based approach (Helmer and Tiao (1982)), the Bayesian seasonal adjustment (Akaike (1980), Akaike and Ishiguro (1980)), the state space modeling (Kitagawa and Gersch (1984)) and the non-parametric regression (Cleveland et al. (1990)).

Here, when we consider the anomaly from the point of view of the prediction, we can recognize that it is the yearly distinctive variablities biased from regularly seasonal variables. Therefore, we adopt the polynomial in order to obtain the regular seasonality rather than the flexible seasonality for yearly variablities.

The long-term trend and the periodicities of the means and the variances are estimated by polynomials included the Fourier form. Specifically, let $\{T_n\ ;\ n = 1, 2, \cdots, N\ ;\ N = 14600\}$ be the original daily mean surface temperature data. Then we assume an independently and identically distributed noise term v_n for each n for the stochastic relation among T_n, the mean μ_n and variance υ_n^2,

$$T_n = \mu_n + \upsilon_n v_n\ ,\ v_n \sim N(0, 1^2)\ , \tag{3.1}$$

where

$$\mu_n = B_n + S_n\ ,$$

$$B_n = \sum_{j=0}^{\overline{O}} a_j n^j\ ,\quad S_n = \sum_{j=1}^{\overline{P}} b_j \sin\frac{2\pi jn}{365} + \sum_{j=1}^{\overline{Q}} c_j \cos\frac{2\pi jn}{365}\ ,$$

and

$$\upsilon_n^2 = \tilde{B}_n + \tilde{S}_n ,$$

$$\tilde{B}_n = \sum_{j=0}^{\tilde{O}} \tilde{a}_j n^j \ , \quad \tilde{S}_n = \sum_{j=1}^{\tilde{P}} \tilde{b}_j \sin\frac{2\pi jn}{365} + \sum_{j=1}^{\tilde{Q}} \tilde{c}_j \cos\frac{2\pi jn}{365} .$$

Here, the integer numbers $\overline{O}$ and $\tilde{O}$ are respective orders of the polynomials, the integer numbers $\overline{P}$, $\overline{Q}$, $\tilde{P}$ and $\tilde{Q}$ are respective orders of the Fourier polynomials, and we assume the Nomal distribution with the mean 0 and the variance 1^2 for the residuals v_n. B_n and S_n represent the long-term trend and the seasonal periodicity of the means respectively, and $\tilde{B}_n$ and $\tilde{S}_n$ represent the long-term trend and seasonal periodicity of the variances respectively. Given the orders $\overline{O}$, $\overline{P}$, $\overline{Q}$, $\tilde{O}$, $\tilde{P}$ and $\tilde{Q}$ we simultaneously estimate the both coefficients of μ_n and variance υ_n^2 by the maximum likelihood procedure, or nonlinear least squares procedure.

Then the optimal orders $\overline{O}$, $\overline{P}$, $\overline{Q}$, $\tilde{O}$, $\tilde{P}$ and $\tilde{Q}$ are determined by making use of the Akaike Information Criterion (AIC ; see Akaike (1974), and Parzen et al. (1998), for example) that is defined by

$$AIC \quad = (-2) \log (\text{maximum likelihood}) + 2k,$$

where k is the total number of adjusted parameters. The AIC is computed for each of models fitted to the same data. The addition of the quantity $2k$, roughly compensates for the additional flexibility which the extra parameters provide in models with different numbers of parameters. The model with the lower AIC value is taken as giving the better choice for forward prediction purposes. In so far as it depends on the likelihood ratio, the AIC can also be used as a rough guide to the model testing. As a rule of thumb, in testing a model with $k+d$ parameters against a null hypothesis with just k parameters, we take a difference of 2 in AIC values as a rough estimate of significance at the 5% level or less depending on d.

The log likelihood $\ell(\theta_S)$ with the parameter vector θ_S of the polynomials (3.1) is

$$\ell(\theta_S) = -\frac{N}{2}\log 2\pi - \frac{1}{2}\sum_{n=1}^{N}\log\upsilon_n^2 - \frac{1}{2}\sum_{n=1}^{N}\frac{(y_n-\mu_n)^2}{\upsilon_n^2},$$

where μ_n and υ_n^2 hold the Fourier form of the polynomials (3.1), and the maximum log likelihood is estimated by the quasi-Newton method.

The optimal order of the polynomials in each station are listed in Table 3.1. The

estimated values of the long-term trend of the mean μ_n in each station are plotted in panels of Figure 3.1. The horizontal axis represents the date for 40 years, and the vertical axis represents the values of the long-term trend of the mean μ_n. We can confirm the increasing trend in all stations. The estimated values of the seasonal periodicity of the mean μ_n in each station are plotted in panels of Figure 3.2. The horizontal axis represents the date within a one-year period, and the vertical axis represents the values of the seasonal periodicity of the mean. We can confirm unimodal curves with a peak in summer season are drawn in all panels.

The estimated values of the long-term trend of the variance υ_n^2 in each station are plotted in panels of Figure 3.3. The horizontal axis represents the date for 40 years, and the vertical axis represents the values of the long-term trend of the variance υ_n^2. Note that there is not always the increasing trend such as the mean. The estimated values of the seasonal periodicity of the variance υ_n^2 in each station are plotted in panels of Figure 3.4. The horizontal axis represents the date for 40 years, and the vertical axis represents the values of the long-term trend of the variance υ_n^2. We can confirm curves with a few peaks are drawn in the panels. Note that the positions and the shape of the peaks are different according to the area.

We are concerned with the yearly distinctive variablities. For their prediction, though the seasonal periodicities which are the yearly regular variablities are removed, the long-term trend is not so, and we can consider it as the information which forms the yearly distinctive variablities. Therefore, we compose the surface air temperature anomaly removing only the seasonal periodicities, this is,

$$\hat{\mu}_n = a + \sum_{j=1}^{\bar{P}} b_j \sin\frac{2\pi jn}{365} + \sum_{j=1}^{\bar{Q}} c_j \cos\frac{2\pi jn}{365}$$

and

$$\hat{\upsilon}_n^2 = \tilde{a} + \sum_{j=1}^{\tilde{P}} \tilde{b}_j \sin\frac{2\pi jn}{365} + \sum_{j=1}^{\tilde{Q}} \tilde{c}_j \cos\frac{2\pi jn}{365}.$$

The realized data of the surface air temperature anomaly $v_n = (T_n - \hat{\mu}_n)/\hat{\upsilon}_n$ is indicated simply by the notation y_n from now on. We will discuss the property of the anomaly in the next chapter.

Table 3.1. The optimal order of applied polynomials in each station.

WMO code	stations	orders $\overline{O}$	$\overline{P}$	$\overline{Q}$	$\tilde{O}$	$\tilde{P}$	$\tilde{Q}$	AIC values	WMO code	stations	orders $\overline{O}$	$\overline{P}$	$\overline{Q}$	$\tilde{O}$	$\tilde{P}$	$\tilde{Q}$	AIC values
47401	Wakkanai	11	19	19	14	24	24	71424.9	47402	Kitamiesashi	11	19	19	12	20	20	75514.9
47404	Haboro	24	19	19	12	24	23	70543.5	47405	Omu	12	19	19	12	20	20	76789.9
47406	Rumoi	25	19	19	12	27	26	69396.7	47407	Asahikawa	11	19	19	8	22	21	74504.0
47409	Abashiri	24	19	19	13	20	20	75493.7	47411	Otaru	12	19	19	13	7	7	68970.5
47412	Sapporo	28	19	19	13	27	26	70182.0	47413	Iwamizawa	47	19	19	11	7	7	71917.1
47417	Obihiro	11	19	19	14	15	15	73323.6	47418	Kushiro	22	19	19	13	7	7	68110.5
47420	Nemuro	27	19	19	14	10	10	69286.4	47421	Suttsu	11	29	28	11	11	11	67100.0
47423	Muroran	26	41	40	12	11	11	67378.2	47424	Tomakomai	35	19	19	13	11	11	66320.8
47426	Urakawa	24	19	19	11	29	28	67304.0	47428	Esashi	63	19	19	26	11	11	66030.4
47430	Hakodate	23	29	28	11	11	11	69654.7	47433	Kutchan	52	19	19	11	27	26	71361.8
47435	Mombetsu	12	19	19	17	20	20	75635.8	47440	Hiroo	51	23	22	13	44	44	72757.8
47520	Shinjo	23	41	40	13	38	38	66740.5	47570	Wakamatsu	17	40	40	10	38	38	67189.3
47574	Fukaura	12	19	19	11	8	7	68606.0	47575	Aomori	11	23	22	8	11	11	68283.7
47576	Mutsu	29	24	23	10	11	11	69729.9	47581	Hachinohe	24	24	23	27	8	7	72220.3
47582	Akita	18	20	20	10	8	7	67686.0	47584	Morioka	15	24	23	11	9	8	69677.1
47585	Miyako	16	24	23	11	8	7	71940.5	47587	Sakata	12	20	20	10	8	7	66214.0
47588	Yamagata	18	42	42	11	27	26	68725.7	47590	Sendai	14	22	22	11	5	5	68490.8
47592	Ishinomaki	12	22	22	10	5	5	67412.7	47595	Fukushima	13	42	42	12	27	26	70137.6
47597	Shirakawa	16	44	44	8	38	38	69032.3	47600	Wajima	12	22	22	3	8	7	67131.0
47602	Aikawa	14	22	22	11	8	7	67637.4	47604	Niigata	11	22	22	4	8	7	65941.0
47605	Kanazawa	12	22	22	12	27	26	68280.0	47606	Fushiki	17	22	22	2	27	26	67595.7
47607	Toyama	18	22	22	3	8	7	69482.2	47610	Nagano	17	22	22	3	31	31	69411.3
47612	Takada	23	22	22	4	15	15	68503.7	47615	Utsunomiya	24	22	22	11	38	38	67685.2
47616	Fukui	17	22	22	3	15	15	67938.2	47617	Takayama	14	15	14	9	27	26	67448.6
47618	Matsumoto	33	15	14	8	27	26	71099.0	47620	Suwa	10	15	14	9	21	21	67316.6
47624	Maebashi	19	33	33	8	27	26	68005.0	47626	Kumagaya	15	22	22	10	38	38	66754.9
47629	Mito	20	22	22	11	15	15	67838.9	47631	Tsuruga	13	22	22	3	8	7	68035.2
47632	Gifu	18	34	33	9	35	35	65334.8	47636	Nagoya	16	15	14	9	27	26	64921.5
47637	Iida	25	22	22	9	27	26	66830.0	47638	Kofu	13	13	13	9	35	35	65373.9
47640	Kawaguchiko	15	7	7	7	38	38	69873.0	47641	Chichibu	14	22	22	5	38	38	66777.3
47648	Choshi	36	10	10	9	15	15	64533.0	47649	Ueno	17	35	34	7	35	35	65409.6
47651	Tsu	24	13	13	9	27	26	63312.5	47653	Irako	27	7	7	12	26	25	60591.1
47654	Hamamatsu	15	7	7	9	26	25	62922.4	47655	Omaezaki	44	22	22	14	27	26	61098.4
47656	Shizuoka	16	7	7	7	26	25	63715.4	47657	Mishima	17	7	7	7	25	25	65621.9

WMO code	stations	orders $\overline{O}$	$\overline{P}$	$\overline{Q}$	$\tilde{O}$	$\tilde{P}$	$\tilde{Q}$	AIC values
47662	Tokyo	14	22	22	19	38	38	67051.9
47666	Irozaki	16	22	22	10	39	39	61602.7
47670	Yokohama	16	22	22	7	38	38	66351.7
47675	Oshima	11	7	7	7	38	38	63951.8
47690	Nikko	17	7	7	17	25	24	70831.6
47741	Matsue	16	22	22	8	27	26	65758.4
47744	Yonago	15	22	22	12	27	26	68704.2
47747	Toyooka	16	34	34	19	27	26	67861.6
47754	Hagi	18	34	34	11	15	15	66728.9
47756	Tsuyama	24	35	34	12	23	22	65315.8
47761	Hikone	18	22	22	15	27	26	63475.3
47765	Hiroshima	18	35	34	13	11	10	63355.2
47768	Okayama	23	34	33	13	27	26	64967.2
47770	Kobe	16	22	22	13	27	26	64908.7
47776	Sumoto	24	22	22	14	25	24	63866.6
47778	Shionomisaki	17	22	22	13	26	25	62911.4
47800	Izuhara	19	22	22	13	27	26	66805.5
47807	Fukuoka	15	22	21	12	15	14	65822.7
47812	Sasebo	19	35	34	13	30	29	64342.4
47814	Hita	25	35	34	13	11	11	67764.4
47817	Nagasaki	18	34	33	13	30	29	64553.6
47821	Asosan	25	35	34	5	26	26	70165.7
47824	Hitoyoshi	25	35	34	13	11	11	66451.8
47829	Miyakonojo	25	35	34	5	11	11	66307.7
47831	Makurazaki	23	35	34	13	11	11	64386.5
47836	Yakushima	21	22	21	5	10	10	60545.6
47838	Ushibuka	14	34	33	13	11	11	63173.1
47890	Tadotsu	43	18	18	15	15	15	61330.0
47892	Uwajima	44	35	34	18	11	11	64423.8
47895	Tokushima	16	35	34	13	27	26	62694.9
47898	Shimizu	26	35	34	13	27	26	62360.7
47909	Naze	31	15	15	5	9	8	58888.2
47918	Ishigakijima	22	17	17	10	14	14	56887.3
47929	Kumejima	30	18	17	5	23	22	57201.7
47945	Minamidaitojima	27	15	15	6	7	7	54439.4

WMO code	stations	orders $\overline{O}$	$\overline{P}$	$\overline{Q}$	$\tilde{O}$	$\tilde{P}$	$\tilde{Q}$	AIC values
47663	Owase	17	7	7	9	26	26	63765.4
47668	Ajiro	20	7	7	7	25	24	66310.3
47674	Katsuura	11	7	7	7	38	38	65771.2
47678	Hachijojima	24	8	8	7	26	25	59323.6
47740	Saigo	14	22	22	9	9	9	67291.6
47742	Sakai	15	22	22	13	27	26	65915.3
47746	Tottori	16	22	22	17	9	9	68860.1
47750	Maizuru	14	22	22	15	31	31	67779.9
47755	Hamada	16	22	22	13	27	26	66084.0
47759	Kyoto	17	34	34	13	27	26	66304.8
47762	Shimonoseki	19	34	34	13	15	14	61821.7
47766	Kure	16	34	33	15	11	10	62188.2
47769	Himeji	18	35	34	12	27	26	64633.0
47772	Osaka	19	34	34	8	35	35	64614.5
47777	Wakayama	21	22	22	9	27	26	63615.2
47780	Nara	19	34	34	7	27	26	65935.3
47805	Hirado	19	22	22	12	27	26	62342.7
47809	Iizuka	16	34	34	13	28	28	66330.4
47813	Saga	26	34	33	13	29	29	65399.2
47815	Oita	19	35	34	12	15	15	64137.7
47819	Kumamoto	19	35	34	7	30	30	66804.2
47823	Akune	15	34	33	13	11	11	64144.6
47827	Kagoshima	28	35	34	13	12	11	65085.1
47830	Miyazaki	21	35	34	14	11	11	65952.6
47835	Aburatsu	24	35	34	14	11	11	64841.7
47837	Tanegashima	19	17	16	2	11	11	59797.1
47887	Matsuyama	19	34	34	15	11	11	64132.6
47891	Takamatsu	18	15	15	13	15	15	63441.1
47893	Kochi	26	35	34	13	10	9	63441.5
47897	Sukumo	23	35	34	12	11	11	63224.8
47899	Murotomisaki	28	22	22	13	13	13	61605.5
47912	Yonagunijima	21	18	18	10	21	20	55168.9
47927	Miyakojima	30	17	16	4	19	18	54538.4
47936	Naha	25	18	18	5	26	25	56109.1

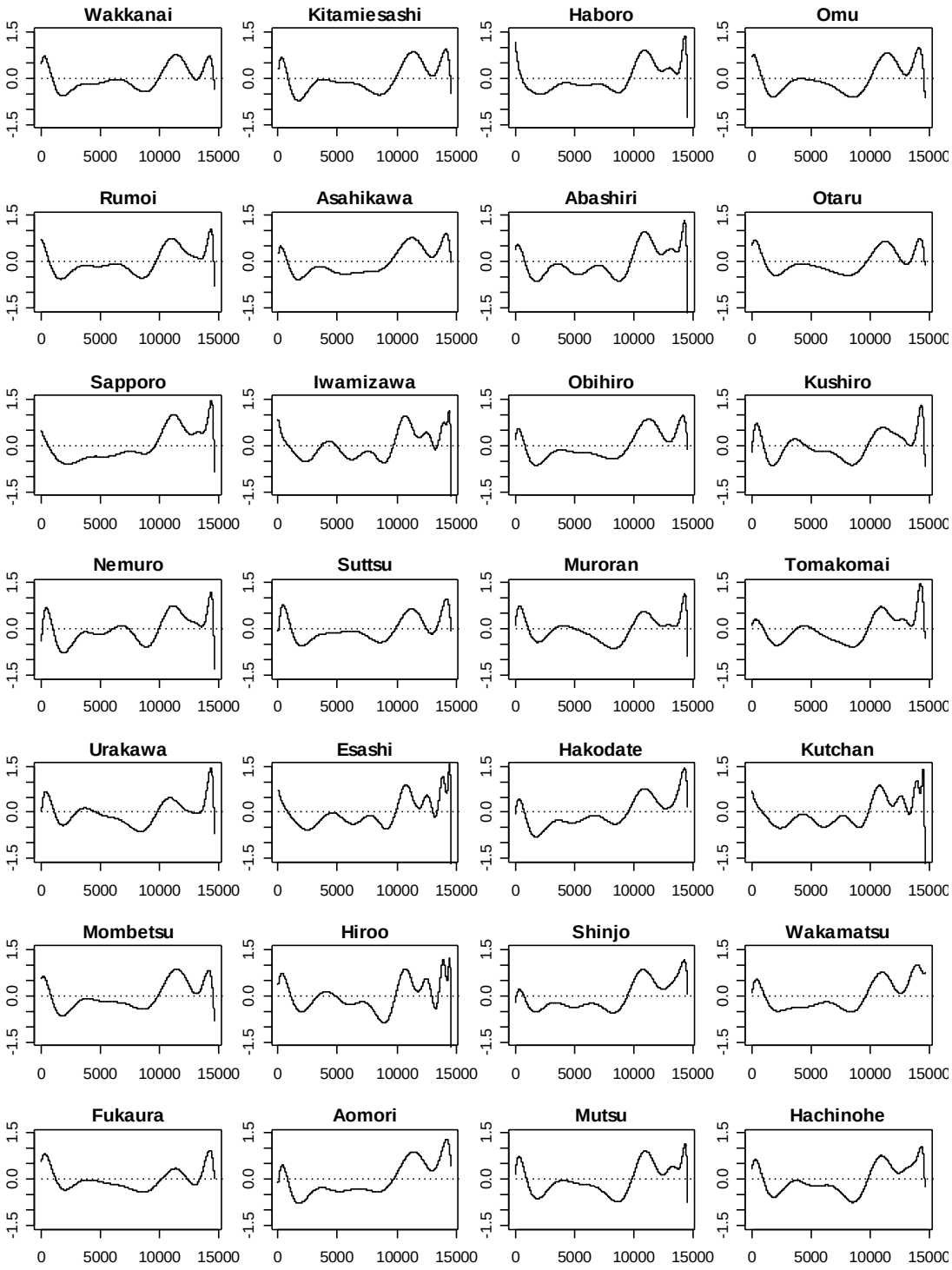

Figure 3.1-1. The estimated long-term trend of the mean μ_n in each station.

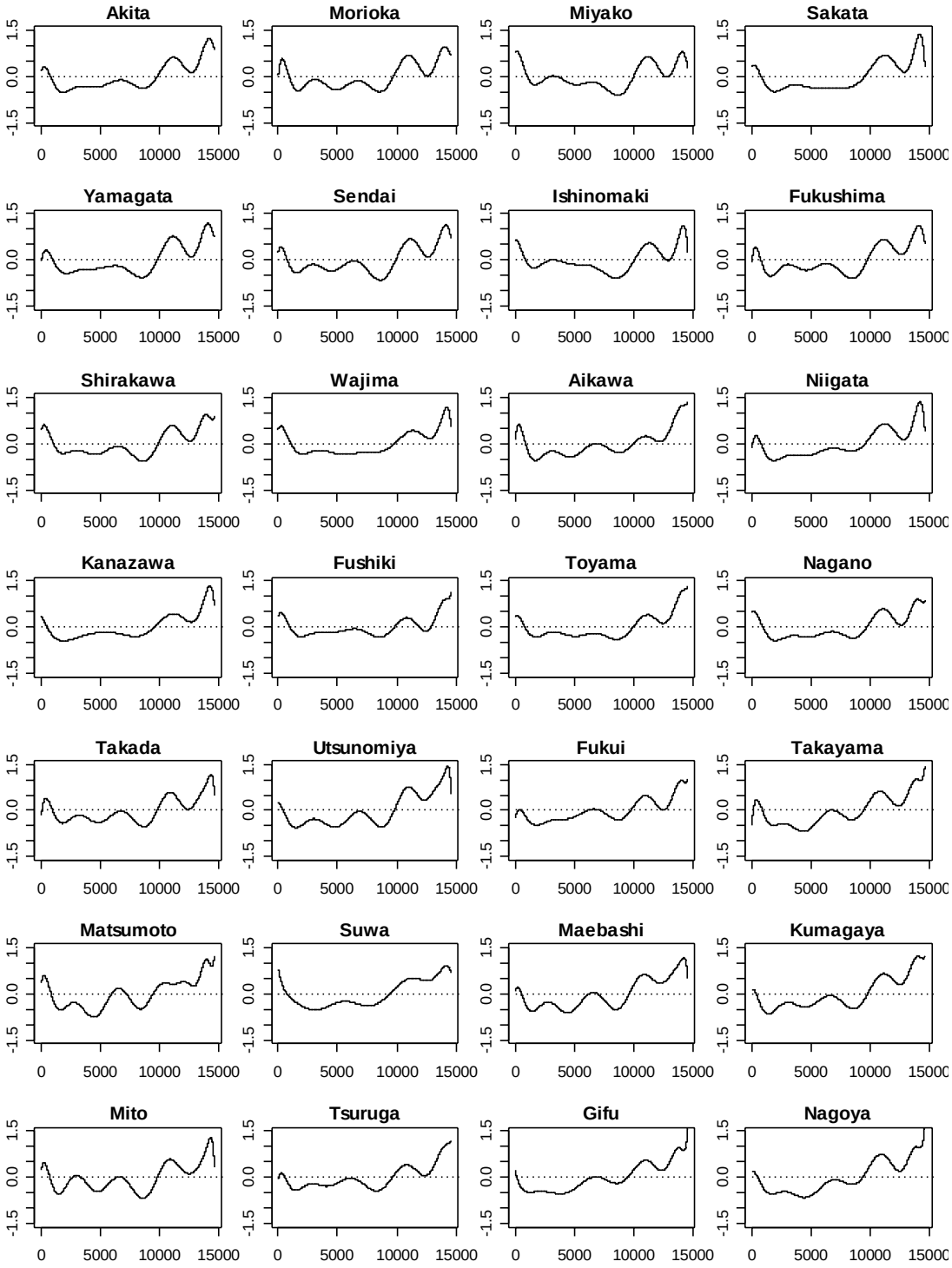

Figure 3.1-2. The estimated long-term trend of the mean μ_n in each station.

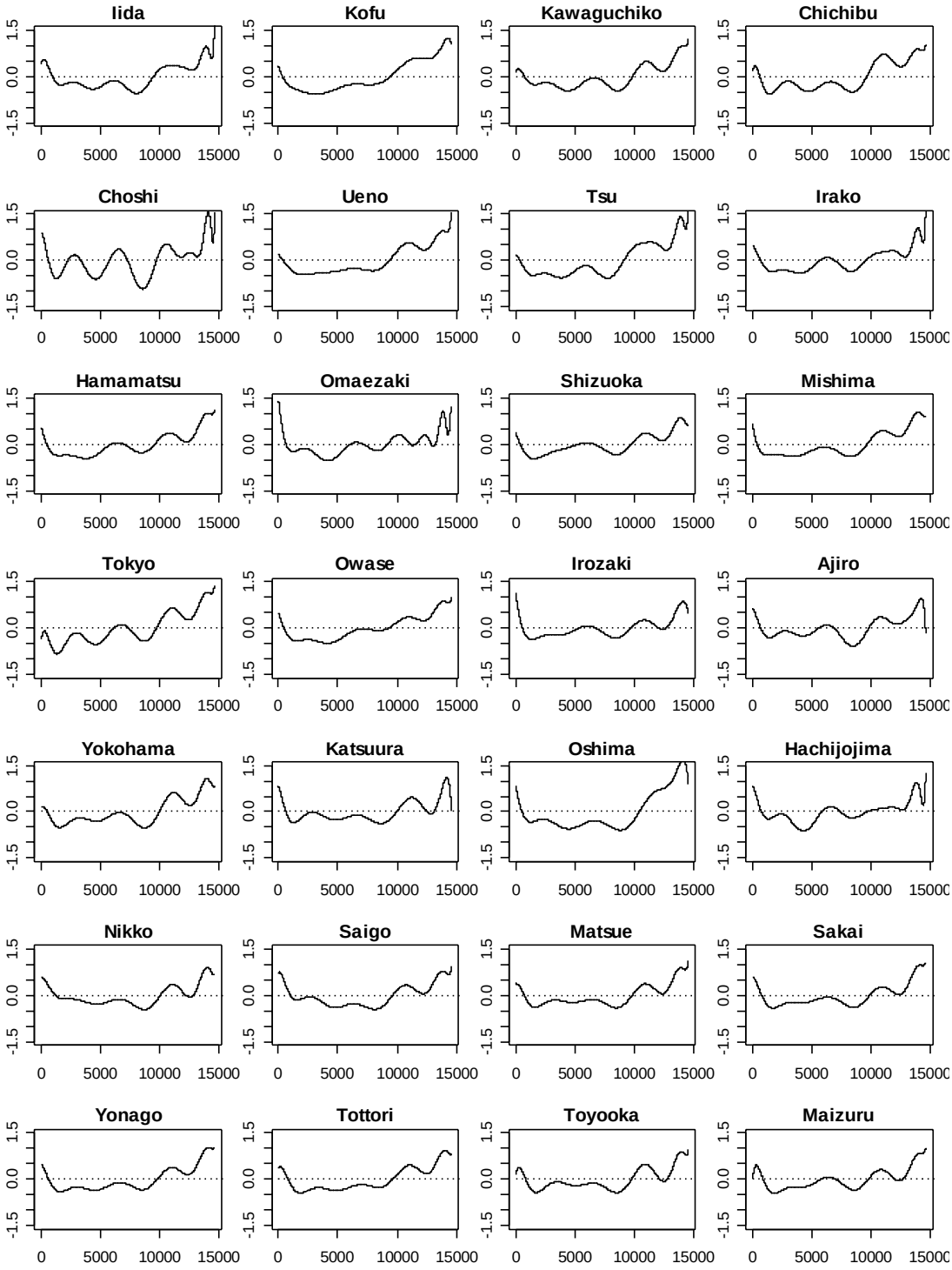

Figure 3.1-3. The estimated long-term trend of the mean μ_n in each station.

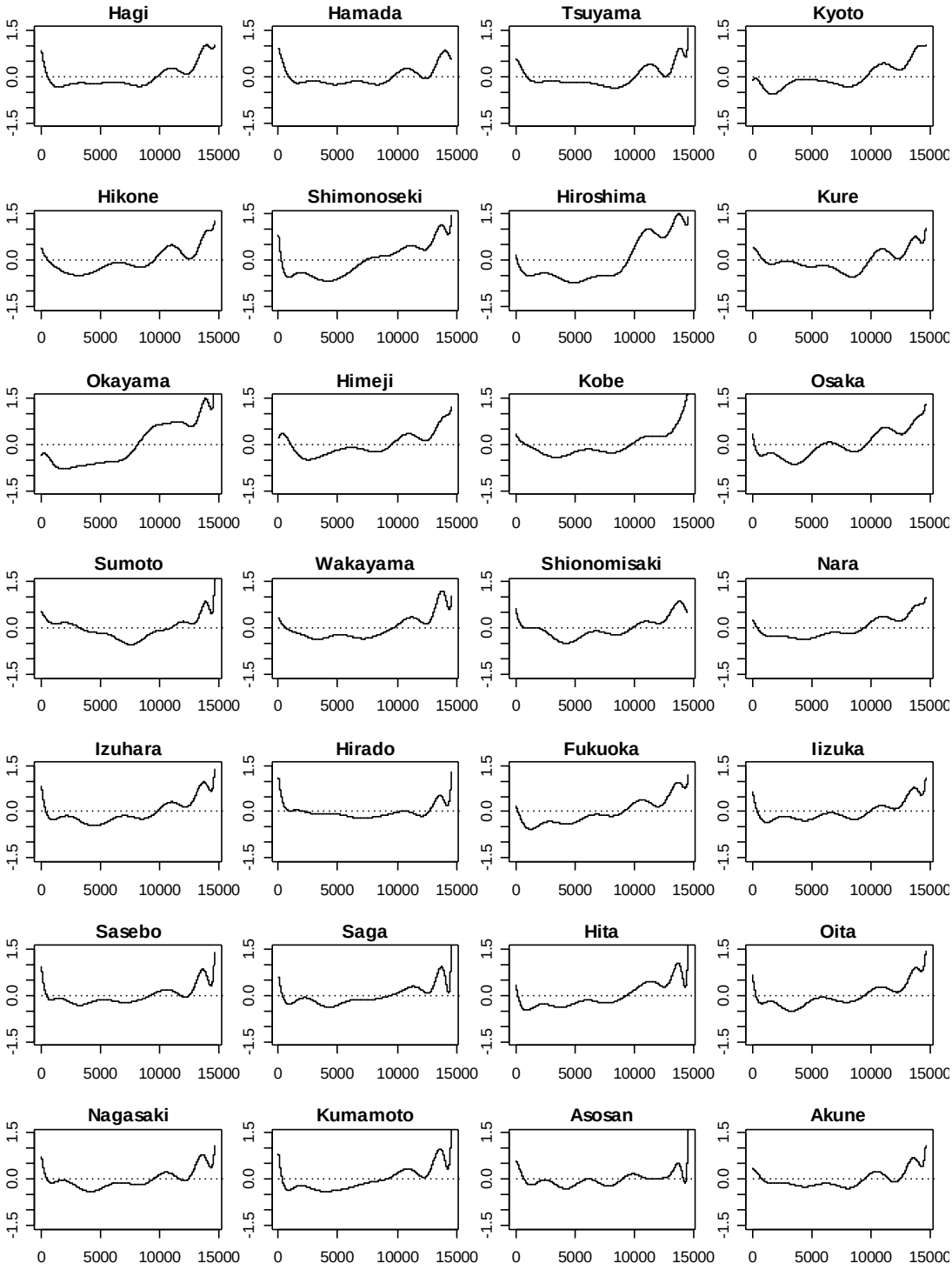

Figure 3.1-4. The estimated long-term trend of the mean μ_n in each station.

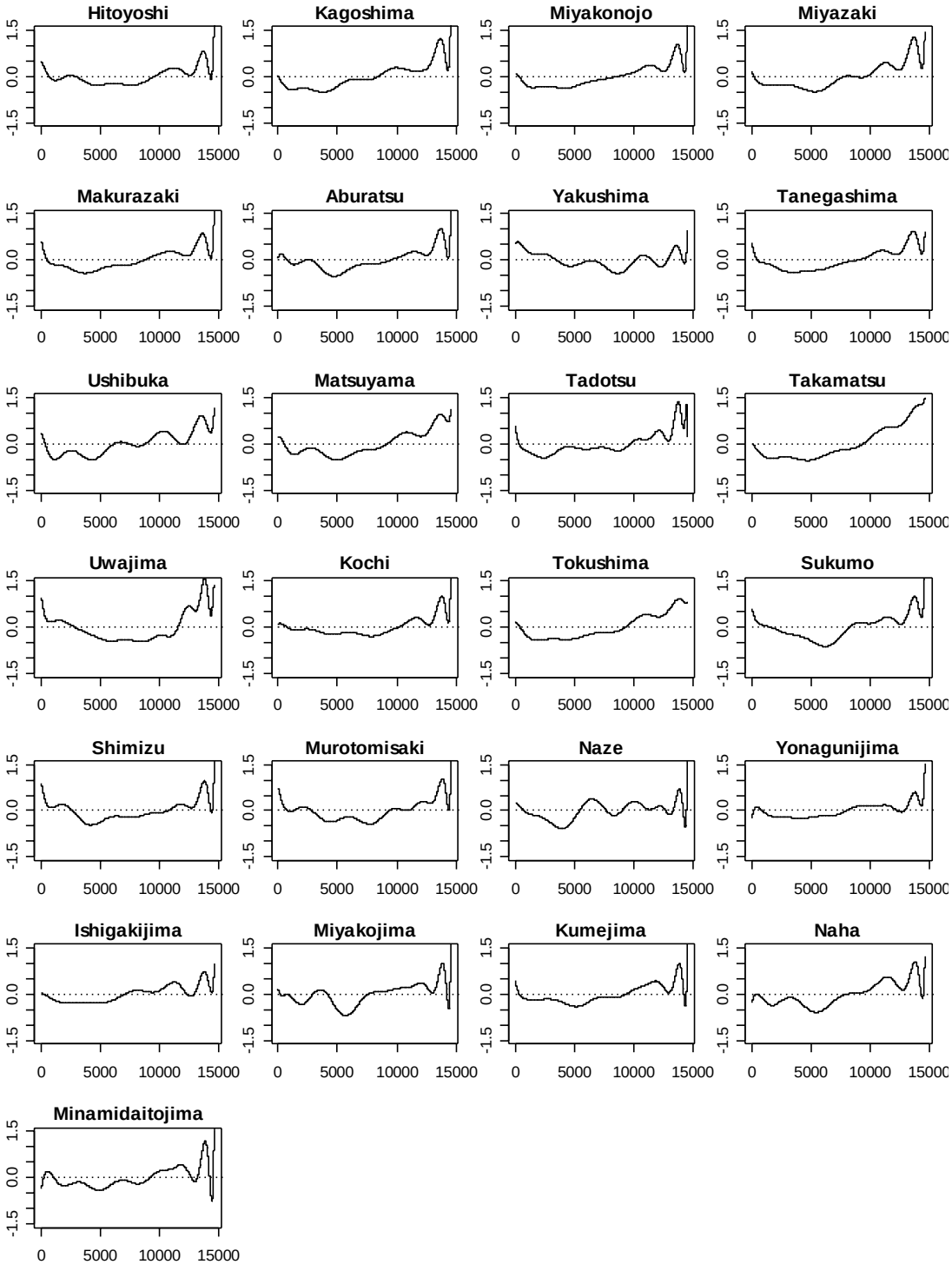

Figure 3.1-5. The estimated long-term trend of the mean μ_n in each station.

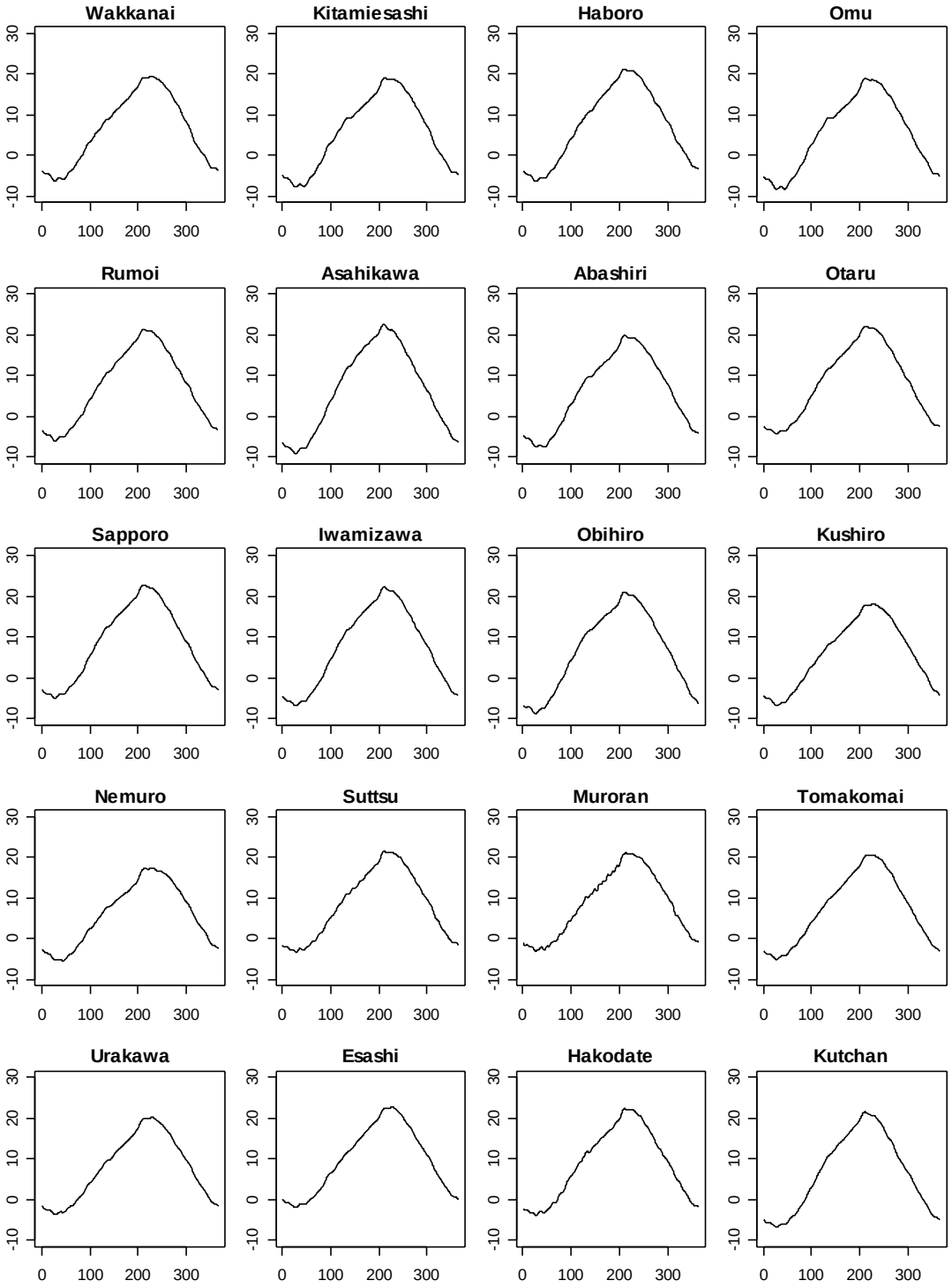

Figure 3.2-1. The estimated seasonal periodicity of the mean μ_n in each station.

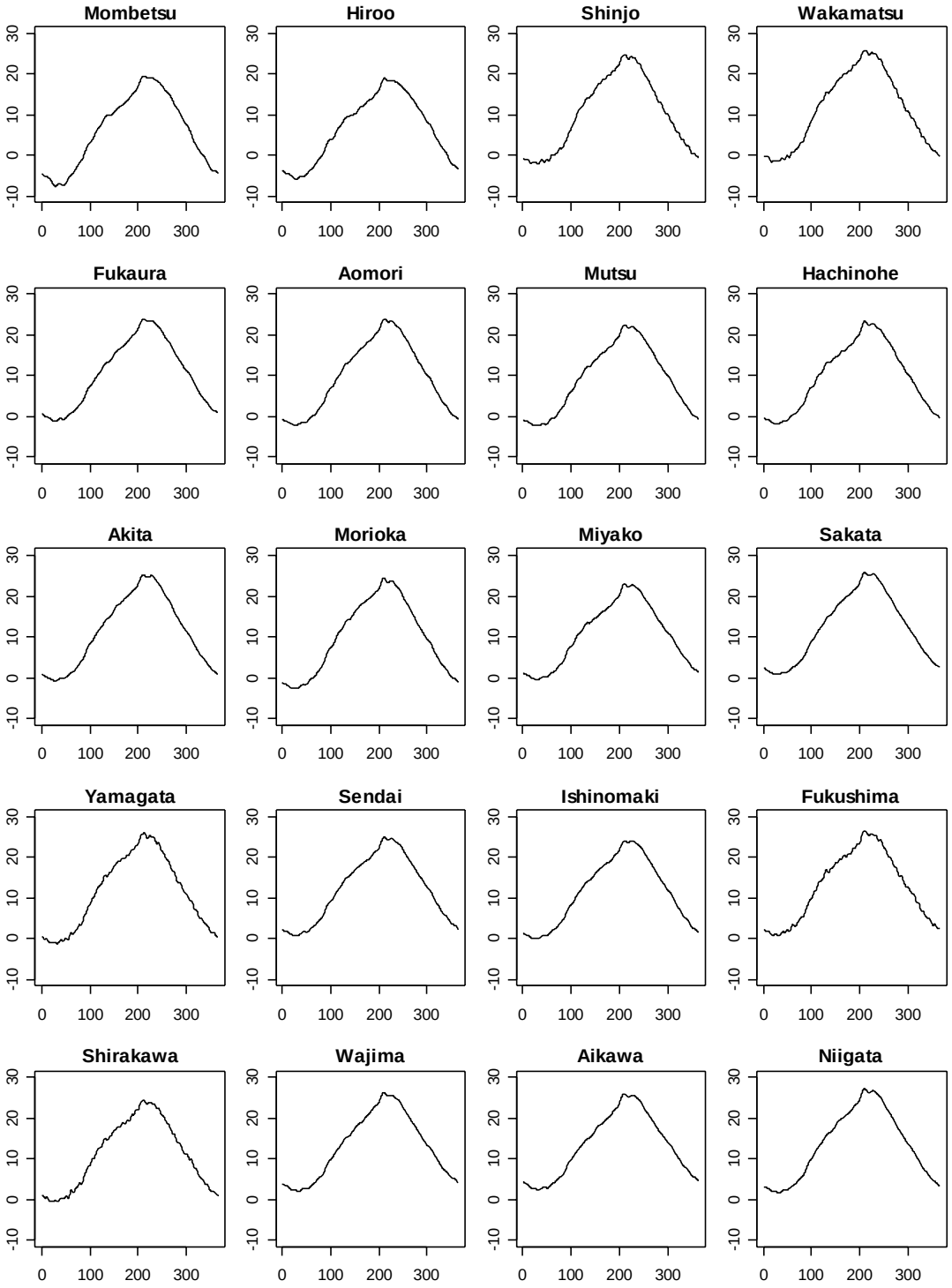

Figure 3.2-2. The estimated seasonal periodicity of the mean μ_n in each station.

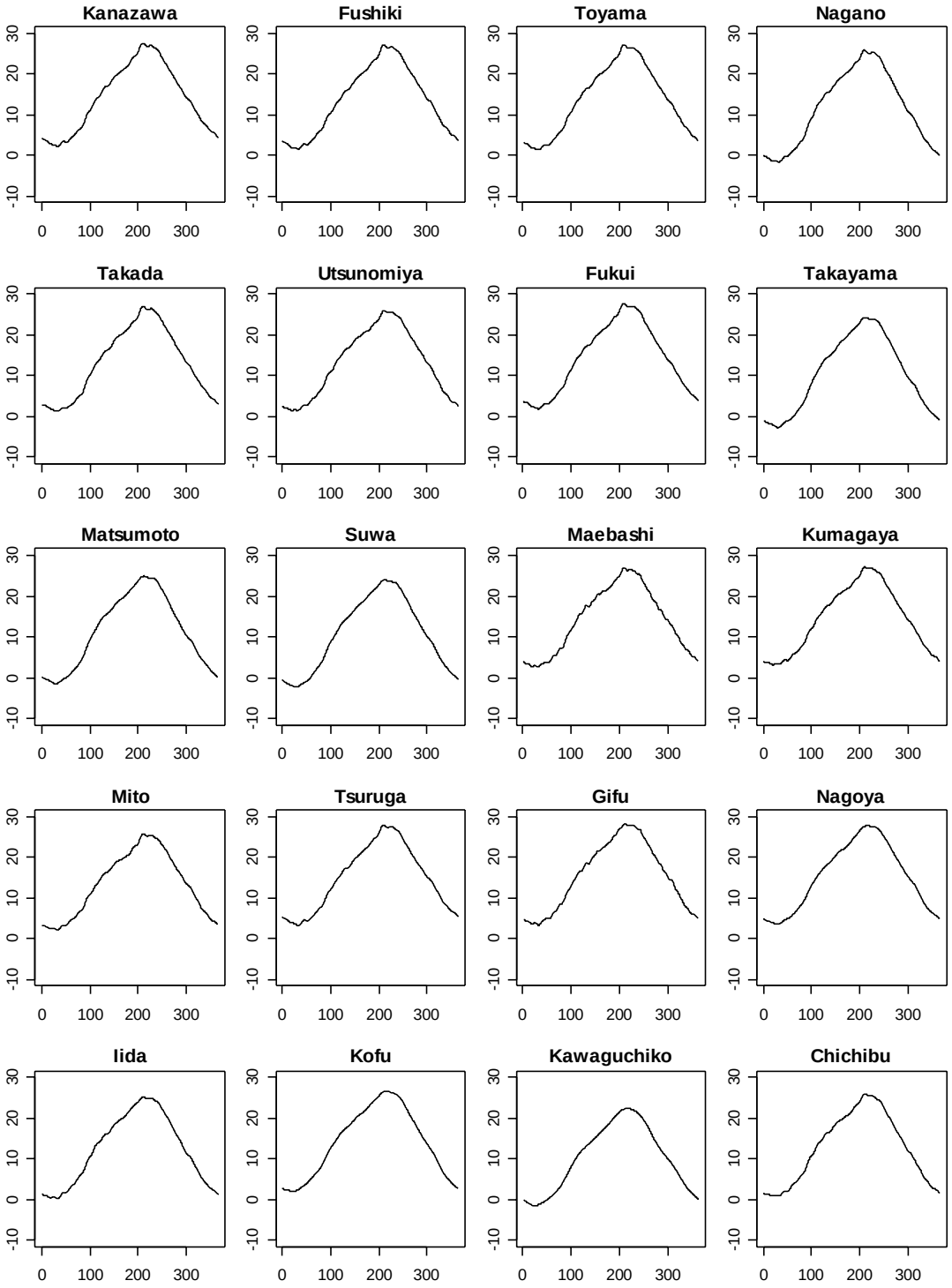

Figure 3.2-3. The estimated seasonal periodicity of the mean μ_n in each station.

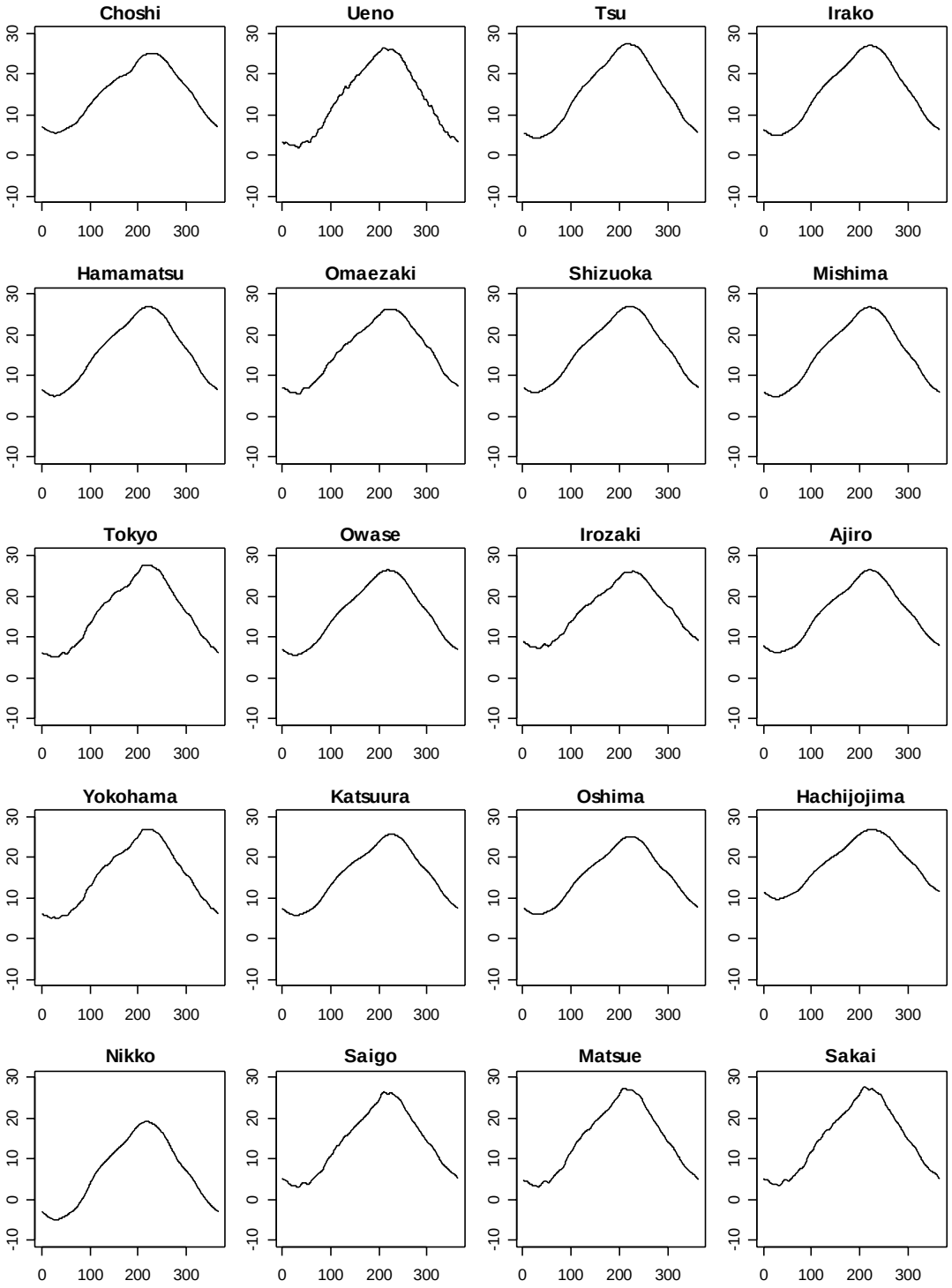

Figure 3.2-4. The estimated seasonal periodicity of the mean μ_n in each station.

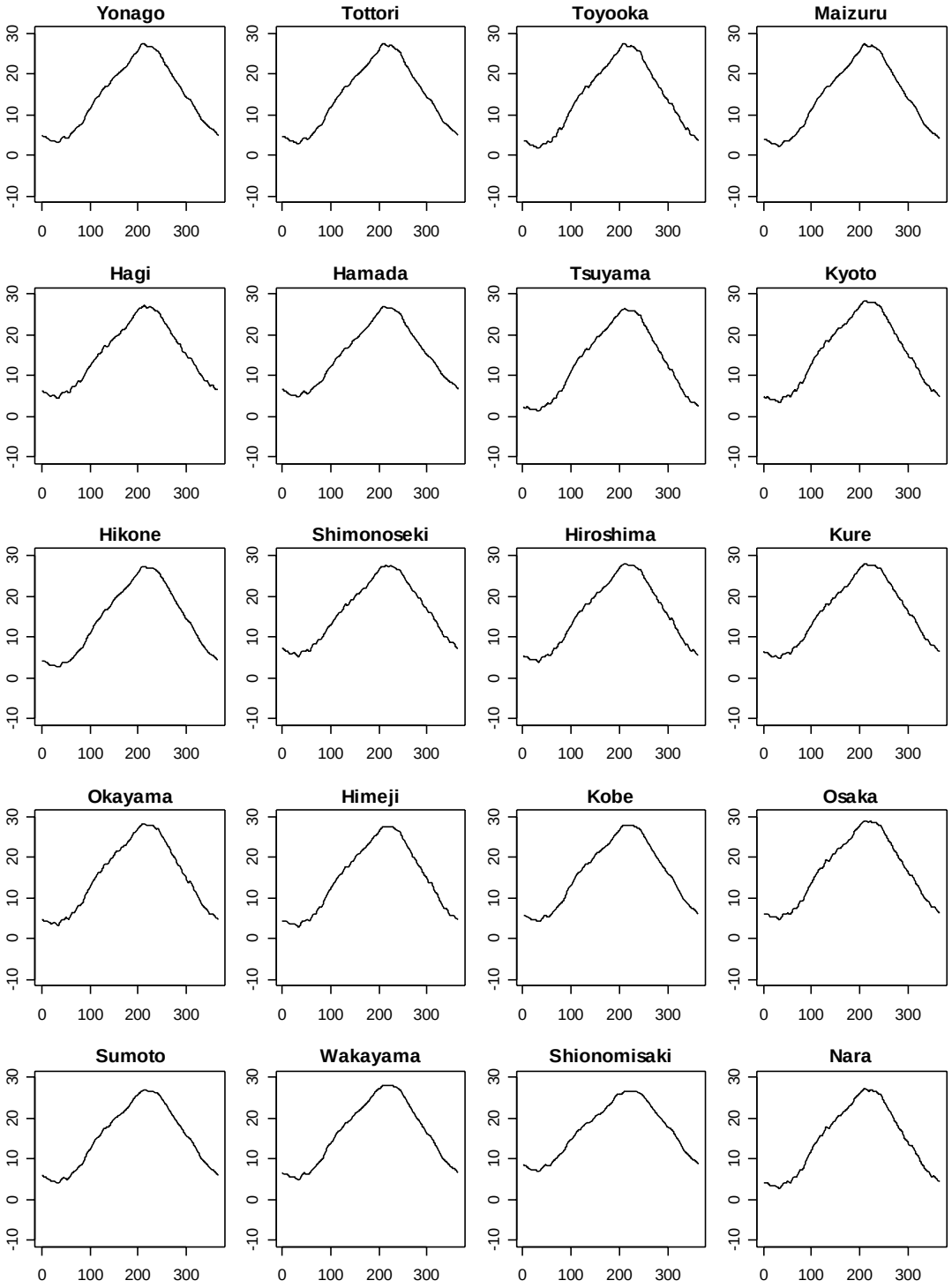

Figure 3.2-5. The estimated seasonal periodicity of the mean μ_n in each station.

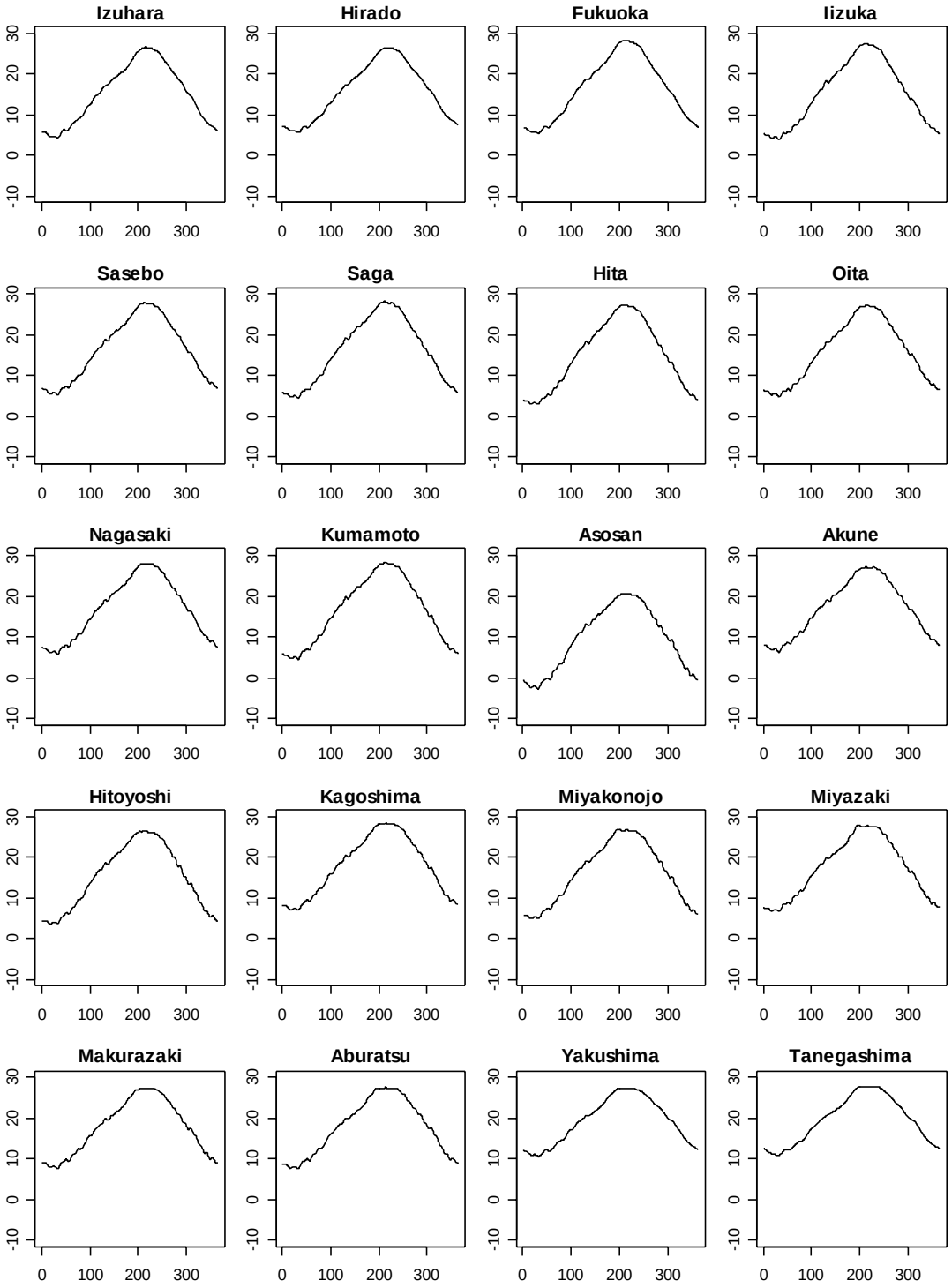

Figure 3.2-6. The estimated seasonal periodicity of the mean μ_n in each station.

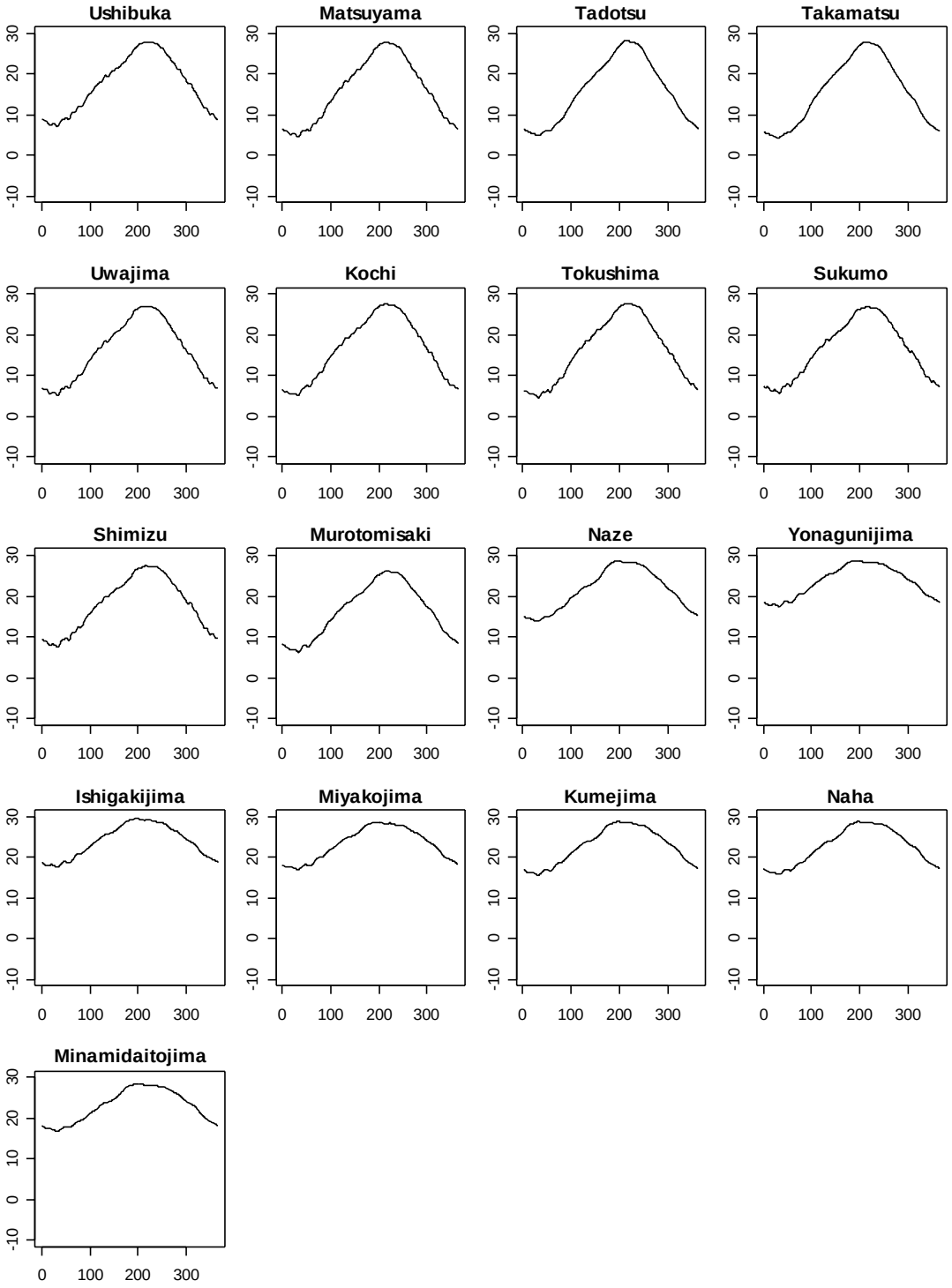

Figure 3.2-7. The estimated seasonal periodicity of the mean μ_n in each station.

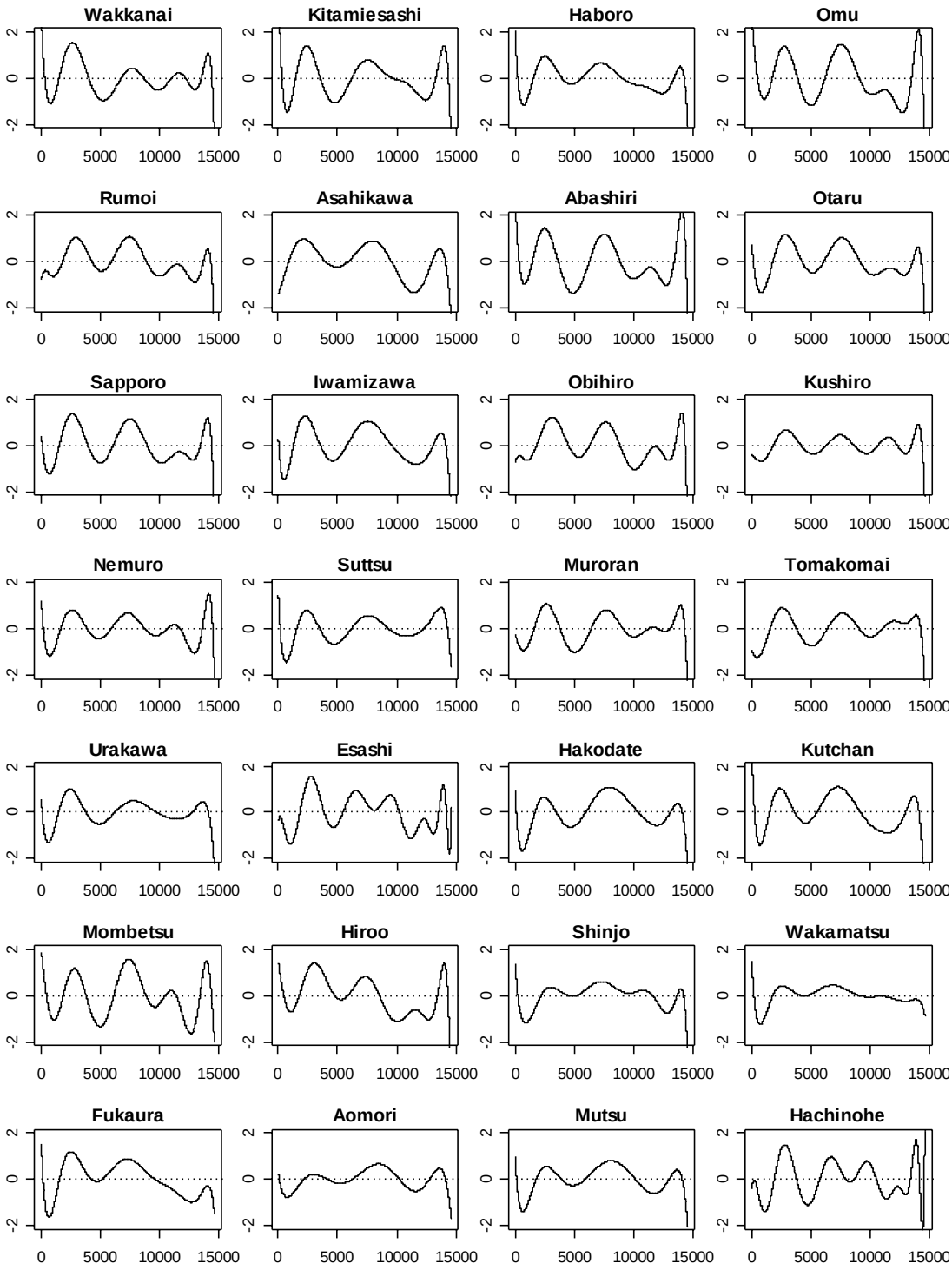

Figure 3.3-1. The estimated long-term trend of the variance υ_n^2 in each station.

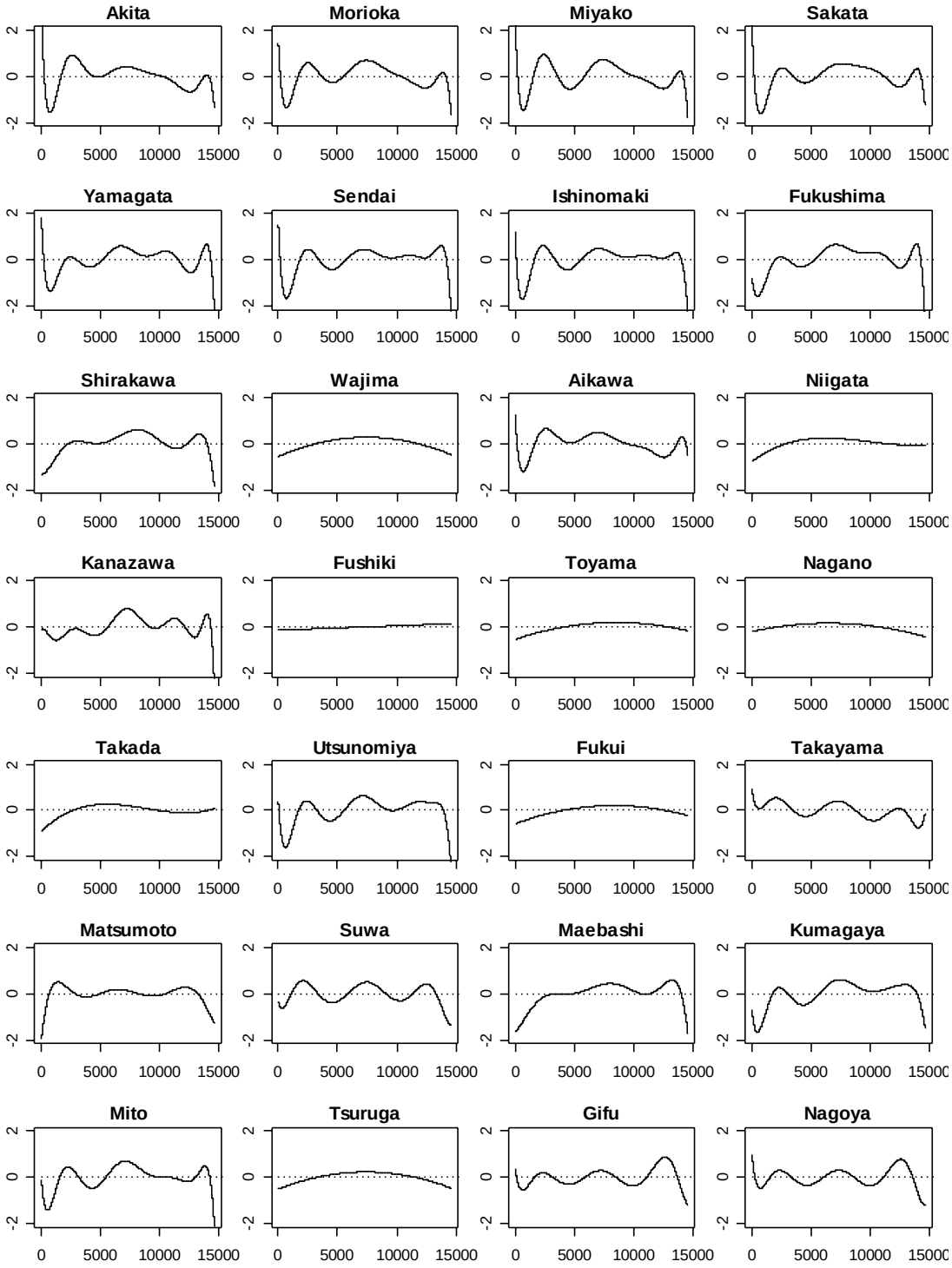

Figure 3.3-2. The estimated long-term trend of the variance υ_n^2 in each station.

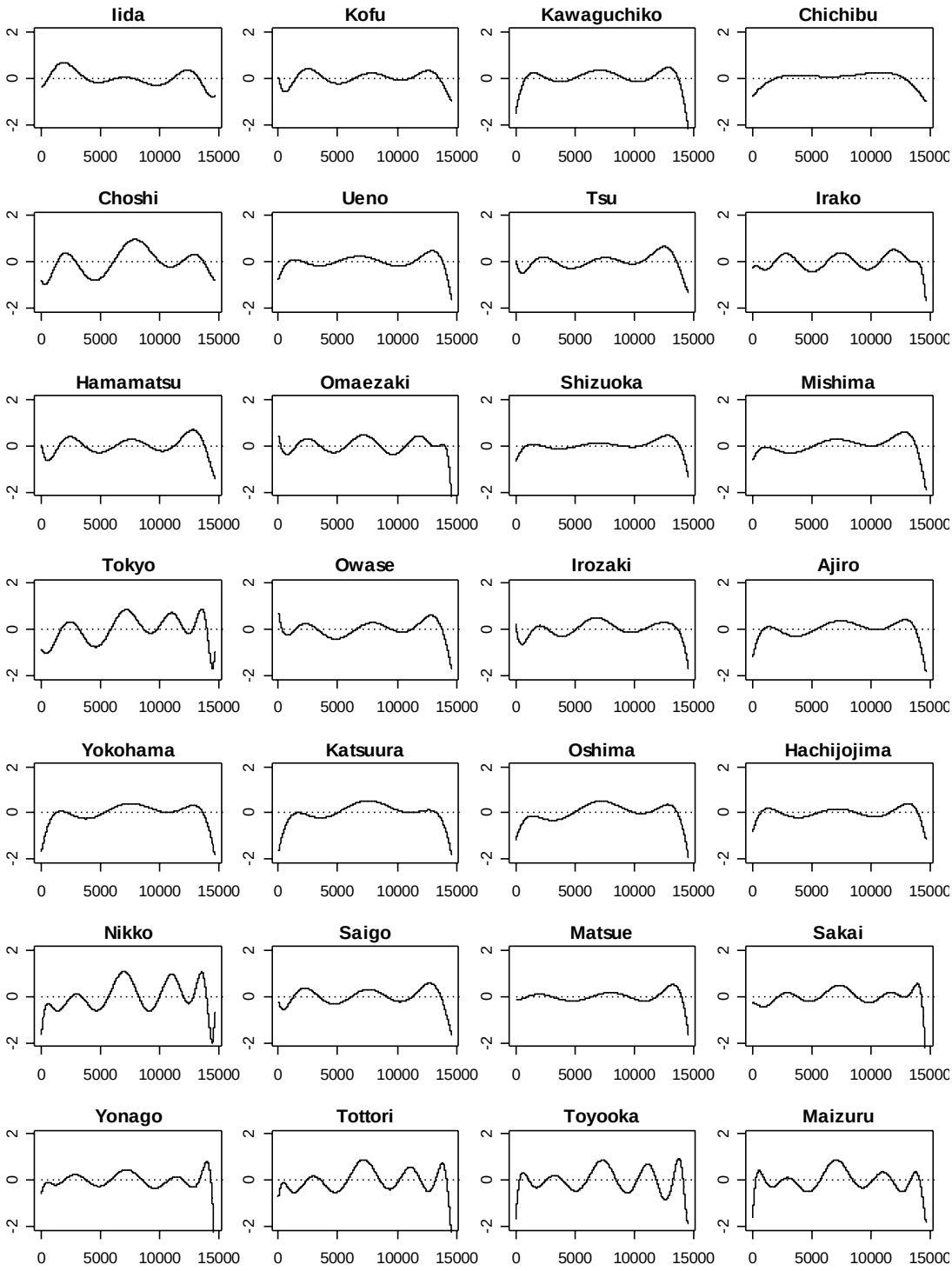

Figure 3.3-3. The estimated long-term trend of the variance υ_n^2 in each station.

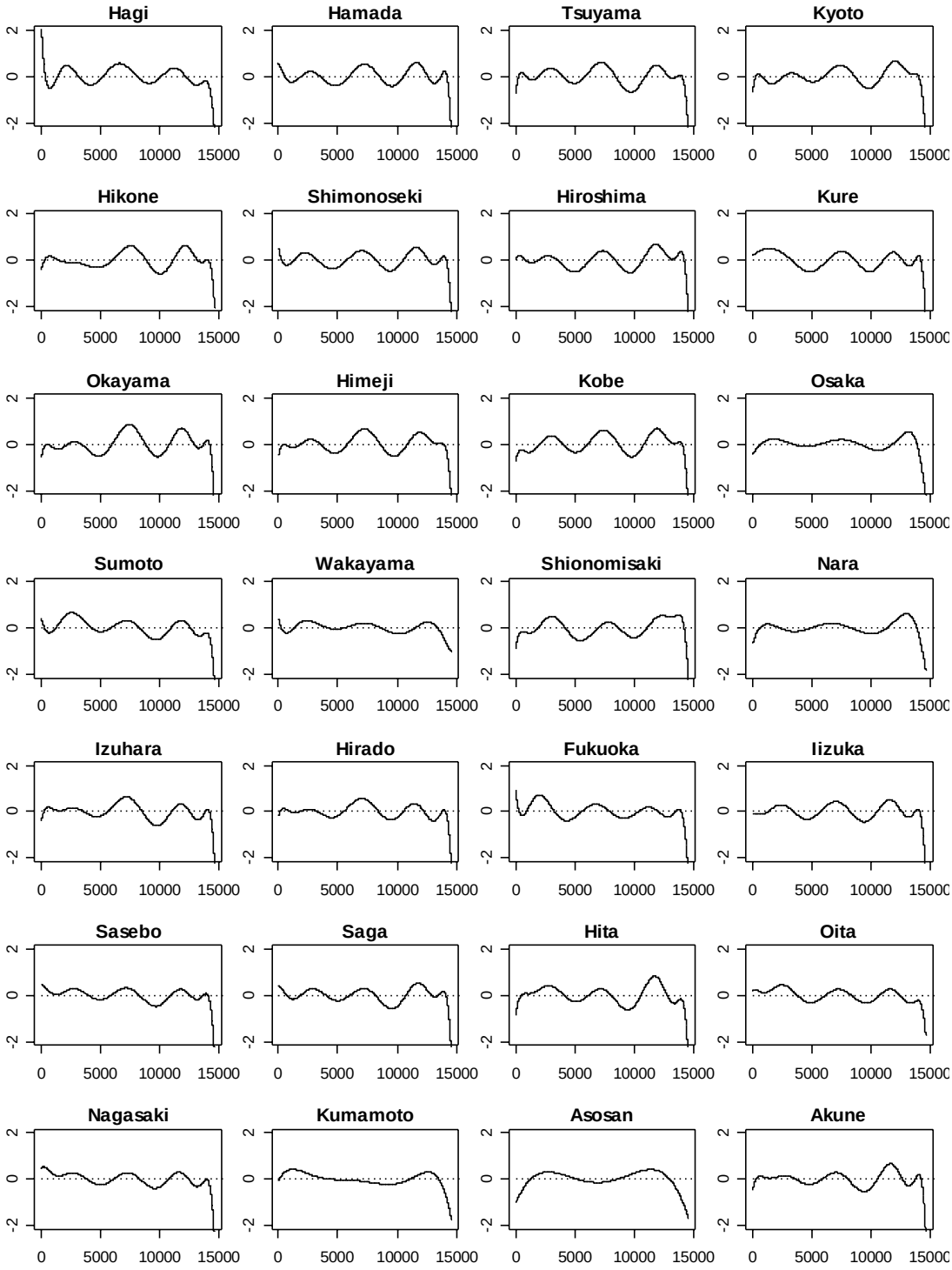

Figure 3.3-4. The estimated long-term trend of the variance υ_n^2 in each station.

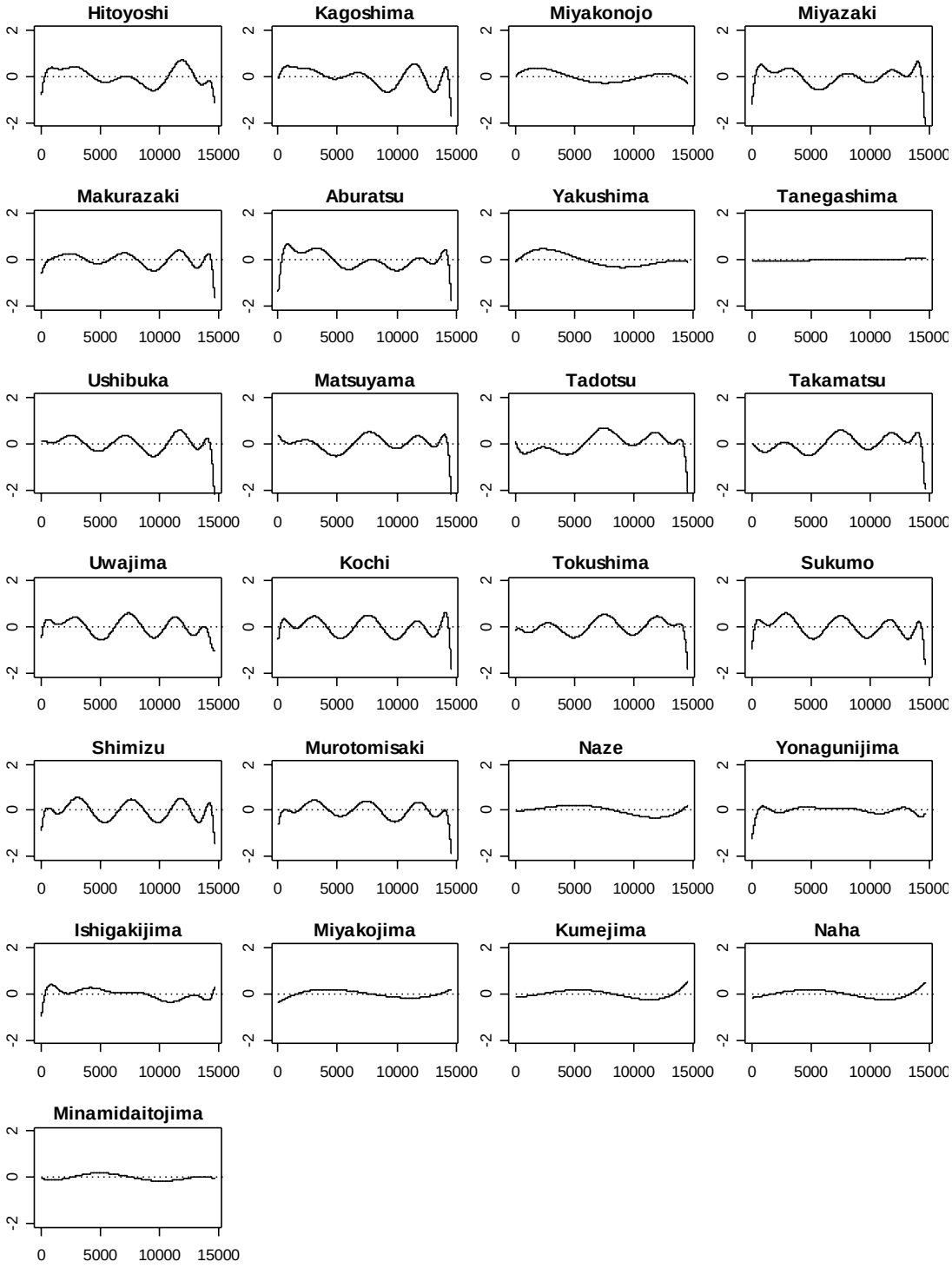

Figure 3.3-5. The estimated long-term trend of the variance υ_n^2 in each station.

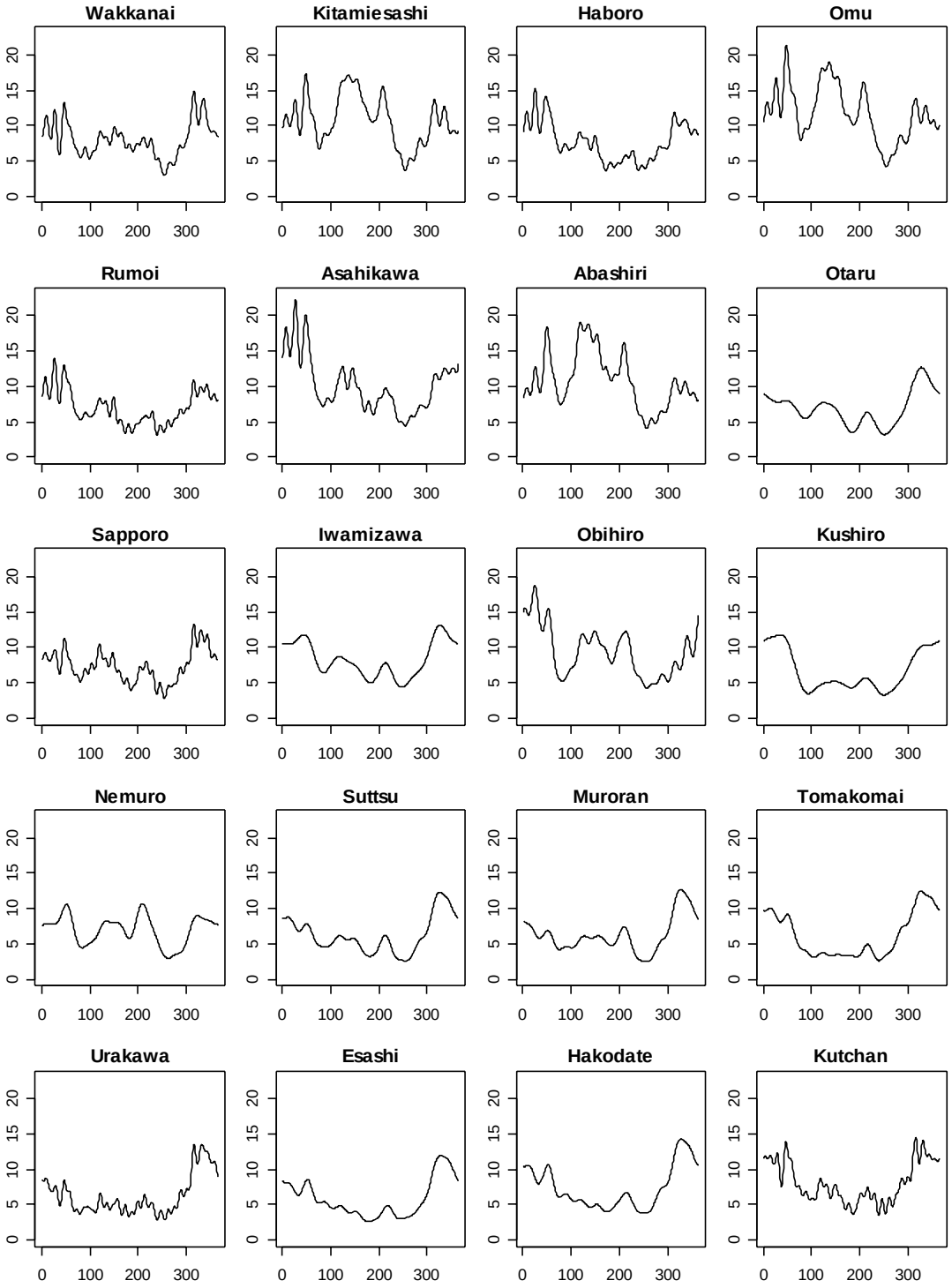

Figure 3.4-1. The estimated seasonal periodicity of the variance υ_n^2 in each station.

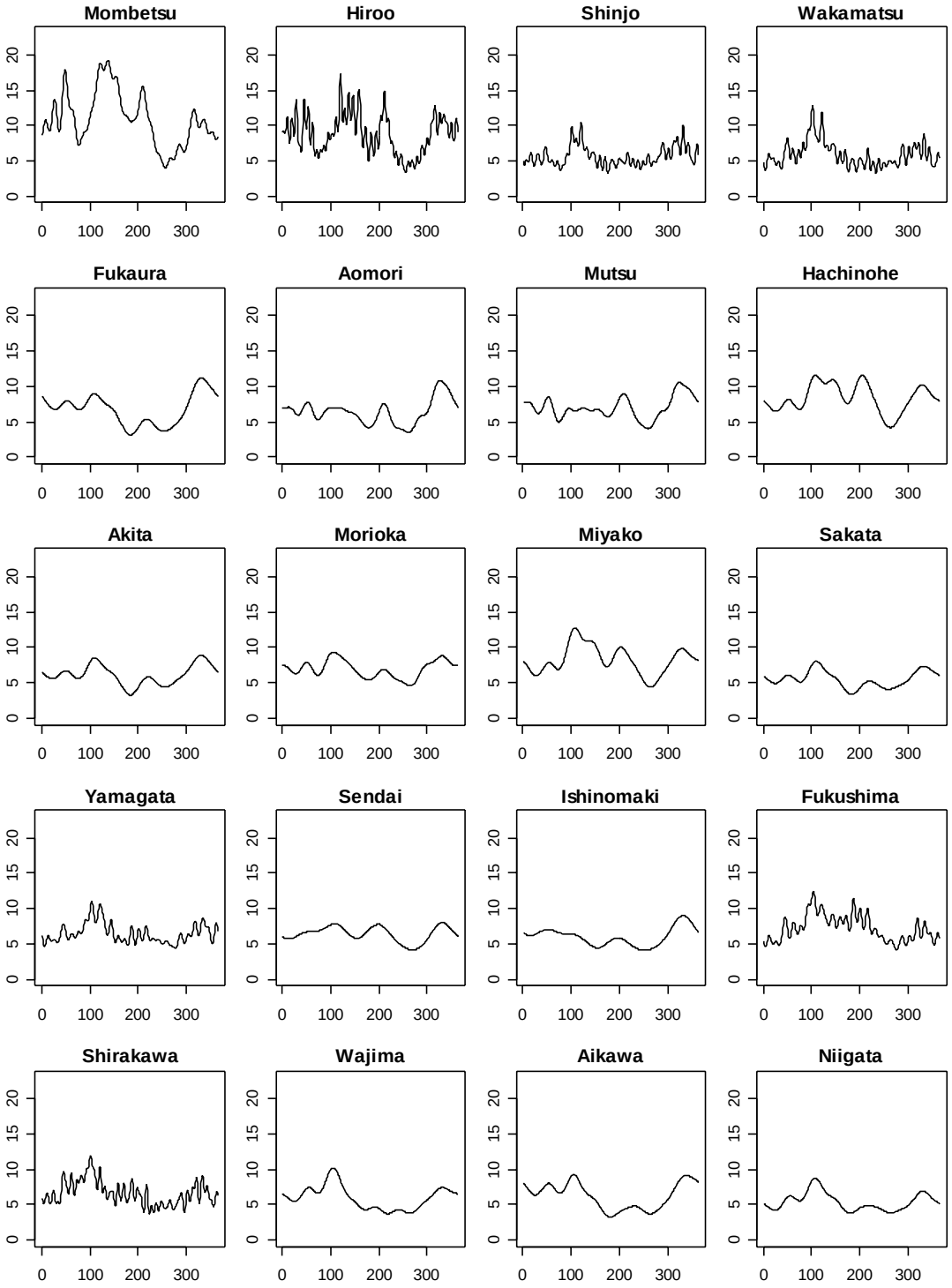

Figure 3.4-2. The estimated seasonal periodicity of the variance υ_n^2 in each station.

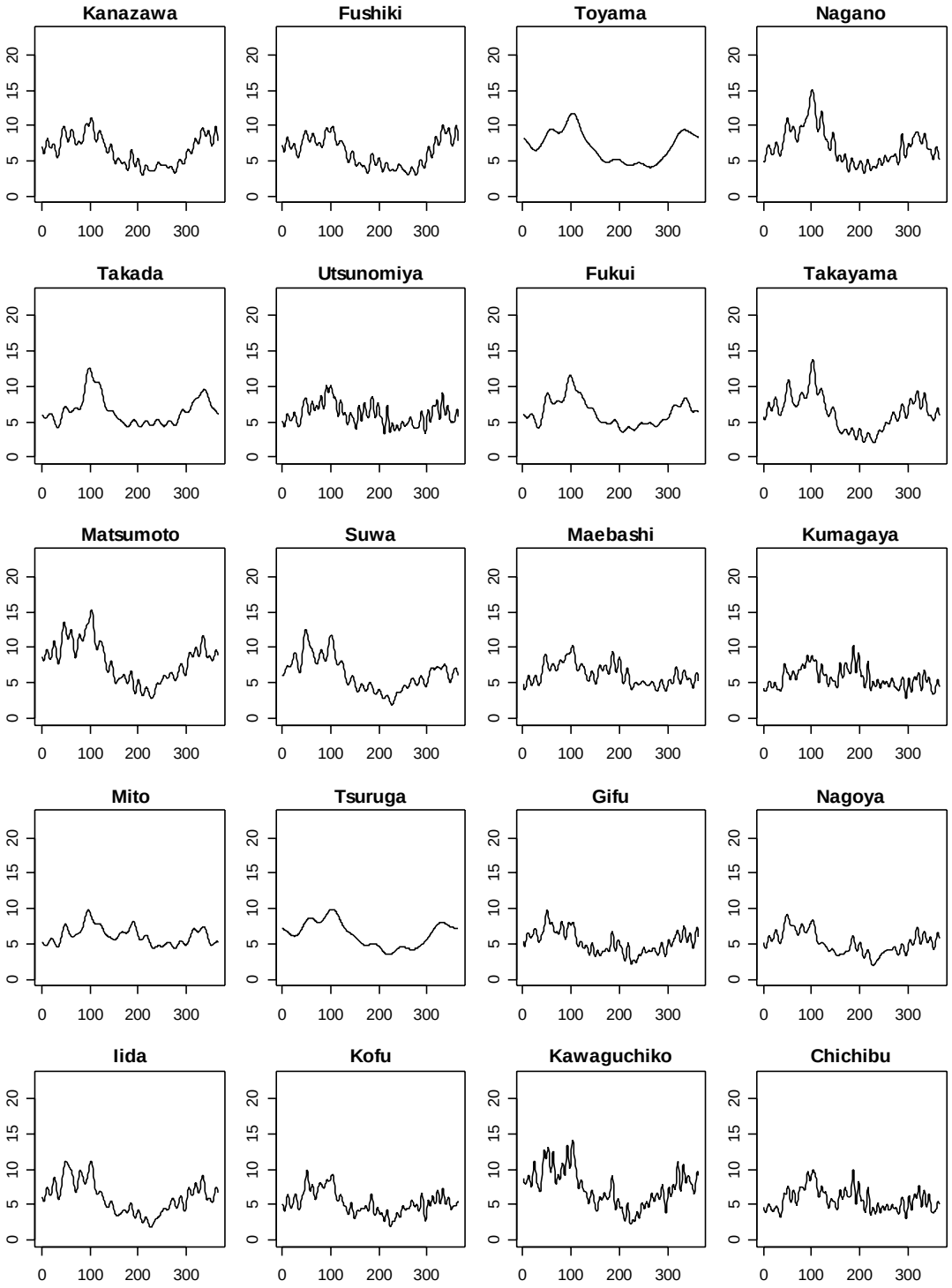

Figure 3.4-3. The estimated seasonal periodicity of the variance υ_n^2 in each station.

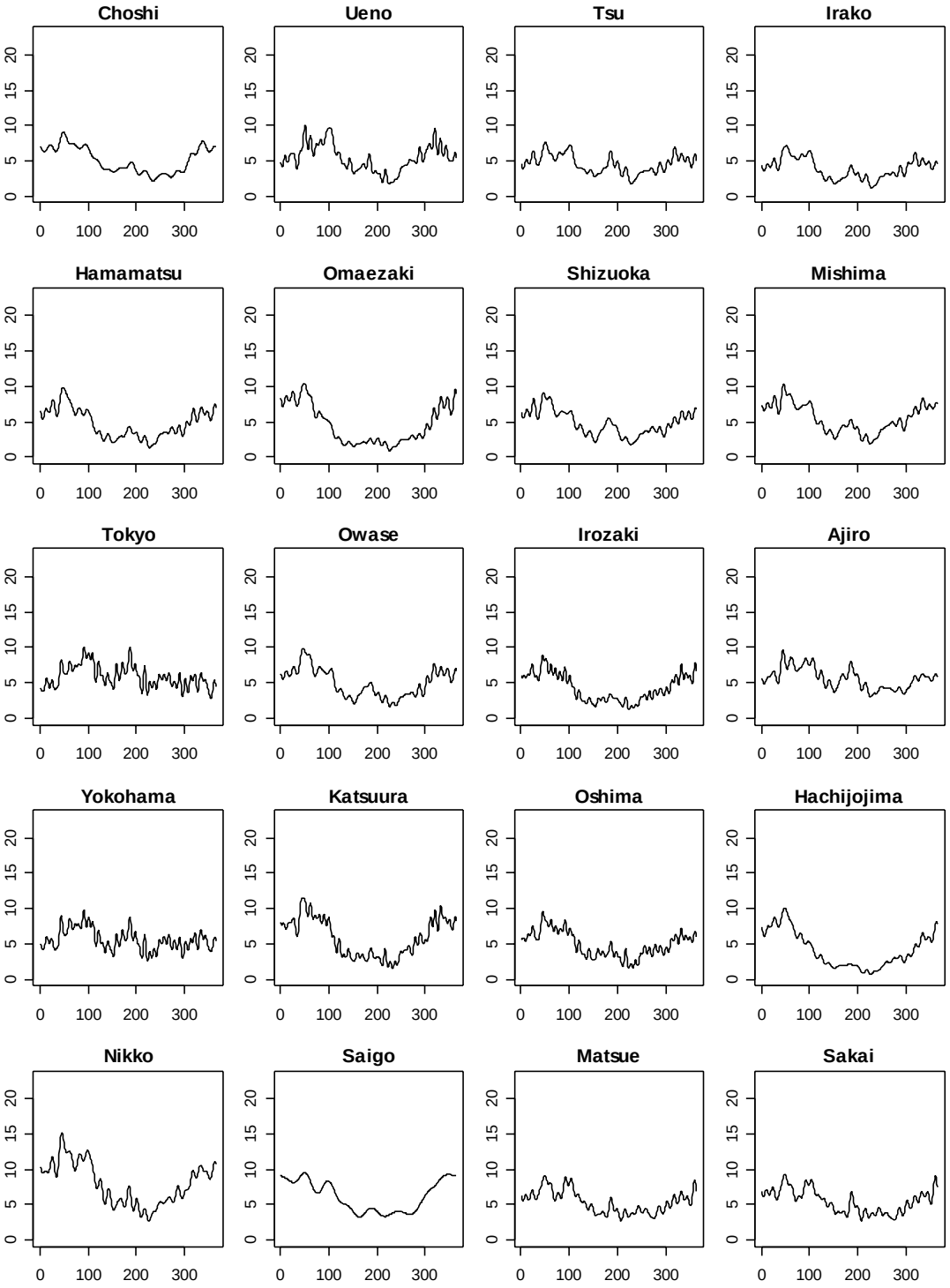

Figure 3.4-4. The estimated seasonal periodicity of the variance υ_n^2 in each station.

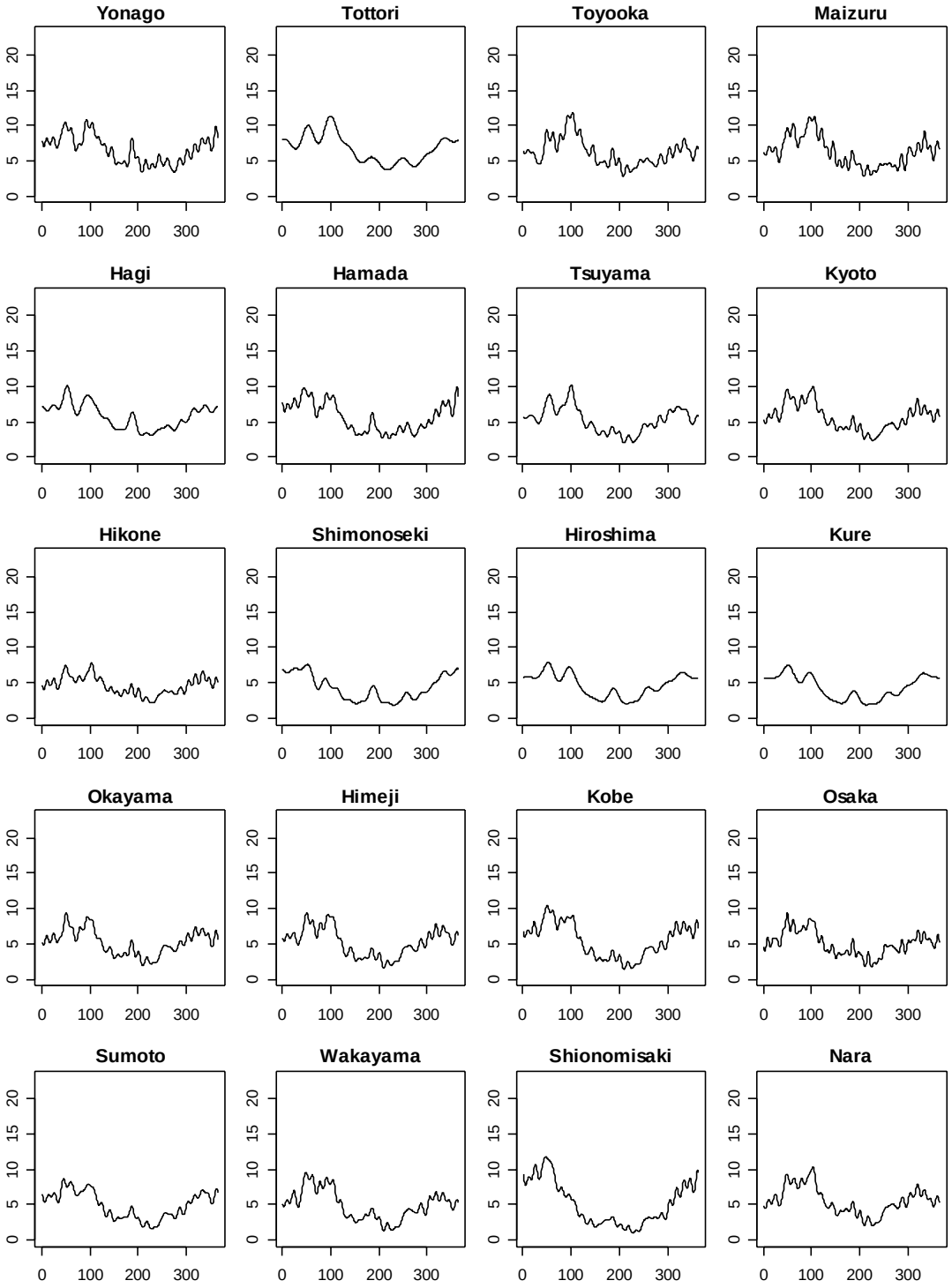

Figure 3.4-5. The estimated seasonal periodicity of the variance υ_n^2 in each station.

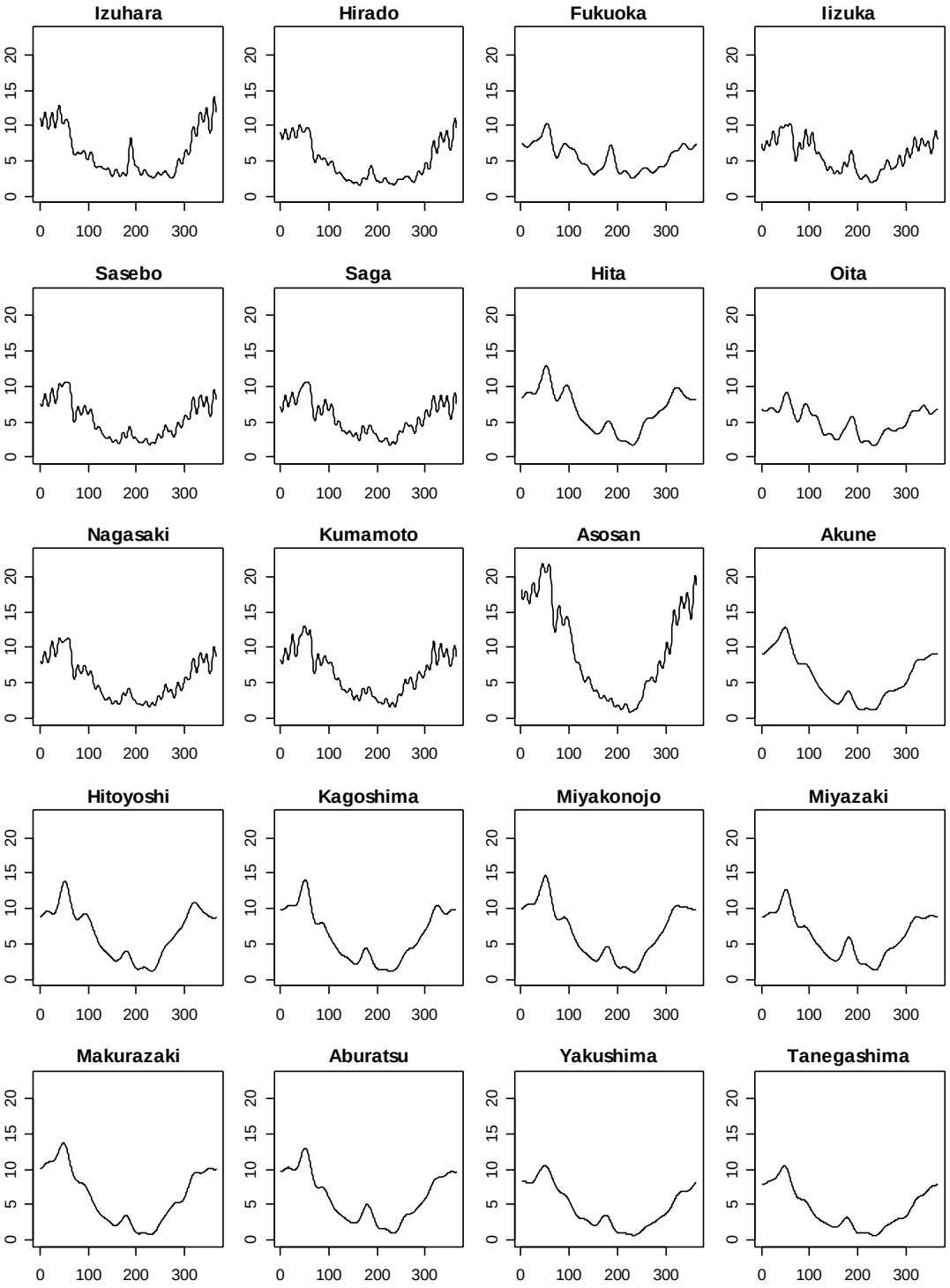

Figure 3.4-6. The estimated seasonal periodicity of the variance υ_n^2 in each station.

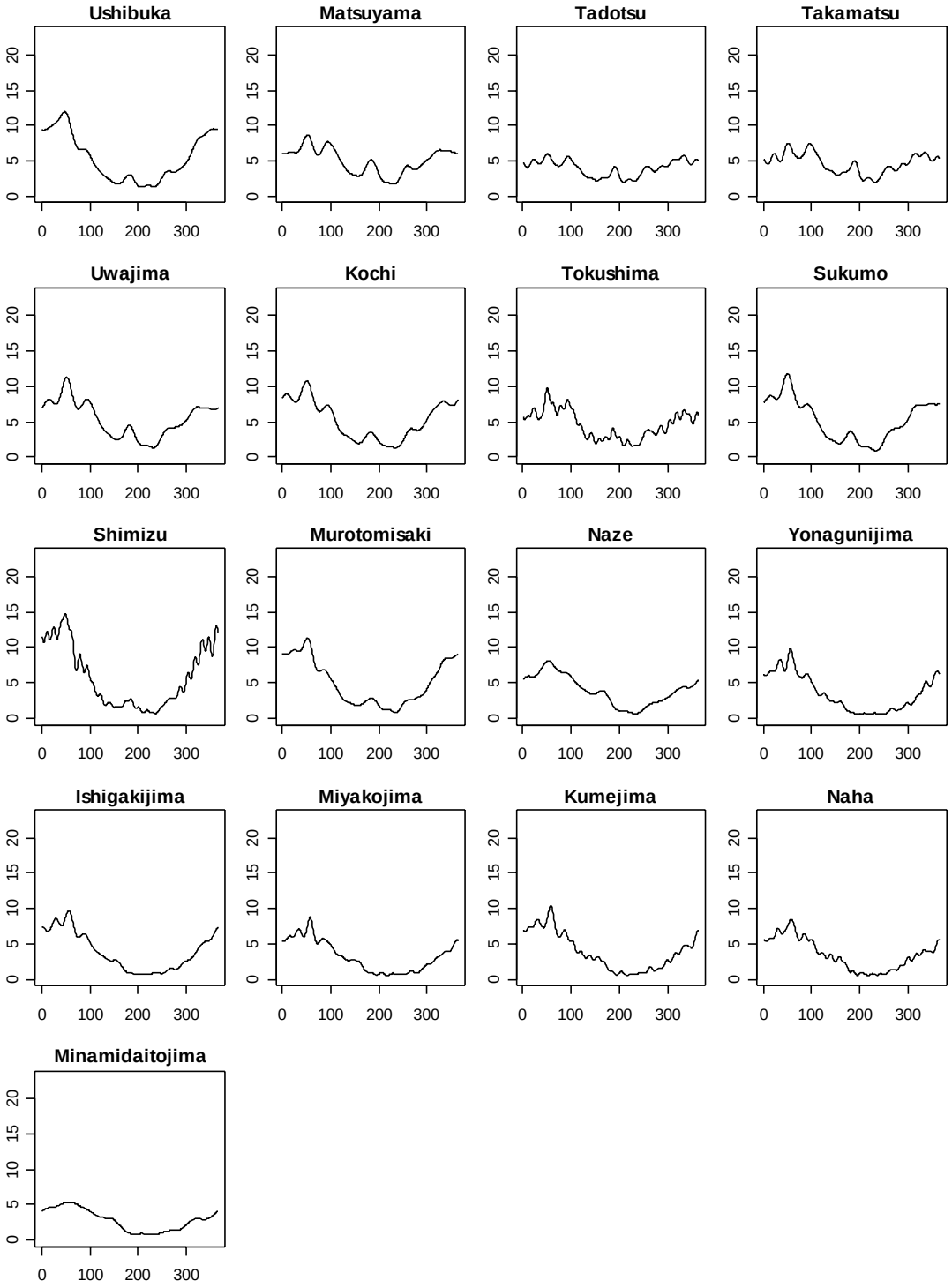

Figure 3.4-7. The estimated seasonal periodicity of the variance υ_n^2 in each station.

Chapter 4

The property of the anomaly

4.1 Low-pass filtered data

To confirm the yearly distinctive variablities, we can get a low frequency anomaly factor using a low-pass filtered data obtained by a running mean with time span covering a period, such as the running mean weighted by the binomial filter,

$$L_n(t) = \sum_{j=1-0.5(t-1)}^{N+0.5(t-1)} w_{n,j} y_j \quad ,$$

$$w_{n,j} = \begin{cases} \dfrac{{}_{t-1}C_{0.5(t-1)+n-j}}{2^{t-1}} & if \quad 0 \le \{0.5(t-1)+n-j\} \le (t-1) \\ 0 & otherwise. \end{cases} . \tag{4.1}$$

We take the span $t = 365$, this is, one year here. Figure 4.1 gives an example of such a low-pass filtered dataset from 1961 through 2000 for the Tokyo station. The horizontal axis represents the date for 10 years; the top panel is from 1961 until 1970,the second panel is from 1971 until 1980, the third panel is from 1981 until 1990, the bottom panel is from 1991 until 2000, and the vertical axis represents the values of the low-pass filtered dataset. The plot shows the feature of the yearly distinctive variablities such as the cool summer and the warm winter; for example, generally it is said that 1980's and 1993's summer are the cool summer, and 1989's and 1990's winter are the warm winter. From this we can recognize that the low-pass filter by weighted running mean extracts the feature of the yearly distinctive variablities clearly and the defined anomaly in the previous chapter holds the information that is the subject of our research.

In from Figure 4.2.1 to Figure 4.2.9, the low-pass filtered datasets with the span *t* = 365 from 1961 through 2000 for all stations are shown according to their regions,

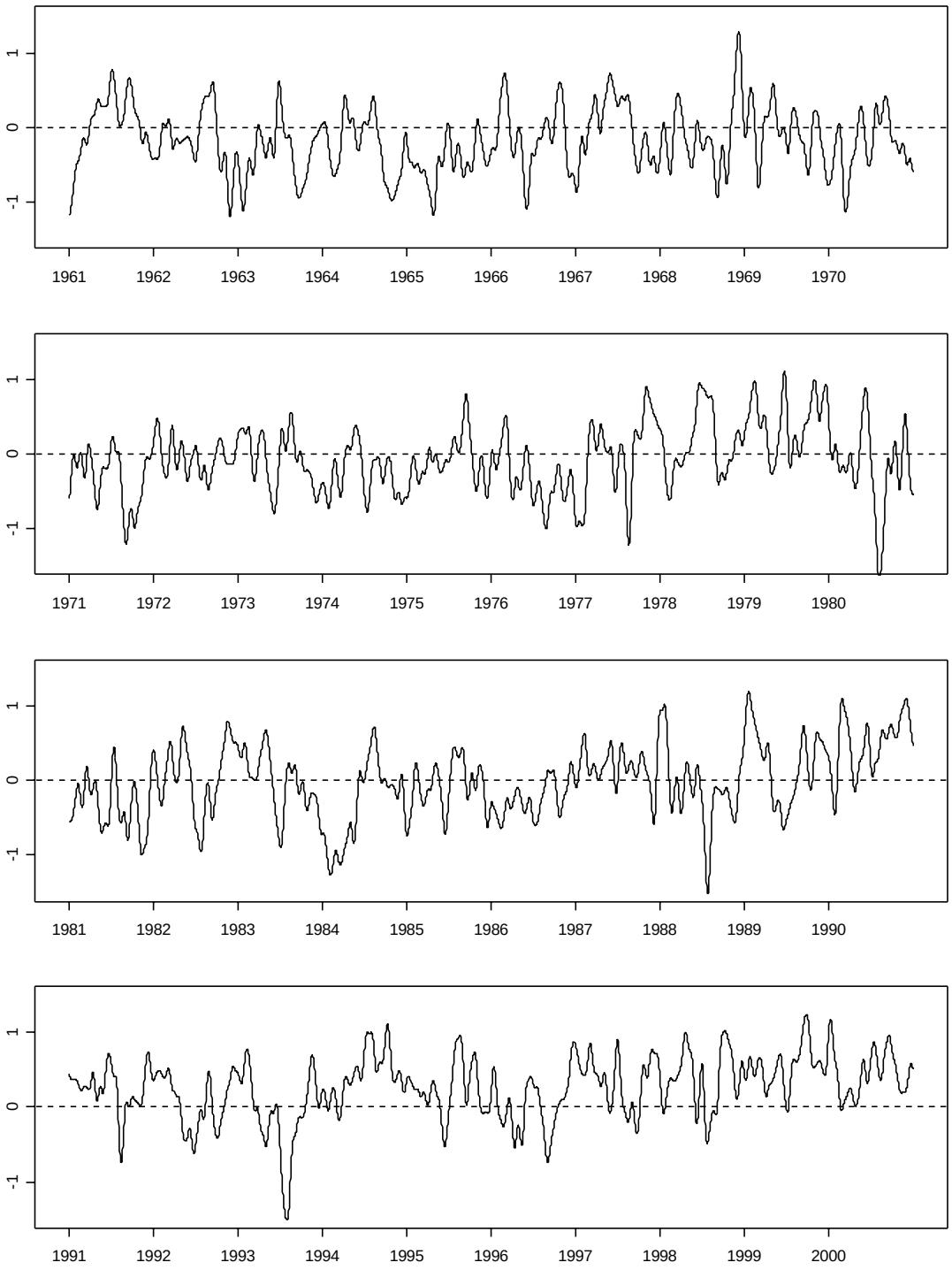

Figure 4.1. The low-pass filtered data from 1961 through 2000 for the Tokyo station. The horizontal axis represents the date for 10 years; the top panel is from 1961 until 1970,the second panel is from 1971 until 1980, the third panel is from 1981 until 1990, the bottom panel is from 1991 until 2000, and the vertical axis represents the values of the low-pass filtered dataset.

Hokkaido, Tohoku region, Kanto region, Chubu region, Kinki region, Chugoku region, Shikoku region, Kyushu region and Nansei Islands. The WMO codes of stations according to each region are as follows: 47401, 47402, 47404, 47405, 47406, 47407, 47409, 47411, 47412, 47413, 47417, 47418, 47420, 47421, 47423, 47424, 47426, 47428, 47430, 47433, 47435 and 47440 belong to Hokkaido; 47520, 47570, 47574, 47575, 47576, 47581, 47582, 47584, 47585, 47587, 47588, 47590, 47592, 47595 and 47597 belong to Tohoku region; 47615, 47624, 47626, 47629, 47638, 47640, 47641, 47648, 47662, 47670, 47674, 47675, 47678 and 47690 belong to Kanto region; 47600, 47602, 47604, 47605, 47606, 47607, 47610, 47612, 47616, 47617, 47618, 47620, 47631, 47632, 47636, 47637, 47653, 47654, 47655, 47656, 47657, 47666 and 47668 belong to Chubu region; 47649, 47651, 47663, 47747, 47750, 47759, 47761, 47769, 47770, 47772, 47776, 47777, 47778 and 47780 belong to Kinki region; 47740, 47741, 47742, 47744, 47746, 47754, 47755, 47756, 47762, 47765, 47766 and 47768 belong to Chugoku region; 47887, 47890, 47891, 47892, 47893, 47895, 47897, 47898 and 47899 belong to Shikoku region; 47800, 47805, 47807, 47809, 47812, 47813, 47814, 47815, 47817, 47819, 47821, 47823, 47824, 47827, 47829, 47830, 47831, 47835, 47836, 47837 and 47838 belong to Kyushu region; 47909, 47912, 47918, 47927, 47929, 47936 and 47945 belong to Nansei Islands. In from Figure 4.2.1 to Figure 4.2.9, the horizontal axis represents the date for 10 years; the top panel is from 1961 until 1970,the second panel is from 1971 until 1980, the third panel is from 1981 until 1990, the bottom panel is from 1991 until 2000, and the vertical axis represents the values of the low-pass filtered dataset. Note that the behavior of each station in the same area is similar. This shows the correlation between stations, and above all, proves to be useful for long-term forecasting. Nevertheless, we are aware that this important factor cannot be predicted solely on the basis of the past time series of temperature records, and that some other geophysical variables and other useful exogenous factors should be investigated in order to predict such anomalies effectively. This is one of the most difficult tasks among the current meteorological research subjects.

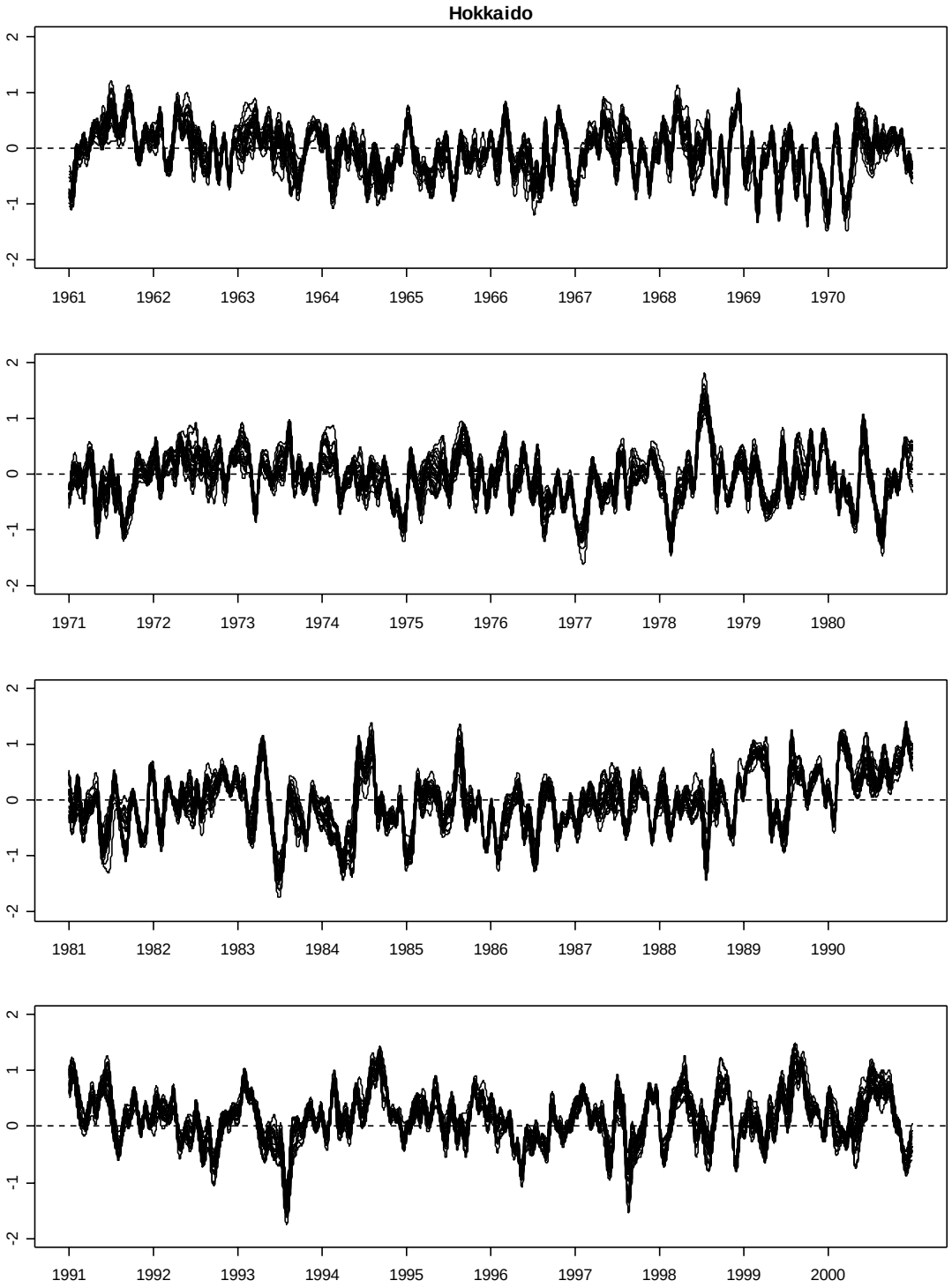

Figure 4.2.1. The low-pass filtered datasets with the span $t = 365$ from 1961 through 2000 for stations in Hokkaido.

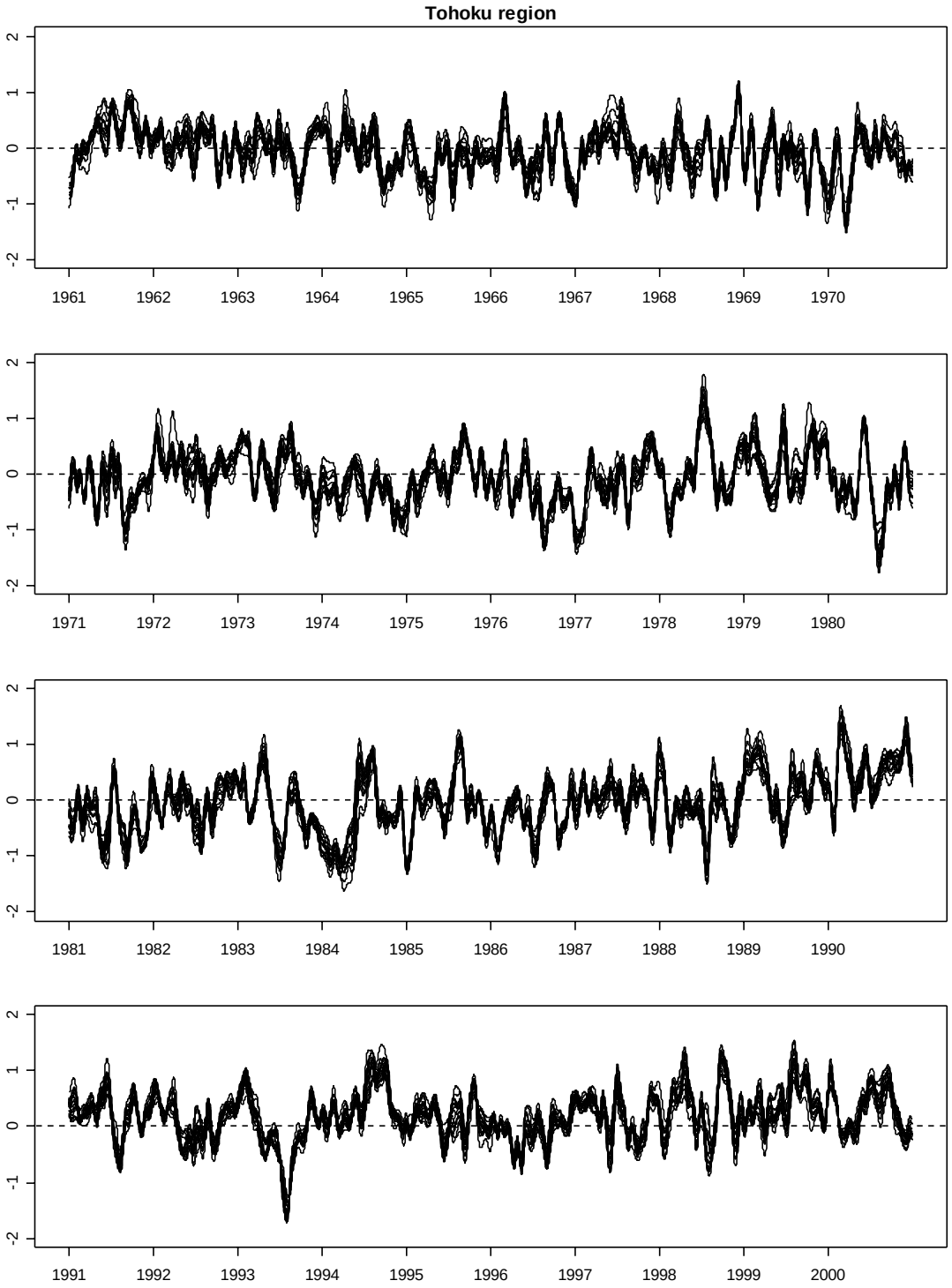

Figure 4.2.2. The low-pass filtered datasets with the span $t = 365$ from 1961 through 2000 for stations in Tohoku region.

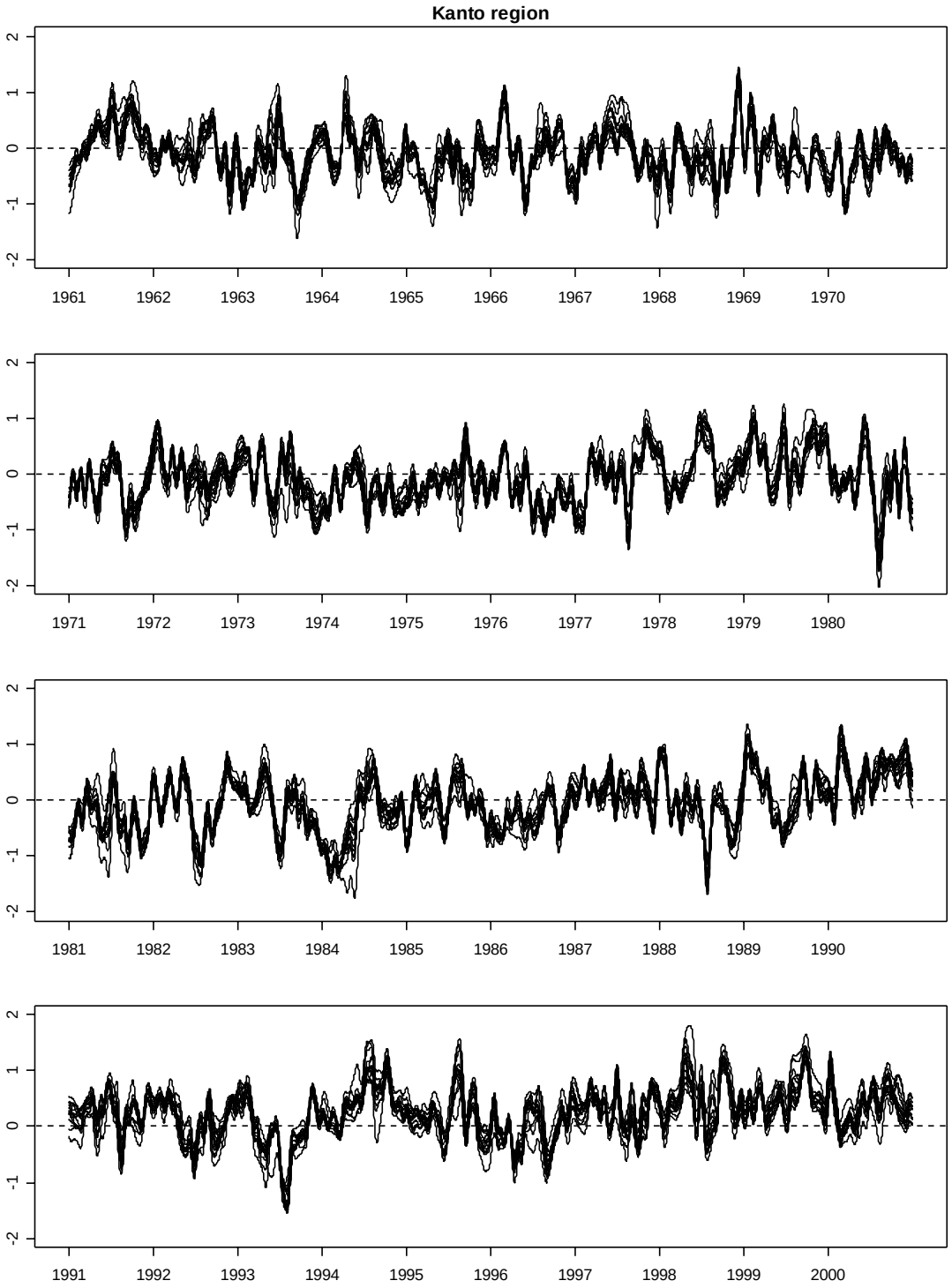

Figure 4.2.3. The low-pass filtered datasets with the span $t = 365$ from 1961 through 2000 for stations in Kanto region.

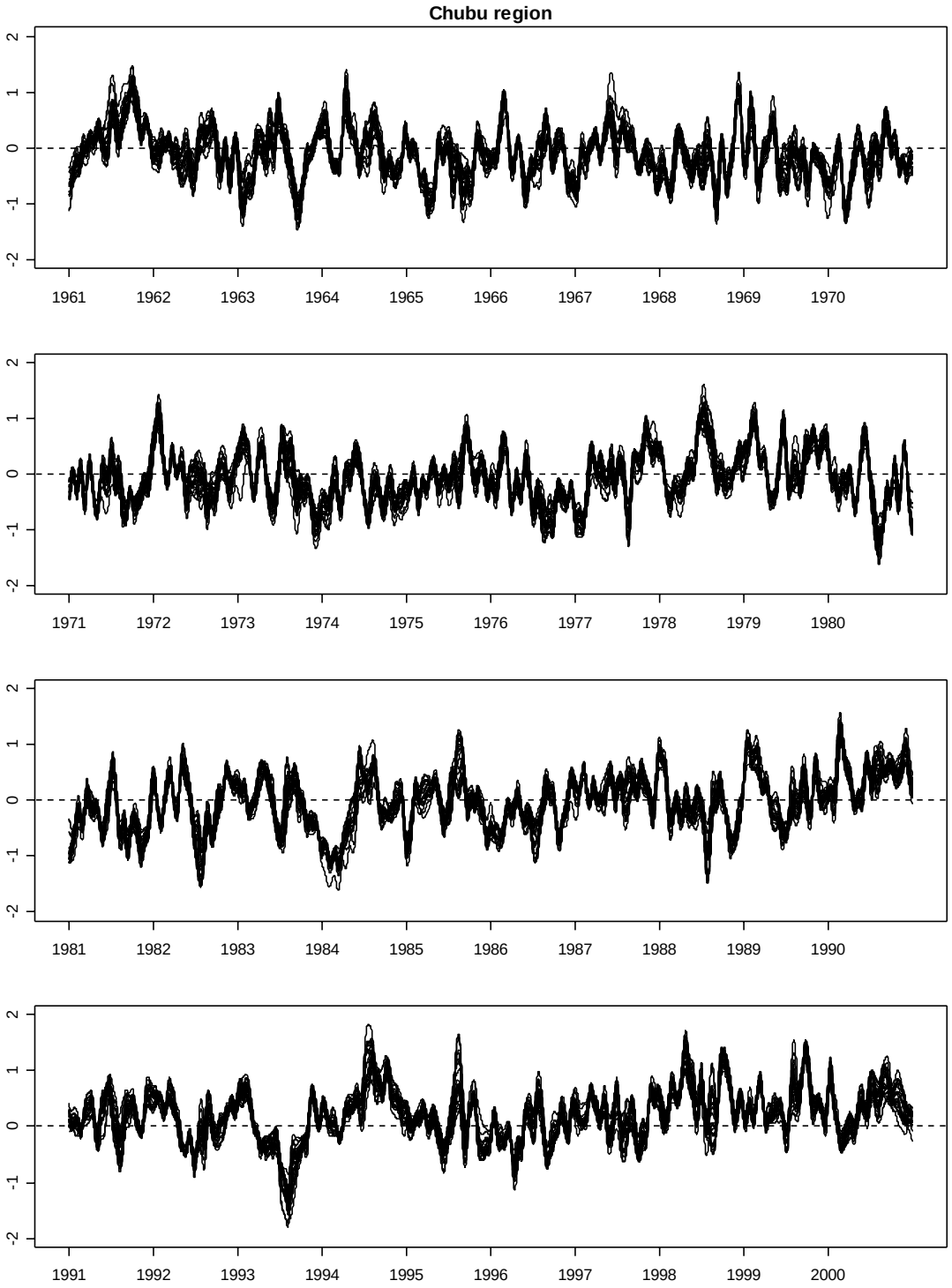

Figure 4.2.4. The low-pass filtered datasets with the span $t = 365$ from 1961 through 2000 for stations in Chubu region.

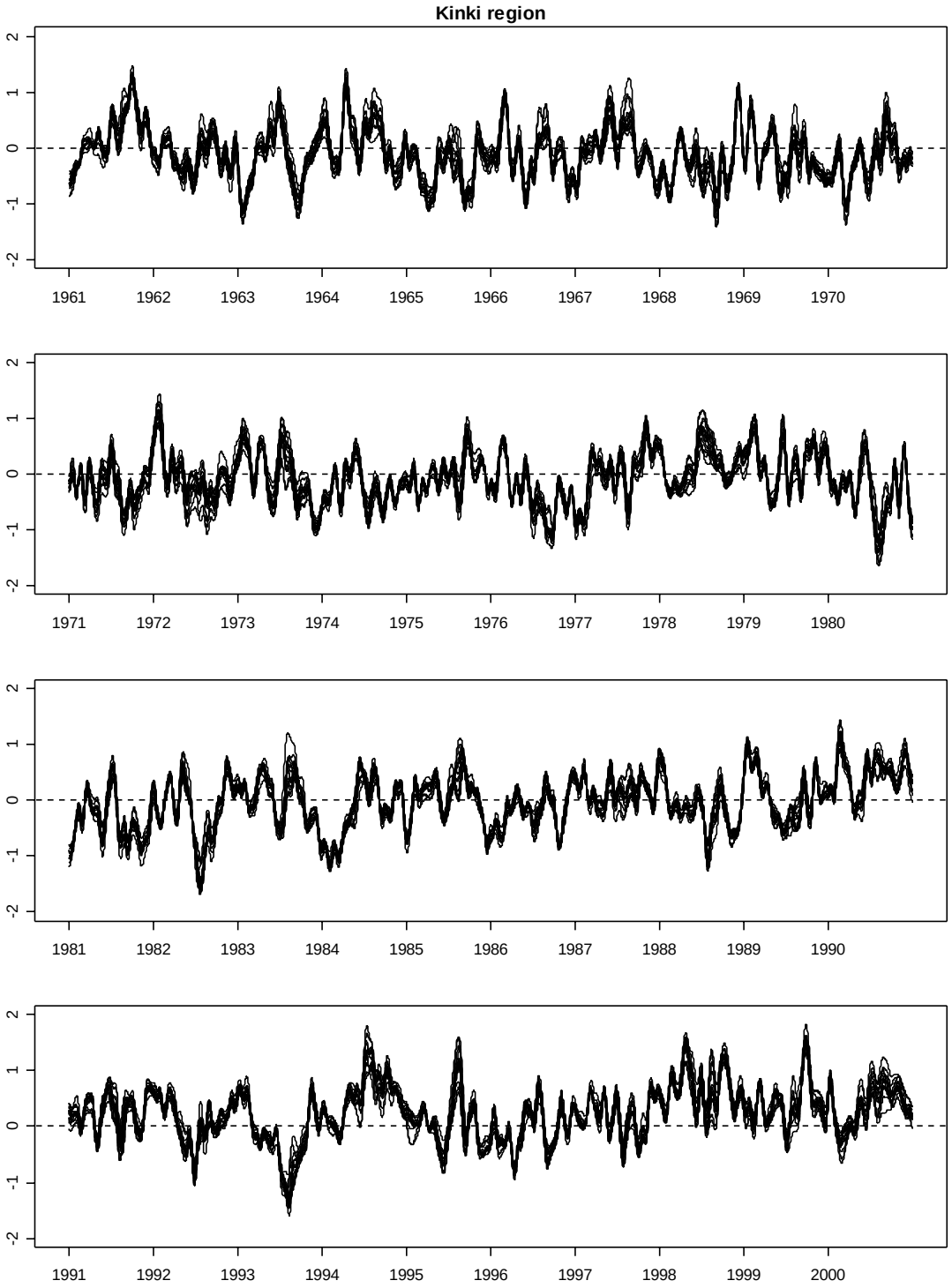

Figure 4.2.5. The low-pass filtered datasets with the span $t = 365$ from 1961 through 2000 for stations in Kinki region.

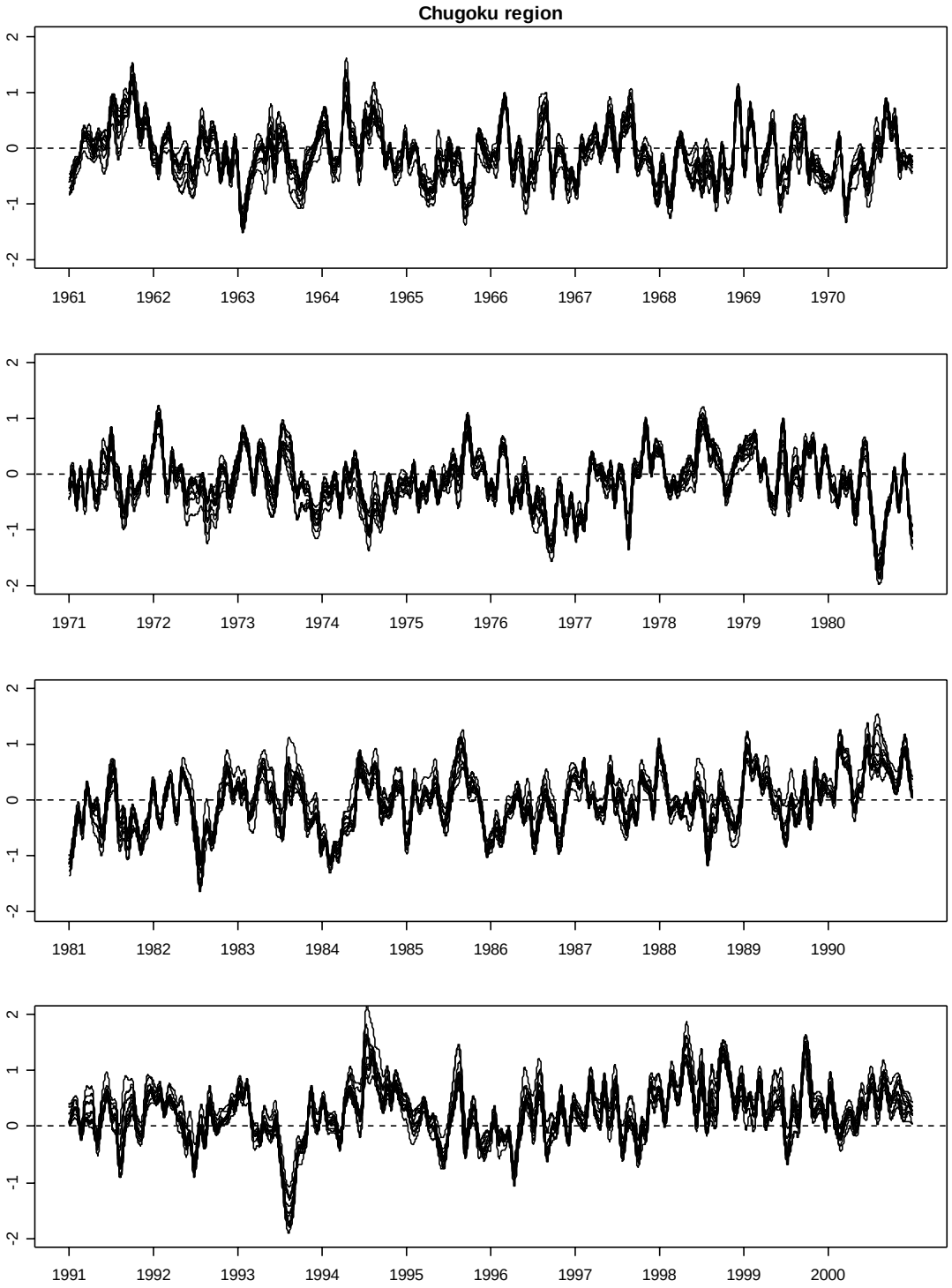

Figure 4.2.6. The low-pass filtered datasets with the span $t = 365$ from 1961 through 2000 for stations in Chugoku region.

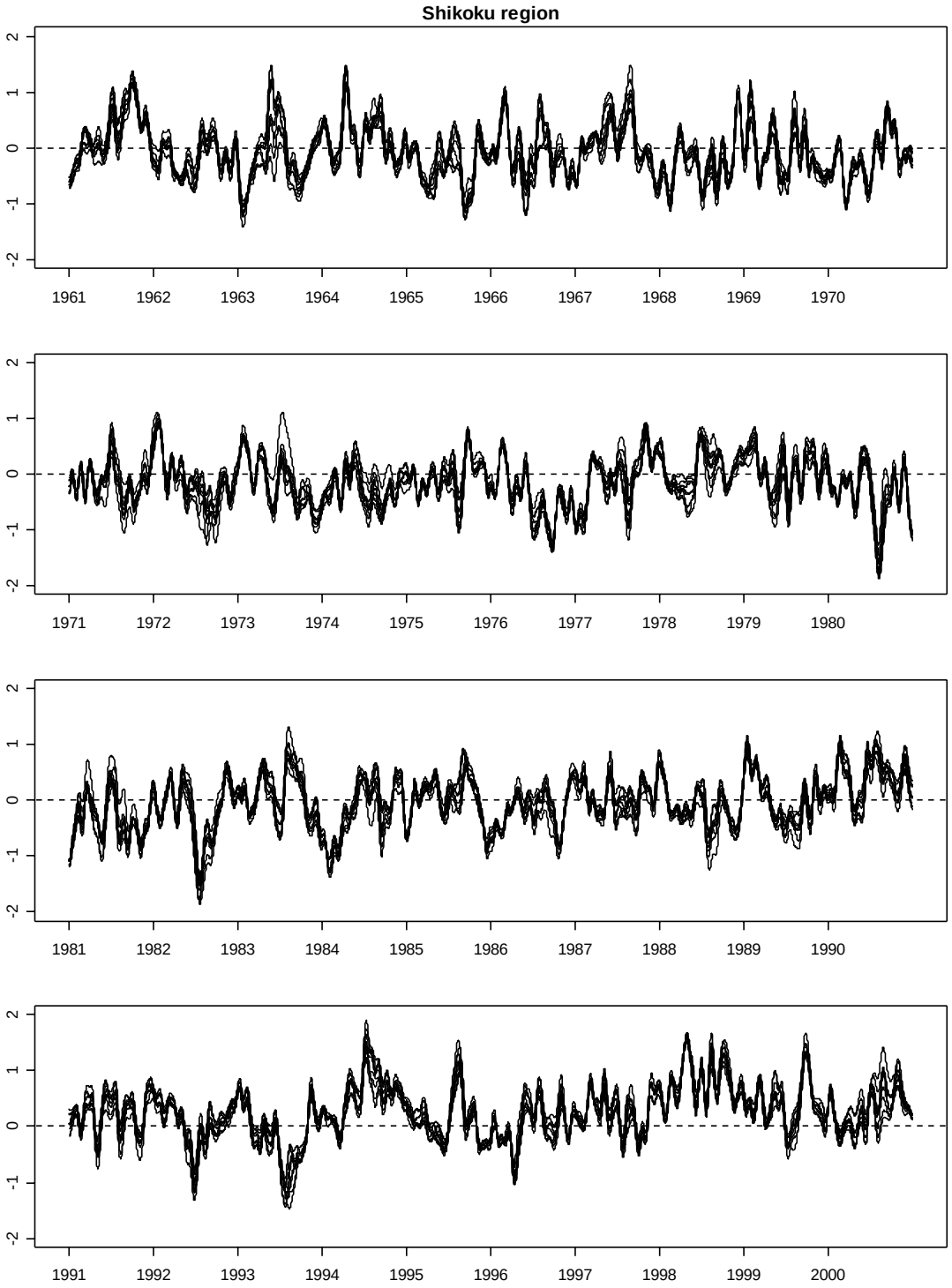

Figure 4.2.7. The low-pass filtered datasets with the span $t = 365$ from 1961 through 2000 for stations in Shikoku region.

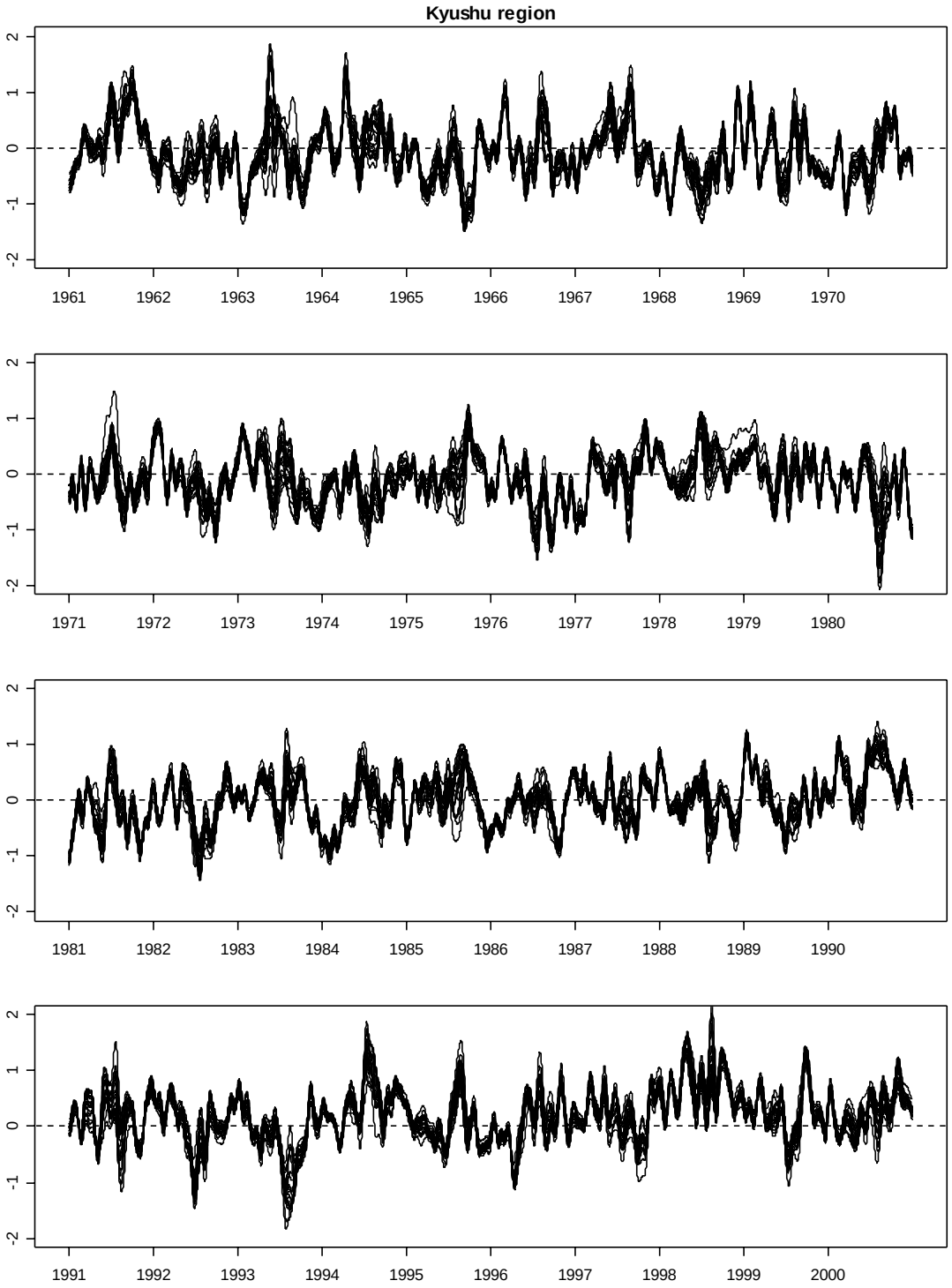

Figure 4.2.8. The low-pass filtered datasets with the span $t = 365$ from 1961 through 2000 for stations in Kyushu region.

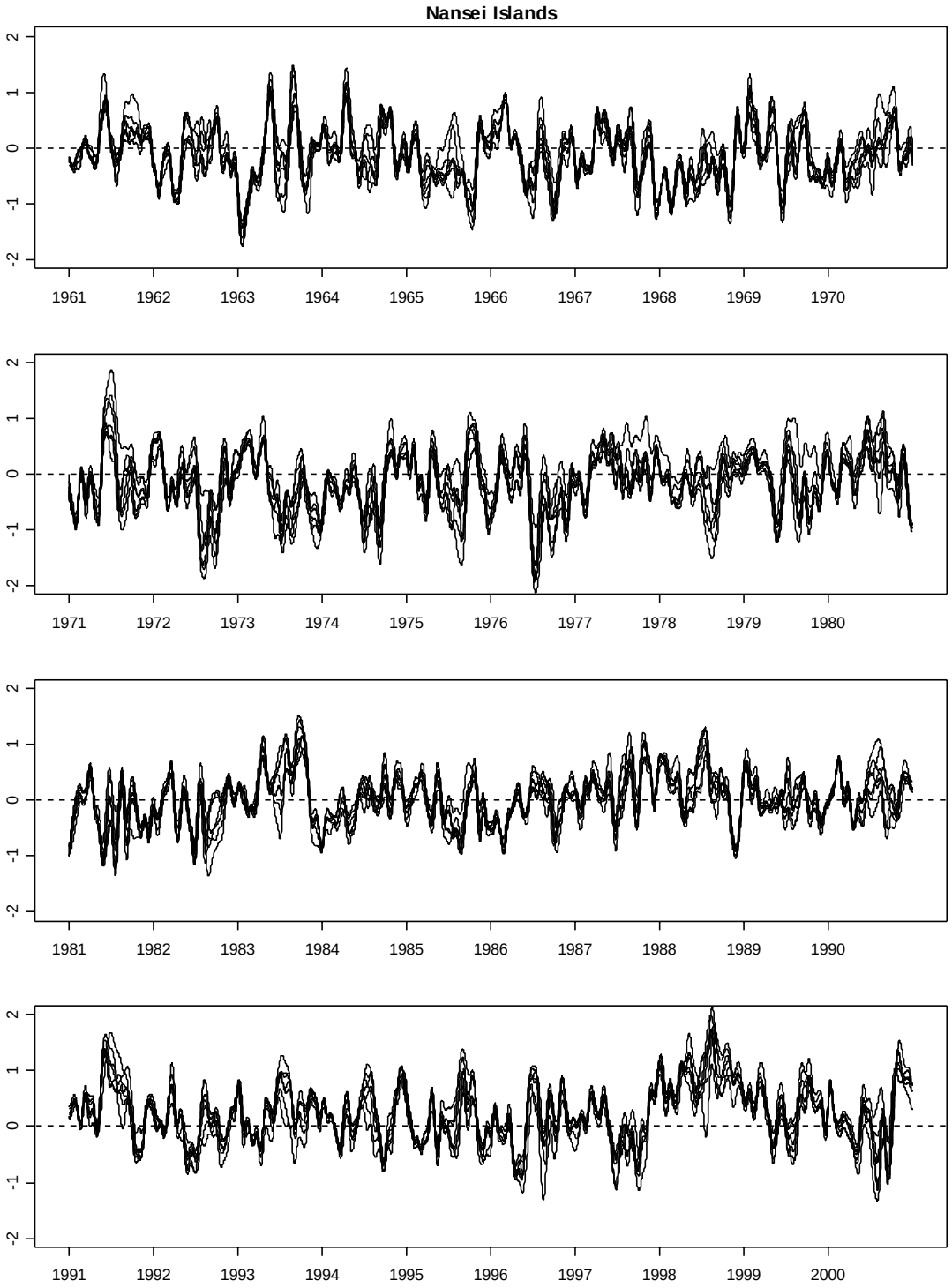

Figure 4.2.9. The low-pass filtered datasets with the span $t = 365$ from 1961 through 2000 for stations in Nansei Islands.

4.2 The autocorrelation and the analysis of AR model

Now, we will turn to the autocorrelation of the surface air temperature anomaly. Each panel in Figure 4.3 shows the sample autocorrelation function of the Sapporo, Sendai, Wajima, Tokyo, Osaka, Fukuoka, Kochi and Naha stations. The horizontal axis represents the lag, the vertical axis represents values of the autocorrelation function and the dashed line represents the 95% confidence interval. We can confirm long autocorrelations in their stations, and the same feature has been shown in other stations as well, though we do not show the plot here.

In order to examine the autocorrelation structure we apply the AR model

$$y_n = \sum_{j=1}^{m} a_j y_{n-j} + v_n, \quad v_n \sim N(0, \sigma^2), \tag{4.2}$$

to the surface air temperature anomaly. The optimal order m are determined by making use of the AIC. For the m-th order AR model, the autocovariance function with lag k ($k \geq 0$) is given as

$$C(0) = \sum_{j=1}^{m} a_j C(j) + \sigma^2 \quad \text{, for } k = 0, \tag{4.3}$$

$$C(k) = \sum_{j=1}^{m} a_j C(|k-j|) \quad \text{, for } k \geq 1. \tag{4.4}$$

Since a normal distribution is assumed for the residuals of the data $\{y_n\,;\ n = 1, 2, \cdots, N\}$, including m adjusting parameters, for the stationary time series $\mathbf{y} = (y_1, \cdots, y_N)^{\mathrm{T}}$, the likelihood $\mathcal{L}(\theta_A)$ with the parameter vector θ_A of the AR model (4.2) is

$$\mathcal{L}(\theta_A) = (2\pi)^{-\frac{N}{2}} \{\det \mathbf{\Sigma}(N)\}^{-\frac{1}{2}} \exp\{-\frac{1}{2}\mathbf{y}^{\mathrm{T}} \mathbf{\Sigma}(N)^{-1} \mathbf{y}\}, \tag{4.5}$$

where the superscript T represents transpose and $\mathbf{\Sigma}(x)$ is a variance-covariance matrix represented by the autocovariance function as follows

$$\mathbf{\Sigma}(x) = \begin{bmatrix} C(0) & C(1) & \cdots & C(x-1) \\ C(1) & C(0) & \cdots & C(x-2) \\ \vdots & \vdots & \ddots & \vdots \\ C(x-1) & C(x-2) & \cdots & C(0) \end{bmatrix}. \tag{4.6}$$

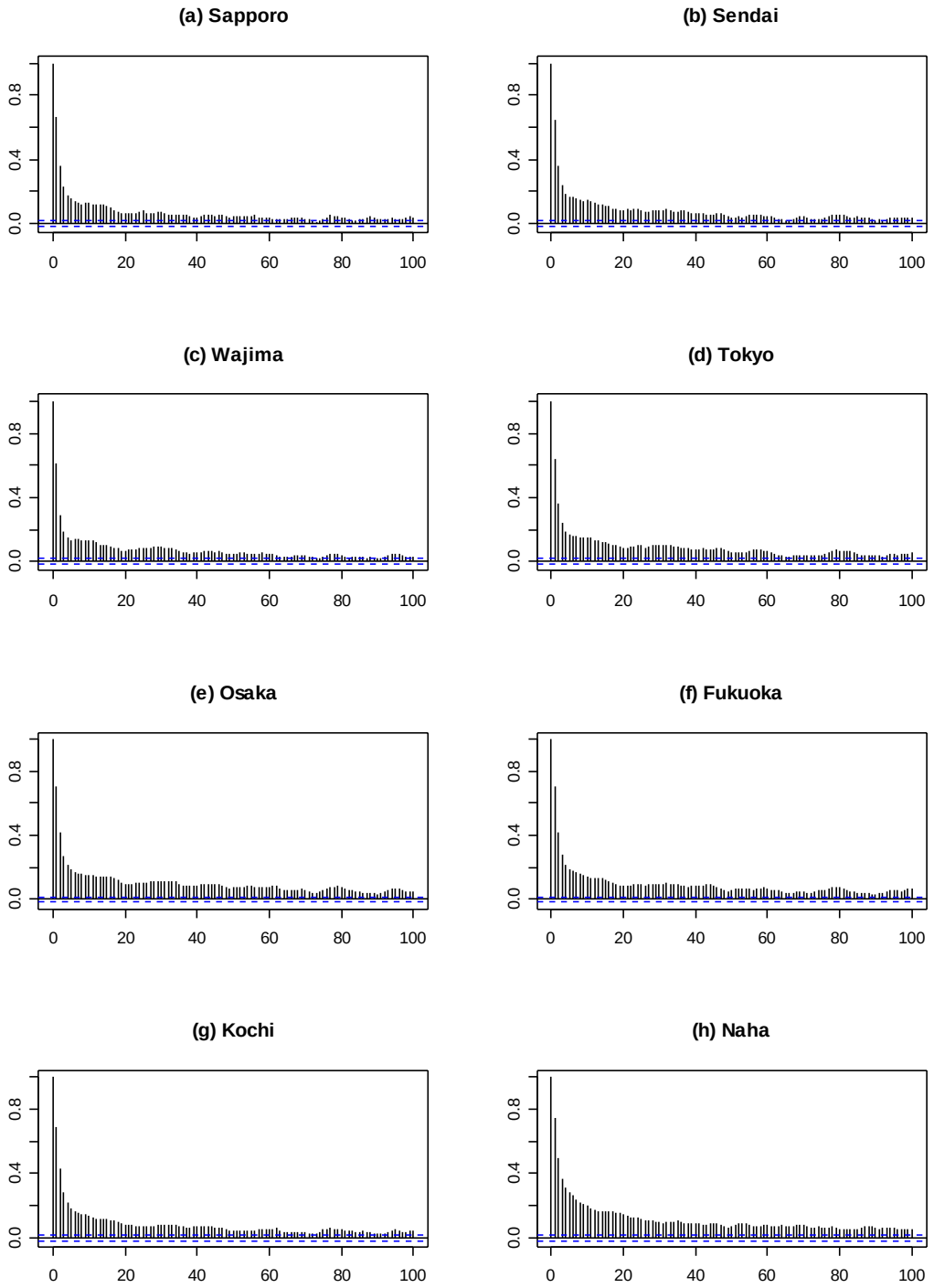

Figure 4.3. The autocorrelation function of the surface air temperature anomalies in the Sapporo, Sendai, Wajima, Tokyo, Osaka, Fukuoka, Kochi and Naha stations. The horizontal axis represents the lag, the vertical axis represents values of the autocorrelation function and the dashed line represents the 95% confidence interval.

Since the distribution of y_n is determined by the values of $y_{n-1}, \cdots, y_{n-m}$ in the m-th order AR model, for the maximum order M ($M \geq m$), the likelihood $\mathcal{L}(\theta_A)$ is represented as follows

$$\mathcal{L}(\theta_A) =$$

$$(2\pi)^{-\frac{M}{2}} \{\det \mathbf{\Sigma}(M)\}^{-\frac{1}{2}} \exp\{-\frac{1}{2}\mathbf{y}^{\mathrm{T}}\mathbf{\Sigma}(M)^{-1}\mathbf{y}\} \prod_{n=M+1}^{N} (2\pi)^{-\frac{1}{2}} (\sigma^2)^{-\frac{1}{2}} \exp\{-\frac{1}{2\sigma^2}(y_n - \sum_{j=1}^{m} a_j y_{n-j})^2\} \tag{4.7}$$

and the log likelihood $\ell(\theta_A)$ is

$$\ell(\theta_A) = \log\left[(2\pi)^{-\frac{M}{2}} \{\det \mathbf{\Sigma}(M)\}^{-\frac{1}{2}} \exp\{-\frac{1}{2}\mathbf{y}^{\mathrm{T}}\mathbf{\Sigma}(M)^{-1}\mathbf{y}\} \right] +$$

$$\sum_{n=M+1}^{N} \log\left[(2\pi)^{-\frac{1}{2}} (\sigma^2)^{-\frac{1}{2}} \exp\{-\frac{1}{2\sigma^2}(y_n - \sum_{j=1}^{m} a_j y_{n-j})^2\} \right]. \tag{4.8}$$

When N is sufficiently large for M, using only the second term of Equation (4.8), the log likelihood is approximately represented as

$$\ell(\theta_A) = -\frac{N-M}{2}\log 2\pi\sigma^2 - \frac{1}{2\sigma^2}\sum_{n=M+1}^{N}(y_n - \sum_{j=1}^{m} a_j y_{n-j})^2 . \tag{4.9}$$

From

$$\frac{\partial \ell(\theta_A)}{\partial \sigma^2} = -\frac{N-M}{2\sigma^2} + \frac{1}{2(\sigma^2)^2}\sum_{n=M+1}^{N}(y_n - \sum_{j=1}^{m} a_j y_{n-j})^2 ,$$

we get

$$\hat{\sigma}_m^2 = \frac{1}{N-M}\sum_{n=M+1}^{N}(y_n - \sum_{j=1}^{m} a_j y_{n-j})^2 , \tag{4.10}$$

then, the maximum log likelihood is represented as

$$\ell(\hat{\theta}_A) = -\frac{N-M}{2}\log 2\pi\hat{\sigma}_m^2 - \frac{N-M}{2}, \tag{4.11}$$

the AIC of the m-th order AR model is given by

$$AIC_m \;=\; (N-M)\,(\log 2\pi\hat{\sigma}_m^2 + 1) + 2(m+1) . \tag{4.12}$$

Here we have set m to get the set of the orders that minimize the AIC. We have used

the least squares algorithm using the standard Householder transformation which is efficient in computing the AIC sequentially to select the best fitted order (Kitagawa and Akaike, (1978)). The optimal order of the AR model in each station are listed in Table 4.1. We can confirm long orders corresponding to days from two weeks to a month.

Once the optimal order of the AR and the coefficients are estimated, the power spectrum density $P(f)$ of the frequency f is given in terms of the transfer function (Akaike(1968)) such that

$$P(f) = \frac{\hat{\sigma}^2}{\left|1 - \sum_{j=1}^{m} \hat{a}_j e^{-i2\pi fj}\right|^2}, \tag{4.13}$$

where $\hat{a}_j$ is the estimated coefficients of the AR model, and the symbol i here represents the imaginary unit of complex number. Each panel in Figure 4.4 shows the periodogram and estimated power spectrum of the Sapporo, Sendai, Wajima, Tokyo, Osaka, Fukuoka, Kochi and Naha stations. The horizontal axis represents the frequency in logarithmic scale indicated in unit of 1/day, where “y” represents the frequency corresponding a year, and the vertical axis represents values of the periodogram and power spectrum density in logarithmic scale. In each panel, the black points and lines represent periodogram, and the red solid line represents the estimated power spectrum. Note that the exceptional peak of a year that has been recognized in Figure 2.3 is removed by seasonal adjustment. We can confirm the feature with the peak in the low frequency, and the same feature has been shown in other stations as well, though we do not show their plot here. From the analysis mentioned above, it is suggested that the surface air temperature anomalies have long memory.

Table 4.1. The optimal order of the AR model applied to the anomaly data of each station.

WMO code	stations	orders	AIC values	WMO code	stations	orders	AIC values
47401	Wakkanai	15	31451.8	47402	Kitamiesashi	15	32334.1
47404	Haboro	15	33497.3	47405	Omu	15	33553.1
47406	Rumoi	28	33281.1	47407	Asahikawa	16	32799.8
47409	Abashiri	15	33277.8	47411	Otaru	15	33331.6
47412	Sapporo	28	32743.8	47413	Iwamizawa	16	32649.2
47417	Obihiro	16	33879.0	47418	Kushiro	37	33596.0
47420	Nemuro	37	33739.1	47421	Suttsu	24	32724.4
47423	Muroran	29	32980.0	47424	Tomakomai	29	33792.9
47426	Urakawa	29	33444.7	47428	Esashi	29	33341.2
47430	Hakodate	24	32587.5	47433	Kutchan	29	33475.6
47435	Mombetsu	15	33148.9	47440	Hiroo	39	35213.2
47520	Shinjo	31	32461.7	47570	Wakamatsu	31	32384.8
47574	Fukaura	15	34092.1	47575	Aomori	24	32844.7
47576	Mutsu	29	33217.2	47581	Hachinohe	24	33597.9
47582	Akita	27	33115.9	47584	Morioka	15	32251.4
47585	Miyako	29	34616.6	47587	Sakata	37	33151.2
47588	Yamagata	32	32861.4	47590	Sendai	36	33592.7
47592	Ishinomaki	37	32721.2	47595	Fukushima	32	33685.2
47597	Shirakawa	33	33339.9	47600	Wajima	30	34299.5
47602	Aikawa	29	34491.2	47604	Niigata	29	32667.1
47605	Kanazawa	30	33495.3	47606	Fushiki	30	33210.4
47607	Toyama	30	33854.3	47610	Nagano	27	31985.6
47612	Takada	30	34182.7	47615	Utsunomiya	46	33036.3
47616	Fukui	27	32277.1	47617	Takayama	29	32499.1
47618	Matsumoto	32	34155.5	47620	Suwa	33	32466.1
47624	Maebashi	46	34185.8	47626	Kumagaya	46	34621.6
47629	Mito	30	33493.4	47631	Tsuruga	33	32864.2
47632	Gifu	33	31883.4	47636	Nagoya	33	31670.4
47637	Iida	32	33972.2	47638	Kofu	44	33880.6
47640	Kawaguchiko	46	34487.5	47641	Chichibu	45	34223.9
47648	Choshi	36	32871.2	47649	Ueno	33	32162.3
47651	Tsu	44	33458.7	47653	Irako	33	32300.7
47654	Hamamatsu	33	32305.9	47655	Omaezaki	33	31523.6
47656	Shizuoka	33	34288.6	47657	Mishima	33	33981.8

WMO code	stations	orders	AIC values	WMO code	stations	orders	AIC values
47662	Tokyo	33	34046.6	47663	Owase	44	33667.3
47666	Irozaki	34	33071.7	47668	Ajiro	33	34667.4
47670	Yokohama	33	34571.3	47674	Katsuura	32	33887.2
47675	Oshima	45	34012.3	47678	Hachijojima	32	32884.7
47690	Nikko	47	33773.1	47740	Saigo	33	32986.3
47741	Matsue	33	31769.9	47742	Sakai	33	31742.0
47744	Yonago	33	32902.0	47746	Tottori	33	32965.1
47747	Toyooka	32	32210.0	47750	Maizuru	32	32474.6
47754	Hagi	29	32694.1	47755	Hamada	33	33024.3
47756	Tsuyama	32	32067.4	47759	Kyoto	32	30969.7
47761	Hikone	42	31613.3	47762	Shimonoseki	41	31620.7
47765	Hiroshima	44	31559.7	47766	Kure	33	31680.6
47768	Okayama	39	31736.3	47769	Himeji	32	31458.7
47770	Kobe	33	31286.7	47772	Osaka	32	31544.2
47776	Sumoto	32	32157.1	47777	Wakayama	32	32621.9
47778	Shionomisaki	32	32830.6	47780	Nara	32	32069.3
47800	Izuhara	42	31811.0	47805	Hirado	32	30998.1
47807	Fukuoka	32	31204.7	47809	Iizuka	14	31726.1
47812	Sasebo	43	31017.4	47813	Saga	43	30469.0
47814	Hita	23	31352.9	47815	Oita	32	33227.5
47817	Nagasaki	23	31081.8	47819	Kumamoto	27	30640.1
47821	Asosan	23	30845.2	47823	Akune	17	31631.1
47824	Hitoyoshi	20	31922.8	47827	Kagoshima	23	30755.3
47829	Miyakonojo	23	31809.8	47830	Miyazaki	20	32799.3
47831	Makurazaki	15	31472.9	47835	Aburatsu	23	32324.0
47836	Yakushima	16	32201.1	47837	Tanegashima	38	31802.5
47838	Ushibuka	44	30969.5	47887	Matsuyama	33	31942.7
47890	Tadotsu	33	33638.3	47891	Takamatsu	44	33329.0
47892	Uwajima	32	31949.2	47893	Kochi	32	32053.7
47895	Tokushima	32	33093.7	47897	Sukumo	32	32424.3
47898	Shimizu	33	32055.5	47899	Murotomisaki	32	32744.8
47909	Naze	17	31456.6	47912	Yonagunijima	21	30885.6
47918	Ishigakijima	20	30405.2	47927	Miyakojima	20	30583.8
47929	Kumejima	27	30354.7	47936	Naha	23	29902.2
47945	Minamidaitojima	27	30694.9				

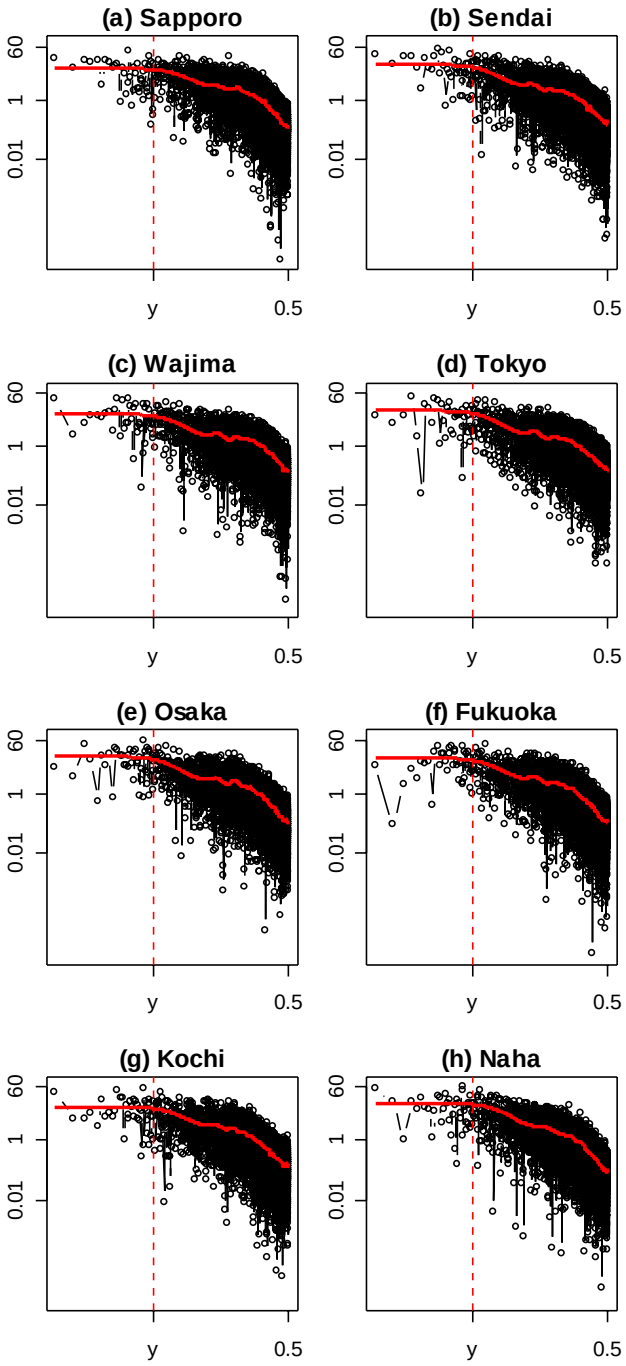

Figure 4.4 The periodogram and estimated power spectrum of the Sapporo, Sendai, Wajima, Tokyo, Osaka, Fukuoka, Kochi and Naha stations. The horizontal axis represents the frequency in logarithmic scale indicated in unit of 1/day, where "y" represents the frequency corresponding a year, and the vertical axis represents values of the periodogram and power spectrum density in logarithmic scale. In each panel, the black points and lines represent periodogram, and the red solid line represents the estimated power spectrum.

Chapter 5

Analysis of the seasonality of the autocorrelation

Jewson and Caballero (2003) discusses the seasonal changes of the autocorrelation of the surface air temperature anomaly in USA. In this chapter, we will discuss the detailed seasonal structure of surface air temperature anomalies in Japan. We then consider a non-stationary extension of the AR model, which hopefully provides knowledge about the features of the data used in the model.

5.1 Seasonality in the autocorrelations of the anomaly temperatures

In order to examine the autocorrelation structure of the seasonal periodicity on the anomalies of surface air temperature $\{y_n\ ;\ n=1, 2, \ldots, 365_{\text{days}} \text{ x } 40_{\text{years}}\}$ for each station, we consider the data of the same month throughout a 40-year period. For example, suppose that the dataset $\{ d^{\,p}_{j,n}\ ;\ n = 1, 2, \ldots , 31\}$ with j =1 represents the January data taken from $\{y_n,\}$ for the year of 1960 + p with p = 1, 2, … , 40. We also use data of the previous m last days in December, denoted by $\{ d^{\,p}_{j,n}; n = -m, -m+1, \ldots, -1, 0 \}$ with j =1, to fit the ordinary AR model of the order m,

$$d^{\,p}_{j,n} = \sum_{k=1}^{m} a_k d^{\,p}_{j,n-k} + v_n\,, \quad v_n \sim N(\,0\,,\sigma^2\,)\,, \tag{5.1}$$

to the January data. Similarly, the AR is applied for other months from February through December. The coefficients $\{ a_k \}$, the order m and the variance σ^2 are assumed to be the same within each month throughout the years p = 1, 2, … , 40, so that we apply the least

squares,

$$\sum_{p=1}^{40}\sum_{n=1}^{\Lambda_j}[d_{1,n}^{p}-\sum_{k=1}^{m}a_k d_{j,n-k}^{p}]^2 \rightarrow \min,$$

for each month $j = 1, 2, \ldots, 12$, and $\Lambda_j = 31, 28, 31, 30, \ldots, 31$ are number of days in respective months. We have used the least squares algorithm using the standard Householder transformation for computing the AIC to select the best fitted order and estimating the coefficients, and have estimated the power spectrum density using the transfer function (4.13).

We analyzed such monthly selected data in the Tokyo station. Table 5.1 lists the AIC values for the optimal orders of the respective AR models applied to the monthly selected datasets from January through December, in addition to the AIC with the optimal order of the AR model applied to the whole data. The sum of the AIC values of the separated data for January till December is substantially smaller than the AIC value for the whole data. This suggests that the combination of the models with monthly varying structure is significantly superior to the stationary AR model throughout the year in the predictive performance.

Figure 5.1 shows the estimated power spectrum of each month. The horizontal axis represents the frequency in logarithmic scale indicated in unit of 1/day, and the vertical axis represents values of the power spectrum density in a linear scale. It is shown that the power spectrum changes substantially from month to month.

Table 5.1. The minimum AIC values associated with the optimal AR orders applied to the monthly separated data and the whole data.

Months of the monthly selected datasets	AIC values	orders
January	4751.1	17
February	4558.8	15
March	5387.2	10
April	5313.6	2
May	5101.8	3
Jun	4744.4	3
July	4593.4	3
August	4353.1	17
September	4705.1	7
October	4838.1	16
November	4797.4	11
December	4691.0	9
Total	57834.9	
The whole data (Non-divided data)	58319.3	33

(a) January, February and March

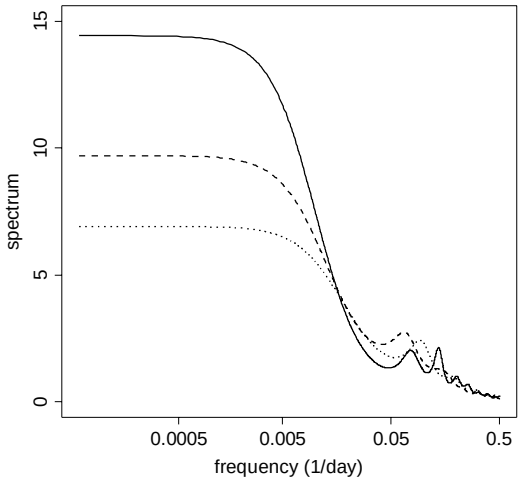

(b) April, May and Jun

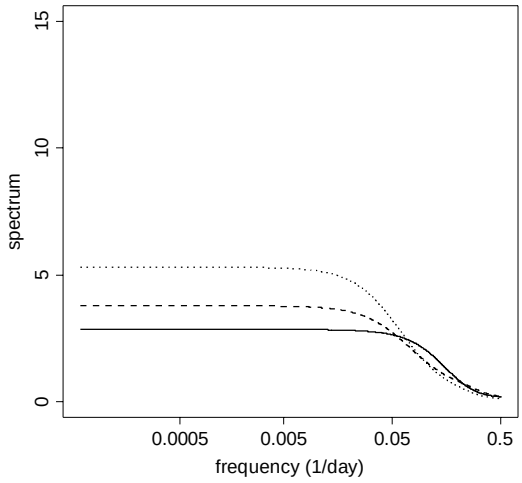

(c) July, August and September

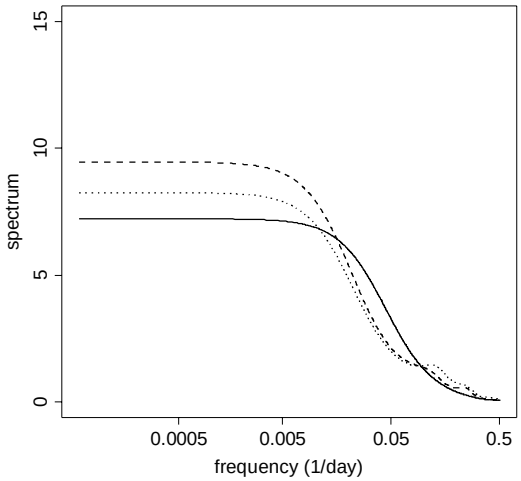

(d) October, November and December

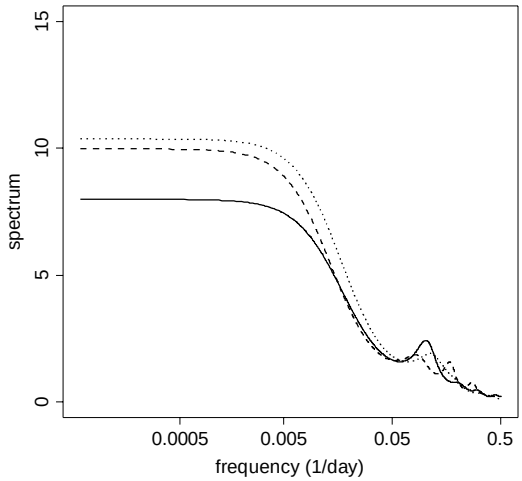

Figure 5.1. The power spectrum density of each month in Tokyo. Panel (a) plots January (solid line), February (broken line) and March (dotted line); panel (b) plots April (solid line), May (broken line) and June (dotted line); panel (c) plots July (solid line), August (broken line) and September (dotted line) and panel (d) plots October(solid line), November (broken line) and December (dotted line). The horizontal axis represents the frequency in a log-scale (1/day) and the vertical axis represents the power spectrum density in a linear scale.

5.2 A Fourier form autoregressive model

From the result of the previous section, we consider a periodic autoregressive model. Gladyshev (1961) and Gladyshev (1963) define a periodically correlated random sequence as a process with periodic structure. Jones and Brelsford (1967) propose an autoregressive model with periodic parameters that are represented by Fourier series consisting of only a few terms. Ogura (1971) gives the spectral representation theorems for periodic nonstationary processes. Ogura and Yoshida (1982) proposed a method for estimating the spectra of periodic stationary processes. Pagano (1978) presented a methodology for analyzing periodic autoregressions, and Parzen and Pagano (1979) analyze the seasonal stationary time series by periodic autoregressive schemes. Troutman (1979) discuss some properties of a periodic autoregressive process. Vecchia and Ballerini (1991) present statistical procedures for detecting if periodicities exist in the autocorrelation function of a seasonal time series after removal of seasonal means and standard deviations. Furthermore, the theorems and models of the periodic autoregressive process are developed to periodic autoregressive-moving average models (for example, Tiao and Grupe (1980), Anderson and Vecchia (1993), Adams and Goodwin (1995), Anderson et al. (1999)).

We consider a non-stationary AR model

$$y_n = \sum_{j=1}^{m} A_j(n) \cdot y_{n-j} + v_n, \qquad v_n \sim N(0, \sigma^2), \tag{5.2}$$

where the coefficients $A_j(n)$ changes with time n. Akaike (1979) and Kitagawa and Gersch (1985a, b) estimate changing spectrum of this type of non-stationary AR model through a Bayesian procedure by imposing a certain smoothness prior against the variability of the coefficients $A_j(n)$ with respect to n. Here, alternatively, we will parameterize the coefficients assuming seasonally varying function as a periodic autoregressive model. Though we can suppose several forms which represent the seasonality, we consider a Fourier form autoregressive model proposed by Jones and Brelsford (1967) such that

$$A_j(n) = a_j + \sum_{k=1}^{p} b_{jk} \sin \frac{2\pi k(n-j)}{365} + \sum_{k=1}^{q} c_{jk} \cos \frac{2\pi k(n-j)}{365}. \tag{5.3}$$

In order to distinguish from the ordinary AR model, for convenience, we refer to this Fourier form autoregressive model as the *FFAR* model hereafter in this paper. The

coefficients $\{b_{jk}\}$ and $\{c_{jk}\}$ of the FFAR model are estimated using the least squares method which uses the Householder transformation. The orders *m*, *p* and *q* are determined so as to minimize the AIC value.

For $\{y_n\ ;\ n = 1, 2, \cdots, N\}$ and the maximum order *M* ($M \geq m$), in the same way as the log likelihood $\ell(\theta_A)$ of the AR model in the previous chapter, the log likelihood $\ell(\theta_F)$ with the parameter vector θ_F of the FFAR model (5.2) and (5.3) is approximately given,

$$\ell(\theta_F) = -\frac{N-M}{2}\log 2\pi\sigma^2 - \frac{1}{2\sigma^2}\sum_{n=M+1}^{N}(y_n - \sum_{j=1}^{m} A_j(n)\cdot y_{n-j})^2\,, \tag{5.4}$$

where the orders *p* and *q* are given in $A_j(n)$. From

$$\frac{\partial\ell(\theta_F)}{\partial\sigma^2} = -\frac{N-M}{2\sigma^2} + \frac{1}{2(\sigma^2)^2}\sum_{n=M+1}^{N}(y_n - \sum_{j=1}^{m} A_j(n)\cdot y_{n-j})^2\,,$$

we get

$$\hat{\sigma}^2_{mpq} = \frac{1}{N-M}\sum_{n=M+1}^{N}(y_n - \sum_{j=1}^{m} A_j(n)\cdot y_{n-j})^2\,, \tag{5.5}$$

then, the maximum log likelihood is represented as

$$\ell(\hat{\theta}_F) = -\frac{N-M}{2}\log 2\pi\hat{\sigma}^2_{mpq} - \frac{N-M}{2}\,, \tag{5.6}$$

the AIC of the (*m* ,*p*, *q*)-th order FFAR model is

$$AIC_{mpq} = (N-M)(\log 2\pi\hat{\sigma}^2_{mpq} + 1) + 2\{(m+p+q)+1\}\,. \tag{5.7}$$

The FFAR model is applied to the temperature anomalies observed throughout the whole period in all stations in the Japan islands. The minimum AIC and the optimal order of the FFAR model in each station in Japan are listed in Table 5.2, where the orders, *m*, *p* and *q*, correspond to those in Equations (5.2) and (5.3); *m* is the length of past history data in $\{y_n\}$, *p* and *q* are the seasonal orders, that is, the orders of the sine and cosine expansions, respectively. The ordinary AR model is included in the FFAR with $p = 0$ and $q = 0$.

The stations in Table 5.2 are listed in the order of the difference of the AIC values between the FFAR model and the ordinary AR. Though a few stations, including Kumagaya (WMO code 47626), Chichibu (WMO code 47641), Tsu (WMO code 47651) and Kofu (WMO code 47638), take the seasonal order of the minimum AIC to

be zero in value (i.e., the ordinary AR model is better fitted than the FFAR model from predictive viewpoint), in the other 133 stations, the AIC difference is substantially smaller than zero (i.e., the FFAR model is much better fitted than the ordinary AR model). Among the stations in Japan, it is in Kagoshima (WMO code 47827) where the AIC difference is the smallest.

The time-varying spectrum of the frequency f in the FFAR model, which we will refer to as *the daily power spectrum* $P_n(f)$, is estimated through the function,

$$p_n(f) = \frac{\hat{\sigma}^2}{\left| 1 - \hat{B}_n(f) \right|^2}, \tag{5.8}$$

where using estimated coefficients of the FFAR model

$$\hat{B}_n(f) = \sum_{j=1}^{\hat{m}} [\, \hat{a}_j + \sum_{k=1}^{\hat{p}} \hat{b}_{jk} \sin \frac{2\pi k(n-j)}{365} + \sum_{k=1}^{\hat{q}} \hat{c}_{jk} \cos \frac{2\pi k(n-j)}{365} \,] e^{-i2\pi fj} \quad . \tag{5.9}$$

The gray scale image with contours in Figure 5.2 displays such a power spectrum of frequency at the time instance of the year on the plane, for each of the six climatically typical stations, Sapporo (WMO code 47412), Sendai (WMO code 47590), Tokyo, Wajima (WMO code 47600), Kagoshima, and Naha (WMO code 47936). The contours on the gray scale image are displayed equidistantly in a linear-scale according to the power spectrum size. We should note that there are a couple of peaks in most of the power spectrum density. Thus we can recognize that the FFAR model represents the quantitative features of the seasonal periodicity in terms of daily power spectrum for the temperature anomalies.

Table 5.2. The minimum AIC value associated with the selected order of the FFAR. The orders *m*, *p* and *q* correspond to those in equation (5) and (6), where *m* is the AR order of data y_n, and *p* and *q* are the seasonal orders, whereas the ordinary AR model takes $p = q = 0$.

WMO code	stations	orders			AIC values		
		m	*p*	*q*	(a) FFAR	(b) AR	(a) - (b)
47827	Kagoshima	14	3	2	30413.1	30755.3	-342.2
47824	Hitoyoshi	11	2	2	31642.5	31922.8	-280.3
47898	Shimizu	8	4	3	31788.7	32055.5	-266.8
47829	Miyakonojo	8	4	3	31545.5	31809.8	-264.3
47912	Yonagunijima	5	3	2	30625.9	30885.6	-259.7
47927	Miyakojima	20	1	1	30325.7	30583.8	-258.1
47893	Kochi	8	4	3	31798.1	32053.7	-255.6
47936	Naha	20	1	1	29661.9	29902.2	-240.3
47814	Hita	7	3	3	31114.7	31352.9	-238.2
47819	Kumamoto	15	2	2	30406.7	30640.1	-233.4
47813	Saga	15	2	2	30240.8	30469.0	-228.2
47918	Ishigakijima	5	3	2	30189.8	30405.2	-215.4
47655	Omaezaki	17	2	1	31312.8	31523.6	-210.8
47899	Murotomisaki	14	2	2	32535.8	32744.8	-209.0
47674	Katsuura	14	2	1	33678.8	33887.2	-208.4
47837	Tanegashima	14	2	2	31598.2	31802.5	-204.3
47836	Yakushima	15	1	1	31999.4	32201.1	-201.7
47821	Asosan	6	2	2	30643.7	30845.2	-201.5
47654	Hamamatsu	14	2	1	32136.2	32305.9	-169.7
47831	Makurazaki	9	3	3	31303.4	31472.9	-169.5
47805	Hirado	13	2	2	30828.9	30998.1	-169.2
47433	Kutchan	15	2	2	33308.9	33475.6	-166.7
47897	Sukumo	8	3	3	32258.3	32424.3	-166.0
47617	Takayama	13	2	2	32333.9	32499.1	-165.2
47838	Ushibuka	15	2	2	30806.3	30969.5	-163.2
47413	Iwamizawa	13	2	2	32486.4	32649.2	-162.8
47620	Suwa	14	2	2	32306.2	32466.1	-159.9
47770	Kobe	16	2	2	31128.0	31286.7	-158.7
47830	Miyazaki	8	4	3	32641.0	32799.3	-158.3
47690	Nikko	10	2	1	33617.0	33773.1	-156.1
47428	Esashi	16	2	2	33188.9	33341.2	-152.3
47835	Aburatsu	8	3	3	32171.9	32324.0	-152.1
47407	Asahikawa	16	2	1	32648.9	32799.8	-150.9
47430	Hakodate	15	2	2	32436.9	32587.5	-150.6
47424	Tomakomai	15	2	1	33646.5	33792.9	-146.4
47426	Urakawa	14	2	2	33300.2	33444.7	-144.5
47606	Fushiki	10	2	2	33066.4	33210.4	-144.0
47780	Nara	10	3	3	31925.7	32069.3	-143.6
47401	Wakkanai	8	2	2	31314.8	31451.8	-137.0
47412	Sapporo	13	2	2	32613.3	32743.8	-130.5
47618	Matsumoto	24	2	2	34025.3	34155.5	-130.2
47776	Sumoto	15	2	1	32032.1	32157.1	-125.0
47759	Kyoto	9	3	3	30844.8	30969.7	-124.9
47807	Fukuoka	14	2	2	31082.5	31204.7	-122.2

WMO code	stations	orders m	p	q	AIC values (a) FFAR	(b) AR	(a) - (b)
47929	Kumejima	9	1	1	30232.5	30354.7	-122.2
47576	Mutsu	15	2	2	33096.0	33217.2	-121.2
47809	Iizuka	6	4	3	31609.0	31726.1	-117.1
47800	Izuhara	16	2	2	31696.6	31811.0	-114.4
47584	Morioka	12	2	2	32137.0	32251.4	-114.4
47607	Toyama	15	2	2	33743.9	33854.3	-110.4
47740	Saigo	10	3	3	32876.0	32986.3	-110.3
47812	Sasebo	7	3	3	30908.8	31017.4	-108.6
47778	Shionomisaki	14	2	1	32723.0	32830.6	-107.6
47823	Akune	8	3	3	31526.4	31631.1	-104.7
47570	Wakamatsu	10	2	2	32280.7	32384.8	-104.1
47411	Otaru	16	2	2	33228.0	33331.6	-103.6
47887	Matsuyama	16	2	2	31839.2	31942.7	-103.5
47581	Hachinohe	9	2	2	33494.9	33597.9	-103.0
47602	Aikawa	17	2	1	34390.1	34491.2	-101.1
47420	Nemuro	14	2	2	33638.8	33739.1	-100.3
47585	Miyako	12	3	3	34517.4	34616.6	-99.2
47574	Fukaura	9	2	2	33993.4	34092.1	-98.7
47421	Suttsu	9	2	2	32626.6	32724.4	-97.8
47772	Osaka	16	3	2	31447.3	31544.2	-96.9
47817	Nagasaki	7	3	3	30987.5	31081.8	-94.3
47575	Aomori	16	2	2	32751.0	32844.7	-93.7
47754	Hagi	14	2	2	32600.6	32694.1	-93.5
47631	Tsuruga	12	2	2	32774.8	32864.2	-89.4
47755	Hamada	9	3	2	32935.2	33024.3	-89.1
47520	Shinjo	12	3	2	32374.2	32461.7	-87.5
47744	Yonago	10	2	2	32814.6	32902.0	-87.4
47892	Uwajima	9	3	3	31862.1	31949.2	-87.1
47435	Mombetsu	13	2	2	33061.9	33148.9	-87.0
47600	Wajima	11	2	2	34214.4	34299.5	-85.1
47406	Rumoi	16	2	2	33196.1	33281.1	-85.0
47404	Haboro	15	2	2	33413.7	33497.3	-83.6
47595	Fukushima	10	2	2	33602.8	33685.2	-82.4
47777	Wakayama	14	2	2	32540.2	32621.9	-81.7
47762	Shimonoseki	15	2	1	31540.4	31620.7	-80.3
47769	Himeji	15	2	2	31382.1	31458.7	-76.6
47746	Tottori	10	2	2	32889.1	32965.1	-76.0
47616	Fukui	10	2	2	32201.2	32277.1	-75.9
47649	Ueno	10	2	2	32087.5	32162.3	-74.8
47409	Abashiri	14	2	2	33203.1	33277.8	-74.7
47582	Akita	14	2	2	33043.7	33115.9	-72.2
47423	Muroran	16	2	1	32908.0	32980.0	-72.0
47592	Ishinomaki	12	2	2	32650.6	32721.2	-70.6
47742	Sakai	8	2	2	31673.1	31742.0	-68.9
47637	Iida	10	2	2	33904.5	33972.2	-67.7
47909	Naze	16	1	1	31389.4	31456.6	-67.2
47670	Yokohama	11	3	3	34504.1	34571.3	-67.2

WMO code	stations	orders m	p	q	AIC values (a) FFAR	(b) AR	(a) - (b)
47678	Hachijojima	20	2	1	32819.4	32884.7	-65.3
47418	Kushiro	15	2	1	33531.0	33596.0	-65.0
47741	Matsue	9	2	2	31705.7	31769.9	-64.2
47766	Kure	16	2	2	31617.4	31680.6	-63.2
47588	Yamagata	12	2	2	32798.8	32861.4	-62.6
47668	Ajiro	10	3	3	34605.0	34667.4	-62.4
47663	Owase	14	2	2	33604.9	33667.3	-62.4
47657	Mishima	14	2	1	33919.7	33981.8	-62.1
47405	Omu	12	2	2	33493.2	33553.1	-59.9
47597	Shirakawa	10	2	2	33280.4	33339.9	-59.5
47640	Kawaguchiko	14	2	1	34429.3	34487.5	-58.2
47675	Oshima	33	1	1	33954.2	34012.3	-58.1
47815	Oita	8	4	3	33170.0	33227.5	-57.5
47605	Kanazawa	16	2	2	33439.1	33495.3	-56.2
47666	Irozaki	32	2	1	33016.1	33071.7	-55.6
47610	Nagano	10	2	2	31930.3	31985.6	-55.3
47747	Toyooka	9	2	2	32155.3	32210.0	-54.7
47890	Tadotsu	14	2	1	33585.0	33638.3	-53.3
47612	Takada	20	2	2	34130.6	34182.7	-52.1
47587	Sakata	14	2	2	33100.1	33151.2	-51.1
47656	Shizuoka	14	2	1	34238.4	34288.6	-50.2
47895	Tokushima	14	2	2	33043.4	33093.7	-50.3
47604	Niigata	12	2	2	32617.6	32667.1	-49.5
47756	Tsuyama	13	2	2	32019.4	32067.4	-48.0
47750	Maizuru	10	3	3	32427.0	32474.6	-47.6
47632	Gifu	10	3	2	31836.7	31883.4	-46.7
47662	Tokyo	10	3	3	34003.5	34046.6	-43.1
47402	Kitamiesashi	9	2	2	32296.8	32334.1	-37.3
47891	Takamatsu	14	2	2	33293.2	33329.0	-35.8
47629	Mito	12	3	2	33458.9	33493.4	-34.5
47945	Minamidaitojima	10	2	1	30661.6	30694.9	-33.3
47590	Sendai	10	2	2	33567.0	33592.7	-25.7
47765	Hiroshima	16	2	2	31539.0	31559.7	-20.7
47768	Okayama	33	1	1	31716.0	31736.3	-20.3
47648	Choshi	24	2	1	32851.4	32871.2	-19.8
47615	Utsunomiya	12	3	2	33018.6	33036.3	-17.7
47440	Hiroo	15	2	1	35196.6	35213.2	-16.6
47636	Nagoya	23	1	1	31657.2	31670.4	-13.2
47653	Irako	13	3	2	32287.5	32300.7	-13.2
47761	Hikone	12	2	2	31604.5	31613.3	-8.8
47624	Maebashi	17	2	1	34180.9	34185.8	-4.9
47417	Obihiro	15	2	1	33874.9	33879.0	-4.1
47626	Kumagaya	46	0	0	34621.6	34621.6	0.0
47641	Chichibu	45	0	0	34223.9	34223.9	0.0
47651	Tsu	44	0	0	33458.7	33458.7	0.0
47638	Kofu	44	0	0	33880.6	33880.6	0.0

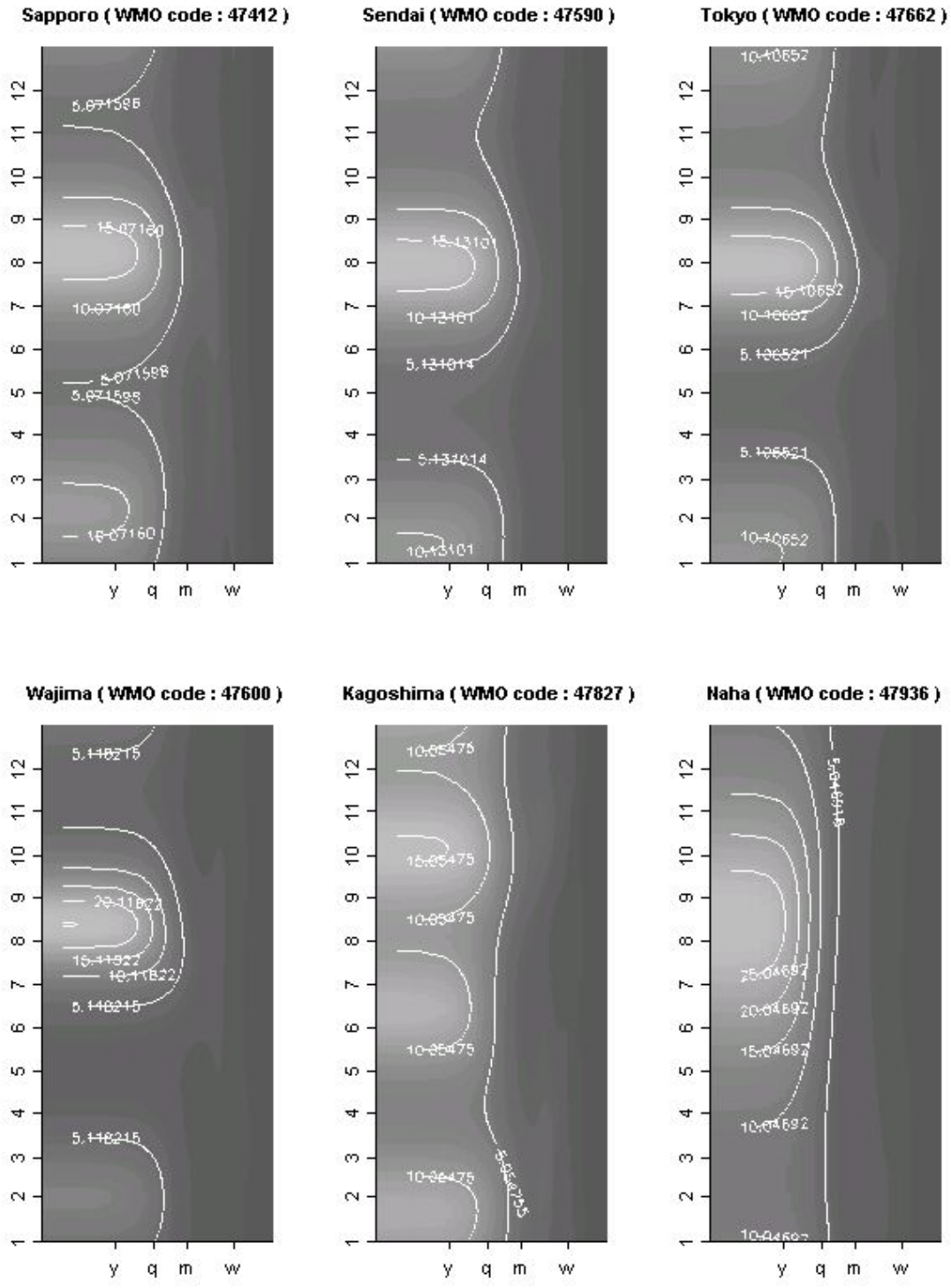

Figure 5.2. The power spectrum of frequency and time instance of the year at 6 stations. The horizontal axis for the frequency f in log-scale, where " y ", "q", "m" and "w" represents the frequency corresponding to a year, a quarter of the year, a month, and a week, respectively. The vertical axis represents the time in the month n of the year, and the contour shows the power spectrum density equidistantly drawn in linear-scale.

5.3 Characteristic yearly temperature anomalies throughout the Japan islands

Here we would like to separate the surface temperature anomalies into a low frequency factor and a remaining factor of the higher frequencies. The low frequency factor is extremely important and valuable for long-term prediction of the temperature as considered in the section 4.1. Specifically, we can get a low frequency anomaly factor using a low-pass filtered data obtained by a running mean with time span covering a period of one to several years using Equation (4.1).

Figure 5.3 gives an example of such a low-pass filtered dataset from 1991 through 2000 for the Tokyo station. The horizontal axis represents the time in years. The panel (a) corresponds to the time span $t = 365$, the panel (b) corresponds to $t = 365 \times 3$ and the panel (c) corresponds to $t = 365 \times 5$. From these panels we can clearly recognize the yearly distinctive feature of the anomalies and the decrease of the high frequency variablity with the increase of the time window span *t*.

we are concerned with the high-pass filtered data obtained by subtracting the low-pass filtered data from the anomalous data

$$\tilde{y}_n(t) = y_n - L_n(t), \tag{5.10}$$

where $L_n(t)$ is the low-pass filtered data defined above. Thus the high-pass filtered data $\tilde{y}_n(t)$ are mainly responsible to the anomalous changes within a year. Figure 5.4 shows the high-pass filtered data from 1991 through 2000 at the Tokyo station, corresponding to the panels in Figure 5.3. The feature seems robust (not very sensitive) when using a window length of 1 - 5 years. Figure 5.5 shows the power spectrum of the high-pass filtered data $\tilde{y}_n(t)$ at the Tokyo station. The horizontal axis represents the frequency in logarithmic scale indicated in unit of 1/day, where “y” represents the frequency corresponding to a year, and the vertical axis represents values of the power spectrum density in a linear scale. The black solid line represents the window span $t = 365$, the red solid line represents the window span $t = 365 \times 3$ and the light green solid line represents the window span $t = 365 \times 5$. We see that the low frequency increases as the window size for the low-pass filter increases.

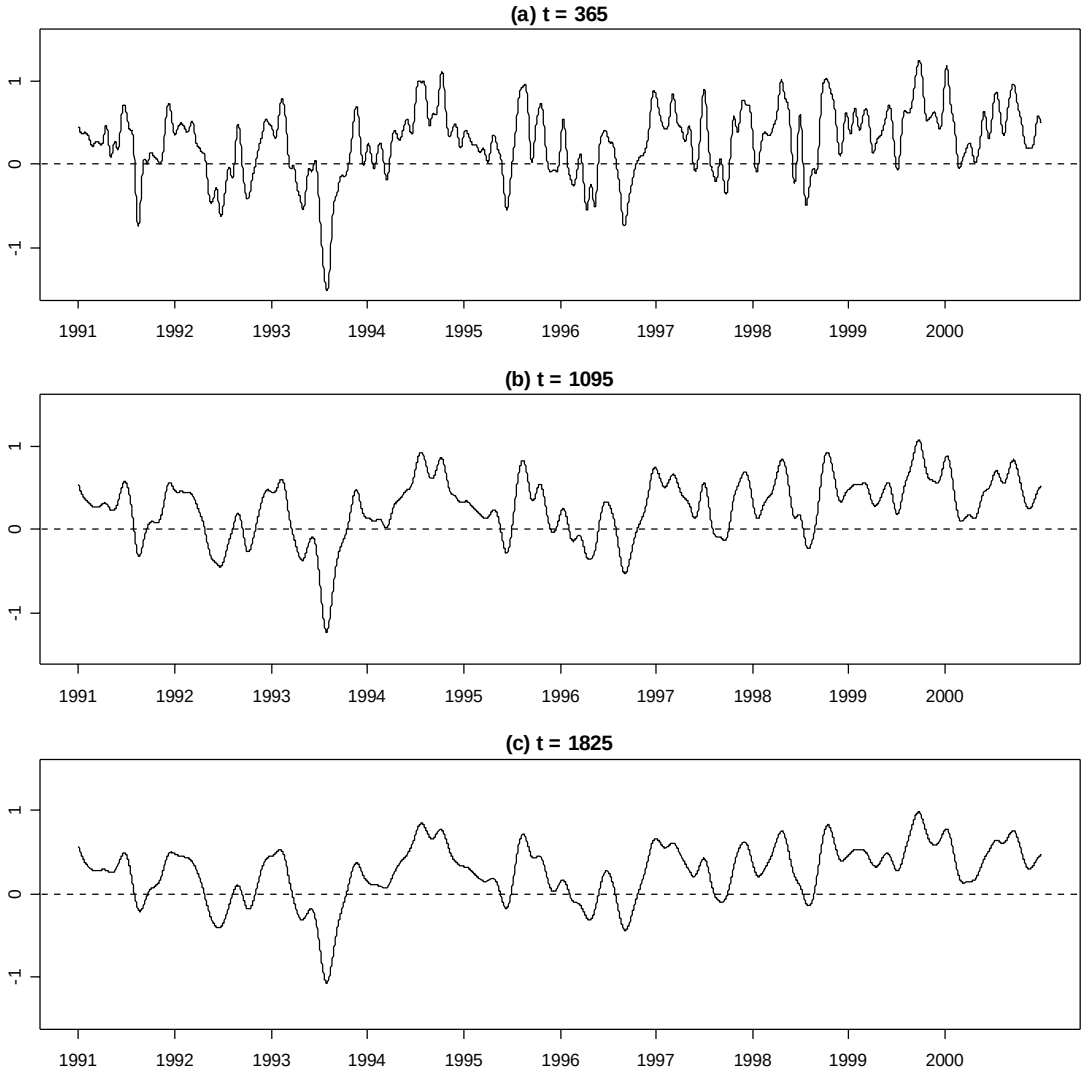

Figure 5.3. The low-pass filter data displayed for the period from 1991 through 2000 at the Tokyo station. The horizontal axis indicates the time in years. Panel (a) stands for the time span $t = 365$, panel (b) for $t = 365 \times 3$ and panel (c) for $t = 365 \times 5$ (see text for the low-pass filter).

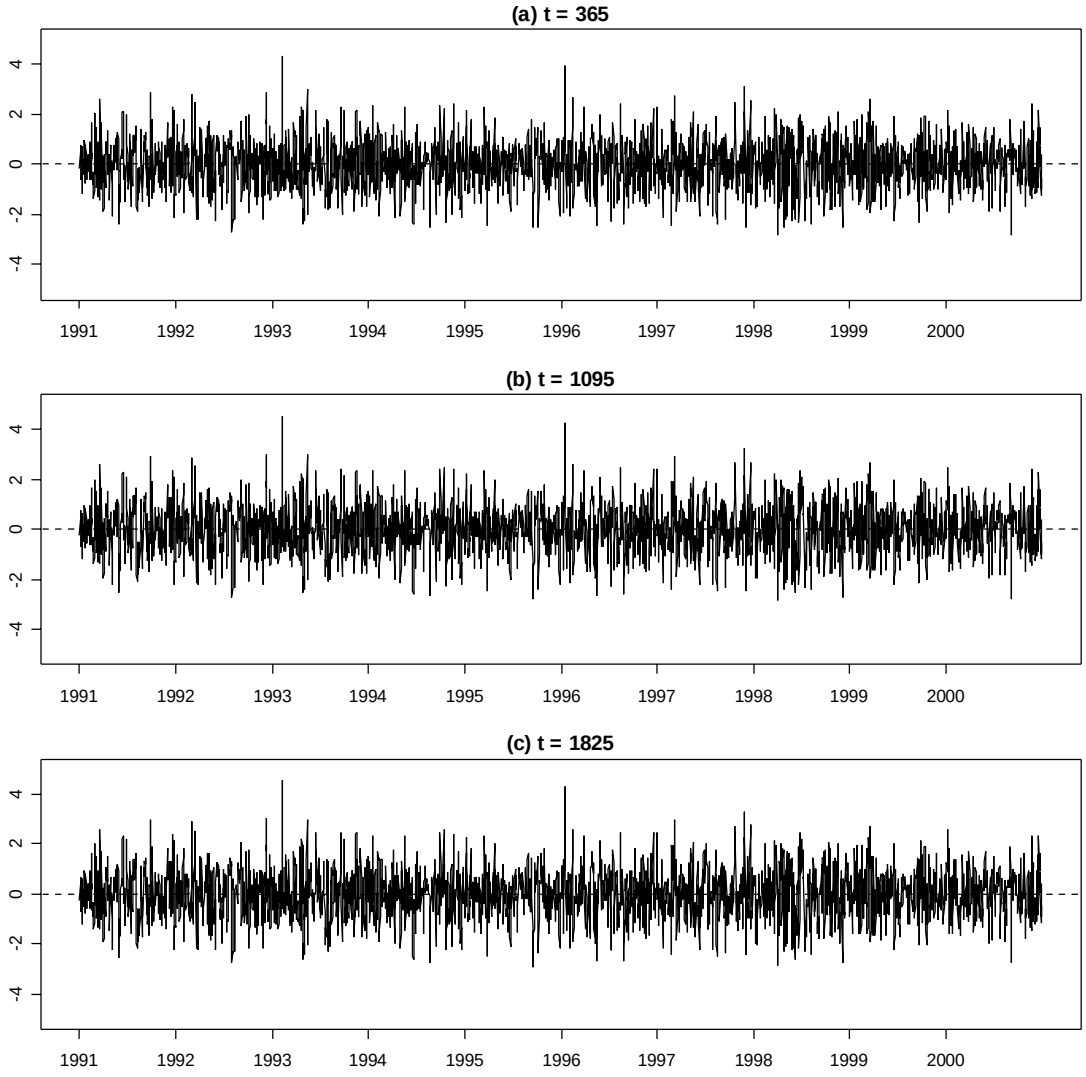

Figure 5.4. The high-pass filter data displayed for the period from 1991 through 2000 in Tokyo. The horizontal axis is the time (years). Panel (a) stands for the time span $t = 365$, panel (b) for $t = 365 \times 3$ and panel (c) for $t = 365 \times 5$ (see text for the high-pass filter).

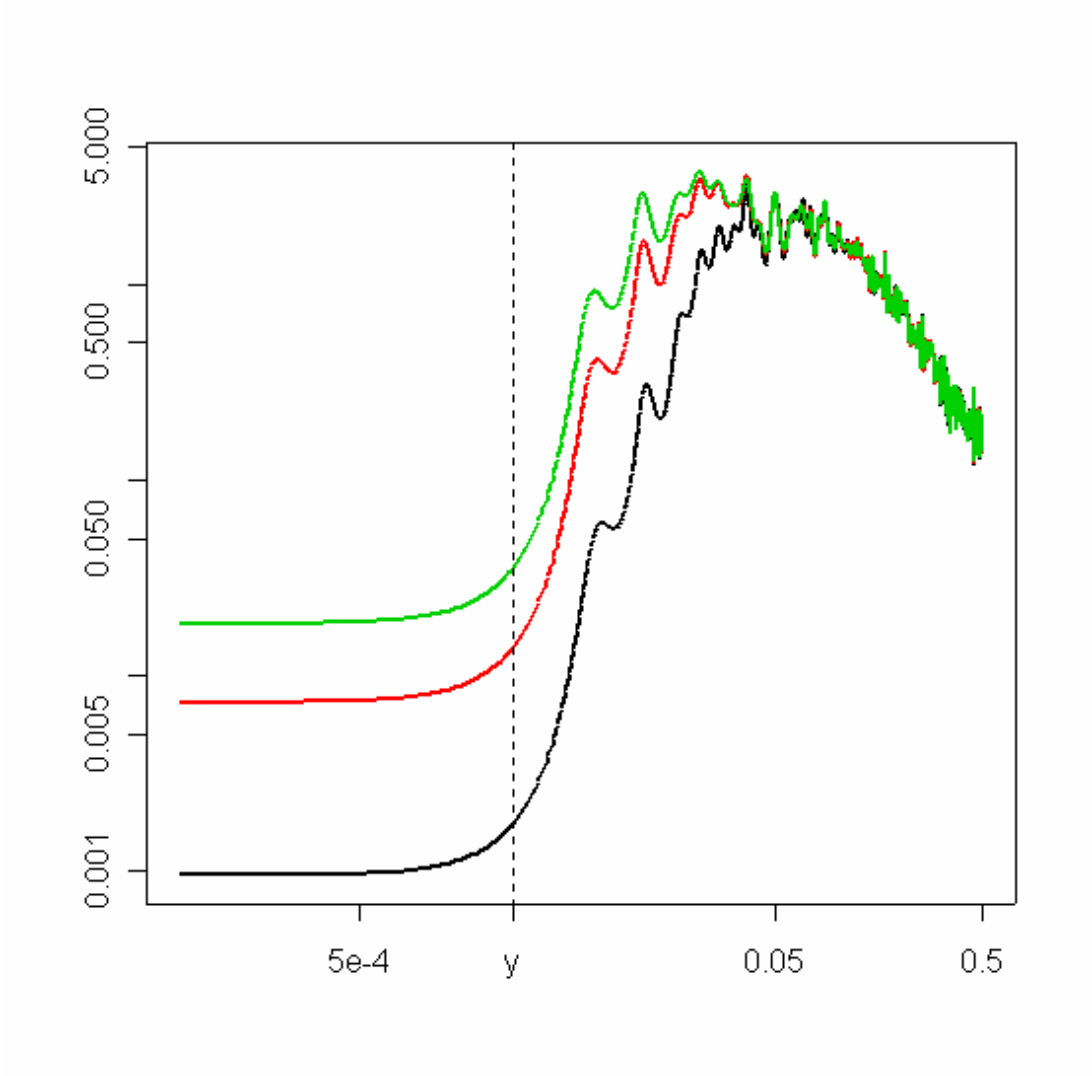

Figure 5.5. The power spectrum of the high-pass filtered data $\tilde{y}_n(t)$ at the Tokyo station. The horizontal axis represents the frequency in logarithmic scale indicated in unit of 1/day, where "y" represents the frequency corresponding to a year, and the vertical axis represents values of the power spectrum density in a linear scale. The black solid line represents the window span $t = 365$, the red solid line represents the window span $t = 365 \times 3$ and the light green solid line represents the window span $t = 365 \times 5$.

We have applied the FFAR model to the high-pass filtered data $\tilde{y}_n(t)$ from all the listed stations. Table 5.3 lists the optimal order with the AIC value for each filtered dataset in the stations where the FFAR model provides a better fit than the ordinary AR model. In Table 5.3, (a) stands for the data of the window span $t = 365$, (b) for the data of the window span $t = 365 \times 3$, and (c) for the data of the window span $t = 365 \times 5$. We see that number of stations increases as the window size for the low-pass filter increases.

Figure 5.6 shows the location of the stations in a map of the Japan islands and the result of applying the FFAR model to the high-pass filtered data. The symbols other than the open circles are used to represent stations where the AIC difference between the FFAR model and the ordinary AR model is negative; the black disks are used to represent the stations of the FFAR being better fit for the filtered data of all time window spans $t = 365$, $t = 365 \times 3$ and $t = 365 \times 5$, black triangles to represent the stations of the better fit for the filtered data of both time window spans $t = 365 \times 3$ and $t = 365 \times 5$, and black squares are used to represent the stations of the better fit for the data of only the time window span $t = 365 \times 5$. In the other stations indicated by open circles, the FFAR model is not superior to the ordinary AR model for the high-pass filtered data, which means that there is no seasonality in the residual data after removing the yearly distinctive variablities. It seems that the number of stations with seasonal anomalies increases to include most stations as the window length *t* increases (cf., Table 5.2 obtained in Section 5.2), whereas time span $t = 365$ for the filtered data should in principle be the minimum for a possible detection of the seasonality.

From Table 5.3 and Figure 16, we see that the stations of the seasonal anomalies are gradually increasing northward from the southern end, as the filtering window span increases, such that there are 6 stations for $t = 365$, 13 stations for $t = 365 \times 3$ and 19 stations for $t = 365 \times 5$. In addition, all of these stations are located at the Okinawa Islands and coast of Kyushu, Shikoku and Honshu. It is our belief that the seasonality in the autocorrelation of the filtered data that is propagating from the south as the frequency of the filtered data get lower, can be explained by the influence of the seasonal movement of the warm currents known as “Kuroshio” and “Tsushima” (arrows on Figure 16).

Table 5.3. Stations where the FFAR model fits better than the AR for each of the high-pass filter datasets; the optimal order and the AIC difference value.

(a) High-pass filtered anomaly data with the time window of $t = 365$.

WMO code	stations	orders m	p	q	AIC values (a) FFAR	(b) AR	(a) - (b)
47827	Kagoshima	91	1	1	27837.9	27898.3	- 60.4
47936	Naha	107	1	1	26990.1	27034.9	- 44.8
47893	Kochi	98	1	1	29183.2	29223.6	- 40.4
47898	Shimizu	97	1	1	29178.0	29199.8	- 21.8
47927	Miyakojima	100	1	1	27709.1	27723.1	- 14.0
47836	Yakushima	98	1	1	29385.8	29399.7	- 13.9

(b) High-pass filtered anomaly data with the time window of $t = 365 \times 3$

WMO code	stations	orders m	p	q	AIC values (a) FFAR	(b) AR	(a) - (b)
47827	Kagoshima	71	1	1	29132.5	29230.3	- 97.8
47893	Kochi	73	1	1	30486.0	30559.1	- 73.1
47936	Naha	84	1	1	28296.6	28369.7	- 73.1
47898	Shimizu	89	1	1	30469.8	30532.2	- 62.4
47836	Yakushima	90	1	1	30685.4	30730.6	- 45.2
47655	Omaezaki	75	1	1	29963.7	30006.9	- 43.2
47899	Murotomisaki	72	1	1	31188.3	31226.1	- 37.8
47674	Katsuura	72	1	1	32359.2	32394.6	- 35.4
47927	Miyakojima	100	1	1	29020.6	29051.0	- 30.4
47837	Tanegashima	90	1	1	30278.5	30291.9	- 13.4
47770	Kobe	89	1	1	29739.7	29745.5	- 5.8
47819	Kumamoto	90	1	1	29126.6	29130.4	- 3.8
47654	Hamamatsu	75	1	1	30774.5	30778.1	- 3.6

(c) High-pass filtered anomaly data with the time window of $t = 365 \times 5$

WMO code	stations	orders m	p	q	AIC values (a) FFAR	(b) AR	(a) - (b)
47827	Kagoshima	70	1	1	29506.3	29634.6	- 128.3
47893	Kochi	72	1	1	30860.9	30963.8	- 102.9
47936	Naha	80	1	1	28684.6	28770.8	- 86.2
47655	Omaezaki	72	1	1	30341.2	30416.8	- 75.6
47899	Murotomisaki	72	1	1	31559.5	31635.0	- 75.5
47898	Shimizu	89	1	1	30859.4	30932.3	- 72.9
47836	Yakushima	73	1	1	31063.5	31133.2	- 69.7
47674	Katsuura	72	1	1	32739.3	32794.8	- 55.5
47927	Miyakojima	81	1	1	29409.6	29451.6	- 42.0
47654	Hamamatsu	75	1	1	31154.5	31191.1	- 36.6
47837	Tanegashima	71	1	1	30654.9	30691.5	- 36.6
47770	Kobe	72	1	1	30122.3	30154.1	- 31.8
47819	Kumamoto	72	1	1	29503.4	29531.4	- 28.0
47829	Miyakonojo	72	1	1	30688.8	30704.1	- 15.3
47912	Yonagunijima	81	1	1	29751.0	29763.7	- 12.7
47813	Saga	71	1	1	29335.5	29345.5	- 10.0
47918	Ishigakijima	81	1	1	29276.0	29281.0	- 5.0
47759	Kyoto	73	1	1	29853.8	29856.1	- 2.3
47838	Ushibuka	72	1	1	29847.1	29848.1	- 1.0

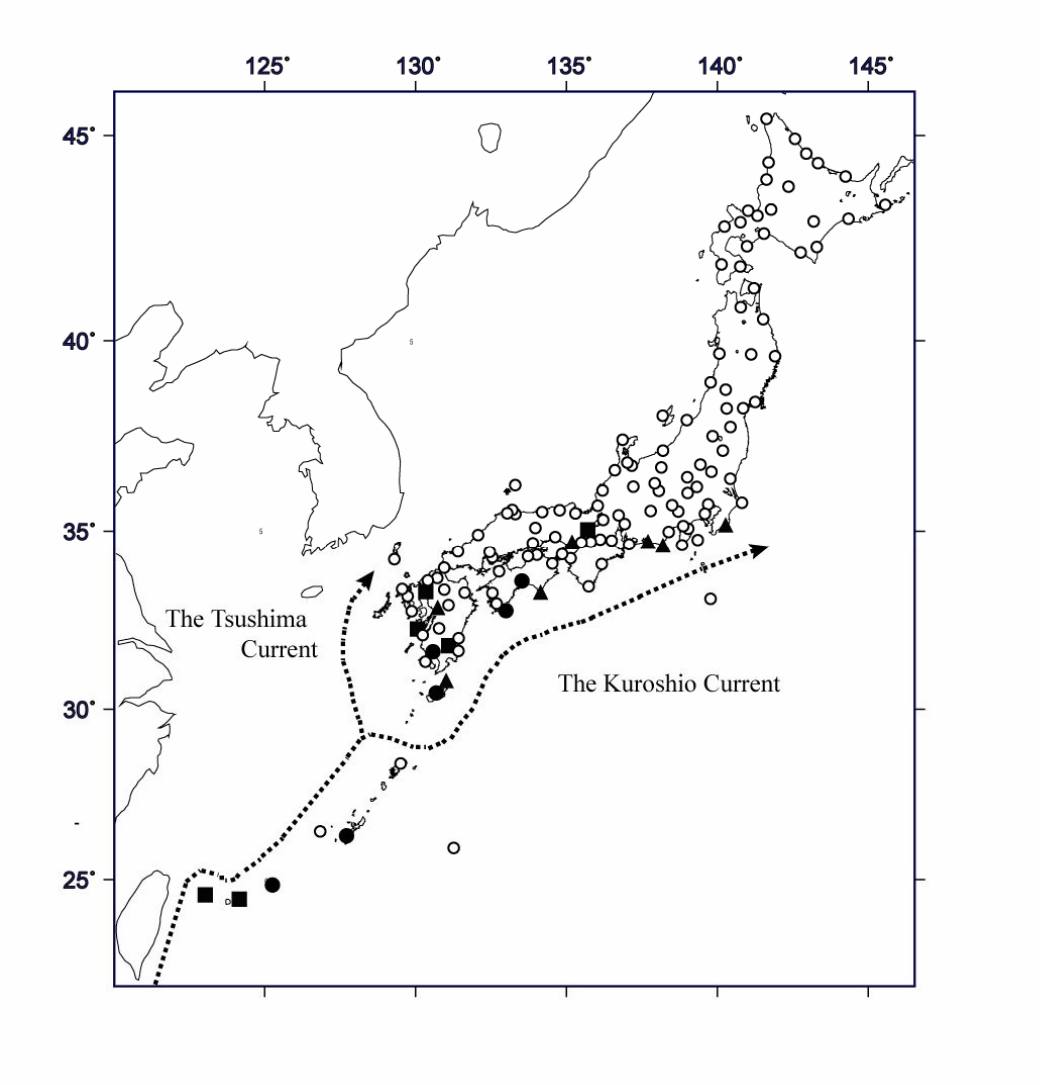

Figure 5.6. The location of the stations and the result of applying the FFAR model to the high-pass filtered data. The symbols other than the open circle represent stations where the FFAR provides a better fit than the ordinary AR in the sense of the AIC: black disks indicate the stations of the better fit for the filtered data of the time span $t = 365$, $t = 365 \times 3$ and $t = 365 \times 5$, black triangles indicate the stations of the better fit for both filtered data of the time span $t = 365 \times 3$ and $t = 365 \times 5$, and black squares indicate the stations of the better fit for only filtered data of the time span $t = 365 \times 5$. Dotted arrow lines indicate the mean current paths of “Kuroshio” and “Tsushima”.

5.4 An example of the application to the risk management

In this section, we will see an example of the application to the risk management using the FFAR model, to put it concretely, an example of pricing of weather derivatives using the FFAR model. Wakaura (2006) argue the article in detail.

Weather derivatives are contingent claims written on weather indices such as temperature and can hedge the fluctuation of profits caused by the change in the weather. The contract of weather derivatives that we take up here is the put option and the structure is:

(a) The underlying index is defined as the measure of weather which governs when and how payouts on the contract will occur. The indices are HDD (the heating degree days) and CDD (the cooling degree days) that is defined as

$$\text{HDD} = \max(18^\circ - T_n, 0) \quad \text{and} \quad \text{CDD} = \max(T_n - 18^\circ, 0),$$

where T_n is the daily mean value of temperature.

(b) The start date and end date that constrain the period over which the underlying index is calculated are defined and the period is called the *term*.

(c) The value of the underlying index at which the contract starts to pay out and the payout amount per unit increment in the index beyond the strike are defined. The former is called the *strike* and the latter is called the *tick size*.

(d) When the accumulated index value within the term falls beyond the strike, the payout is calculated by the accumulated index value and the tick size.

The price of weather derivatives is determined by discounting their expected payoff and simulating the probability distribution of the index valuates the expected payoff. We simulate the probability distributions of the index using the AR model and the FFAR model, and compare the prices based the AR model and the FFAR model.

The steps of the pricing are as follows:

(a) Simulating the surface air temperature anomalies y_n's for the appointed period by Monte Carlo simulation with the initial value that is the real value of the

appointed date after from 1/1/2001 and coefficients of the AR model and the FFAR model which were estimated from the data in the station for 40 years period from 1961 through 2000. The number of simulation is set to 1000.

(b) Calculating the set of weather indices (HDD and CDD) from the set of the simulated value $\hat{y}_n$, where the daily mean value of temperature T_n is estimated as $\hat{T}_n = \hat{\mu}_n + \hat{\upsilon}_n^2\ \hat{y}_n$.

(c) The price of put option is valuated as

$$Y\sum_{I=0}^{K}(K-I)\hat{F}(I),$$

where I is the index value, $\hat{F}(I)$ is the probability distribution of cumulative HDD or CDD for the appointed period (the term), which is estimated from the set of weather indices calculated in step (b), K is the strike and Y is the tick size.

The supposed contracts are follows (the tick sizes are all 100,000yen) :

(a) Contract 1
Station : Tokyo
Index : HDD
Term : from January 1 until February 28
Strike : 650 DD

(b) Contract 2
Station : Osaka
Index : HDD
Term : from January 1 until February 28
Strike : 650 DD

(c) Contract 3
Station : Tokyo
Index : CDD
Term : from Jun 1 until August 31
Strike : 450 DD

(d) Contract 4
Station : Osaka
Index : CDD

Term : from Jun 1 until August 31
Strike : 530 DD

Figure 5.7 shows the predicted distribution of cumulative HDD and CDD in each supposed contract. The left panel is the distribution using the AR model and the right panel is the distribution using FFAR model. Table 5.4 shows their valuated prices. We recognize that the defference of the prices of the contract in summer season (the contract 3 and 4) is remarkable. In also Jewson and Caballero (2003), it is pointed out that the prices in summer season depend upon the seasonality of the autocorrelation. That is also expected from the defference of their power spectrum. It is suggested that we cannot disregard the seasonalty in the pricing of weather derivatives or the risk management.

Table 5.4. The list of prices based the AR model and the FFAR model in each supposed contract (the monetary unit is the yen).

	contract 1	contract 2	contract 3	contract 4
AR model	223,734	322,889	282,834	49,192
FFAR model	115,374	234,769	656,664	166,359

(a) Contract 1

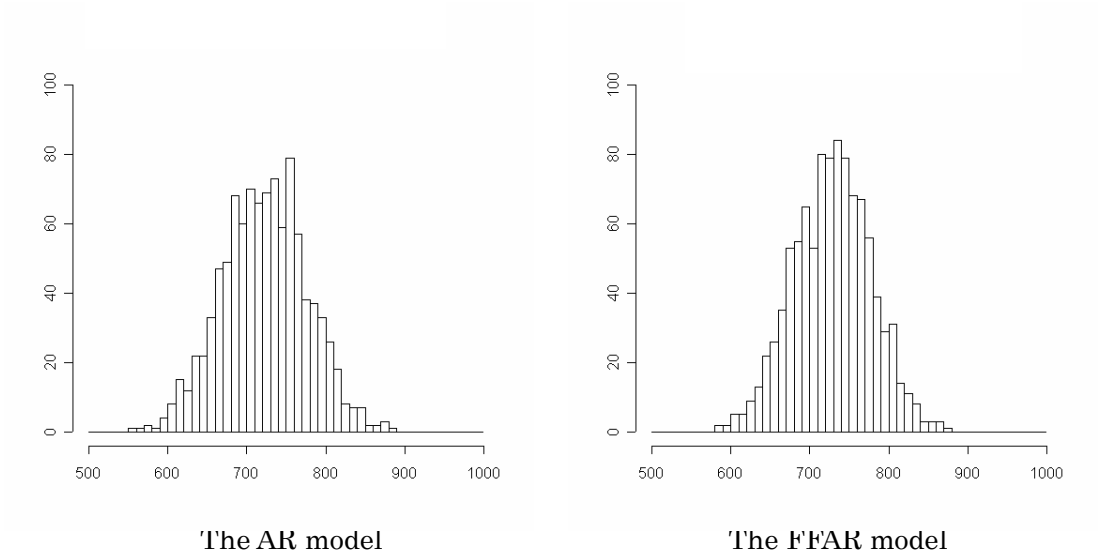

(b) Contract 2

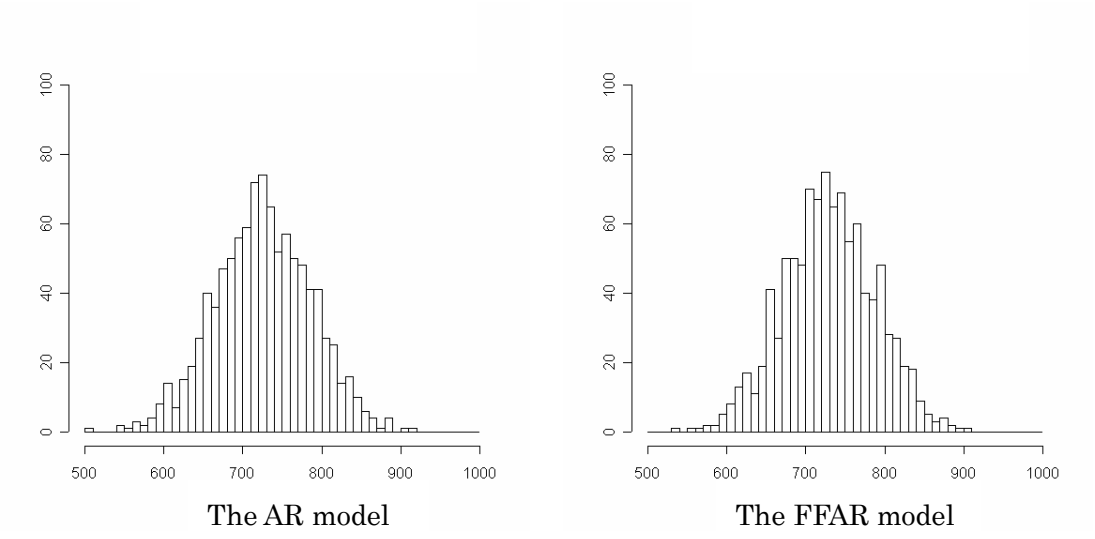

Figure 5.7-1. The predicted distribution of cumulative HDD and CDD in each supposed contract. The left panel is the distribution using the AR model and the right panel is the distribution using FFAR model.

(c) Contract 3

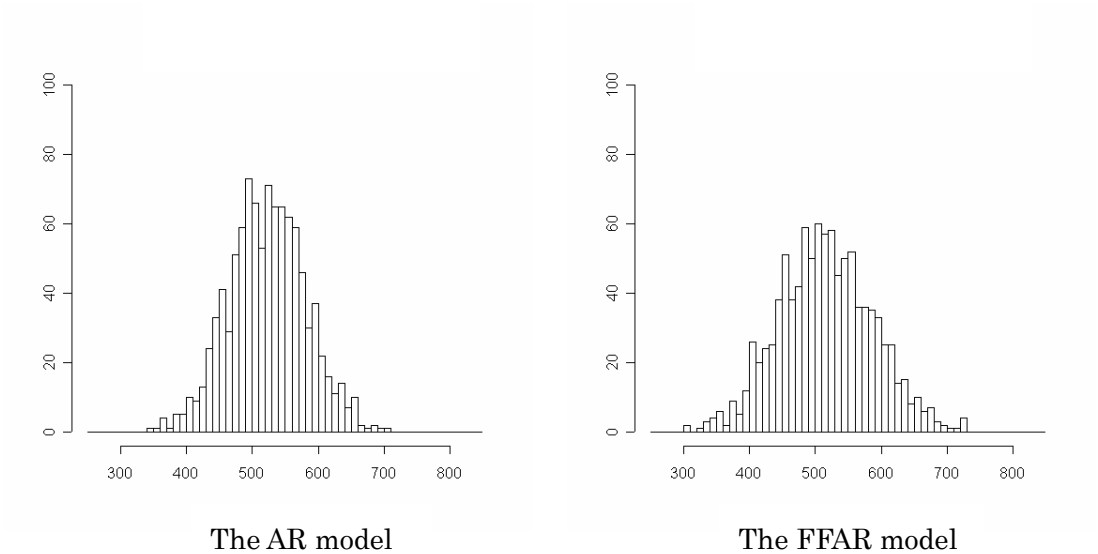

The AR model The FFAR model

(d) Contract 4

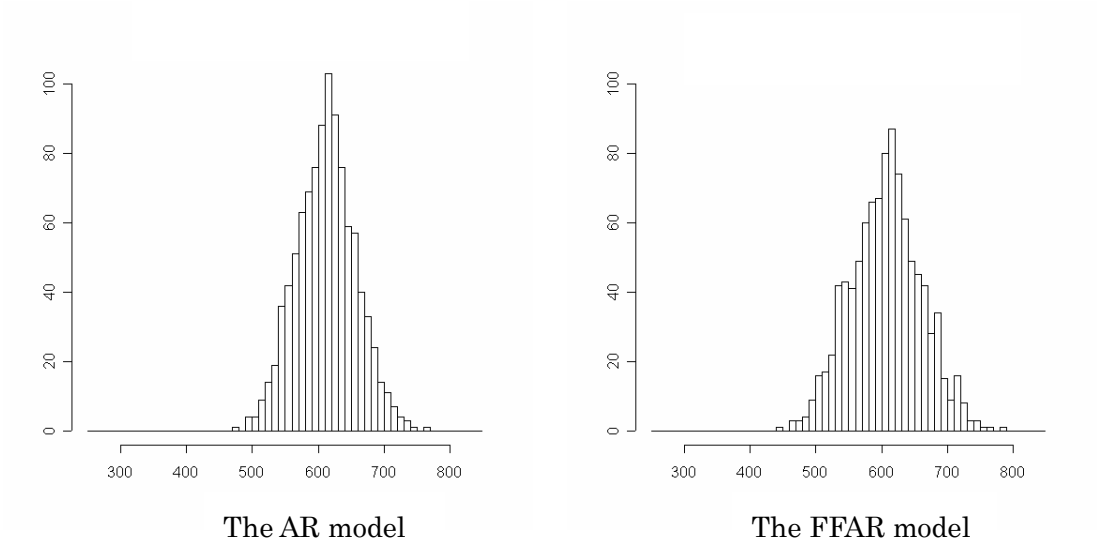

The AR model The FFAR model

Figure 5.7-2. The predicted distribution of cumulative HDD and CDD in each supposed contract. The left panel is the distribution using the AR model and the right panel is the distribution using FFAR model.

Chapter 6

Extension to a multivariate model

6.1 The concept

In this chapter, we consider a multivariate model. AR processes consist of a dynamically determined component and a stochastic component. The dynamically determined component is linear differential equations that can approximate the dynamics of physical processes. The stochastic component represents external force. It is commonly assumed that the stochastic component is the white noise, and if we consider the frequency response function, we can understand that AR processes are the response of the linear system for the input of the white noise, in the frequency domain. An AR process can be generalized to a multivariate setting. Multivariate AR processes can describe joint evolution between processes as a system.

We can consider that the surface air temperature is a product that various factors such as heat fluxes are intricately intertwined. If we assume that the external factors are random variables, and that the mechanism which generate the anomalies of the surface air temperature, is a linear system of the factors, we can describe the anomalies of the surface air temperature as a linear system driven by external force, using the AR model. Then, by assuming that the anomalies of the surface air temperature observed in each station are the output of the AR model and they influence mutually as linear systems, we can apply the multivariate AR model to them as a climate system for analysis of the relation and the evolution of them, and by considering the input of white noise as the atmospheric external forces in each station, we can quantitatively discuss the relation between the stations.

The relationship between the stations considered in this chapter is the causality. The causality between variables in multivariate models has been developed in economics. The cross-correlation function is a concise measurement for multiple variables. the Pierce-Haugh (1977) test is a method for the detection of the causality using the

cross-correlation function. The causality in the sense of Granger (1969) is utilized broadly in economic analysis and Sims (1972) proposed a test for the causality. In the comparison of tests due to Granger (1969) and Sims (1972) for the absence of a Granger causal ordering in stationary Gaussian time series, Geweke (1983) recommends the Wald variants of a test attributed to Granger and the lagged dependent variable version of Sims's test. The impulse response function which represent the progress of the influence between variables in the time domain is also utilized for analysis of the causality; however Otomo et al. (1972) shows the case that the impulse response function is not useful in analysis of variables with feedback relation. The variance decomposition represents the causality between variables using the diagonal elements of the orthogonalized variance-covariance matrix of the prediction error in the multivariate model. In the context of the variance decomposition, Sims (1980) proposes the relative variance contribution. For the arbitrary choice of the arrange between variables in the orthogonalization of the variance decomposition, the structural VAR (vector autoregressive) model is proposed (Bernanke (1986), Sims (1986) and Blanchard (1989)). On the other hand, Geweke (1982) defines a measure of linear dependence and feedback for multiple time series; the measure of linear dependence is the sum of the measure of instantaneous linear feedback and measures of each linear feedback between variables, and the measure of linear feedback is additively decomposed by frequency. Furthermore, Geweke (1984) proposes a measure of linear dependence and feedback for two multiple time series conditional on a third.

Akaike (1968) defines quantitatively the degree of contribution of the noise terms correspond to the input for variables correspond to the response in the linear system such as the multivariate AR model and that is called the *noise contribution*. In this chapter, we will apply multivariate AR model to surface air temperature anomalies, and analyze the relation between the stations using the noise contribution. In the definition of noise contributions, however, it is assumed that the components of the white noise are mutually uncorrelated. There are the correlations between the anomalies of the surface air temperature of each station as shown in Chapter 4. Though it seems that they depend on the distance between stations and weather events which influence among stations in a local and the whole area, we would like to analyze the structure of the influence between individual station in the general situation. As for the correlated noise, Tanokura and Kitagawa (2004) discuss the general form incorporated noise contributions of correlated noise sources, and Wong and Ozaki (2006) discuss the approach of the state space framework. Strictly speaking, if the innovations are mutually correlated, we must consider the influence of the correlated noise and recognize the

contribution of the diagonal noise in the variance covariance matrix as the contribution containing the influence of not only itself but also the cross-correlated noise in the case of variance covariance matrix of the innovations with significant correlation. The noise contribution is, however, stable in terms of the estimation of diagonal noise in the variance covariance matrix, even in the case of the mutually correlated innovations (Tanokura (2004), Wong (2005) and Wong and Ozaki (2006)), and so from the conciseness of the argument we will argue without the consideration of their influence.

On the other hand, as described in the previous chapter, there is the seasonal periodicity of power spectrum in most area of Japan. This suggests that the structure of the anomalies of the surface air temperature, in other words, the climatic mechanism that generates them, varies depending on the season. Even if it cannot say to that, it is clear at least that the model with seasonally varying structure has higher performance than the normal model. If the object of our analysis is extended to multivariate, we can study the relation of the seasonal change and the influence between stations simultaneously. Therefore, FFAR is extended to a multivariate model (for convenience, we refer to it as the *MFFAR* model hereafter in this paper).

6.2 The model and the noise contribution

Let $\mathbf{y}_n$ be a K-element vector with time point n,

$$\mathbf{y}_n = (y_n(1), \cdots, y_n(K))^{\mathrm{T}}, n = \{1,2,\cdots,N\},$$

then the FFAR model is extended to a multivariate model,

$$\mathbf{y}_n = \sum_{s=1}^{m} \mathbf{G}_s(n)\mathbf{y}_{n-s} + \mathbf{v}_n, \quad \mathbf{v}_n \sim N(0, \mathbf{V}), \tag{6.1}$$

$$\mathbf{G}_s(n) = \mathbf{A}_s + \sum_{l=1}^{p} \mathbf{B}_{sl} \sin\frac{2\pi l(n-s)}{365} + \sum_{l=1}^{q} \mathbf{C}_{sl} \cos\frac{2\pi l(n-s)}{365},$$

where $\mathbf{A}_s$, $\mathbf{B}_{sl}$, $\mathbf{C}_{sl}$ is a $K \times K$-matrix, and

$$E[\mathbf{v}_n]=\begin{bmatrix}0\\ \vdots \\ 0\end{bmatrix},\quad \mathbf{V}=E[\mathbf{v}_n\mathbf{v}_n^{\mathrm{T}}]=\begin{bmatrix}\sigma_{11} & \cdots & \sigma_{1K}\\ \vdots & \ddots & \vdots \\ \sigma_{K1} & \cdots & \sigma_{KK}\end{bmatrix}.$$

Furthermore, a frequency response function with *n* is defined as

$$\mathbf{H}_n(f)=(-\sum_{s=0}^{m}\mathbf{G}_s(n)e^{-i2\pi fs})^{-1}, \tag{6.2}$$

where $-1/2\le f\le 1/2$ for discrete time series, and $\mathbf{G}_0(n)$ is a diagonal matrix with diagonal elements = -1, then, using the frequency response function a *daily cross spectrum matrix* $\mathbf{P}_n(f)$ can be represented by

$$\mathbf{P}_n(f)=\mathbf{H}_n(f)\ \mathbf{V}\ (\mathbf{H}_n(f))^{*}, \tag{6.3}$$

where $(\cdot)^{*}$ is an complex transposed matrix. By assuming $\mathbf{V}$ is an diagonal matrix, diag($\sigma_1^2\cdots\sigma_K^2$), the *j*-th diagonal element $p_{njj}(f)$ of the daily cross spectrum matrix in the MFFAR model is

$$p_{njj}(f)=\sum_{k=1}^{K}h_{njk}(f)\sigma_k^2h_{njk}(f)^{*}=\sum_{k=1}^{K}\left|h_{njk}(f)\right|^2\sigma_k^2, \tag{6.4}$$

where, h_{njk} is the (*j*, *k*) element of $\mathbf{H}_n(f)$. It shows that the power spectrum of the j-th element on the frequency *f* is decomposed into *K*-noises of which the quantity is $\left|h_{njk}(f)\right|^2\sigma_k^2$ given by coefficient matrices of MFFAR. The quantity $\left|h_{jk}(f)\right|^2\sigma_k^2$ without *n* in the ordinary multivariate AR model is called the *noise contribution* (Akaike (1968)), in particular, we call the noise contribution with the daily parameter *n*,

$$z_{njk}(f)=\left|h_{njk}(f)\right|^2\sigma_k^2, \tag{6.5}$$

the *daily noise contribution* in this paper, and call the relative noise contribution with the daily parameter *n*,

$$r_{njk}(f)=\frac{z_{njk}(f)}{p_{njj}(f)}, \tag{6.6}$$

the *daily relative noise contribution* in this paper.

Furthermore, since it is unnecessary to focus on the specific frequency in our argument, the daily noise contribution integrated on the frequency is defined as a new index,

$$\tilde{z}_{njk} = \int_{-1/2}^{1/2} z_{njk}(f)df \ , \tag{6.7}$$

also the daily relative noise contribution,

$$\tilde{r}_{njk} = \frac{\tilde{z}_{njk}}{\int_{-1/2}^{1/2} p_{njj}(f)df} \ . \tag{6.8}$$

The AR model is a linear system driven by the input of the noise. In our climate system of the anomalies of the surface air temperature based on the multivariate AR model, we can consider the noise as external force in the station such as heat fluxes which influence the surface air temperature, and argue the relation between stations quantitatively using the noise contribution. Moreover, we can argue not only the effect between stations but also the relation of seasonal effect by applying the MFFAR.

In the following section, the example of the analysis of the daily noise contribution for the Tokyo and Osaka station estimated by MFFAR is shown. The coefficients of the MFFAR model are estimated using the instantaneous response model by the least squares method via Householder transformations (see Kitagawa and Akaike (1981) and Kitagawa (1993)), and the orders are determined so as to minimize the AIC value. The instantaneous response model of the MFFAR model (6.1) is

$$\mathbf{y}_n = \tilde{\mathbf{G}}_0 \mathbf{y}_n + \sum_{s=1}^{m} \tilde{\mathbf{G}}_s(n)\mathbf{y}_{n-s} + \mathbf{w}_n, \quad \mathbf{w}_n \sim N(0, \mathbf{W}) , \tag{6.9}$$

$$\tilde{\mathbf{G}}_s(n) = \tilde{\mathbf{A}}_s + \sum_{l=1}^{p} \tilde{\mathbf{B}}_{sl} \sin\frac{2\pi l(n-s)}{365} + \sum_{l=1}^{q} \tilde{\mathbf{C}}_{sl} \cos\frac{2\pi l(n-s)}{365} ,$$

where $\tilde{\mathbf{G}}_0$ is a matrix of which upper triangular elements are all zero,

$$\tilde{\mathbf{G}}_0 = \begin{bmatrix} 0 & 0 & \cdots & 0 \\ g_0(2,1) & 0 & \cdots & 0 \\ \vdots & \ddots & \ddots & \vdots \\ g_0(K,1) & \cdots & g_0(K,K-1) & 0 \end{bmatrix},$$

and $\mathbf{W}$ is a diagonal matrix,

$$\mathbf{W} = \begin{bmatrix} \sigma_1^2 & & & O \\ & \sigma_2^2 & & \\ & & \ddots & \\ O & & & \sigma_K^2 \end{bmatrix}.$$

For $(\mathbf{I}-\tilde{\mathbf{G}}_0)^{-1}$,

$$\mathbf{G}_s(n)=(\mathbf{I}-\tilde{\mathbf{G}}_0)^{-1}\,\tilde{\mathbf{G}}_s(n),$$

$$\mathbf{V}\ =(\mathbf{I}-\tilde{\mathbf{G}}_0)^{-1}\,\mathbf{W}\,(\mathbf{I}-\tilde{\mathbf{G}}_0)^{-1},$$

where $\mathbf{I}$ is an identity matrix, therefore the instantaneous response form is equivalent to Equation (8). Since the variance-covariance matrix $\mathbf{W}$ is a diagonal matrix in the instantaneous response model, coefficients of each variable of the vector $\mathbf{y}_n$ can be estimated independently as a (*m*, *p*, *q*)-th order FFAR model with {*K*(*m*+*p*+*q*)+*k*} parameters, and for the maximum order of *m*, *M* (*M* ≥ *m*), the AIC of the *k*-th variable is

$$AIC(k)=(N-M)(\log 2\pi\hat{\sigma}^2_{mpq}(k)+1)+2\{K(m+P+Q)+k\}, \tag{6.10}$$

where $\hat{\sigma}^2_{mpq}(k)$ is the least residual variance of the model of the *k*-th variable and is determined by parameters *m*, *p* and *q* from the form of Equation (6.1), furthermore the AIC of the multivariate model is

$$AIC=\sum_{k=1}^{K}(N-M)(\log 2\pi\hat{\sigma}^2_{mpq}(k)+1)+2\{K(m+p+q)+k\}. \tag{6.11}$$

On the other hand, the indices (6.7) and (6.8) are approximated by the sum of the daily noise contribution over all frequencies $f_l=l/N$ (l = 0, …, [$N/2$]), where [x] represents the maximum integer of not more than x,

$$S_{njk}=\sum_{l=0}^{[N/2]}z_{njk}(f_l), \tag{6.12}$$

and the relative form of the index S_{njk},

$$R_{njk}=\frac{S_{njk}}{\sum_{k=1}^{K}S_{njk}}, \tag{6.13}$$

where, the denominator $\sum_{k=1}^{K}S_{njk}$ corresponds to $\sum_{l=0}^{[N/2]}p_{njj}(f_l)$. Furthermore R_{njk} is averaged for each month in a year, this is, the number of *n* can be transformed from the length of 40 years (14600) into the length of a year (365), because *n* can be represented as n - $365\cdot[n/366]$ from Fourier form $\sin\frac{2\pi j(n-m)}{365}$ and $\sin\frac{2\pi j(n-m)}{365}$ in Equation (6.1), and for { $R_{\tau_{\tilde{n}}jk}$; τ = 1, …12; $\tilde{n}$ = 1, 2, … , Λ_τ } with τ represents the

order of months in a year, Λ_τ = 31, 28, 31, 30, … , 31 are number of days in respective months,

$$\tilde{R}_{mjk} = \frac{1}{\Lambda_\tau} \sum_{\tilde{n}=1}^{\Lambda_\tau} R_{\tau_{\tilde{n}} jk} \,. \tag{6.14}$$

Hereafter we call the index the monthly averaged *SDNC* (**S**um of **D**aily **N**oise **C**ontribution over all frequencies) in this paper.

6.3 Analysis of Tokyo and Osaka

For analysis we selected the Tokyo station as a station representing stations in the east area of Japan and the Osaka station as a station representing stations in the west area of Japan. We will consider the relation between the Tokyo station and other 136 stations in Japan and the relation between the Osaka station and other 136 stations in Japan. Since the instability of the high dimensional model, the bivariate models are respectively applied to 136 bivariate datasets of the Tokyo station or the Osaka station and each other station, and the daily noise contributions are respectively estimated from coefficients of their models.

Table 6.1 shows the orders and the AIC values of applying MFFAR to the Tokyo station and other 136 stations in Japan. We select the Fukaura station (WMO code 47574) as a representative from the stations which the daily noise contribution for Tokyo is high through a year and show the seasonal change of the daily noise contribution of Fukaura in Figure 6.1, where each panel represents the daily noise contribution of the first day in each month, and in each panel the horizontal axis represents the frequency, the vertical axis represents values of the daily noise contribution and the shadow area represents the contribution of oneself for Tokyo. Figure 6.2 shows the daily relative noise contribution of Fukaura, where axes and explanatory notes correspond to Figure 6.1. Figure 6.3 shows monthly maps of the monthly averaged SDNC from other 136 stations to Tokyo; the values of the monthly averaged SDNC are shown in the section 6.5 Appendix (the later section of this chapter). In Figure 6.3 the stations are represented as the solid circles with color separated by values of the monthly averaged SDNC: the red corresponds to the value that is more than 0.4, the yellow corresponds to the value that is from 0.3 (exclusive) to 0.4 (inclusive), the green corresponds to the value that is from 0.2 (exclusive) to 0.3

Table 6.1. The orders and the AIC values of the MFFAR model applied to the Tokyo station between other stations, where m, p and q are orders in Equation (6.1).

WMO code	stations	orders m	p	q	AIC values	WMO code	stations	orders m	p	q	AIC values
47401	Wakkanai	10	2	2	62862.8	47402	Kitamiesashi	7	5	4	63968.4
47404	Haboro	10	2	2	64479.7	47405	Omu	7	5	4	65174.9
47406	Rumoi	9	3	2	64327.3	47407	Asahikawa	9	3	3	63964.7
47409	Abashiri	10	2	2	64486.2	47411	Otaru	9	2	2	63696.6
47412	Sapporo	9	2	2	63117.8	47413	Iwamizawa	9	2	2	62937.5
47417	Obihiro	10	5	4	65259.4	47418	Kushiro	10	3	3	64608.7
47420	Nemuro	10	3	3	64839.9	47421	Suttsu	10	2	2	62879.7
47423	Muroran	9	3	3	62997.2	47424	Tomakomai	10	3	3	63731.0
47426	Urakawa	10	2	2	62749.4	47428	Esashi	9	2	2	62837.6
47430	Hakodate	10	2	2	61488.8	47433	Kutchan	10	2	2	63499.3
47435	Mombetsu	10	2	2	64569.6	47440	Hiroo	10	2	2	66195.4
47520	Shinjo	10	3	2	60643.5	47570	Wakamatsu	5	6	6	59742.3
47574	Fukaura	9	2	2	62829.4	47575	Aomori	10	2	2	61331.4
47576	Mutsu	10	2	2	61876.0	47581	Hachinohe	11	3	3	61520.2
47582	Akita	9	3	3	61940.5	47584	Morioka	11	2	2	59106.1
47585	Miyako	10	2	2	61466.6	47587	Sakata	9	2	2	60962.5
47588	Yamagata	10	2	2	57911.5	47590	Sendai	10	2	2	55448.0
47592	Ishinomaki	11	3	3	56395.1	47595	Fukushima	12	2	2	54238.1
47597	Shirakawa	10	2	2	50387.3	47600	Wajima	10	2	2	61193.6
47602	Aikawa	8	5	5	61404.6	47604	Niigata	9	2	2	59552.6
47605	Kanazawa	9	2	2	59954.8	47606	Fushiki	9	2	2	60140.9
47607	Toyama	10	2	2	59996.8	47610	Nagano	10	2	2	58672.9
47612	Takada	9	2	2	61057.4	47615	Utsunomiya	10	3	2	46346.2
47616	Fukui	4	5	5	59802.0	47617	Takayama	10	2	2	60952.2
47618	Matsumoto	10	2	2	59216.1	47620	Suwa	10	2	2	57643.9
47624	Maebashi	5	6	6	46945.1	47626	Kumagaya	10	2	2	43041.1
47629	Mito	10	2	2	48311.4	47631	Tsuruga	4	5	5	60619.3
47632	Gifu	7	3	2	58703.2	47636	Nagoya	10	2	2	57897.9
47637	Iida	10	2	2	60662.9	47638	Kofu	10	3	3	56653.1
47640	Kawaguchiko	10	2	2	54255.5	47641	Chichibu	11	2	2	50633.6
47648	Choshi	16	2	2	53314.7	47649	Ueno	10	2	2	60254.1
47651	Tsu	10	3	2	60339.5	47653	Irako	10	3	2	58411.2
47654	Hamamatsu	9	3	2	57306.3	47655	Omaezaki	10	2	2	56798.8

WMO code	stations	orders m	p	q	AIC values	WMO code	stations	orders m	p	q	AIC values
47656	Shizuoka	10	2	2	57079.9	47657	Mishima	10	2	1	55013.3
47663	Owase	10	2	2	61603.1	47666	Irozaki	14	2	2	52292.3
47668	Ajiro	10	2	2	46914.1	47670	Yokohama	15	2	2	27641.2
47674	Katsuura	10	2	2	53174.8	47675	Oshima	20	2	2	50424.8
47678	Hachijojima	11	2	2	62426.0	47690	Nikko	10	2	2	54201.3
47740	Saigo	9	3	3	61649.5	47741	Matsue	10	2	2	60524.8
47742	Sakai	10	2	2	60917.3	47744	Yonago	10	2	2	61254.1
47746	Tottori	10	2	2	61149.5	47747	Toyooka	10	2	2	60874.4
47750	Maizuru	10	2	2	60993.8	47754	Hagi	10	2	2	62444.1
47755	Hamada	10	2	2	61994.9	47756	Tsuyama	11	2	2	61808.0
47759	Kyoto	10	2	2	58699.3	47761	Hikone	10	2	2	59636.1
47762	Shimonoseki	14	2	2	61695.5	47765	Hiroshima	16	2	2	61792.9
47766	Kure	10	2	2	61600.6	47768	Okayama	14	2	2	60871.3
47769	Himeji	10	2	2	60293.1	47770	Kobe	10	2	2	59222.8
47772	Osaka	10	2	2	58632.7	47776	Sumoto	10	2	2	59699.5
47777	Wakayama	6	5	5	60772.9	47778	Shionomisaki	10	2	2	60969.7
47780	Nara	10	2	2	59598.0	47800	Izuhara	10	2	2	62479.2
47805	Hirado	10	2	2	61629.0	47807	Fukuoka	10	2	2	61404.1
47809	Iizuka	5	5	5	61924.3	47812	Sasebo	9	3	3	62383.7
47813	Saga	12	2	2	61615.6	47814	Hita	3	5	5	62598.8
47815	Oita	10	2	2	64016.9	47817	Nagasaki	7	5	5	62443.1
47819	Kumamoto	6	5	5	62278.8	47821	Asosan	10	2	2	62161.6
47823	Akune	7	5	5	63080.5	47824	Hitoyoshi	10	2	2	64040.2
47827	Kagoshima	10	2	2	62783.1	47829	Miyakonojo	10	3	3	63478.9
47830	Miyazaki	10	2	2	64019.8	47831	Makurazaki	10	3	2	63498.5
47835	Aburatsu	10	2	2	64004.1	47836	Yakushima	13	1	1	64580.1
47837	Tanegashima	10	2	2	63484.4	47838	Ushibuka	5	5	5	62502.9
47887	Matsuyama	10	2	2	61860.2	47890	Tadotsu	10	2	2	62600.1
47891	Takamatsu	10	2	2	62381.5	47892	Uwajima	13	2	2	62865.1
47893	Kochi	10	2	2	62859.0	47895	Tokushima	10	2	2	61680.3
47897	Sukumo	10	2	2	63374.8	47898	Shimizu	10	3	3	62813.9
47899	Murotomisaki	10	2	2	61515.6	47909	Naze	10	3	3	64400.4
47912	Yonagunijima	6	3	2	63817.6	47918	Ishigakijima	10	2	2	63384.0
47927	Miyakojima	10	2	2	63588.6	47929	Kumejima	10	2	2	63472.7
47936	Naha	10	3	3	62766.0	47945	Minamidaitojima	10	3	2	64100.3

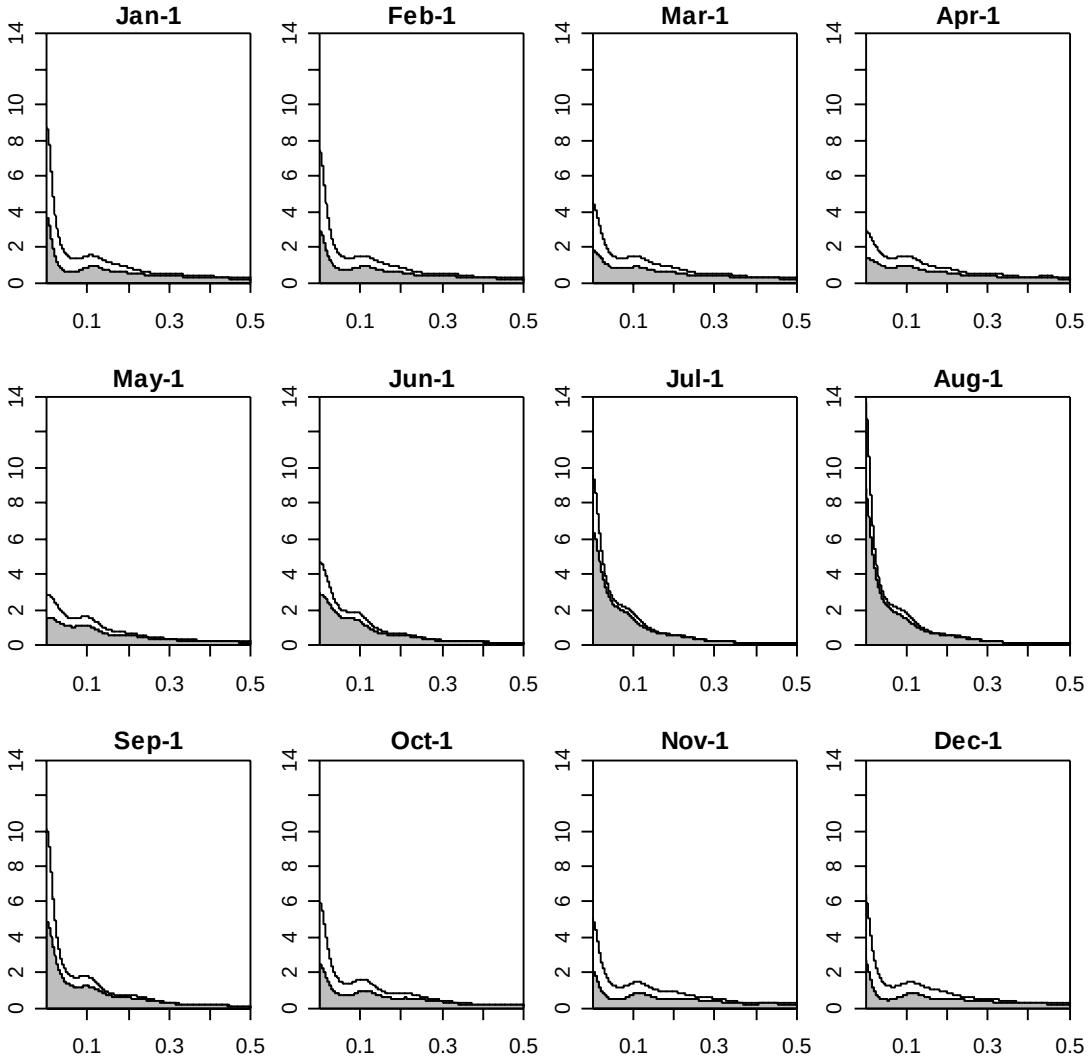

Figure 6.1. The daily noise contribution of Fukaura. Each panel represents the daily noise contribution of the first day in each month, and in each panel the horizontal axis represents the frequency, the vertical axis represents values of the daily noise contribution and the shadow area represents the contribution of oneself for Tokyo.

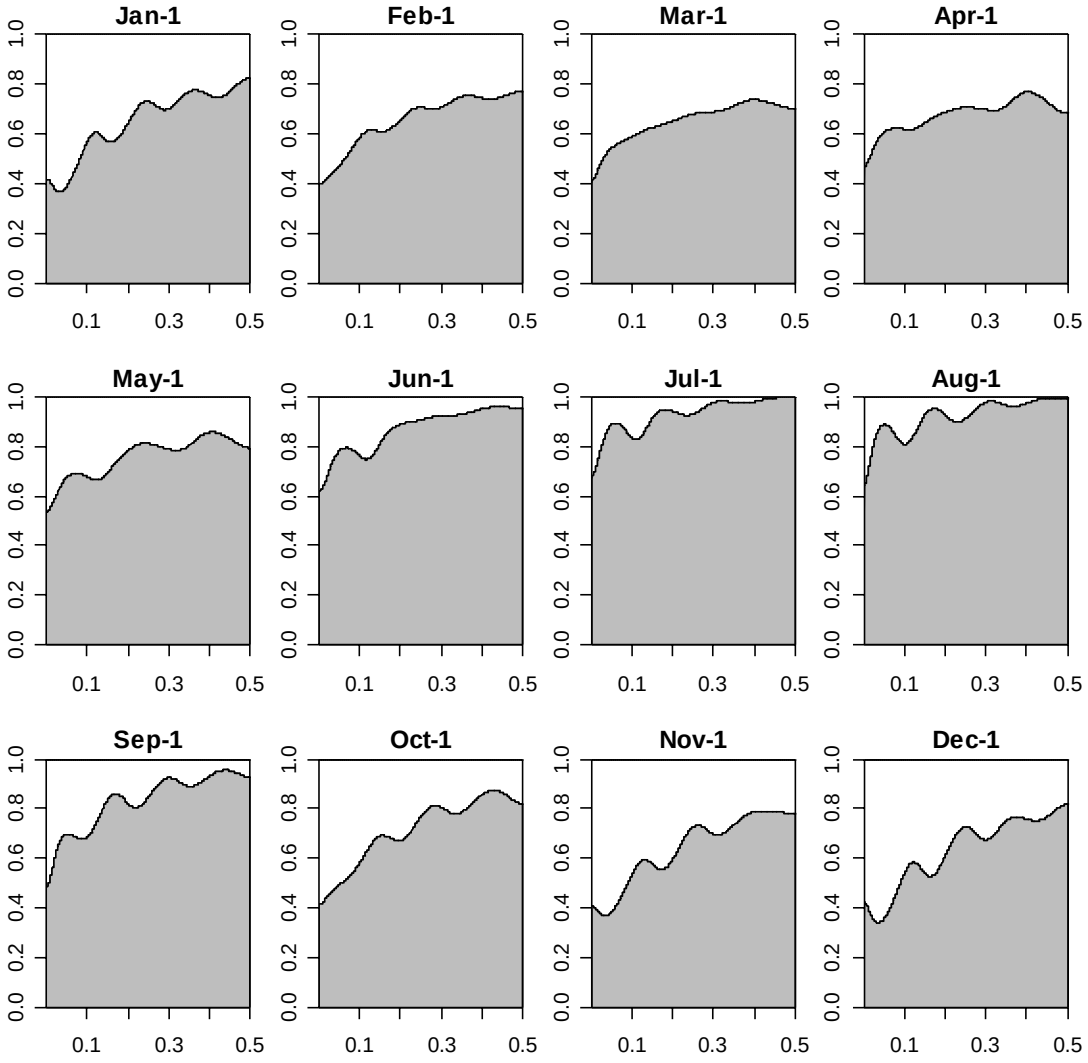

Figure 6.2. The daily relative noise contribution of Fukaura. Each panel represents the daily relative noise contribution of the first day in each month, and in each panel the horizontal axis represents the frequency, the vertical axis represents values of the daily relative noise contribution and the shadow area represents the contribution of oneself for Tokyo.

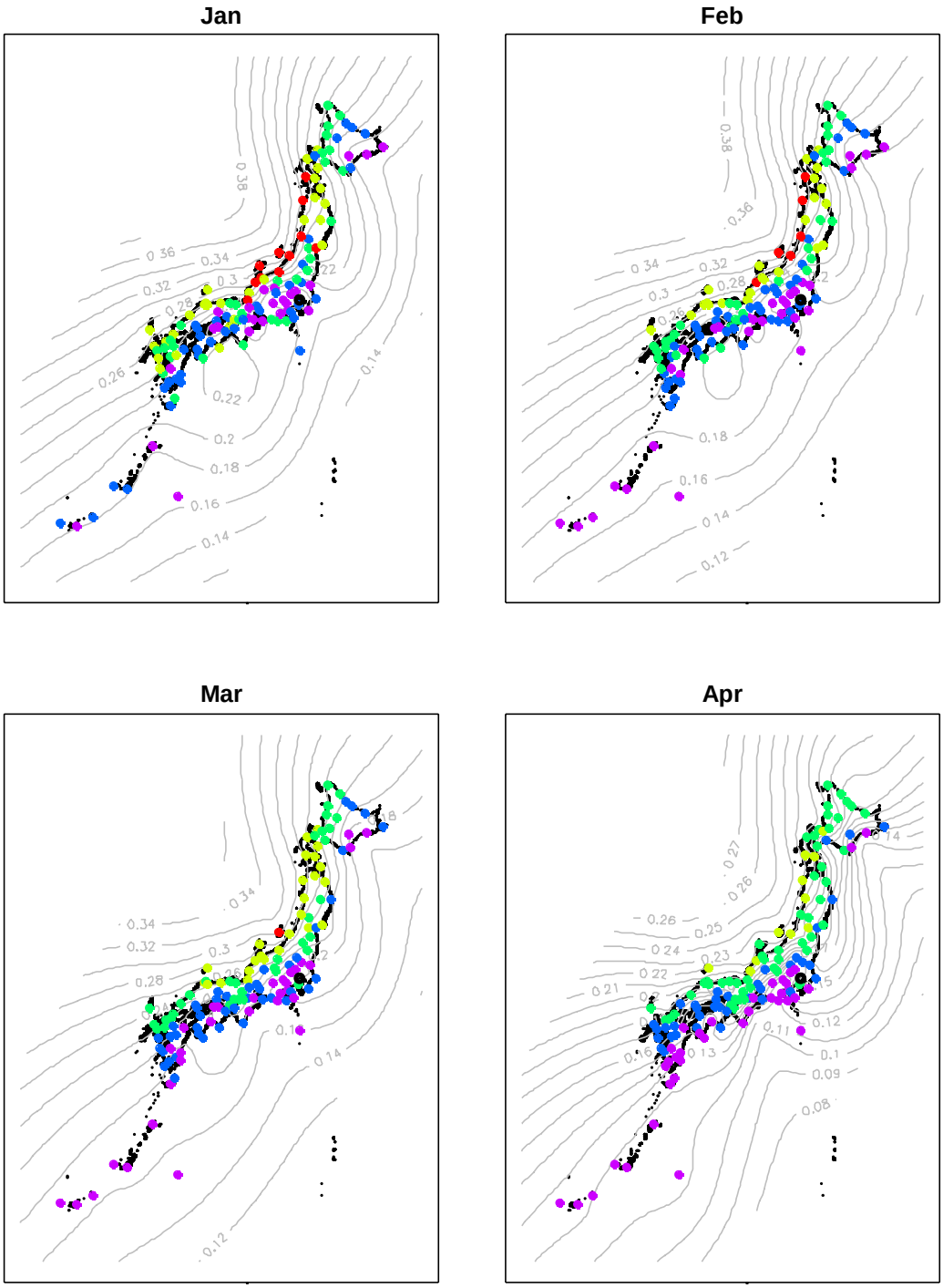

Figure 6.3-1 The monthly maps (from January until April) of the monthly averaged SDNC from other 136 stations to Tokyo, where the stations are represented as the solid circles with color separated by values of the monthly averaged SDNC: the red corresponds to the value that is more than 0.4, the yellow corresponds to the value that is from 0.3 (exclusive) to 0.4 (inclusive), the green corresponds to the value that is from 0.2 (exclusive) to 0.3 (inclusive), the blue corresponds to the value that is from 0.1 (exclusive) to 0.2 (inclusive), the violet corresponds to the value that is equal to or less than 0.1 and the black is the Tokyo station.

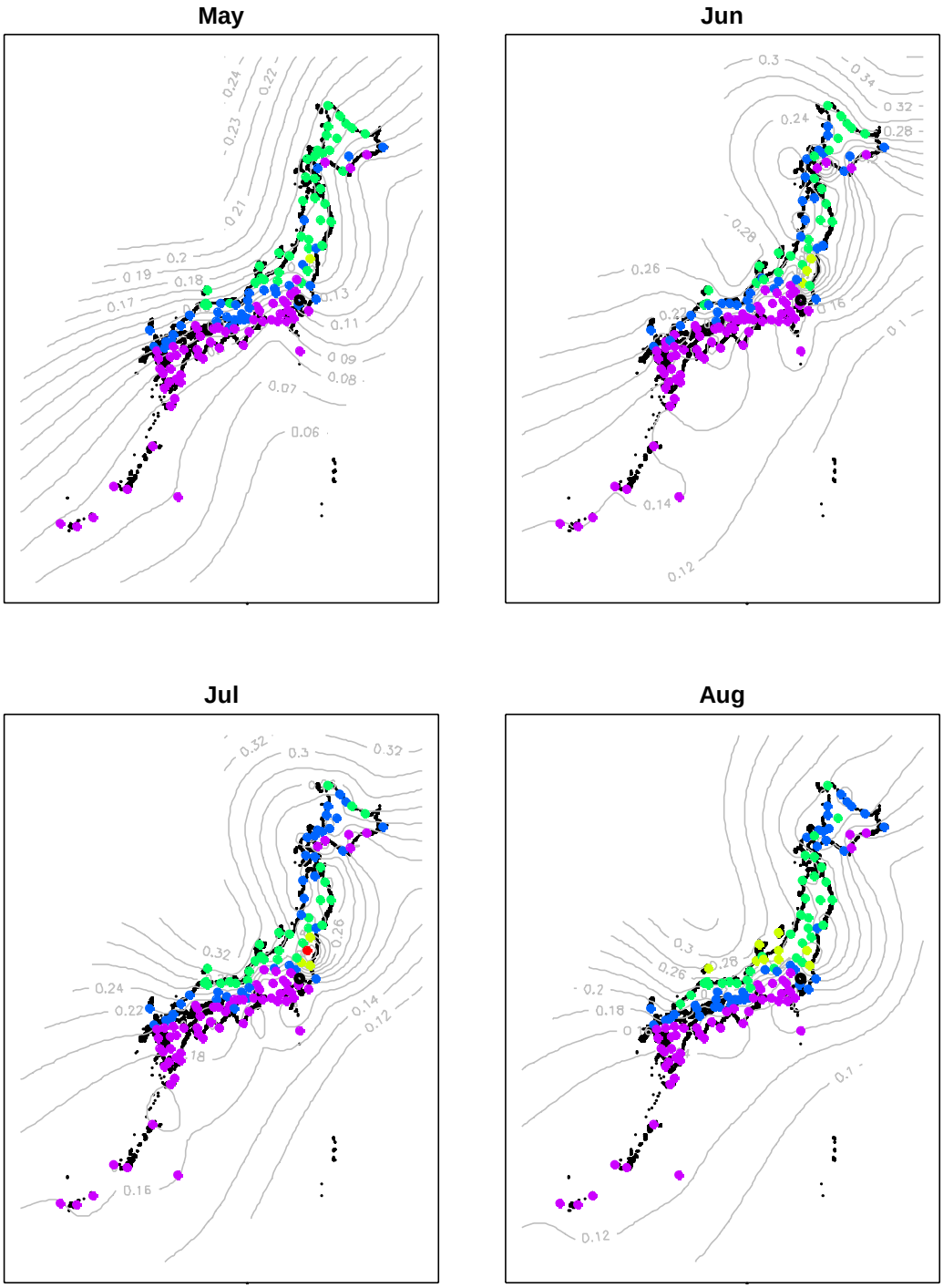

Figure 6.3-2 The monthly maps (from May until August) of the monthly averaged SDNC from other 136 stations to Tokyo, where the stations are represented as the solid circles with color separated by values of the monthly averaged SDNC: the red corresponds to the value that is more than 0.4, the yellow corresponds to the value that is from 0.3 (exclusive) to 0.4 (inclusive), the green corresponds to the value that is from 0.2 (exclusive) to 0.3 (inclusive), the blue corresponds to the value that is from 0.1 (exclusive) to 0.2 (inclusive), the violet corresponds to the value that is equal to or less than 0.1 and the black is the Tokyo station.

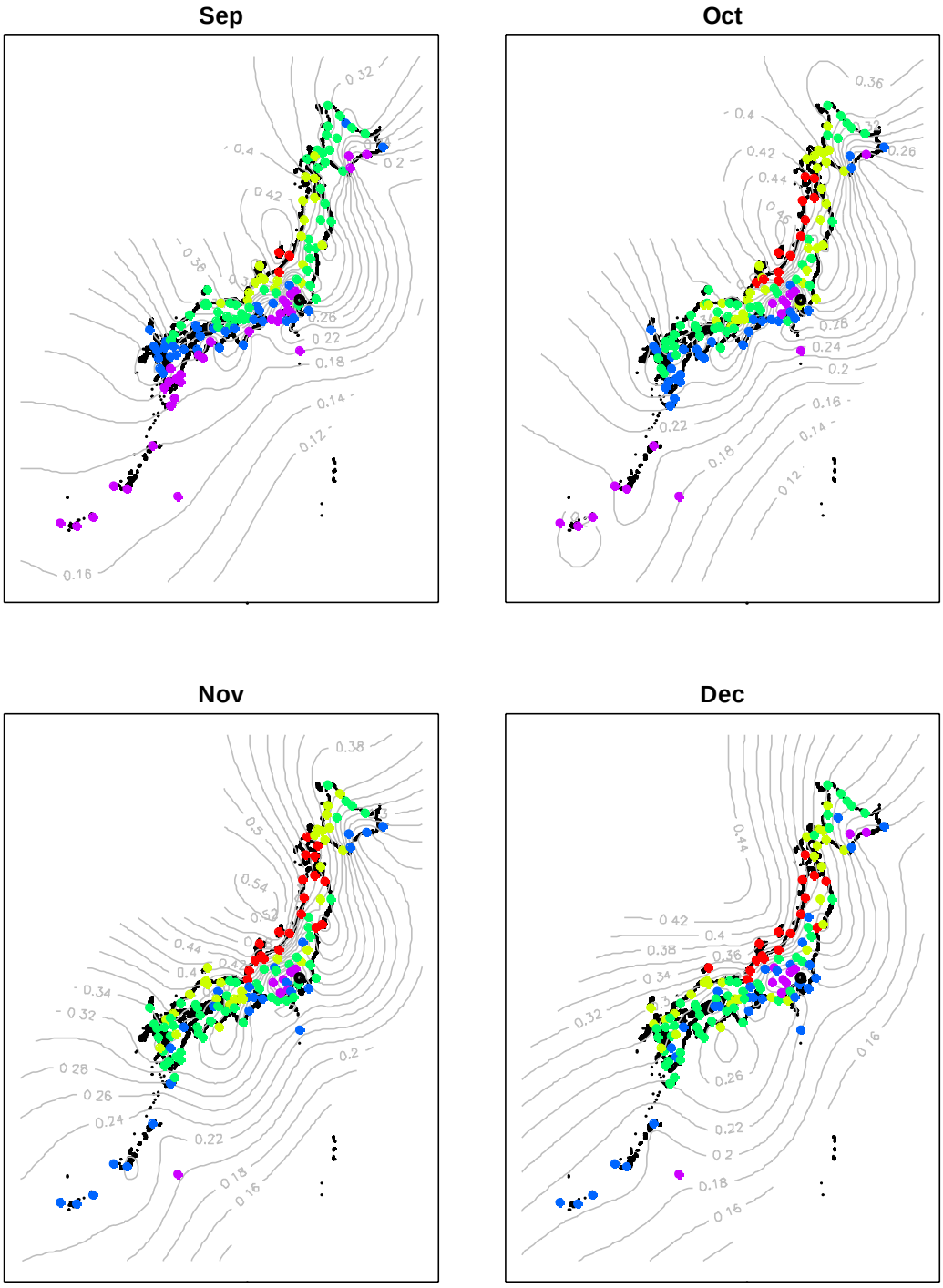

Figure 6.3-3. The monthly maps (from September until December) of the monthly averaged SDNC from other 136 stations to Tokyo, where the stations are represented as the solid circles with color separated by values of the monthly averaged SDNC: the red corresponds to the value that is more than 0.4, the yellow corresponds to the value that is from 0.3 (exclusive) to 0.4 (inclusive), the green corresponds to the value that is from 0.2 (exclusive) to 0.3 (inclusive), the blue corresponds to the value that is from 0.1 (exclusive) to 0.2 (inclusive), the violet corresponds to the value that is equal to or less than 0.1 and the black is the Tokyo station.

(inclusive), the blue corresponds to the value that is from 0.1 (exclusive) to 0.2 (inclusive), the violet corresponds to the value that is equal to or less than 0.1 and the black is the Tokyo station, and the contour is estimate by the thin plate spline regression (for example, see Green and Silverman (1994)), where the smoothing parameter is adjusted by GCV (the Generalized Cross Validation), and the value is scaled by the range between the minimum and maximum values. From Figure 6.3 we can obtain the following recognition. The stations of which values of the monthly averaged SDNC is more than 0.4 is confirmed in a cold season (October, November, December, January and February) and their stations is located on the Sea of Japan side in the northern part of Honshu Island. In particular in November and December, the stations of which values of the monthly averaged SDNC is less than 0.1, this is the violet circles, seldom exist and the value of the monthly averaged SDNC of each station is high as a whole. The propagation of influence estimated from the contour is from the northwest in December, January, February, March, April and May, on the other hand, the core areas on the contour exist locally around the Tohoku region in Jun, July, August, September, October and November. This suggests that summer and autumn differ from winter and spring as for the climatic system that influence to temperature of Tokyo.

Table 6.2 shows the orders and the AIC values of applying MFFAR to the Osaka station and other 136 stations in Japan. We select the Shimonoseki station (WMO code 47762) as a representative from the stations which the daily noise contribution for Osaka is high through a year and show the seasonal change of the daily noise contribution of Shimonoseki in Figure 6.4, where each panel represents the daily noise contribution of the first day in each month, and in each panel the horizontal axis represents the frequency, the vertical axis represents values of the daily noise contribution and the shadow area represents the contribution of oneself for Osaka. Figure 6.5 shows the daily relative noise contribution of Shimonoseki, where axes and explanatory notes correspond to Figure 6.4. Figure 6.6 shows monthly maps of the monthly averaged SDNC from other 136 stations to Osaka and explanatory notes are the same as Figure 6.3; the values of the monthly averaged SDNC are shown in the section 6.5 Appendix (the later section of this chapter). From Figure 6.6 we can obtain the following recognition. The stations of which values of the monthly averaged SDNC are more than 0.4 are confirmed in a cold season (November, December, January and February) and their stations is located in the west of Japan. The propagation of influence estimated from the contour is from the west-northwest in all season. It seems that the seasonal variation in Osaka is poorer than that of Tokyo.

Table 6.2. The orders and the AIC values of the MFFAR model applied to the Osaka station between other stations, where *m*, *p* and *q* are orders in Equation (6.1).

WMO code	stations	orders *m*	*p*	*q*	AIC values	WMO code	stations	orders *m*	*p*	*q*	AIC values
47401	Wakkanai	9	2	2	61375.6	47402	Kitamiesashi	9	2	2	62449.5
47404	Haboro	8	3	2	63302.6	47405	Omu	9	2	2	63747.1
47406	Rumoi	8	3	2	63115.8	47407	Asahikawa	9	3	3	62579.8
47409	Abashiri	9	2	2	63319.8	47411	Otaru	9	2	2	62723.1
47412	Sapporo	9	2	2	62102.4	47413	Iwamizawa	9	2	2	62034.9
47417	Obihiro	9	3	3	64185.8	47418	Kushiro	9	3	3	63888.5
47420	Nemuro	9	3	3	63721.3	47421	Suttsu	9	2	2	61959.9
47423	Muroran	9	2	2	62213.5	47424	Tomakomai	9	3	3	63300.1
47426	Urakawa	15	2	2	62711.1	47428	Esashi	9	3	2	62179.7
47430	Hakodate	9	2	2	61146.2	47433	Kutchan	9	3	2	62806.2
47435	Mombetsu	9	2	2	63256.9	47440	Hiroo	9	2	2	65454.5
47520	Shinjo	8	3	2	60108.1	47570	Wakamatsu	8	3	2	57692.9
47574	Fukaura	9	3	2	62046.2	47575	Aomori	11	2	2	61107.4
47576	Mutsu	9	2	2	62015.5	47581	Hachinohe	13	2	2	61862.8
47582	Akita	9	3	2	61127.4	47584	Morioka	8	3	2	59755.6
47585	Miyako	13	3	2	62775.5	47587	Sakata	13	3	2	60306.3
47588	Yamagata	5	4	4	59421.2	47590	Sendai	11	2	2	60588.9
47592	Ishinomaki	11	2	2	59847.5	47595	Fukushima	11	2	2	59746.6
47597	Shirakawa	10	2	2	57628.9	47600	Wajima	9	3	2	57838.3
47602	Aikawa	9	3	2	60070.7	47604	Niigata	9	4	4	57819.0
47605	Kanazawa	5	5	5	53698.1	47606	Fushiki	16	2	2	54934.8
47607	Toyama	9	3	2	55545.1	47610	Nagano	8	4	4	53128.6
47612	Takada	9	3	2	58149.8	47615	Utsunomiya	13	2	2	56851.5
47616	Fukui	5	5	5	50922.9	47617	Takayama	8	3	2	51854.6
47618	Matsumoto	6	5	5	54064.6	47620	Suwa	6	5	5	50850.8
47624	Maebashi	6	5	5	57321.0	47626	Kumagaya	10	2	2	58841.2
47629	Mito	13	2	2	58367.4	47631	Tsuruga	13	2	2	51186.8
47632	Gifu	8	4	4	46399.9	47636	Nagoya	15	1	1	45462.8
47637	Iida	6	5	5	53558.1	47638	Kofu	8	2	2	56193.0
47640	Kawaguchiko	3	6	5	56956.1	47641	Chichibu	8	2	2	57927.6
47648	Choshi	15	2	2	57880.5	47649	Ueno	11	2	2	40913.1
47651	Tsu	12	4	3	48856.3	47653	Irako	13	2	1	47654.3
47654	Hamamatsu	5	4	4	51231.5	47655	Omaezaki	13	2	2	51932.0

WMO code	stations	orders m	p	q	AIC values	WMO code	stations	orders m	p	q	AIC values
47656	Shizuoka	3	5	5	56547.0	47657	Mishima	6	5	5	56309.0
47662	Tokyo	9	2	2	58629.6	47663	Owase	5	4	4	53290.3
47666	Irozaki	13	2	2	55457.9	47668	Ajiro	9	3	2	57901.2
47670	Yokohama	9	2	2	58859.3	47674	Katsuura	9	3	2	58422.7
47675	Oshima	13	2	2	57572.7	47678	Hachijojima	9	2	2	57995.2
47690	Nikko	16	3	2	56291.0	47740	Saigo	13	3	2	55510.1
47741	Matsue	13	3	2	51719.9	47742	Sakai	16	2	2	52482.3
47744	Yonago	13	3	2	53874.6	47746	Tottori	13	3	2	52897.0
47747	Toyooka	13	3	2	51417.1	47750	Maizuru	13	2	2	50443.5
47754	Hagi	8	3	2	55256.4	47755	Hamada	5	4	4	54808.0
47756	Tsuyama	13	2	2	48308.0	47759	Kyoto	18	1	1	31113.2
47761	Hikone	12	2	2	43626.5	47762	Shimonoseki	5	5	5	53232.1
47765	Hiroshima	14	2	2	51024.7	47766	Kure	9	4	4	50403.2
47768	Okayama	20	3	2	43638.2	47769	Himeji	6	5	5	39956.0
47770	Kobe	13	3	2	31900.0	47776	Sumoto	14	3	2	39404.3
47777	Wakayama	12	3	2	41283.1	47778	Shionomisaki	7	4	4	52357.2
47780	Nara	15	2	2	29525.8	47800	Izuhara	9	2	2	56898.3
47805	Hirado	11	2	2	55316.5	47807	Fukuoka	6	3	2	54233.0
47809	Iizuka	16	2	1	54021.9	47812	Sasebo	10	2	2	55673.6
47813	Saga	13	2	2	54198.4	47814	Hita	13	2	2	54975.2
47815	Oita	7	5	5	55932.6	47817	Nagasaki	6	3	2	55815.7
47819	Kumamoto	3	5	5	55130.3	47821	Asosan	13	3	2	55543.5
47823	Akune	16	3	2	57051.0	47824	Hitoyoshi	5	5	5	58508.6
47827	Kagoshima	9	2	2	57308.9	47829	Miyakonojo	9	3	3	58034.5
47830	Miyazaki	9	3	3	58263.6	47831	Makurazaki	13	3	2	58178.0
47835	Aburatsu	9	3	2	58622.1	47836	Yakushima	11	3	2	59998.0
47837	Tanegashima	11	3	2	58381.8	47838	Ushibuka	5	5	5	56142.5
47887	Matsuyama	13	3	2	50496.8	47890	Tadotsu	14	2	2	49566.6
47891	Takamatsu	13	4	3	47563.1	47892	Uwajima	16	2	2	54488.8
47893	Kochi	9	3	2	53832.7	47895	Tokushima	10	3	3	45733.5
47897	Sukumo	13	2	2	55583.6	47898	Shimizu	9	3	3	54974.0
47899	Murotomisaki	11	2	2	51666.9	47909	Naze	6	5	5	60580.8
47912	Yonagunijima	10	3	3	60260.4	47918	Ishigakijima	6	5	5	59928.9
47927	Miyakojima	10	3	2	60112.2	47929	Kumejima	6	5	5	59907.9
47936	Naha	6	5	5	59101.2	47945	Minamidaitojima	9	2	2	60784.1

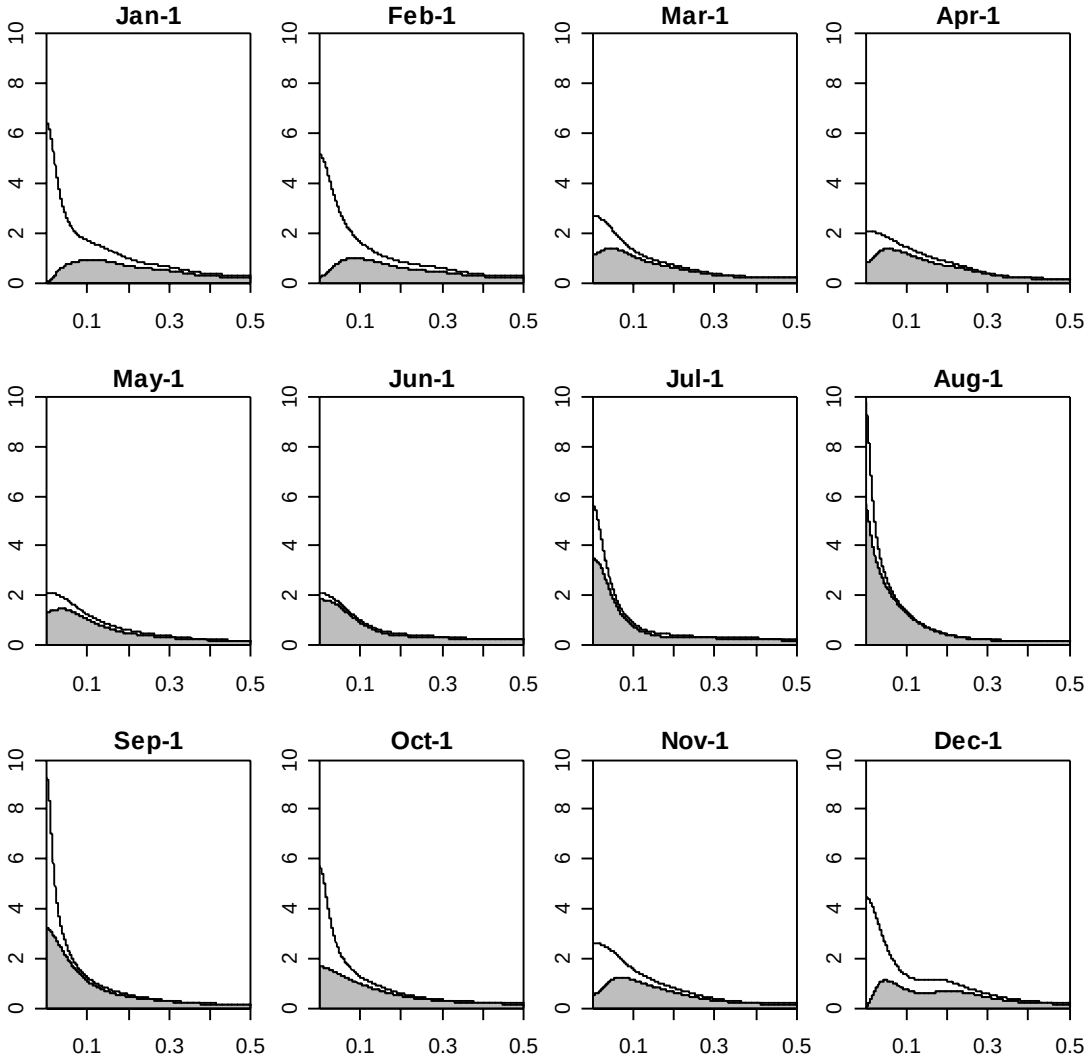

Figure 6.4. The daily noise contribution of Shimonoseki. Each panel represents the daily noise contribution of the first day in each month, and in each panel the horizontal axis represents the frequency, the vertical axis represents values of the daily noise contribution and the shadow area represents the contribution of oneself for Osaka.

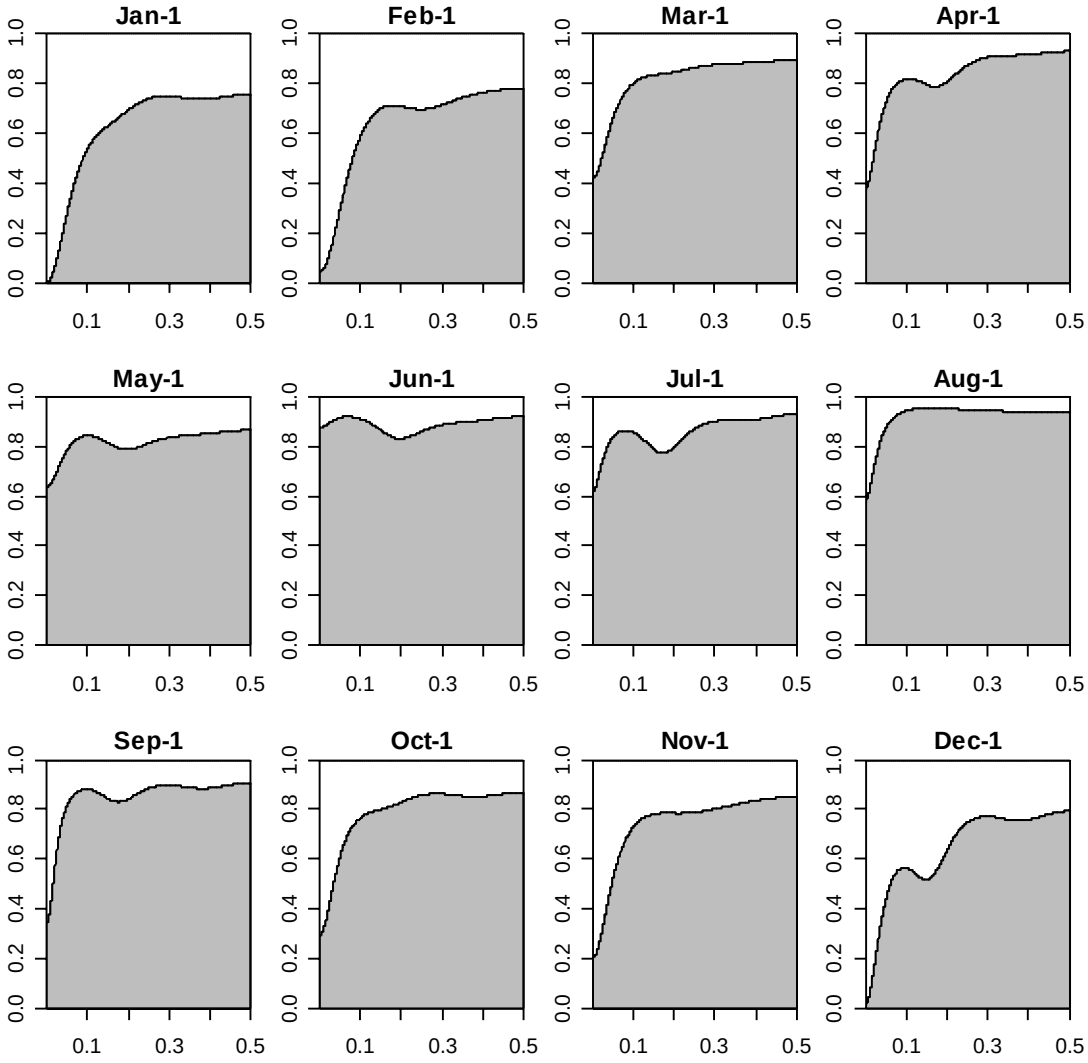

Figure 6.5. The daily relative noise contribution of Shimonoseki. Each panel represents the daily relative noise contribution of the first day in each month, and in each panel the horizontal axis represents the frequency, the vertical axis represents values of the daily relative noise contribution and the shadow area represents the contribution of oneself for Osaka.

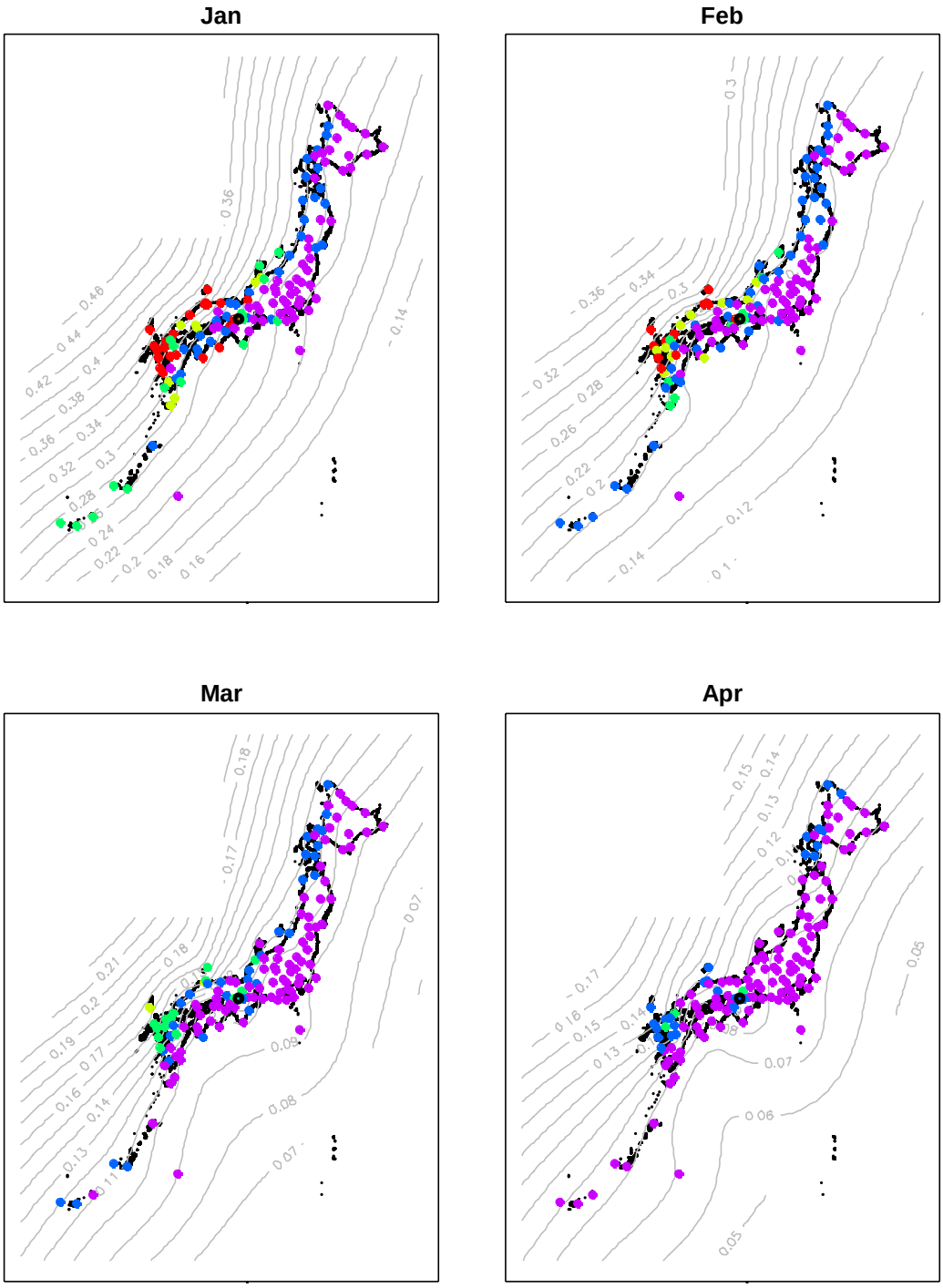

Figure 6.6-1 The monthly maps (from January until April) of the monthly averaged SDNC from other 136 stations to Osaka, where the stations are represented as the solid circles with color separated by values of the monthly averaged SDNC: the red corresponds to the value that is more than 0.4, the yellow corresponds to the value that is from 0.3 (exclusive) to 0.4 (inclusive), the green corresponds to the value that is from 0.2 (exclusive) to 0.3 (inclusive), the blue corresponds to the value that is from 0.1 (exclusive) to 0.2 (inclusive), the violet corresponds to the value that is equal to or less than 0.1 and the black is the Osaka station.

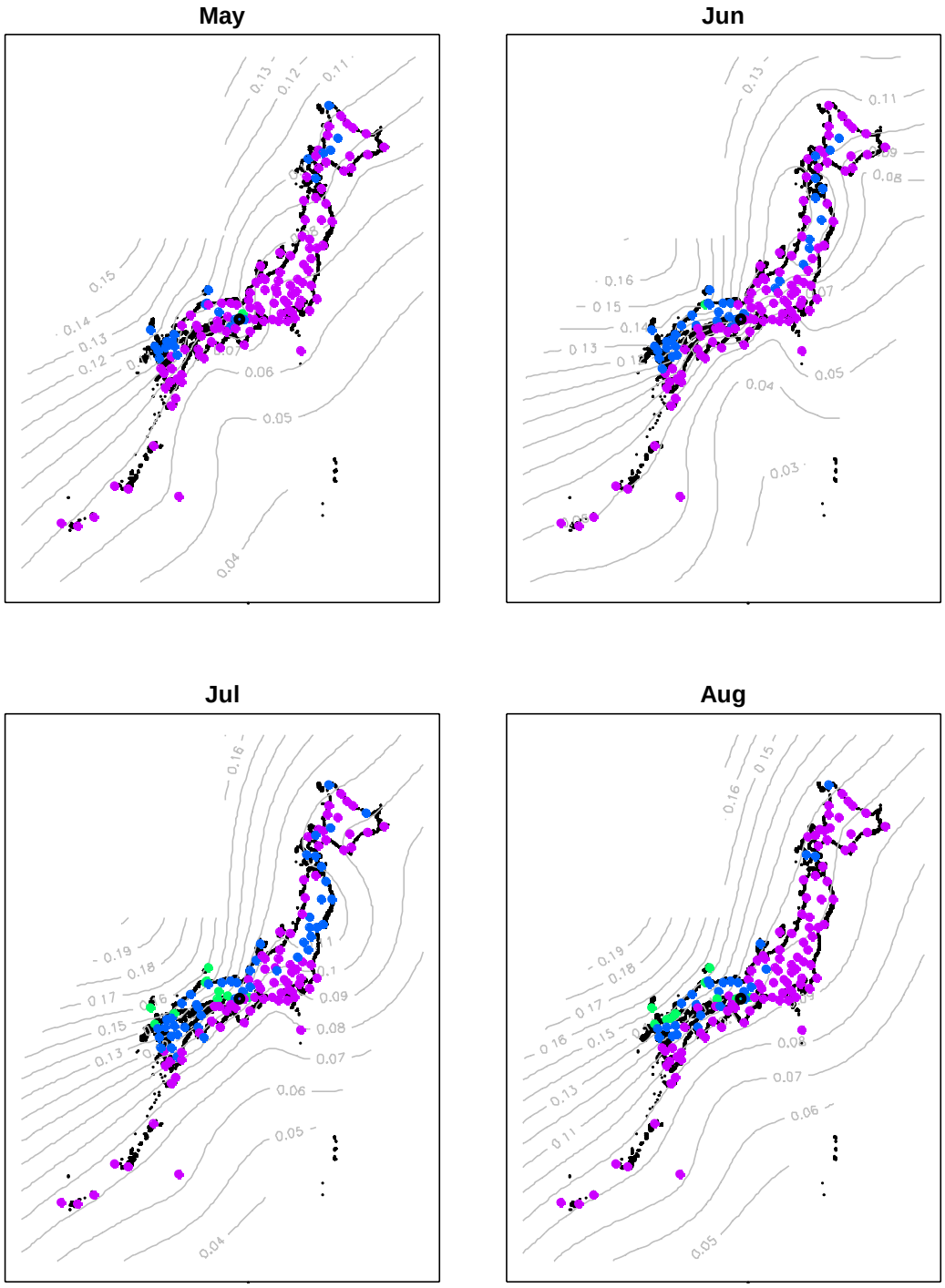

Figure 6.6-2 The monthly maps (from May until August) of the monthly averaged SDNC from other 136 stations to Osaka, where the stations are represented as the solid circles with color separated by values of the monthly averaged SDNC: the red corresponds to the value that is more than 0.4, the yellow corresponds to the value that is from 0.3 (exclusive) to 0.4 (inclusive), the green corresponds to the value that is from 0.2 (exclusive) to 0.3 (inclusive), the blue corresponds to the value that is from 0.1 (exclusive) to 0.2 (inclusive), the violet corresponds to the value that is equal to or less than 0.1 and the black is the Osaka station.

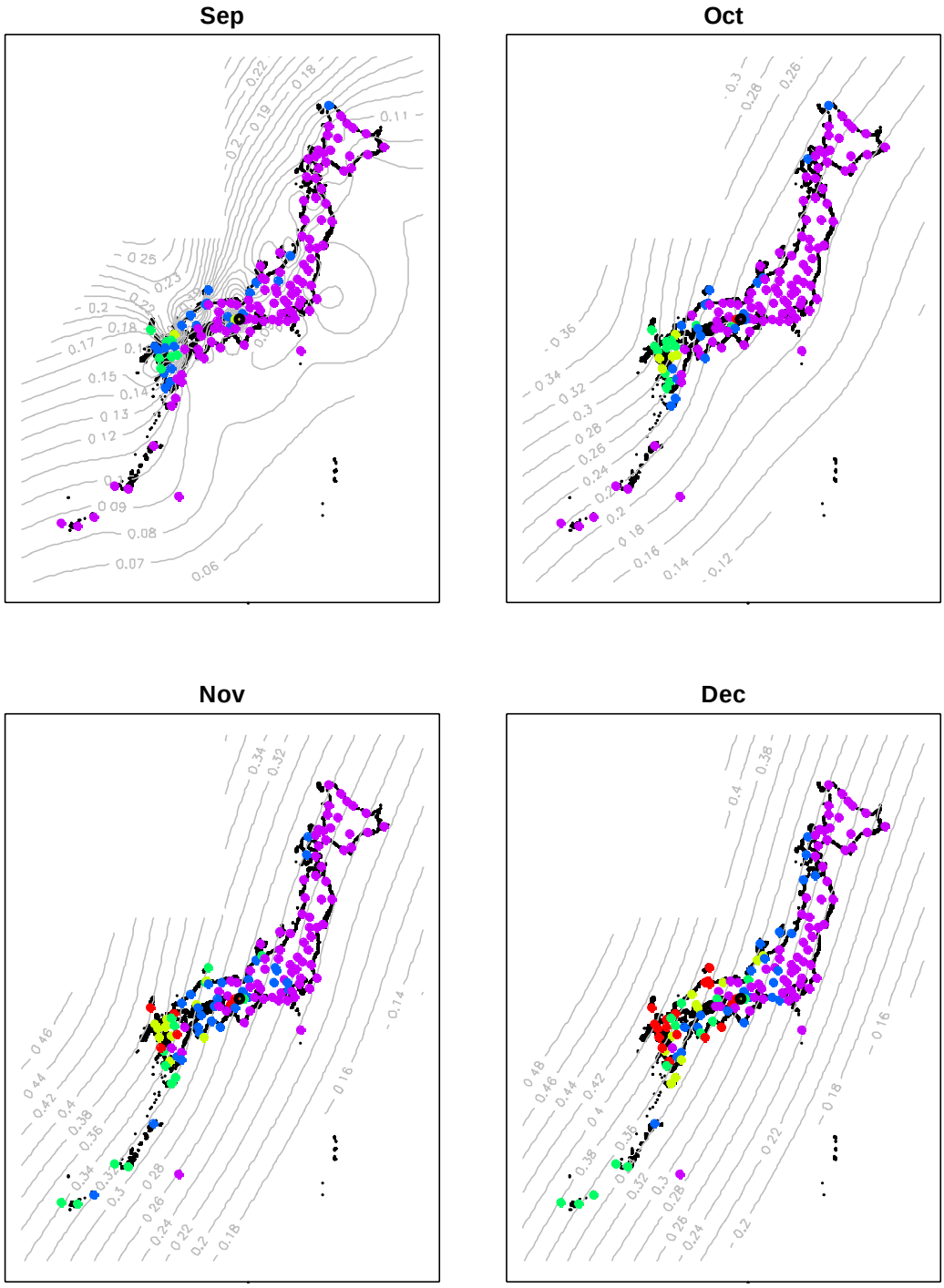

Figure 6.6-3. The monthly maps (from September until December) of the monthly averaged SDNC from other 136 stations to Osaka, where the stations are represented as the solid circles with color separated by values of the monthly averaged SDNC: the red corresponds to the value that is more than 0.4, the yellow corresponds to the value that is from 0.3 (exclusive) to 0.4 (inclusive), the green corresponds to the value that is from 0.2 (exclusive) to 0.3 (inclusive), the blue corresponds to the value that is from 0.1 (exclusive) to 0.2 (inclusive), the violet corresponds to the value that is equal to or less than 0.1 and the black is the Osaka station.

From analysis of the Tokyo station and the Osaka station, we can recognize that the area that influence to a station is not always close locally and the propagation and the pattern of influence are various according to the area and the season. This suggests the existence of the seasonal relation and pattern of local teleconnection. By examining such relations carefully, we may find clues to the detection of other useful exogenous factors in the prediction of temperature. Therefore it is expected that the detailed investigation of the infuluence and the causality presents greatfully available knowledge in terms of the prediction of temperature and the method of analysys as mentioned above can be a useful tool for the invetigation.

On the other hamd, Figure 6.7 shows monthly maps of the monthly averaged SDNC from Tokyo to other 136 stations and Figure 6.8 shows monthly maps of the monthly averaged SDNC from Osaka to other 136 stations, where explanatory notes are the same as Figure 6.3 and Figure 6.6 respectively. The values of the monthly averaged SDNC from Tokyo to other 136 stations and from Osaka to other 136 stations are shown in the section 6.5 Appendix (the later section of this chapter). In their maps we attract the feature that the area to which Tokyo influence is limited extremely in comparison with Osaka.

Here, we propose an idea of the usage of maps such as Figure 6.7 and Figure 6.8 from the viewpoint of weather risk management. There is the issue of the *basis risk* in the trade of weather derivatives that can hedge the weather risk. It is the risk due to the contract being written by weather index, such as temperature, in a different location than the area that the user wishes to cover. Since the indices of weather derivatives are often used the values of weather variables in big cities such as Tokyo and Osaka which much contacts are made a deal, the mismatched contact between the area and the index may be made a deal. In such a case, the information of the area that provides the index for the area that the weather risk exists is useful. For example, one can control the amount and the propriety of dealing according to the degree of the influence and the risk. The SDNC is the quantitative measure of the causality and, as for the maps such as Figure 6.7 and Figure 6.8, the practical use is expected as the information that represents potential basis risk quantitatively.

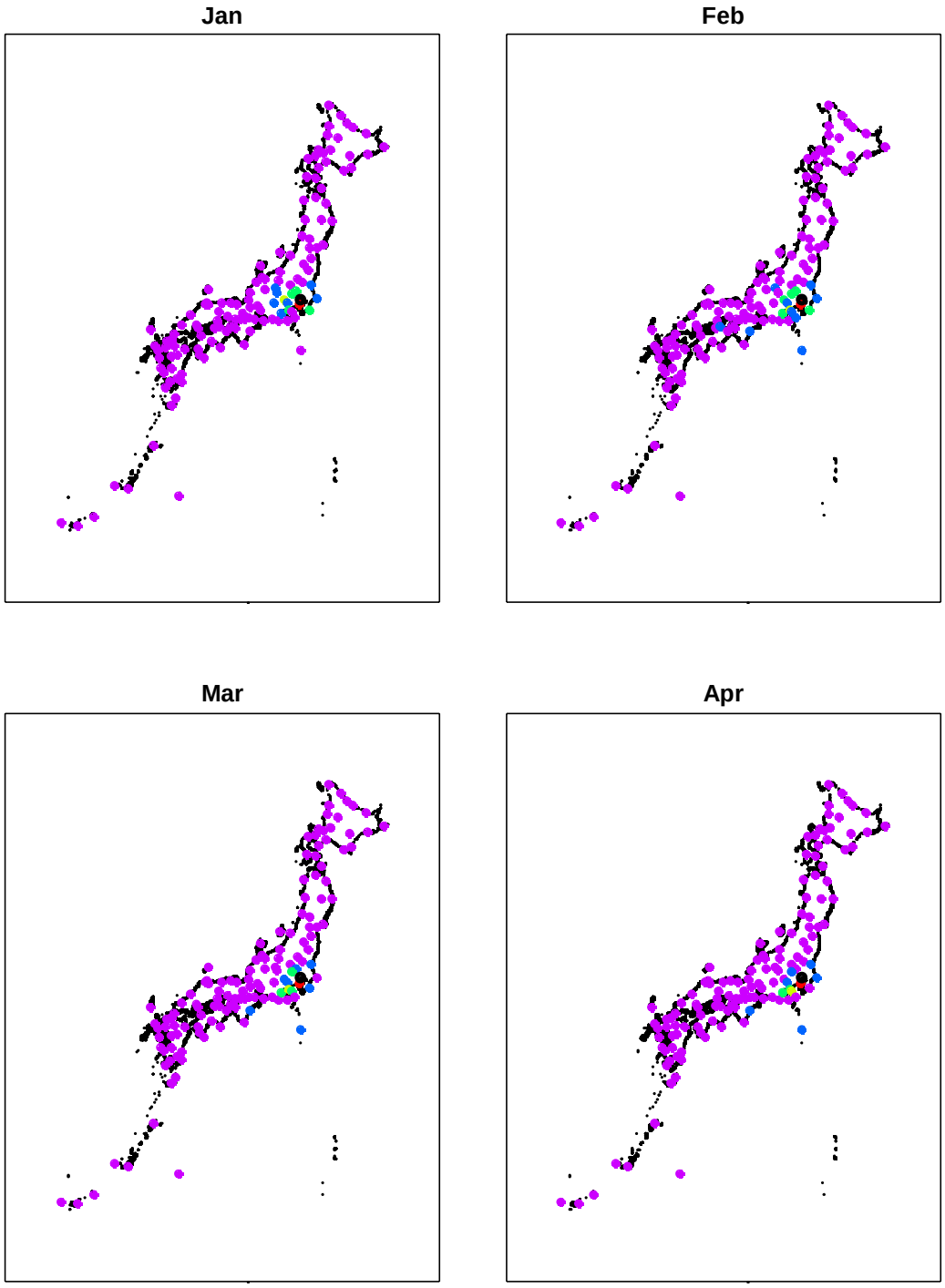

Figure 6.7-1 The monthly maps (from January until April) of the monthly averaged SDNC from Tokyo to other 136 stations, where the stations are represented as the solid circles with color separated by values of the monthly averaged SDNC: the red corresponds to the value that is more than 0.4, the yellow corresponds to the value that is from 0.3 (exclusive) to 0.4 (inclusive), the green corresponds to the value that is from 0.2 (exclusive) to 0.3 (inclusive), the blue corresponds to the value that is from 0.1 (exclusive) to 0.2 (inclusive), the violet corresponds to the value that is equal to or less than 0.1 and the black is the Tokyo station.

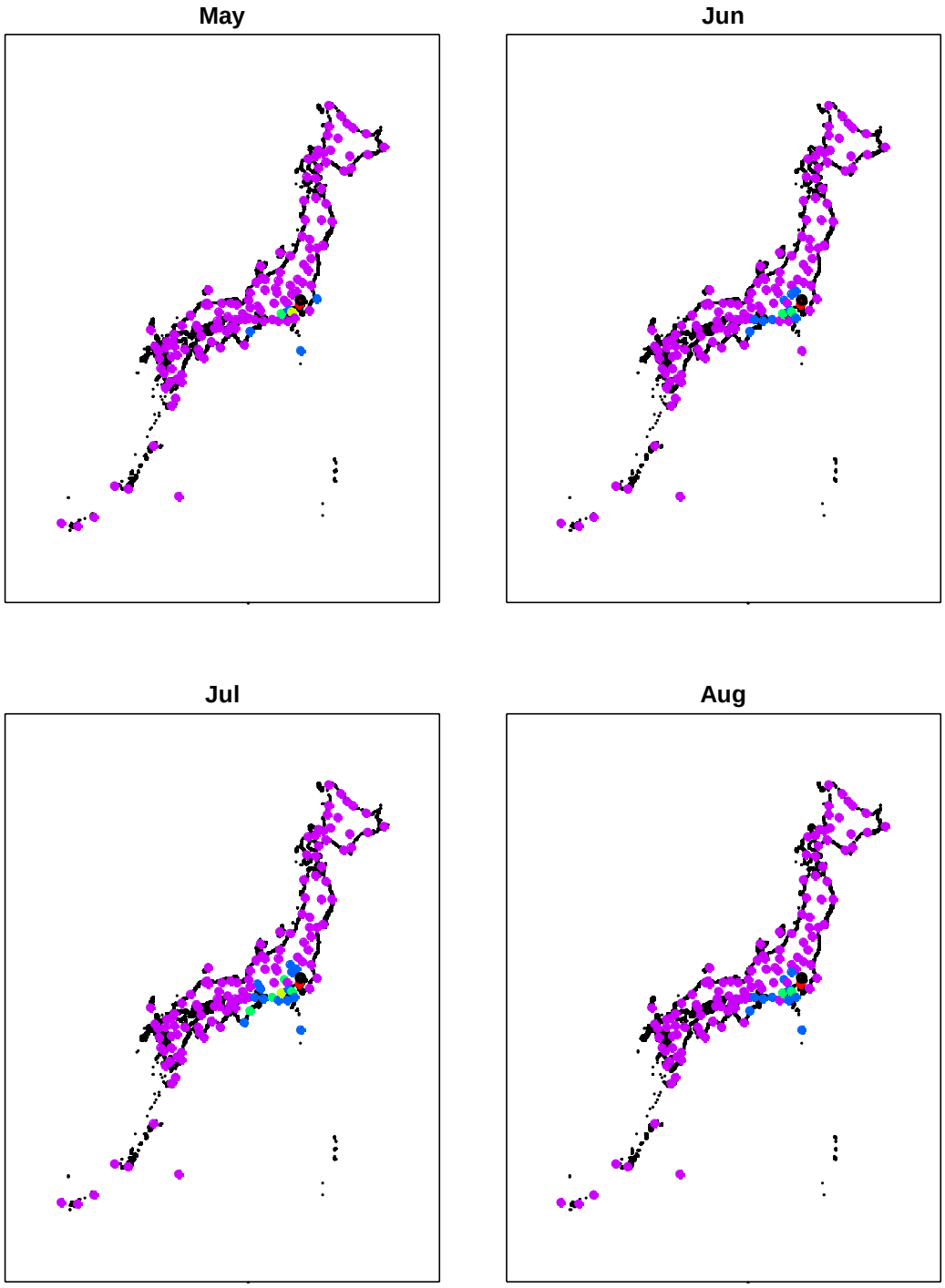

Figure 6.7-2 The monthly maps (from May until August) of the monthly averaged SDNC from Tokyo to other 136 stations, where the stations are represented as the solid circles with color separated by values of the monthly averaged SDNC: the red corresponds to the value that is more than 0.4, the yellow corresponds to the value that is from 0.3 (exclusive) to 0.4 (inclusive), the green corresponds to the value that is from 0.2 (exclusive) to 0.3 (inclusive), the blue corresponds to the value that is from 0.1 (exclusive) to 0.2 (inclusive), the violet corresponds to the value that is equal to or less than 0.1 and the black is the Tokyo station.

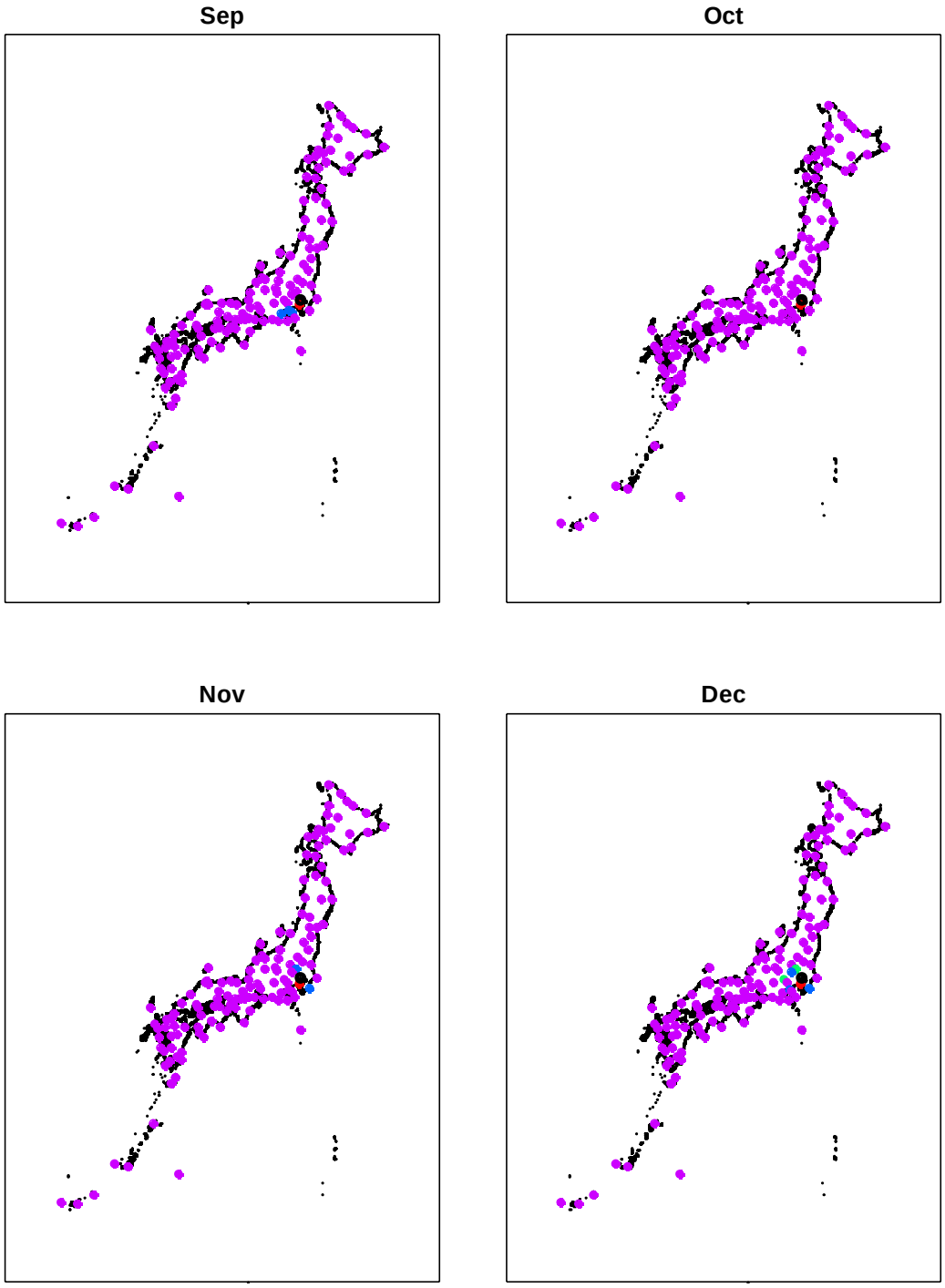

Figure 6.7-3. The monthly maps (from September until December) of the monthly averaged SDNC from Tokyo to other 136 stations, where the stations are represented as the solid circles with color separated by values of the monthly averaged SDNC: the red corresponds to the value that is more than 0.4, the yellow corresponds to the value that is from 0.3 (exclusive) to 0.4 (inclusive), the green corresponds to the value that is from 0.2 (exclusive) to 0.3 (inclusive), the blue corresponds to the value that is from 0.1 (exclusive) to 0.2 (inclusive), the violet corresponds to the value that is equal to or less than 0.1 and the black is the Tokyo station.

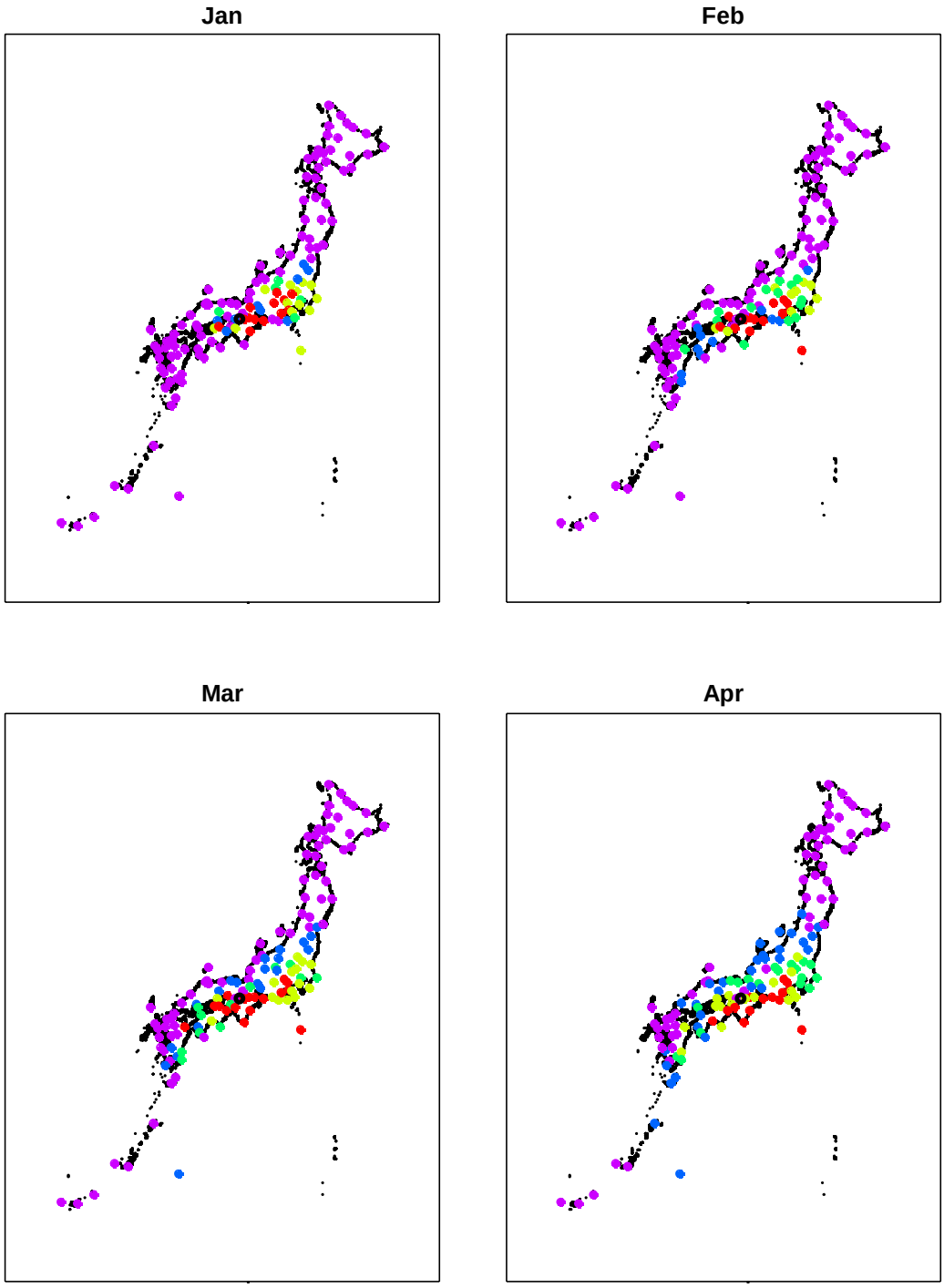

Figure 6.8-1 The monthly maps (from January until April) of the monthly averaged SDNC from Osaka to other 136 stations, where the stations are represented as the solid circles with color separated by values of the monthly averaged SDNC: the red corresponds to the value that is more than 0.4, the yellow corresponds to the value that is from 0.3 (exclusive) to 0.4 (inclusive), the green corresponds to the value that is from 0.2 (exclusive) to 0.3 (inclusive), the blue corresponds to the value that is from 0.1 (exclusive) to 0.2 (inclusive), the violet corresponds to the value that is equal to or less than 0.1 and the black is the Osaka station.

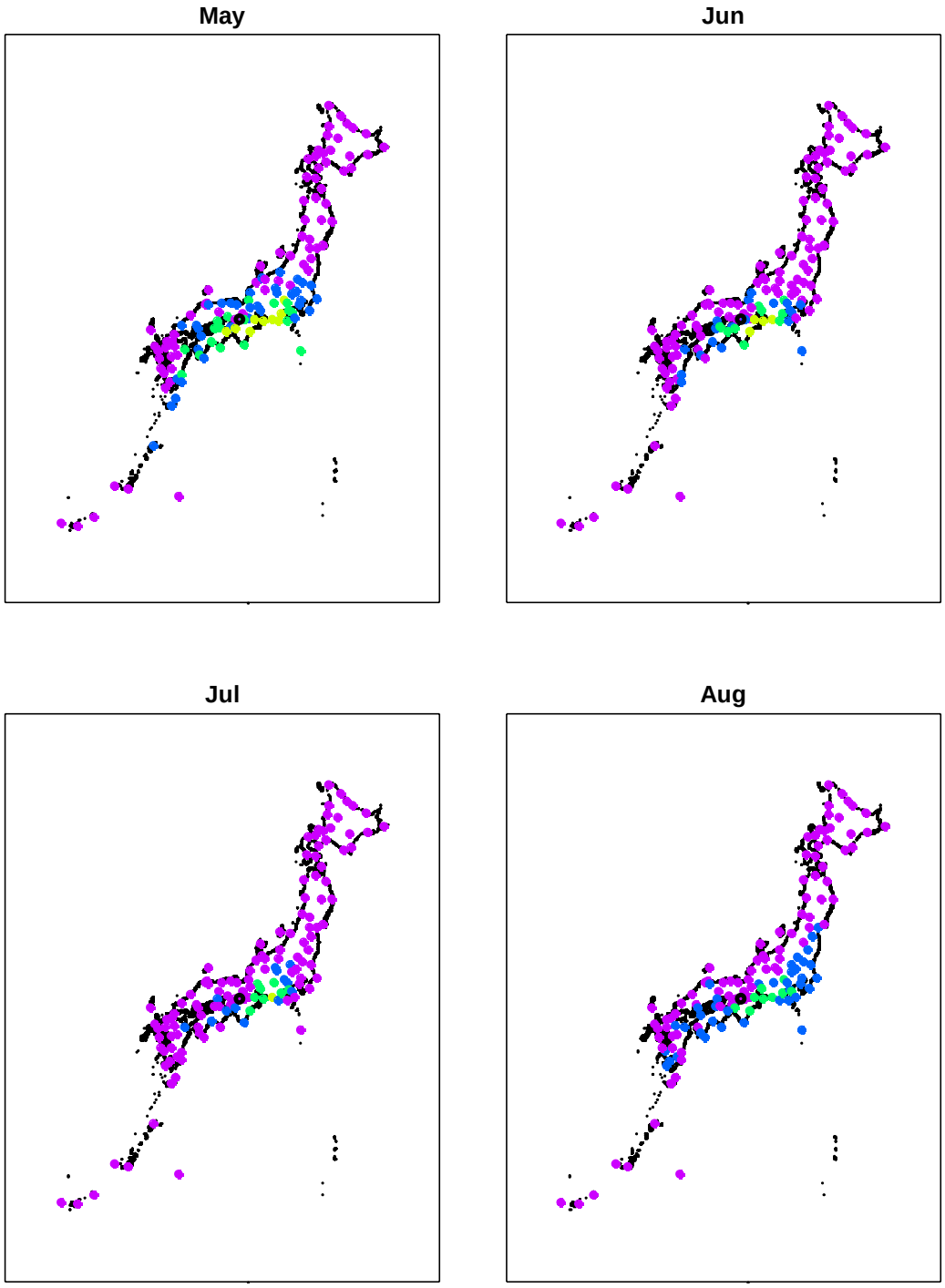

Figure 6.8-2 The monthly maps (from May until August) of the monthly averaged SDNC from Osaka to other 136 stations, where the stations are represented as the solid circles with color separated by values of the monthly averaged SDNC: the red corresponds to the value that is more than 0.4, the yellow corresponds to the value that is from 0.3 (exclusive) to 0.4 (inclusive), the green corresponds to the value that is from 0.2 (exclusive) to 0.3 (inclusive), the blue corresponds to the value that is from 0.1 (exclusive) to 0.2 (inclusive), the violet corresponds to the value that is equal to or less than 0.1 and the black is the Osaka station.

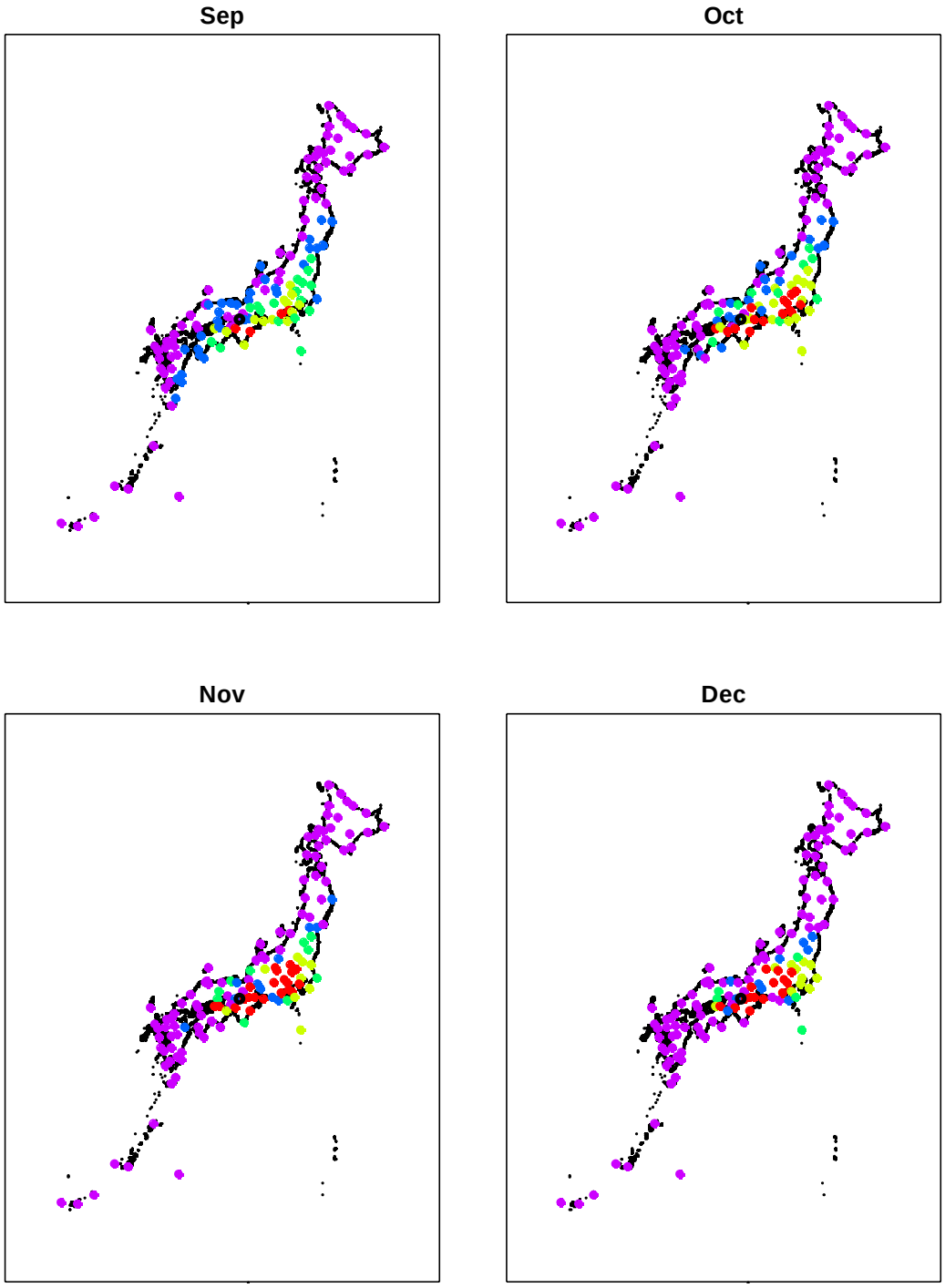

Figure 6.8-3. The monthly maps (from September until December) of the monthly averaged SDNC from Osaka to other 136 stations, where the stations are represented as the solid circles with color separated by values of the monthly averaged SDNC: the red corresponds to the value that is more than 0.4, the yellow corresponds to the value that is from 0.3 (exclusive) to 0.4 (inclusive), the green corresponds to the value that is from 0.2 (exclusive) to 0.3 (inclusive), the blue corresponds to the value that is from 0.1 (exclusive) to 0.2 (inclusive), the violet corresponds to the value that is equal to or less than 0.1 and the black is the Osaka station.

6.4 Analysis of the upper atmosphere

We will now turn to analysis of the upper atmosphere; using the aerological data, we will analyze the relation between the surface in Tokyo and the upper atmosphere. The typical isobaric surface heights are 500 hpa and 850 hpa; the cold airmass which influence to surface air temperature are observed at the 500 hpa isobaric surface, and the 850 hpa isobaric surface is the lowest layer not to take a influence from the surface friction. Therefore, we will analyze the air temperature data at the 850 hpa and 500 hpa isobaric surface, which are observed at 9:00 for the 10-year period from 1991 through 2000; the whole data size is 3650 days for each station, omitting February 29 in the leap years.

Since the seasonal periodicity is recognized in the upper atmosphere as shown in the section 2.2, we apply seasonal adjustment to the aerological data as Chapter 3 and obtained the anomaly data of the upper atmosphere. The optimal order of applied polynomials in each aerological observatory is listed in Table 6.3. The anomaly data of the upper atmosphere at 17 aerological observatories and the surface air temperature at the Tokyo station for the 10-year period from 1991 through 2000 are the object of analysis in this section. The bivariate MFFAR models are respectively applied to 17 bivariate datasets of the Tokyo station and the aerological data at the 500 hpa and 850 hpa isobaric surface, and the monthly averaged SDNC are respectively estimated from coefficients of their models. Table 6.4 shows the orders and the AIC values of applying MFFAR to the Tokyo station and observed points at the 500 hpa and 850 hpa isobaric surface. Figure 6.9 shows monthly maps of the monthly averaged SDNC from observed points at the 500 hpa isobaric surface to Tokyo and Figure 6.10 shows monthly maps of the monthly averaged SDNC from observed points at the 850 hpa isobaric surface to Tokyo, where explanatory notes are the same as Figure 6.3; the values of the monthly averaged SDNC from observed points at the isobaric surface to Tokyo are shown in the section 6.5 Appendix (the later section of this chapter).

From Figure 6.9 we can obtain the following recognition. Values of the monthly averaged SDNC are low as a whole in comparison with the surface; the points of which value is more than 0.3 are nothing. The influence from the west or northwest sea area of Hokkaido Island is recognized through a year and the propagation of influence estimated from the contour is from the north-northwest. This may suggest the position of the cold airmass.

From Figure 6.10 we can obtain the following recognition. Same as at the 500 hpa

isobaric surface, values of the monthly averaged SDNC are low as a whole in comparison with the surface; the points of which value is more than 0.4 are nothing. The area that gives the influence shifts to the south area in comparison of the 500 hpa isobaric surface; the influence from northwest sea area of Honshu Island is recognized through a year. The propagation of influence estimated from the contour is from the northwest or the west-northwest and the distribution in July is characteristic. The seasonal variation of upper atmosphere is scanty in comparison with the surface.

Table 6.3. The optimal order of applied polynomials in each aerological observatory, where $\overline{O}$, $\overline{P}$, $\overline{Q}$, $\tilde{O}$, $\tilde{P}$ and $\tilde{Q}$ are orders in Equation (3.1).

(a) The temperature at the 500 hpa isobaric surface.

WMO code	stations	orders						AIC values
		$\overline{O}$	$\overline{P}$	$\overline{Q}$	$\tilde{O}$	$\tilde{P}$	$\tilde{Q}$	
47401	Wakkanai	10	8	8	9	7	7	20584.9
47412	Sapporo	10	8	8	6	8	8	20538.1
47420	Nemuro	10	9	8	5	8	8	20717.3
47582	Akita	10	9	8	4	5	4	20377.1
47590	Sendai	9	9	8	2	27	27	20024.8
47600	Wajima	9	13	12	2	44	43	19885.4
47646	Tateno	9	13	12	8	17	17	19248.5
47678	Hachijojima	8	11	11	12	17	16	17926.3
47744	Yonago	12	9	9	2	29	29	19071.9
47778	Shionomisaki	13	10	9	13	32	31	18055.0
47807	Fukuoka	14	11	11	2	30	29	18405.1
47827	Kagoshima	15	10	9	13	32	31	17346.6
47909	Naze	12	4	3	8	9	9	15963.6
47918	Ishigakijima	39	25	24	2	29	28	14480.2
47936	Naha	13	8	8	8	24	23	15067.9
47945	Minamidaitojima	41	25	24	9	43	42	14843.6
47971	Chichijima	37	13	13	9	39	38	14705.4

(b) The temperature at the 850 hpa isobaric surface.

WMO code	stations	orders						AIC values
		$\overline{O}$	$\overline{P}$	$\overline{Q}$	$\tilde{O}$	$\tilde{P}$	$\tilde{Q}$	
47401	Wakkanai	10	12	12	6	18	18	20346.7
47412	Sapporo	10	27	26	8	17	16	20021.6
47420	Nemuro	10	27	26	11	15	15	20563.5
47582	Akita	10	7	7	7	8	8	19696.2
47590	Sendai	11	24	23	7	3	3	19821.8
47600	Wajima	10	7	7	6	3	3	19454.8
47646	Tateno	10	20	19	6	3	2	19435.7
47678	Hachijojima	9	18	17	3	5	5	18244.0
47744	Yonago	11	16	16	2	15	15	19424.3
47778	Shionomisaki	11	18	17	2	6	5	18206.6
47807	Fukuoka	9	16	16	8	5	4	19168.2
47827	Kagoshima	9	19	18	2	20	20	17880.9
47909	Naze	9	19	18	9	3	3	17458.3
47918	Ishigakijima	8	24	24	6	42	42	16217.3
47936	Naha	8	24	24	9	10	9	16557.4
47945	Minamidaitojima	8	24	24	8	19	18	15701.3
47971	Chichijima	9	18	17	6	41	41	15729.3

Table 6.4. The orders and the AIC values of the MFFAR model applied to the Tokyo station between the upper atmosphere, where m, p and q are orders in Equation (6.1).

(a) The 500 hpa isobaric surface.

the WMO code	station name	orders m	p	q	AIC values
47401	Wakkanai	3	5	5	17307.0
47412	Sapporo	3	5	5	17285.8
47420	Nemuro	3	5	5	17489.2
47582	Akita	3	5	4	17442.5
47590	Sendai	3	2	2	17702.6
47600	Wajima	3	2	2	17586.2
47646	Tateno	3	5	5	17735.6
47678	Hachijojima	4	2	2	17879.1
47744	Yonago	3	4	4	17593.8
47778	Shionomisaki	2	5	5	17750.3
47807	Fukuoka	3	3	2	17660.6
47827	Kagoshima	3	2	2	17715.9
47909	Naze	3	2	2	17605.2
47918	Ishigakijima	2	6	5	17776.5
47936	Naha	2	4	4	17761.6
47945	Minamidaitojima	3	2	2	17796.4
47971	Chichijima	2	4	4	18018.8

(b) The 850 hpa isobaric surface.

the WMO code	station name	orders m	p	q	AIC values
47401	Wakkanai	3	2	5	17318.0
47412	Sapporo	3	2	5	17272.1
47420	Nemuro	2	1	5	17249.0
47582	Akita	6	6	2	17217.2
47590	Sendai	6	5	3	16457.1
47600	Wajima	5	5	3	17146.4
47646	Tateno	3	2	5	16093.5
47678	Hachijojima	2	2	3	17594.7
47744	Yonago	6	5	3	17099.1
47778	Shionomisaki	3	2	3	17141.7
47807	Fukuoka	4	3	3	17268.9
47827	Kagoshima	2	2	3	17488.6
47909	Naze	3	2	3	17655.4
47918	Ishigakijima	3	2	3	17630.2
47936	Naha	3	2	3	17615.4
47945	Minamidaitojima	6	5	3	17751.0
47971	Chichijima	2	2	3	18072.9

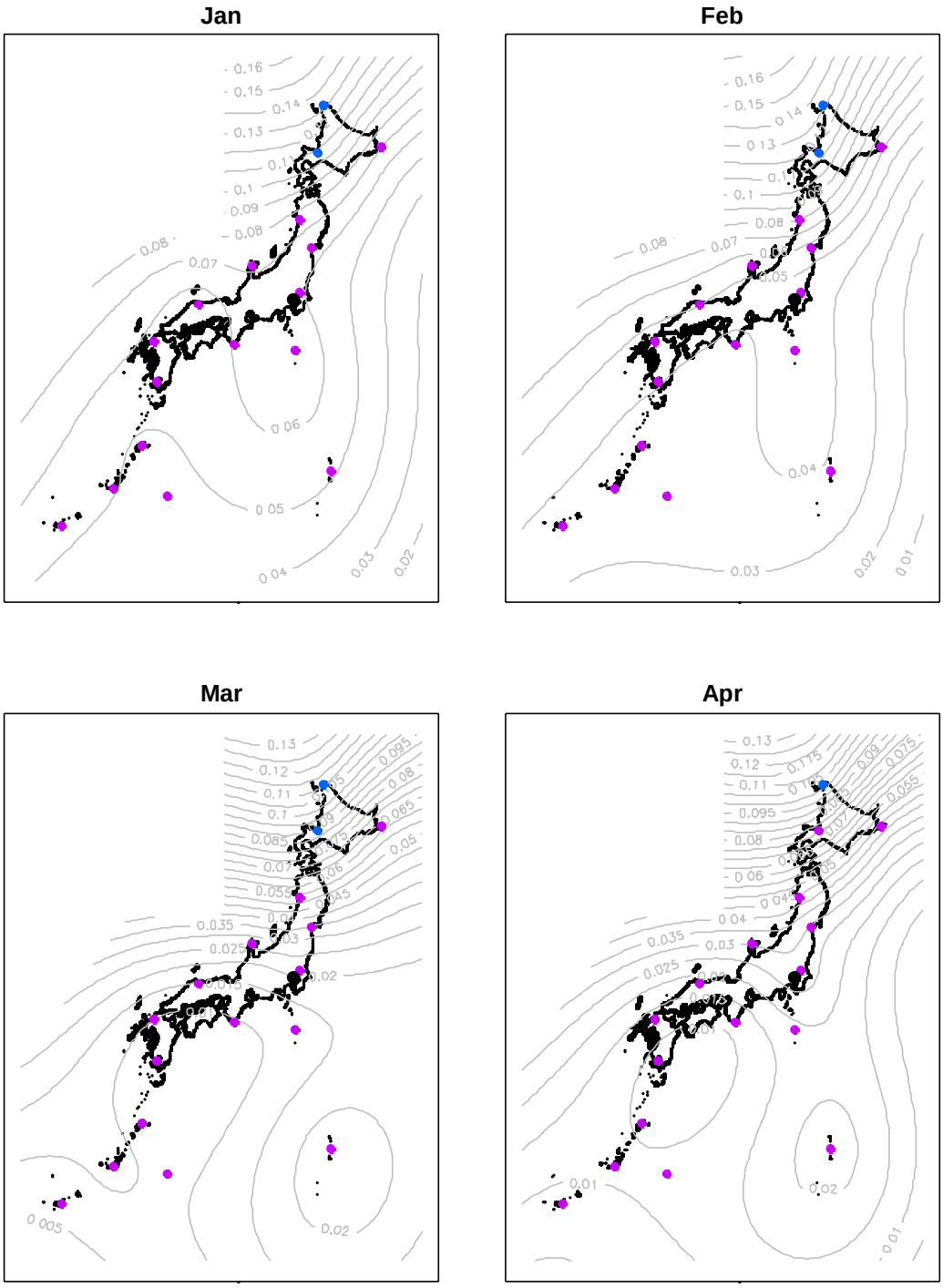

Figure 6.9-1 The monthly maps (from January until April) of the monthly averaged SDNC from observed points at the 500 hpa isobaric surface to Tokyo, where the observation points are represented as the solid circles with color separated by values of the monthly averaged SDNC: the red corresponds to the value that is more than 0.4, the yellow corresponds to the value that is from 0.3 (exclusive) to 0.4 (inclusive), the green corresponds to the value that is from 0.2 (exclusive) to 0.3 (inclusive), the blue corresponds to the value that is from 0.1 (exclusive) to 0.2 (inclusive), the violet corresponds to the value that is equal to or less than 0.1 and the black is the Tokyo station.

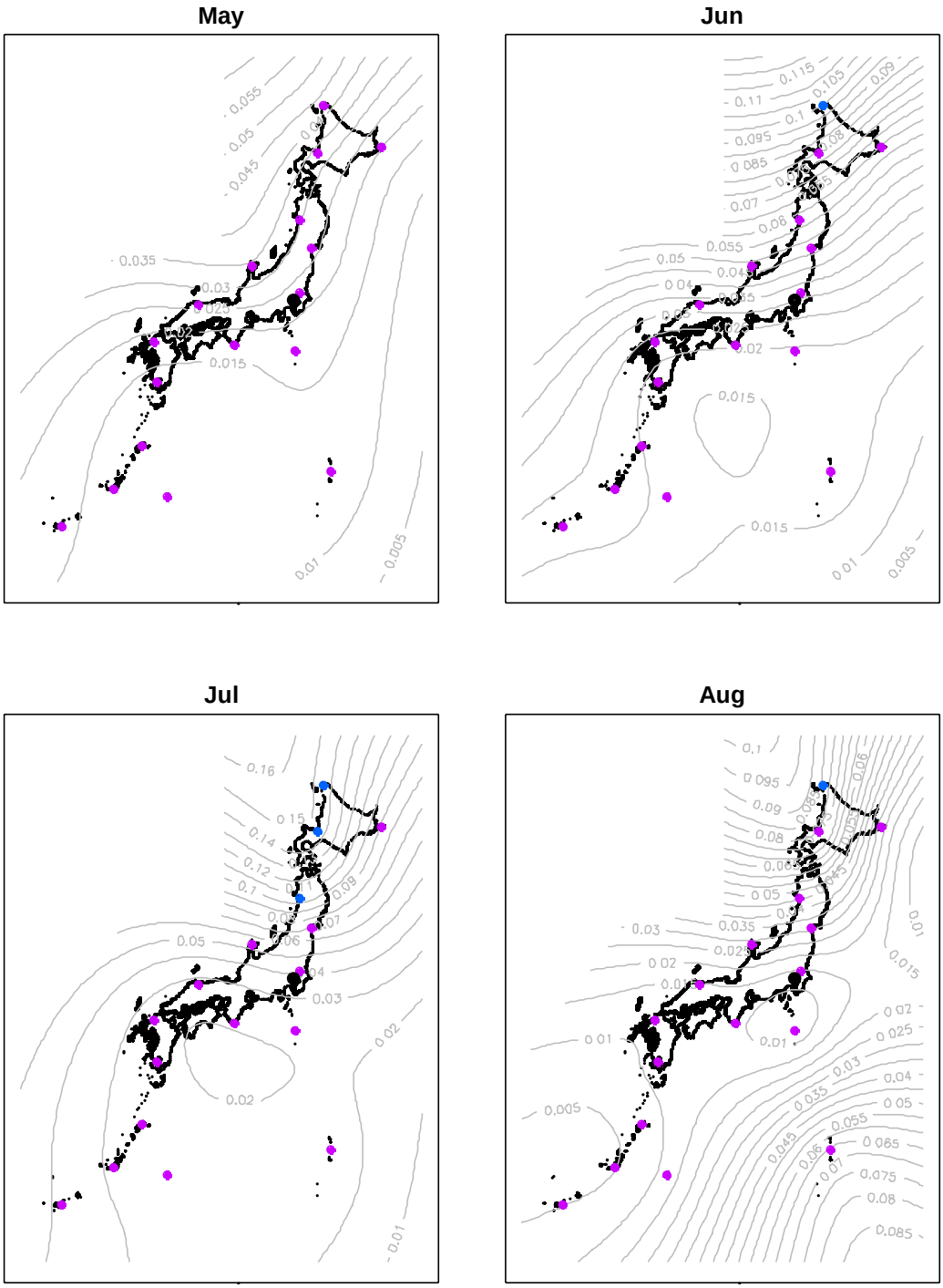

Figure 6.9-2 The monthly maps (from May until August) of the monthly averaged SDNC from observed points at the 500 hpa isobaric surface to Tokyo, where the observation points are represented as the solid circles with color separated by values of the monthly averaged SDNC: the red corresponds to the value that is more than 0.4, the yellow corresponds to the value that is from 0.3 (exclusive) to 0.4 (inclusive), the green corresponds to the value that is from 0.2 (exclusive) to 0.3 (inclusive), the blue corresponds to the value that is from 0.1 (exclusive) to 0.2 (inclusive), the violet corresponds to the value that is equal to or less than 0.1 and the black is the Tokyo station.

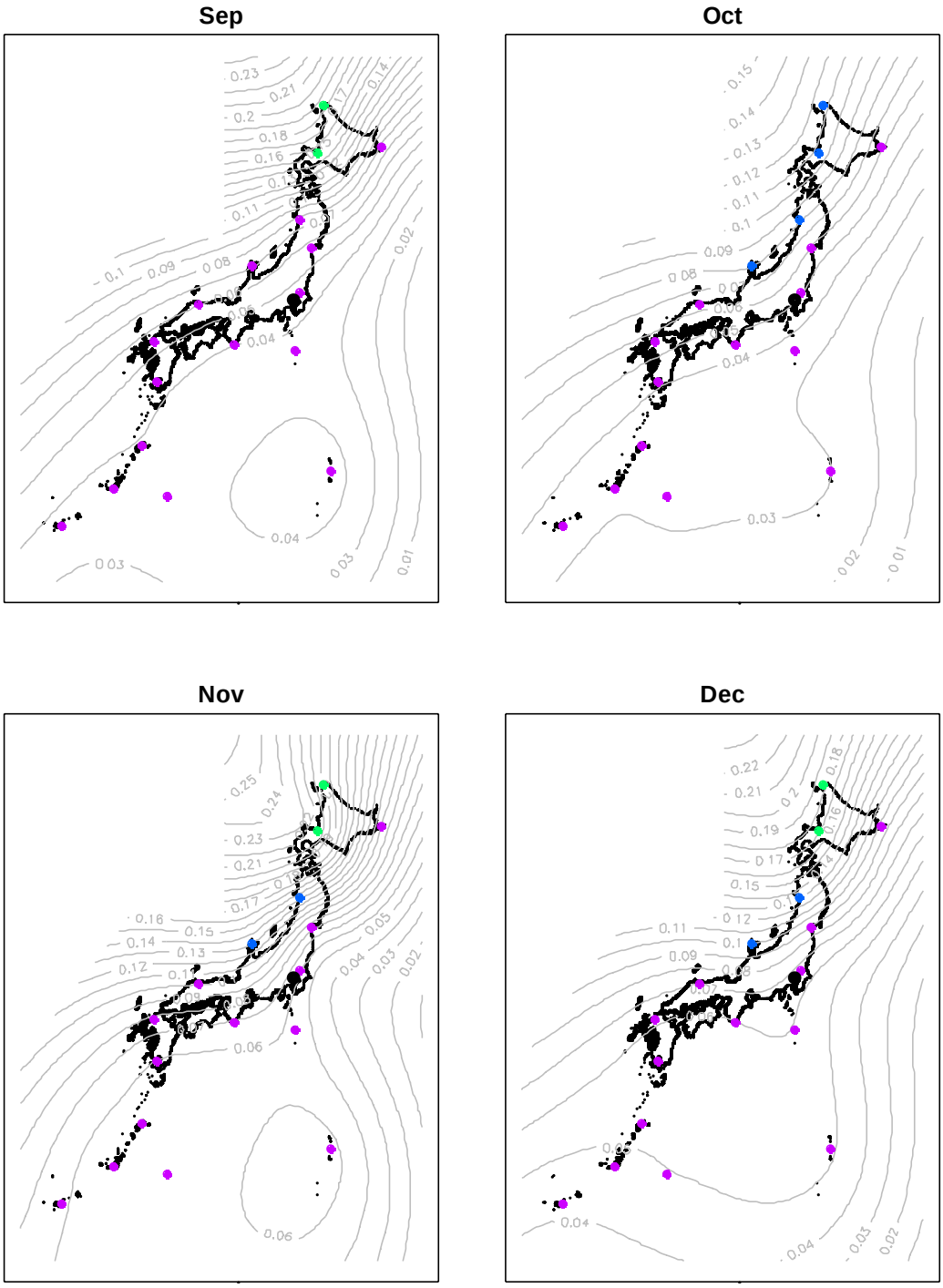

Figure 6.9-3. The monthly maps (from September until December) of the monthly averaged SDNC from observed points at the 500 hpa isobaric surface to Tokyo, where the observation points are represented as the solid circles with color separated by values of the monthly averaged SDNC: the red corresponds to the value that is more than 0.4, the yellow corresponds to the value that is from 0.3 (exclusive) to 0.4 (inclusive), the green corresponds to the value that is from 0.2 (exclusive) to 0.3 (inclusive), the blue corresponds to the value that is from 0.1 (exclusive) to 0.2 (inclusive), the violet corresponds to the value that is equal to or less than 0.1 and the black is the Tokyo station.

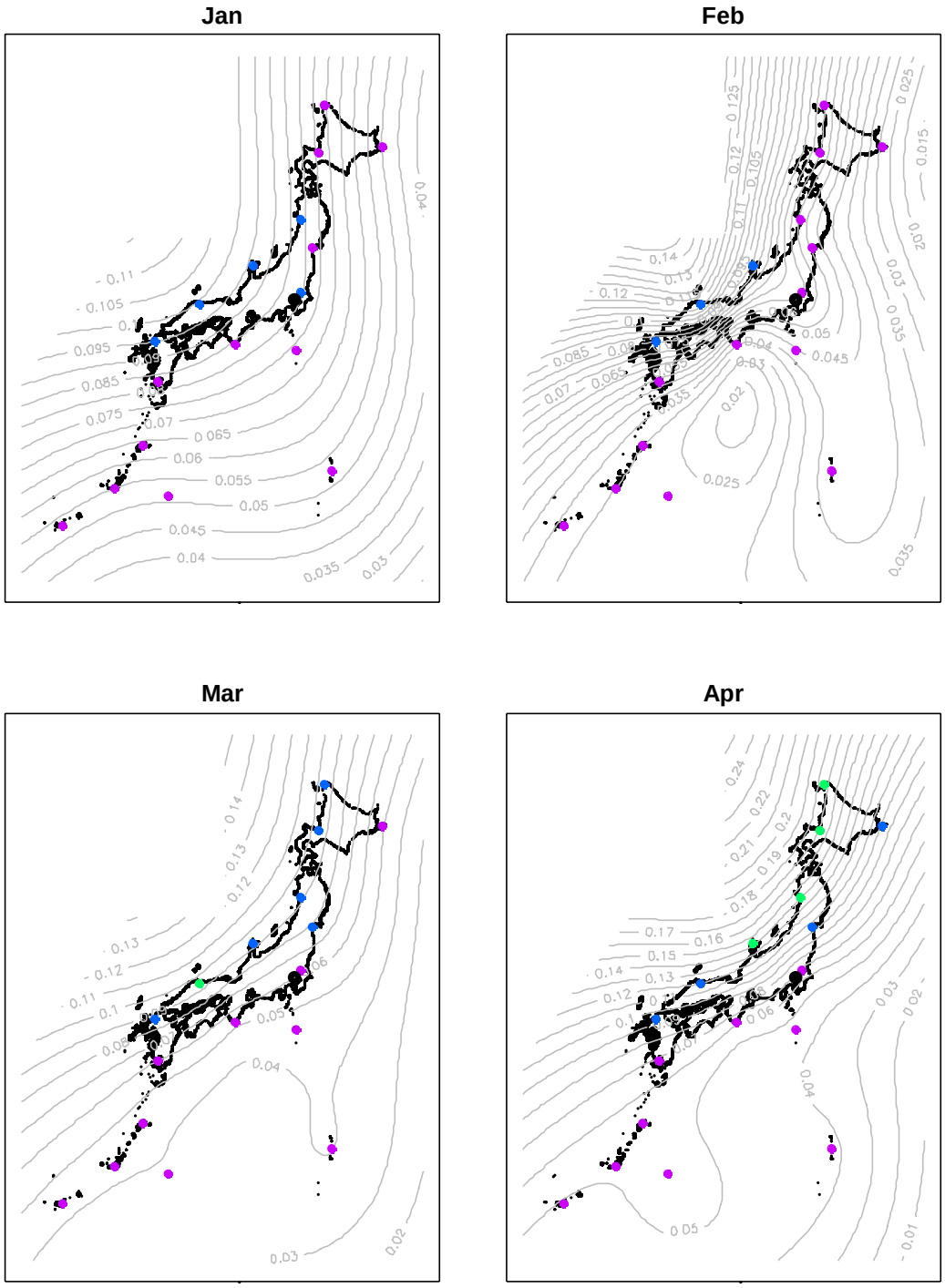

Figure 6.10-1 The monthly maps (from January until April) of the monthly averaged SDNC from observed points at the 850 hpa isobaric surface to Tokyo, where the observation points are represented as the solid circles with color separated by values of the monthly averaged SDNC: the red corresponds to the value that is more than 0.4, the yellow corresponds to the value that is from 0.3 (exclusive) to 0.4 (inclusive), the green corresponds to the value that is from 0.2 (exclusive) to 0.3 (inclusive), the blue corresponds to the value that is from 0.1 (exclusive) to 0.2 (inclusive), the violet corresponds to the value that is equal to or less than 0.1 and the black is the Tokyo station.

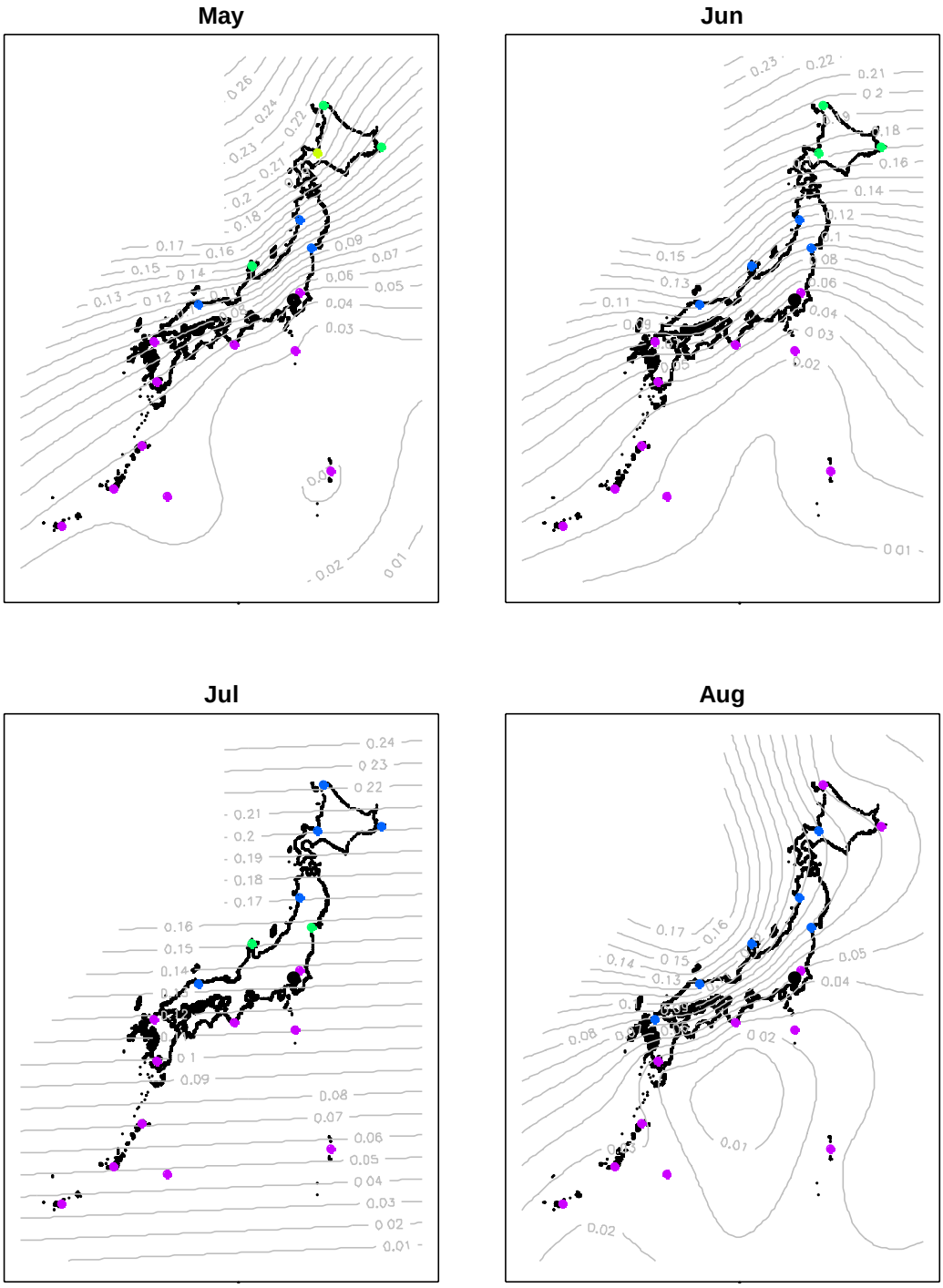

Figure 6.10-2 The monthly maps (from May until August) of the monthly averaged SDNC from observed points at the 850 hpa isobaric surface to Tokyo, where the observation points are represented as the solid circles with color separated by values of the monthly averaged SDNC: the red corresponds to the value that is more than 0.4, the yellow corresponds to the value that is from 0.3 (exclusive) to 0.4 (inclusive), the green corresponds to the value that is from 0.2 (exclusive) to 0.3 (inclusive), the blue corresponds to the value that is from 0.1 (exclusive) to 0.2 (inclusive), the violet corresponds to the value that is equal to or less than 0.1 and the black is the Tokyo station.

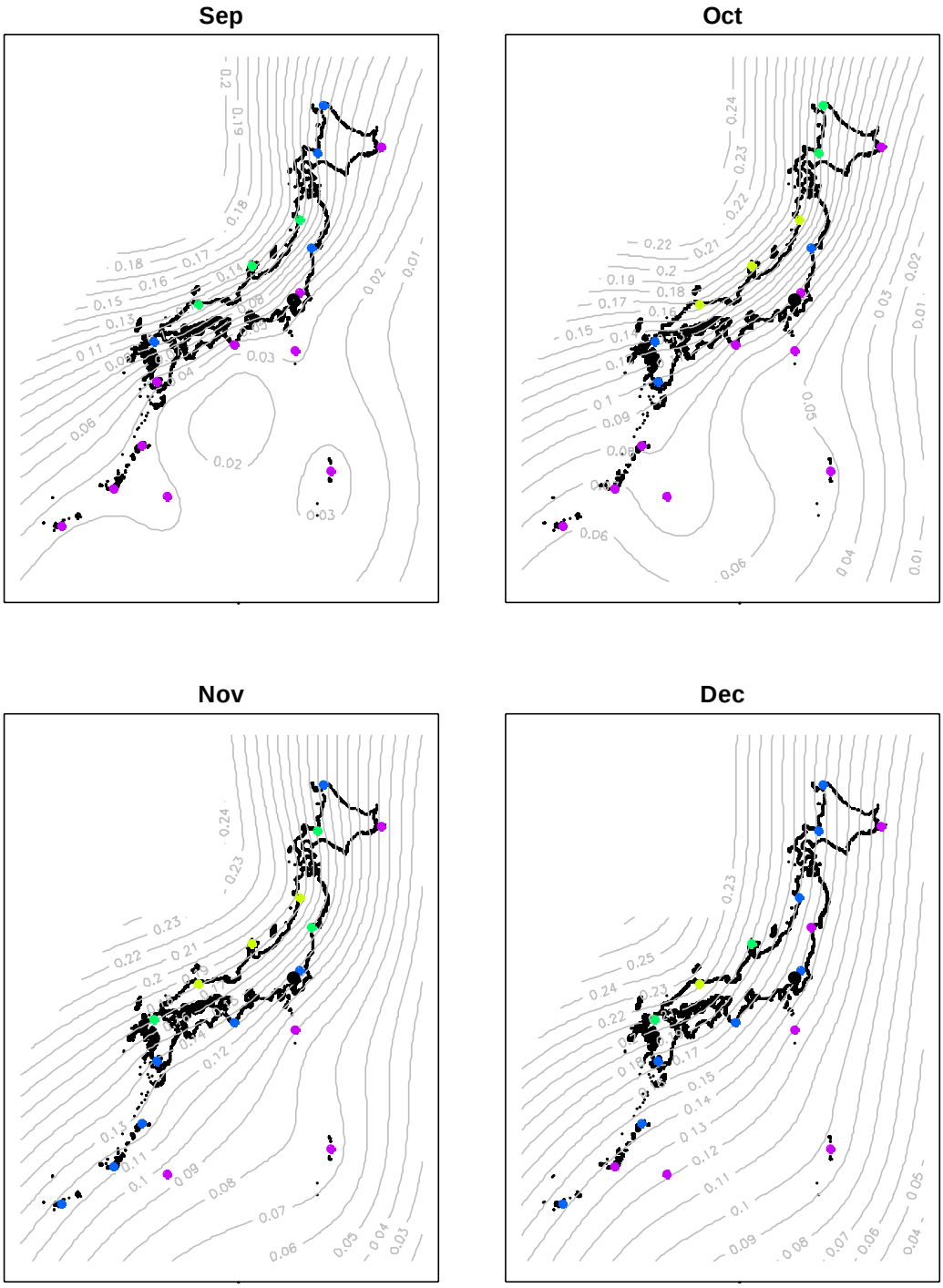

Figure 6.10-3. The monthly maps (from September until December) of the monthly averaged SDNC from observed points at the 850 hpa isobaric surface to Tokyo, where the observation points are represented as the solid circles with color separated by values of the monthly averaged SDNC: the red corresponds to the value that is more than 0.4, the yellow corresponds to the value that is from 0.3 (exclusive) to 0.4 (inclusive), the green corresponds to the value that is from 0.2 (exclusive) to 0.3 (inclusive), the blue corresponds to the value that is from 0.1 (exclusive) to 0.2 (inclusive), the violet corresponds to the value that is equal to or less than 0.1 and the black is the Tokyo station.

6.5 Appendix

Appendix #1. The values of the monthly averaged SDNC from other 136 stations to Tokyo.

Appendix #2. The values of the monthly averaged SDNC from other 136 stations to Osaka.

Appendix #3. The values of the monthly averaged SDNC from Tokyo to other 136 stations.

Appendix #4. The values of the monthly averaged SDNC from Osaka to other 136 stations.

Appendix #5. The values of the monthly averaged SDNC from observed points at the isobaric surface to Tokyo.

Appendix #1. The values of the monthly averaged SDNC from other 136 stations to Tokyo.

WMO code	Jan	Feb	Mar	Apr	May	Jun	Jul	Aug	Sep	Oct	Nov	Dec
47401	0.2649	0.2464	0.2547	0.2634	0.2548	0.2351	0.2122	0.2170	0.2517	0.2781	0.2899	0.2876
47402	0.2161	0.2189	0.2399	0.2325	0.2100	0.2266	0.1736	0.1531	0.2115	0.2886	0.3241	0.2572
47404	0.2719	0.2589	0.2742	0.2747	0.2361	0.1763	0.1368	0.1817	0.2765	0.3275	0.3316	0.3079
47405	0.1939	0.1671	0.1991	0.2157	0.2002	0.2338	0.1793	0.1566	0.1899	0.2406	0.2726	0.2228
47406	0.2275	0.2293	0.2921	0.2948	0.2195	0.1611	0.1656	0.1964	0.2230	0.2672	0.3103	0.2951
47407	0.1211	0.1112	0.2025	0.2873	0.2772	0.2133	0.1703	0.2132	0.2339	0.2402	0.2418	0.1902
47409	0.1342	0.1160	0.1568	0.2149	0.2486	0.2463	0.2074	0.1817	0.2066	0.2415	0.2462	0.2024
47411	0.3270	0.3056	0.3062	0.2991	0.2584	0.1899	0.1446	0.1922	0.2862	0.3446	0.3660	0.3575
47412	0.2920	0.2737	0.2936	0.3017	0.2653	0.1957	0.1418	0.1805	0.2852	0.3523	0.3672	0.3402
47413	0.2291	0.2241	0.2639	0.2983	0.2878	0.2320	0.1745	0.1880	0.2616	0.3184	0.3254	0.2823
47417	0.0314	0.0174	0.0678	0.1324	0.1327	0.1150	0.0787	0.0884	0.0736	0.1074	0.1420	0.0682
47418	0.0323	0.0333	0.0615	0.0830	0.0927	0.0960	0.0997	0.0988	0.0874	0.0984	0.1037	0.0651
47420	0.0544	0.0584	0.1061	0.1370	0.1605	0.1794	0.1546	0.1042	0.1101	0.1580	0.1889	0.1252
47421	0.3507	0.3195	0.3127	0.2934	0.2422	0.1688	0.1195	0.1699	0.2895	0.3707	0.4018	0.3931
47423	0.3089	0.3145	0.3100	0.2218	0.1426	0.0966	0.0815	0.1176	0.2179	0.3658	0.4357	0.3845
47424	0.2398	0.2298	0.2141	0.1387	0.0746	0.0381	0.0553	0.1573	0.2433	0.3286	0.3580	0.3020
47426	0.2206	0.1733	0.1840	0.2141	0.2223	0.1903	0.1509	0.1816	0.2597	0.3231	0.3472	0.3075
47428	0.4335	0.4239	0.3900	0.3265	0.2409	0.1675	0.1596	0.2622	0.3660	0.4075	0.4208	0.4276
47430	0.3505	0.3472	0.3541	0.3389	0.2940	0.2267	0.1922	0.2651	0.3639	0.4100	0.4144	0.3856
47433	0.1889	0.1881	0.2498	0.2992	0.2851	0.2200	0.1700	0.2106	0.3114	0.3666	0.3450	0.2648
47435	0.1982	0.1586	0.1690	0.2026	0.2301	0.2360	0.2062	0.1819	0.2033	0.2381	0.2599	0.2506
47440	0.1171	0.0920	0.0869	0.0933	0.0969	0.0797	0.0491	0.0404	0.0619	0.1047	0.1453	0.1475
47520	0.1618	0.1682	0.2009	0.2227	0.2185	0.2230	0.2474	0.2751	0.2896	0.2899	0.2482	0.1937
47570	0.1202	0.1580	0.2020	0.2555	0.1676	0.2172	0.2239	0.2536	0.3593	0.2527	0.1755	0.1862
47574	0.4574	0.4308	0.3950	0.3398	0.2644	0.1954	0.1715	0.2476	0.3636	0.4317	0.4604	0.4669
47575	0.3932	0.3622	0.3331	0.2966	0.2480	0.1973	0.1847	0.2642	0.3631	0.4100	0.4251	0.4189
47576	0.3388	0.3200	0.3016	0.2890	0.2775	0.2584	0.2373	0.2468	0.2809	0.3170	0.3410	0.3475
47581	0.3587	0.3642	0.3453	0.2669	0.2244	0.2387	0.2617	0.2436	0.2630	0.3664	0.4293	0.4005
47582	0.3897	0.3971	0.3998	0.3163	0.1991	0.1309	0.1398	0.2687	0.3672	0.4331	0.4618	0.4296
47584	0.3124	0.2850	0.2763	0.2707	0.2537	0.2332	0.2227	0.2410	0.2892	0.3412	0.3597	0.3447
47585	0.2686	0.2227	0.1911	0.1868	0.2034	0.2264	0.2363	0.2249	0.2291	0.2660	0.2967	0.2981
47587	0.4542	0.4289	0.3748	0.2981	0.2175	0.1756	0.1923	0.2940	0.3863	0.4207	0.4307	0.4433
47588	0.2778	0.2971	0.3183	0.3142	0.2936	0.2898	0.2933	0.2940	0.3000	0.3060	0.2939	0.2779
47590	0.4344	0.3002	0.1974	0.1613	0.1705	0.1842	0.1766	0.1907	0.2501	0.3414	0.4313	0.4818

WMO code	Jan	Feb	Mar	Apr	May	Jun	Jul	Aug	Sep	Oct	Nov	Dec
47592	0.3601	0.3334	0.3212	0.2689	0.2197	0.1946	0.2175	0.2974	0.3305	0.3748	0.4079	0.3948
47595	0.2627	0.2639	0.2741	0.2867	0.3089	0.3567	0.3595	0.2863	0.2273	0.2247	0.2383	0.2533
47597	0.2910	0.2531	0.2446	0.2548	0.2867	0.3582	0.4052	0.3587	0.2976	0.3085	0.3223	0.3178
47600	0.4162	0.3873	0.3428	0.2895	0.2515	0.2505	0.2810	0.3270	0.3463	0.3734	0.4051	0.4216
47602	0.5293	0.5113	0.4558	0.3397	0.2324	0.2354	0.2615	0.3245	0.4603	0.4822	0.5494	0.5658
47604	0.5251	0.4635	0.3926	0.3199	0.2485	0.2045	0.2045	0.2985	0.4092	0.4749	0.5114	0.5335
47605	0.4732	0.4442	0.3977	0.3212	0.2431	0.2115	0.2460	0.3327	0.3994	0.4421	0.4696	0.4826
47606	0.4331	0.3757	0.3126	0.2514	0.2070	0.1954	0.2214	0.2763	0.3118	0.3576	0.4110	0.4458
47607	0.3882	0.3659	0.3386	0.2927	0.2477	0.2319	0.2638	0.3402	0.3800	0.4081	0.4234	0.4129
47610	0.2090	0.2335	0.2813	0.2752	0.2140	0.1733	0.2055	0.3039	0.3892	0.4149	0.3637	0.2649
47612	0.4320	0.3870	0.3391	0.2849	0.2319	0.2001	0.2142	0.3130	0.4019	0.4515	0.4733	0.4648
47615	0.1071	0.0584	0.0832	0.1380	0.2688	0.3805	0.3599	0.2995	0.3141	0.3353	0.3199	0.2244
47616	0.3458	0.3013	0.3299	0.3086	0.1685	0.1855	0.2349	0.2459	0.3544	0.3652	0.4211	0.4243
47617	0.0653	0.1000	0.1770	0.1978	0.1264	0.0717	0.0938	0.1786	0.2793	0.3039	0.2165	0.1049
47618	0.0845	0.1384	0.2246	0.2340	0.1495	0.1034	0.1610	0.2686	0.3133	0.2797	0.1778	0.0950
47620	0.1200	0.1661	0.2282	0.2068	0.1094	0.0570	0.0881	0.1839	0.2770	0.2958	0.2279	0.1443
47624	0.1684	0.1209	0.1679	0.1507	0.1009	0.0630	0.1230	0.1177	0.1179	0.1921	0.2199	0.1949
47626	0.0082	0.0121	0.0287	0.0481	0.0602	0.0702	0.1020	0.1269	0.0809	0.0319	0.0113	0.0093
47629	0.0868	0.0670	0.0870	0.1135	0.1725	0.2705	0.3349	0.3099	0.2780	0.2845	0.2574	0.1672
47631	0.4073	0.3555	0.3083	0.2543	0.1077	0.1522	0.2006	0.2140	0.3646	0.3378	0.4048	0.4410
47632	0.1758	0.1675	0.1984	0.1556	0.0598	0.0227	0.0399	0.0988	0.1571	0.2272	0.2893	0.2570
47636	0.1873	0.1836	0.1897	0.1513	0.0723	0.0247	0.0268	0.0779	0.1911	0.2787	0.2846	0.2345
47637	0.0429	0.0537	0.0737	0.0655	0.0301	0.0187	0.0369	0.0723	0.1001	0.0980	0.0708	0.0481
47638	0.0306	0.0310	0.0245	0.0134	0.0140	0.0096	0.0167	0.0185	0.0120	0.0330	0.0227	0.0237
47640	0.0725	0.0692	0.0749	0.0622	0.0279	0.0115	0.0317	0.0372	0.0548	0.0895	0.1047	0.0915
47641	0.0171	0.0261	0.0304	0.0271	0.0258	0.0342	0.0399	0.0249	0.0200	0.0330	0.0287	0.0157
47648	0.1266	0.1244	0.1465	0.1601	0.1469	0.1215	0.1149	0.1735	0.2659	0.3024	0.2748	0.1922
47649	0.0662	0.0956	0.1614	0.1889	0.1390	0.0919	0.1085	0.1734	0.2464	0.2636	0.1928	0.1005
47651	0.0427	0.0352	0.0574	0.0678	0.0333	0.0091	0.0231	0.0711	0.1202	0.1739	0.1706	0.1019
47653	0.0731	0.0948	0.1444	0.1309	0.0486	0.0072	0.0177	0.0688	0.1316	0.1812	0.1693	0.1095
47654	0.2687	0.1887	0.1232	0.0497	0.0111	0.0050	0.0109	0.0299	0.0529	0.1440	0.2874	0.3438
47655	0.2725	0.1894	0.0941	0.0311	0.0085	0.0077	0.0274	0.0504	0.0679	0.1195	0.2066	0.2797
47656	0.0518	0.0472	0.0646	0.0683	0.0451	0.0168	0.0044	0.0013	0.0057	0.0257	0.0574	0.0699
47657	0.0744	0.0728	0.0618	0.0420	0.0232	0.0116	0.0130	0.0210	0.0225	0.0383	0.0625	0.0728
47663	0.0871	0.0538	0.0471	0.0350	0.0149	0.0035	0.0048	0.0173	0.0618	0.1368	0.1786	0.1510

WMO code	Jan	Feb	Mar	Apr	May	Jun	Jul	Aug	Sep	Oct	Nov	Dec
47666	0.2450	0.1744	0.1368	0.0956	0.0497	0.0350	0.0648	0.0835	0.1280	0.2197	0.2890	0.3026
47668	0.1711	0.1047	0.1287	0.1346	0.0882	0.0367	0.0238	0.0309	0.0611	0.1113	0.1832	0.2325
47670	0.1087	0.1502	0.2201	0.2448	0.1950	0.0850	0.0413	0.1265	0.2602	0.3153	0.2899	0.1864
47674	0.0828	0.0841	0.1035	0.0980	0.0609	0.0411	0.0723	0.1136	0.1422	0.1795	0.1606	0.1128
47675	0.1289	0.0947	0.0973	0.0821	0.0522	0.0603	0.0877	0.0982	0.1235	0.1866	0.2230	0.1955
47678	0.1055	0.0729	0.0473	0.0299	0.0202	0.0202	0.0266	0.0349	0.0541	0.0913	0.1293	0.1359
47690	0.2197	0.1961	0.1591	0.1060	0.0842	0.1357	0.2201	0.2440	0.2405	0.2503	0.2518	0.2405
47740	0.3995	0.3670	0.3501	0.3003	0.2283	0.2151	0.2978	0.3428	0.2781	0.2946	0.3708	0.4182
47741	0.3463	0.3265	0.3171	0.2832	0.2320	0.2139	0.2442	0.2697	0.2835	0.3147	0.3409	0.3561
47742	0.3479	0.3190	0.2948	0.2584	0.2201	0.2159	0.2498	0.2628	0.2495	0.2678	0.3058	0.3444
47744	0.3854	0.3473	0.3091	0.2543	0.2039	0.1981	0.2388	0.2710	0.2787	0.3087	0.3493	0.3861
47746	0.3662	0.3519	0.3254	0.2625	0.1972	0.1850	0.2313	0.2796	0.3069	0.3366	0.3558	0.3675
47747	0.2178	0.2298	0.2523	0.2418	0.2026	0.1965	0.2423	0.2764	0.2836	0.2877	0.2661	0.2337
47750	0.2068	0.2248	0.2366	0.2097	0.1712	0.1790	0.2315	0.2592	0.2548	0.2484	0.2297	0.2104
47754	0.2653	0.2541	0.2458	0.1985	0.1311	0.1119	0.1611	0.2134	0.2350	0.2644	0.2774	0.2770
47755	0.3559	0.3255	0.2892	0.2273	0.1492	0.1188	0.1716	0.2271	0.2477	0.2875	0.3203	0.3482
47756	0.0875	0.1195	0.1811	0.1966	0.1470	0.1198	0.1513	0.1883	0.2154	0.2177	0.1687	0.1092
47759	0.2395	0.2396	0.2598	0.2324	0.1531	0.0994	0.1085	0.1659	0.2639	0.3395	0.3423	0.2904
47761	0.0902	0.1268	0.1877	0.2050	0.1625	0.1286	0.1501	0.2041	0.2424	0.2412	0.1846	0.1136
47762	0.3378	0.2853	0.2493	0.2058	0.1385	0.0938	0.1019	0.1414	0.2103	0.2962	0.3533	0.3679
47765	0.1978	0.1477	0.1385	0.1201	0.0812	0.0681	0.0918	0.1271	0.1892	0.2638	0.2944	0.2671
47766	0.1895	0.1371	0.1220	0.1054	0.0711	0.0636	0.0970	0.1213	0.1554	0.2197	0.2570	0.2446
47768	0.1860	0.1498	0.1601	0.1606	0.1244	0.1010	0.1266	0.1736	0.2396	0.3008	0.3072	0.2582
47769	0.1684	0.1458	0.1548	0.1424	0.1020	0.0908	0.1249	0.1623	0.2150	0.2749	0.2831	0.2336
47770	0.3140	0.2875	0.2791	0.2274	0.1351	0.0794	0.0874	0.1384	0.2428	0.3476	0.3895	0.3685
47772	0.2555	0.2492	0.2712	0.2430	0.1502	0.0802	0.0756	0.1369	0.2706	0.3707	0.3760	0.3177
47776	0.3205	0.2722	0.2494	0.2034	0.1230	0.0689	0.0787	0.1258	0.2206	0.3280	0.3790	0.3719
47777	0.1762	0.1550	0.1742	0.2146	0.0700	0.0666	0.1051	0.0376	0.1920	0.2721	0.2812	0.2021
47778	0.2287	0.1606	0.1118	0.0666	0.0289	0.0152	0.0342	0.0622	0.1057	0.1806	0.2479	0.2721
47780	0.1734	0.1886	0.2335	0.2285	0.1530	0.0905	0.0888	0.1452	0.2618	0.3430	0.3202	0.2331
47800	0.3609	0.3220	0.2714	0.2235	0.1724	0.1347	0.1262	0.1361	0.1501	0.1959	0.2665	0.3357
47805	0.3262	0.2830	0.2455	0.1970	0.1342	0.1000	0.1093	0.1118	0.1258	0.1877	0.2642	0.3223
47807	0.3062	0.2699	0.2475	0.2040	0.1352	0.0974	0.1116	0.1426	0.1850	0.2531	0.3062	0.3259
47809	0.2736	0.2149	0.2096	0.2613	0.1393	0.1307	0.1345	0.1175	0.2393	0.2614	0.2720	0.2478
47812	0.2610	0.2250	0.2030	0.1547	0.0837	0.0563	0.0635	0.0799	0.1138	0.1807	0.2506	0.2741

WMO code	Jan	Feb	Mar	Apr	May	Jun	Jul	Aug	Sep	Oct	Nov	Dec
47813	0.2311	0.2042	0.2014	0.1702	0.1064	0.0718	0.0773	0.0869	0.1324	0.2190	0.2709	0.2680
47814	0.2281	0.1582	0.1525	0.1912	0.0799	0.0847	0.0812	0.0559	0.1885	0.2568	0.2516	0.2190
47815	0.1203	0.0909	0.0932	0.0898	0.0669	0.0612	0.0829	0.0932	0.1143	0.1669	0.1960	0.1729
47817	0.3062	0.2199	0.1835	0.1845	0.0582	0.0712	0.0664	0.0545	0.1563	0.2115	0.2773	0.2806
47819	0.2574	0.1750	0.1427	0.1496	0.0535	0.0654	0.0770	0.0549	0.1455	0.1980	0.2615	0.2716
47821	0.3061	0.2444	0.1979	0.1386	0.0709	0.0405	0.0519	0.0662	0.1123	0.2144	0.3016	0.3354
47823	0.2699	0.1999	0.1588	0.1468	0.0322	0.0658	0.0556	0.0344	0.1602	0.2177	0.2784	0.2600
47824	0.0841	0.0750	0.0888	0.0848	0.0539	0.0361	0.0380	0.0456	0.0827	0.1463	0.1649	0.1269
47827	0.1986	0.1358	0.1050	0.0734	0.0415	0.0297	0.0277	0.0286	0.0671	0.1646	0.2553	0.2649
47829	0.1454	0.1218	0.1020	0.0625	0.0429	0.0450	0.0329	0.0237	0.0690	0.1827	0.2384	0.1919
47830	0.1439	0.0999	0.0889	0.0730	0.0449	0.0301	0.0292	0.0347	0.0821	0.1683	0.2255	0.2097
47831	0.1670	0.1266	0.1065	0.0783	0.0384	0.0249	0.0204	0.0275	0.0779	0.1672	0.2119	0.2052
47835	0.1804	0.1190	0.0888	0.0593	0.0316	0.0239	0.0280	0.0303	0.0673	0.1490	0.2267	0.2414
47836	0.1943	0.1550	0.0983	0.0472	0.0183	0.0064	0.0038	0.0170	0.0564	0.1150	0.1697	0.2002
47837	0.2139	0.1565	0.1168	0.0754	0.0375	0.0218	0.0186	0.0211	0.0628	0.1468	0.2268	0.2536
47838	0.3501	0.2432	0.1794	0.1563	0.0428	0.0597	0.0480	0.0412	0.1505	0.2207	0.3205	0.3356
47887	0.1788	0.1449	0.1433	0.1261	0.0863	0.0712	0.0850	0.1008	0.1534	0.2318	0.2654	0.2383
47890	0.0690	0.0655	0.0925	0.1108	0.0859	0.0603	0.0829	0.1309	0.1850	0.2193	0.1883	0.1174
47891	0.0679	0.0637	0.0940	0.1184	0.0995	0.0746	0.0914	0.1441	0.2118	0.2487	0.2098	0.1252
47892	0.1625	0.1406	0.1456	0.1298	0.0859	0.0700	0.0869	0.0897	0.1272	0.1949	0.2268	0.2075
47893	0.1771	0.1049	0.0776	0.0545	0.0327	0.0265	0.0312	0.0292	0.0552	0.1377	0.2297	0.2513
47895	0.1671	0.1429	0.1521	0.1406	0.0887	0.0523	0.0605	0.0882	0.1593	0.2495	0.2755	0.2313
47897	0.1613	0.1208	0.1129	0.0935	0.0562	0.0404	0.0488	0.0537	0.0883	0.1672	0.2256	0.2184
47898	0.2460	0.2119	0.1691	0.0964	0.0481	0.0414	0.0600	0.0548	0.0766	0.1774	0.2804	0.2892
47899	0.3015	0.2306	0.1938	0.1469	0.0840	0.0506	0.0590	0.0730	0.1385	0.2536	0.3423	0.3618
47909	0.0907	0.0717	0.0704	0.0376	0.0077	0.0022	0.0025	0.0070	0.0249	0.0621	0.1054	0.1115
47912	0.1096	0.0890	0.0867	0.0617	0.0172	0.0010	0.0015	0.0019	0.0106	0.0519	0.1166	0.1388
47918	0.0944	0.0732	0.0735	0.0586	0.0227	0.0034	0.0059	0.0086	0.0190	0.0669	0.1208	0.1281
47927	0.1006	0.0713	0.0631	0.0455	0.0166	0.0024	0.0054	0.0095	0.0134	0.0492	0.1071	0.1311
47929	0.1070	0.0795	0.0657	0.0432	0.0166	0.0036	0.0021	0.0029	0.0131	0.0513	0.1043	0.1295
47936	0.1054	0.0822	0.0744	0.0355	0.0081	0.0048	0.0045	0.0034	0.0104	0.0729	0.1536	0.1551
47945	0.0431	0.0293	0.0403	0.0296	0.0065	0.0042	0.0028	0.0023	0.0030	0.0244	0.0770	0.0851

Appendix #2. The values of the monthly averaged SDNC from other 136 stations to Osaka.

WMO code	Jan	Feb	Mar	Apr	May	Jun	Jul	Aug	Sep	Oct	Nov	Dec
47401	0.0860	0.1050	0.1196	0.1158	0.1020	0.0991	0.1139	0.1360	0.1333	0.1123	0.0923	0.0815
47402	0.0512	0.0715	0.0940	0.1017	0.0961	0.0867	0.0799	0.0861	0.0891	0.0765	0.0613	0.0502
47404	0.1031	0.1033	0.0853	0.0685	0.0656	0.0725	0.0702	0.0671	0.0782	0.0792	0.0806	0.0906
47405	0.0438	0.0543	0.0668	0.0772	0.0864	0.0919	0.0849	0.0725	0.0614	0.0496	0.0424	0.0407
47406	0.1068	0.1174	0.1042	0.0803	0.0666	0.0750	0.0834	0.0704	0.0607	0.0570	0.0654	0.0853
47407	0.0568	0.0450	0.0414	0.0855	0.1330	0.1268	0.0892	0.0786	0.0725	0.0371	0.0258	0.0390
47409	0.0107	0.0202	0.0387	0.0591	0.0797	0.0989	0.1010	0.0760	0.0463	0.0270	0.0166	0.0113
47411	0.1079	0.1204	0.1186	0.1051	0.0894	0.0761	0.0690	0.0780	0.0877	0.0888	0.0918	0.0971
47412	0.0845	0.1053	0.1200	0.1190	0.1095	0.0990	0.0908	0.0905	0.0883	0.0800	0.0768	0.0762
47413	0.0621	0.0781	0.0905	0.0998	0.1095	0.1158	0.1057	0.0761	0.0506	0.0417	0.0456	0.0516
47417	0.0078	0.0081	0.0309	0.0688	0.0755	0.0588	0.0519	0.0487	0.0339	0.0180	0.0138	0.0133
47418	0.0021	0.0093	0.0169	0.0266	0.0364	0.0404	0.0562	0.0511	0.0215	0.0119	0.0101	0.0040
47420	0.0047	0.0140	0.0167	0.0341	0.0702	0.0779	0.0571	0.0416	0.0360	0.0196	0.0125	0.0067
47421	0.1148	0.1313	0.1425	0.1350	0.1140	0.0892	0.0715	0.0765	0.0955	0.1063	0.1106	0.1104
47423	0.1030	0.1228	0.1291	0.1148	0.0898	0.0633	0.0517	0.0744	0.0976	0.0972	0.0953	0.0945
47424	0.0529	0.0632	0.0609	0.0499	0.0384	0.0304	0.0522	0.0912	0.0641	0.0305	0.0280	0.0362
47426	0.0190	0.0220	0.0279	0.0330	0.0440	0.0590	0.0728	0.0771	0.0598	0.0428	0.0350	0.0267
47428	0.1682	0.1717	0.1554	0.1094	0.0725	0.0707	0.1020	0.1116	0.0826	0.0833	0.1163	0.1548
47430	0.0910	0.1163	0.1223	0.1156	0.1132	0.1148	0.1144	0.1037	0.0778	0.0601	0.0592	0.0692
47433	0.0434	0.0534	0.0595	0.0736	0.0964	0.1200	0.1117	0.0629	0.0433	0.0371	0.0354	0.0375
47435	0.0437	0.0503	0.0604	0.0713	0.0842	0.0975	0.0969	0.0796	0.0612	0.0478	0.0417	0.0417
47440	0.0143	0.0273	0.0377	0.0433	0.0496	0.0496	0.0364	0.0216	0.0145	0.0096	0.0067	0.0082
47520	0.0542	0.0603	0.0427	0.0329	0.0486	0.1047	0.1565	0.0800	0.0105	0.0091	0.0046	0.0233
47570	0.0454	0.0518	0.0290	0.0231	0.0371	0.1020	0.1600	0.0865	0.0114	0.0094	0.0037	0.0141
47574	0.1818	0.1667	0.1138	0.0716	0.0602	0.0651	0.0633	0.0548	0.0559	0.0657	0.0991	0.1501
47575	0.1448	0.1459	0.1191	0.0956	0.0933	0.1014	0.0981	0.0938	0.0974	0.0873	0.0902	0.1167
47576	0.1002	0.1187	0.1000	0.0848	0.0958	0.1220	0.1234	0.0781	0.0368	0.0231	0.0273	0.0556
47581	0.1143	0.1164	0.0804	0.0573	0.0649	0.0989	0.1151	0.0777	0.0418	0.0320	0.0364	0.0679
47582	0.1332	0.1445	0.0871	0.0470	0.0460	0.0651	0.0721	0.0655	0.0556	0.0400	0.0384	0.0717
47584	0.0868	0.1071	0.0833	0.0613	0.0655	0.1064	0.1482	0.0914	0.0200	0.0075	0.0106	0.0361
47585	0.0280	0.0468	0.0333	0.0267	0.0390	0.0788	0.1027	0.0533	0.0160	0.0176	0.0125	0.0074
47587	0.1513	0.1396	0.0766	0.0409	0.0399	0.0708	0.0965	0.0737	0.0446	0.0346	0.0389	0.0904
47588	0.0743	0.0616	0.0762	0.0498	0.0724	0.1416	0.1205	0.0803	0.0329	0.0199	0.0067	0.0649
47590	0.1200	0.0973	0.0419	0.0177	0.0232	0.0679	0.1034	0.0607	0.0238	0.0225	0.0252	0.0642

WMO code	Jan	Feb	Mar	Apr	May	Jun	Jul	Aug	Sep	Oct	Nov	Dec
47592	0.1156	0.1087	0.0502	0.0198	0.0242	0.0684	0.1148	0.0747	0.0220	0.0144	0.0152	0.0517
47595	0.0634	0.0815	0.0530	0.0313	0.0405	0.0942	0.1274	0.0621	0.0164	0.0249	0.0200	0.0203
47597	0.0420	0.0598	0.0381	0.0231	0.0300	0.0769	0.1210	0.0614	0.0086	0.0177	0.0146	0.0093
47600	0.2033	0.1897	0.0814	0.0315	0.0342	0.0850	0.1202	0.1101	0.0650	0.0346	0.0412	0.1045
47602	0.2905	0.2494	0.1177	0.0474	0.0395	0.0636	0.0721	0.0631	0.0679	0.0693	0.0997	0.1966
47604	0.1583	0.1526	0.1377	0.0325	0.0295	0.0999	0.0690	0.0776	0.1149	0.0286	0.0539	0.1856
47605	0.3289	0.3085	0.2141	0.0625	0.0553	0.0924	0.1090	0.0976	0.1275	0.1084	0.1362	0.3003
47606	0.3780	0.2495	0.1003	0.0425	0.0429	0.0683	0.0776	0.0780	0.0824	0.1115	0.2229	0.3513
47607	0.2077	0.1720	0.0695	0.0294	0.0328	0.0747	0.0931	0.0763	0.0517	0.0436	0.0756	0.1403
47610	0.0351	0.0342	0.0545	0.0356	0.0297	0.1181	0.1000	0.0550	0.1056	0.0358	0.0564	0.0309
47612	0.1391	0.1115	0.0306	0.0135	0.0216	0.0592	0.0674	0.0576	0.0549	0.0452	0.0475	0.0788
47615	0.0131	0.0143	0.0224	0.0237	0.0269	0.0548	0.0805	0.0496	0.0194	0.0309	0.0440	0.0329
47616	0.1344	0.1029	0.1012	0.0548	0.0521	0.0839	0.1026	0.0618	0.1009	0.0377	0.0576	0.1826
47617	0.0511	0.0429	0.0512	0.0377	0.0252	0.0509	0.0786	0.1107	0.0635	0.0248	0.0750	0.0843
47618	0.0653	0.0386	0.0331	0.0195	0.0205	0.1039	0.0987	0.0651	0.0427	0.0647	0.1135	0.0888
47620	0.0584	0.0227	0.0641	0.0483	0.0176	0.0738	0.1164	0.0762	0.0419	0.0605	0.1185	0.1017
47624	0.0090	0.0462	0.0786	0.0155	0.0329	0.0380	0.0698	0.0604	0.0136	0.0378	0.0302	0.0176
47626	0.0296	0.0477	0.0388	0.0210	0.0135	0.0282	0.0552	0.0454	0.0171	0.0247	0.0322	0.0218
47629	0.0174	0.0112	0.0146	0.0135	0.0107	0.0352	0.0698	0.0379	0.0176	0.0416	0.0533	0.0387
47631	0.4116	0.3374	0.1405	0.0461	0.0248	0.0383	0.0849	0.0904	0.0314	0.0334	0.1052	0.2690
47632	0.0891	0.1460	0.1125	0.0652	0.0673	0.0255	0.0337	0.0900	0.0259	0.0559	0.0773	0.0818
47636	0.0777	0.0641	0.0532	0.0415	0.0284	0.0166	0.0103	0.0169	0.0413	0.0743	0.0946	0.0924
47637	0.0583	0.0133	0.0235	0.0260	0.0128	0.0271	0.0365	0.0328	0.0152	0.0447	0.1020	0.1275
47638	0.0172	0.0138	0.0117	0.0085	0.0047	0.0068	0.0271	0.0287	0.0107	0.0344	0.0557	0.0412
47640	0.0207	0.0239	0.0199	0.0190	0.0056	0.0143	0.0538	0.0261	0.0140	0.0625	0.1052	0.0756
47641	0.0258	0.0311	0.0193	0.0072	0.0049	0.0210	0.0485	0.0319	0.0076	0.0363	0.0523	0.0337
47648	0.0233	0.0153	0.0117	0.0097	0.0084	0.0199	0.0458	0.0555	0.0446	0.0370	0.0382	0.0336
47649	0.1544	0.1281	0.0982	0.0574	0.0240	0.0719	0.2173	0.2267	0.0462	0.0644	0.1330	0.1620
47651	0.0650	0.0584	0.0288	0.0159	0.0088	0.0129	0.0134	0.0484	0.0218	0.0489	0.0427	0.0418
47653	0.0509	0.0397	0.0318	0.0302	0.0308	0.0152	0.0110	0.0327	0.0145	0.0370	0.0681	0.0685
47654	0.1754	0.0859	0.0118	0.0209	0.0155	0.0036	0.0152	0.0227	0.0180	0.0213	0.0265	0.1385
47655	0.2401	0.1221	0.0233	0.0173	0.0158	0.0049	0.0295	0.0670	0.0487	0.0316	0.0720	0.1974
47656	0.0232	0.0607	0.0304	0.0230	0.0131	0.0022	0.0120	0.0143	0.0103	0.0236	0.0667	0.0480
47657	0.0801	0.0789	0.0515	0.0395	0.0159	0.0062	0.0367	0.0343	0.0099	0.0448	0.1190	0.0983
47662	0.0302	0.0365	0.0247	0.0134	0.0088	0.0238	0.0583	0.0464	0.0133	0.0218	0.0309	0.0240

WMO code	Jan	Feb	Mar	Apr	May	Jun	Jul	Aug	Sep	Oct	Nov	Dec
47663	0.0676	0.1185	0.1039	0.0683	0.0359	0.0126	0.0087	0.0095	0.0117	0.0359	0.0612	0.0554
47666	0.0370	0.0345	0.0196	0.0183	0.0107	0.0168	0.0650	0.0541	0.0134	0.0160	0.0116	0.0134
47668	0.0138	0.0139	0.0194	0.0199	0.0056	0.0090	0.0363	0.0230	0.0081	0.0349	0.0484	0.0316
47670	0.0275	0.0330	0.0223	0.0104	0.0040	0.0119	0.0454	0.0384	0.0076	0.0293	0.0478	0.0352
47674	0.0320	0.0206	0.0166	0.0125	0.0042	0.0182	0.0637	0.0451	0.0053	0.0292	0.0633	0.0599
47675	0.0200	0.0212	0.0204	0.0174	0.0104	0.0261	0.0781	0.0802	0.0346	0.0359	0.0397	0.0267
47678	0.0421	0.0364	0.0333	0.0345	0.0173	0.0161	0.0411	0.0269	0.0077	0.0098	0.0149	0.0288
47690	0.0222	0.0246	0.0312	0.0410	0.0270	0.0630	0.1000	0.0477	0.0090	0.0474	0.0752	0.0471
47740	0.5522	0.4959	0.2967	0.1466	0.1237	0.1565	0.2164	0.2702	0.1947	0.1884	0.2685	0.4440
47741	0.5742	0.5168	0.3155	0.1681	0.1706	0.2096	0.2130	0.2138	0.1866	0.1951	0.2623	0.4542
47742	0.5725	0.4817	0.2876	0.1509	0.1224	0.1686	0.2283	0.1950	0.1249	0.1520	0.3030	0.4905
47744	0.5798	0.4756	0.1813	0.0544	0.0760	0.1500	0.1573	0.1266	0.0868	0.0885	0.1712	0.4124
47746	0.4549	0.3861	0.1814	0.0753	0.0667	0.1136	0.1451	0.1329	0.0967	0.0981	0.1543	0.3042
47747	0.1331	0.1326	0.0503	0.0349	0.0492	0.1087	0.1426	0.1156	0.0552	0.0350	0.0398	0.0533
47750	0.1034	0.0759	0.0384	0.0186	0.0177	0.0588	0.1268	0.1000	0.0260	0.0121	0.0235	0.0665
47754	0.3844	0.3166	0.1479	0.0611	0.0565	0.1100	0.1786	0.1913	0.1664	0.1369	0.1443	0.2578
47755	0.5427	0.3946	0.1876	0.0811	0.0670	0.1297	0.1899	0.1744	0.1878	0.0895	0.1020	0.3945
47756	0.0264	0.0435	0.0884	0.1295	0.1390	0.1615	0.2142	0.1772	0.0706	0.0263	0.0136	0.0188
47759	0.2251	0.2477	0.2510	0.2387	0.2164	0.1884	0.1570	0.1269	0.1091	0.1129	0.1409	0.1842
47761	0.0397	0.0134	0.0135	0.0151	0.0311	0.0691	0.1250	0.1137	0.0288	0.0440	0.0730	0.0739
47762	0.5779	0.4348	0.2330	0.2562	0.1399	0.1497	0.2252	0.2111	0.3608	0.3574	0.4519	0.5600
47765	0.3010	0.1677	0.0733	0.0480	0.0685	0.1187	0.1610	0.1547	0.1485	0.2049	0.3020	0.3524
47766	0.3393	0.0746	0.0441	0.0414	0.0269	0.0885	0.1778	0.0882	0.0976	0.1289	0.1174	0.3035
47768	0.1319	0.0502	0.0390	0.0413	0.0742	0.1541	0.2394	0.2391	0.0965	0.0751	0.1607	0.2227
47769	0.1172	0.1373	0.1150	0.0389	0.0308	0.1321	0.2574	0.0585	0.1852	0.0691	0.0756	0.0878
47770	0.6302	0.5117	0.2974	0.1677	0.1857	0.1951	0.1581	0.2355	0.3468	0.4816	0.5921	0.6464
47776	0.5240	0.2772	0.0737	0.0812	0.1234	0.1615	0.0868	0.0896	0.1116	0.2294	0.4102	0.5547
47777	0.0896	0.0996	0.0992	0.1114	0.0648	0.0293	0.0178	0.0175	0.0474	0.1134	0.1173	0.0840
47778	0.2025	0.0681	0.0371	0.0263	0.0241	0.0070	0.0555	0.0232	0.0105	0.0078	0.0314	0.1440
47780	0.2664	0.2283	0.1959	0.1635	0.1072	0.0655	0.0865	0.1076	0.0767	0.1698	0.2455	0.2764
47800	0.5734	0.4878	0.3173	0.1819	0.1342	0.1453	0.2000	0.2474	0.2432	0.2884	0.4101	0.5329
47805	0.5472	0.4504	0.2939	0.1810	0.1365	0.1524	0.2067	0.2010	0.1654	0.2312	0.3791	0.5110
47807	0.5323	0.4360	0.2315	0.1224	0.1303	0.1703	0.2000	0.2159	0.2472	0.2848	0.3386	0.4545
47809	0.2452	0.2523	0.2320	0.1923	0.1606	0.1478	0.1751	0.2260	0.2131	0.2020	0.2198	0.2348
47812	0.4543	0.3752	0.2727	0.1850	0.1267	0.1199	0.1529	0.1644	0.1770	0.2593	0.3712	0.4500

WMO code	Jan	Feb	Mar	Apr	May	Jun	Jul	Aug	Sep	Oct	Nov	Dec
47813	0.4041	0.3264	0.2645	0.2093	0.1554	0.1347	0.1525	0.1631	0.1926	0.2967	0.3909	0.4306
47814	0.2433	0.1967	0.1699	0.1465	0.1193	0.1135	0.1399	0.1511	0.1582	0.2317	0.2916	0.2889
47815	0.1617	0.0308	0.0128	0.0040	0.0186	0.0517	0.1391	0.0544	0.0731	0.0196	0.0326	0.1255
47817	0.4839	0.4005	0.2285	0.1259	0.1118	0.1218	0.1258	0.1476	0.2343	0.3136	0.3557	0.4293
47819	0.4291	0.3515	0.1856	0.1583	0.0890	0.1283	0.1835	0.1103	0.2505	0.3151	0.3633	0.3931
47821	0.5403	0.4326	0.2995	0.1927	0.1324	0.1101	0.1132	0.1610	0.2333	0.3680	0.4821	0.5551
47823	0.4235	0.3151	0.1496	0.0740	0.0429	0.0542	0.0780	0.0990	0.1467	0.2250	0.2799	0.3700
47824	0.0857	0.1005	0.0505	0.0506	0.0289	0.0845	0.1225	0.0453	0.1404	0.1441	0.0938	0.0536
47827	0.3561	0.2085	0.1083	0.0575	0.0402	0.0528	0.0687	0.0719	0.1162	0.2520	0.4000	0.4435
47829	0.1886	0.1447	0.0557	0.0228	0.0237	0.0698	0.1007	0.0563	0.0461	0.1318	0.1959	0.1989
47830	0.1443	0.0877	0.0294	0.0304	0.0216	0.0473	0.0724	0.0342	0.0258	0.0652	0.0924	0.1321
47831	0.2892	0.1993	0.0942	0.0551	0.0379	0.0429	0.0519	0.0632	0.1153	0.2051	0.2401	0.2810
47835	0.2969	0.1372	0.0368	0.0291	0.0142	0.0275	0.0480	0.0347	0.0399	0.0989	0.1929	0.3126
47836	0.3627	0.2300	0.0835	0.0320	0.0138	0.0145	0.0161	0.0196	0.0644	0.1541	0.2541	0.3573
47837	0.3920	0.2663	0.0979	0.0334	0.0189	0.0366	0.0608	0.0509	0.0565	0.1144	0.2181	0.3561
47838	0.5448	0.4567	0.2333	0.1357	0.0539	0.1081	0.1365	0.0776	0.2099	0.3475	0.4572	0.4977
47887	0.1806	0.0973	0.0245	0.0102	0.0470	0.0843	0.1061	0.1109	0.0950	0.1387	0.1683	0.1985
47890	0.0476	0.0392	0.0372	0.0354	0.0373	0.0426	0.0743	0.0596	0.0227	0.0752	0.1108	0.0881
47891	0.0488	0.0521	0.0563	0.0268	0.0288	0.0437	0.0816	0.1818	0.0564	0.0338	0.0568	0.0485
47892	0.1708	0.1002	0.0599	0.0479	0.0313	0.0467	0.1121	0.1040	0.0735	0.0995	0.1520	0.1945
47893	0.1822	0.0733	0.0279	0.0170	0.0084	0.0221	0.0454	0.0173	0.0113	0.0236	0.1119	0.2488
47895	0.1388	0.0317	0.0494	0.0430	0.0211	0.0160	0.0196	0.0781	0.0232	0.0455	0.0265	0.1157
47897	0.1716	0.0734	0.0328	0.0270	0.0131	0.0269	0.0694	0.0476	0.0235	0.0500	0.1264	0.2012
47898	0.4109	0.3330	0.1383	0.0249	0.0145	0.0511	0.1265	0.0611	0.0249	0.1503	0.3398	0.4225
47899	0.4262	0.1841	0.0346	0.0292	0.0132	0.0294	0.0848	0.0336	0.0068	0.0330	0.1990	0.4213
47909	0.1906	0.1301	0.0575	0.0139	0.0124	0.0170	0.0075	0.0119	0.0555	0.0626	0.1023	0.1535
47912	0.2366	0.1997	0.1416	0.0651	0.0204	0.0085	0.0061	0.0103	0.0114	0.0923	0.2230	0.2625
47918	0.2187	0.1677	0.1219	0.0470	0.0220	0.0129	0.0063	0.0043	0.0072	0.0755	0.2307	0.2504
47927	0.2232	0.1483	0.0982	0.0482	0.0157	0.0142	0.0072	0.0026	0.0084	0.0615	0.1858	0.2676
47929	0.2356	0.1841	0.1151	0.0408	0.0101	0.0105	0.0028	0.0158	0.0374	0.0883	0.2427	0.2625
47936	0.2621	0.1741	0.1022	0.0415	0.0122	0.0118	0.0045	0.0127	0.0357	0.0877	0.2229	0.2648
47945	0.0540	0.0294	0.0193	0.0138	0.0054	0.0014	0.0022	0.0046	0.0152	0.0396	0.0690	0.0771

Appendix #3. The values of the monthly averaged SDNC from Tokyo to other 136 stations.

WMO code	Jan	Feb	Mar	Apr	May	Jun	Jul	Aug	Sep	Oct	Nov	Dec
47401	0.0485	0.0308	0.0251	0.0277	0.0311	0.0207	0.0037	0.0031	0.0063	0.0263	0.0510	0.0616
47402	0.0425	0.0047	0.0304	0.0427	0.0083	0.0170	0.0141	0.0098	0.0090	0.0182	0.0648	0.0446
47404	0.0247	0.0171	0.0118	0.0125	0.0152	0.0109	0.0029	0.0028	0.0044	0.0149	0.0249	0.0285
47405	0.0347	0.0034	0.0217	0.0358	0.0058	0.0122	0.0145	0.0111	0.0083	0.0114	0.0453	0.0324
47406	0.0091	0.0051	0.0190	0.0235	0.0112	0.0103	0.0027	0.0045	0.0054	0.0063	0.0304	0.0348
47407	0.0056	0.0051	0.0180	0.0357	0.0165	0.0110	0.0086	0.0035	0.0045	0.0108	0.0234	0.0132
47409	0.0289	0.0152	0.0109	0.0164	0.0234	0.0156	0.0030	0.0062	0.0049	0.0198	0.0410	0.0450
47411	0.0600	0.0447	0.0325	0.0231	0.0156	0.0100	0.0146	0.0085	0.0070	0.0280	0.0506	0.0647
47412	0.0328	0.0239	0.0195	0.0170	0.0145	0.0120	0.0179	0.0115	0.0045	0.0200	0.0353	0.0402
47413	0.0189	0.0156	0.0166	0.0204	0.0218	0.0146	0.0102	0.0072	0.0056	0.0172	0.0251	0.0240
47417	0.0166	0.0155	0.0216	0.0335	0.0180	0.0340	0.0713	0.0387	0.0410	0.0190	0.0334	0.0137
47418	0.0074	0.0057	0.0134	0.0277	0.0376	0.0355	0.0203	0.0152	0.0095	0.0027	0.0119	0.0170
47420	0.0140	0.0064	0.0095	0.0126	0.0133	0.0130	0.0087	0.0077	0.0080	0.0062	0.0309	0.0429
47421	0.0691	0.0454	0.0275	0.0191	0.0182	0.0195	0.0213	0.0074	0.0110	0.0404	0.0660	0.0783
47423	0.0491	0.0362	0.0333	0.0228	0.0180	0.0340	0.0473	0.0266	0.0071	0.0346	0.0711	0.0741
47424	0.0284	0.0151	0.0203	0.0227	0.0298	0.0500	0.0295	0.0103	0.0086	0.0154	0.0371	0.0474
47426	0.0361	0.0191	0.0157	0.0239	0.0288	0.0199	0.0101	0.0052	0.0126	0.0318	0.0484	0.0513
47428	0.0497	0.0380	0.0251	0.0213	0.0255	0.0215	0.0099	0.0018	0.0104	0.0268	0.0403	0.0500
47430	0.0329	0.0240	0.0237	0.0276	0.0291	0.0212	0.0168	0.0049	0.0120	0.0367	0.0503	0.0463
47433	0.0163	0.0144	0.0170	0.0207	0.0203	0.0143	0.0104	0.0032	0.0095	0.0244	0.0284	0.0225
47435	0.0329	0.0189	0.0129	0.0145	0.0186	0.0133	0.0030	0.0059	0.0051	0.0185	0.0400	0.0482
47440	0.0128	0.0100	0.0099	0.0115	0.0192	0.0400	0.0686	0.0578	0.0213	0.0058	0.0087	0.0140
47520	0.0134	0.0057	0.0141	0.0247	0.0110	0.0145	0.0158	0.0039	0.0073	0.0167	0.0202	0.0167
47570	0.0037	0.0115	0.0119	0.0223	0.0052	0.0184	0.0116	0.0108	0.0278	0.0173	0.0092	0.0099
47574	0.0337	0.0158	0.0091	0.0146	0.0215	0.0246	0.0249	0.0066	0.0084	0.0270	0.0418	0.0465
47575	0.0319	0.0212	0.0237	0.0253	0.0228	0.0272	0.0408	0.0156	0.0171	0.0479	0.0640	0.0545
47576	0.0448	0.0263	0.0228	0.0291	0.0309	0.0183	0.0155	0.0118	0.0034	0.0195	0.0456	0.0579
47581	0.0287	0.0082	0.0193	0.0233	0.0155	0.0191	0.0235	0.0159	0.0038	0.0109	0.0454	0.0634
47582	0.0443	0.0124	0.0141	0.0164	0.0196	0.0443	0.0359	0.0055	0.0058	0.0141	0.0401	0.0651
47584	0.0289	0.0169	0.0176	0.0195	0.0182	0.0176	0.0253	0.0129	0.0082	0.0342	0.0548	0.0499
47585	0.0132	0.0044	0.0115	0.0231	0.0243	0.0156	0.0194	0.0193	0.0046	0.0130	0.0300	0.0297
47587	0.0515	0.0259	0.0086	0.0156	0.0311	0.0351	0.0244	0.0034	0.0083	0.0237	0.0436	0.0592
47588	0.0214	0.0125	0.0137	0.0127	0.0072	0.0073	0.0133	0.0061	0.0079	0.0239	0.0350	0.0338
47590	0.0425	0.0121	0.0094	0.0183	0.0207	0.0231	0.0523	0.0405	0.0090	0.0397	0.0819	0.0820

WMO code	Jan	Feb	Mar	Apr	May	Jun	Jul	Aug	Sep	Oct	Nov	Dec
47592	0.0423	0.0106	0.0111	0.0294	0.0273	0.0340	0.0508	0.0098	0.0112	0.0201	0.0405	0.0687
47595	0.0308	0.0101	0.0089	0.0136	0.0162	0.0254	0.0284	0.0180	0.0080	0.0118	0.0252	0.0390
47597	0.0197	0.0085	0.0109	0.0131	0.0109	0.0175	0.0161	0.0090	0.0228	0.0485	0.0539	0.0401
47600	0.0143	0.0132	0.0225	0.0301	0.0268	0.0253	0.0352	0.0281	0.0097	0.0077	0.0161	0.0198
47602	0.0266	0.0122	0.0207	0.0221	0.0297	0.0243	0.0127	0.0123	0.0123	0.0116	0.0237	0.0365
47604	0.0477	0.0142	0.0047	0.0186	0.0261	0.0239	0.0197	0.0052	0.0046	0.0224	0.0501	0.0661
47605	0.0190	0.0190	0.0185	0.0187	0.0205	0.0251	0.0303	0.0218	0.0134	0.0197	0.0272	0.0243
47606	0.0142	0.0139	0.0159	0.0167	0.0186	0.0239	0.0298	0.0198	0.0112	0.0199	0.0292	0.0242
47607	0.0192	0.0216	0.0244	0.0228	0.0193	0.0194	0.0208	0.0113	0.0061	0.0117	0.0190	0.0198
47610	0.0572	0.0465	0.0240	0.0119	0.0075	0.0064	0.0072	0.0051	0.0117	0.0228	0.0264	0.0372
47612	0.0152	0.0032	0.0102	0.0263	0.0301	0.0252	0.0224	0.0099	0.0069	0.0141	0.0238	0.0271
47615	0.0802	0.0966	0.0744	0.0210	0.0309	0.0398	0.0321	0.0213	0.0428	0.0763	0.0351	0.0393
47616	0.0083	0.0141	0.0264	0.0093	0.0263	0.0310	0.0216	0.0233	0.0214	0.0142	0.0146	0.0202
47617	0.0772	0.0496	0.0144	0.0053	0.0041	0.0081	0.0155	0.0064	0.0111	0.0238	0.0285	0.0505
47618	0.1399	0.1031	0.0396	0.0129	0.0051	0.0031	0.0095	0.0081	0.0165	0.0295	0.0418	0.0922
47620	0.1214	0.0799	0.0254	0.0106	0.0046	0.0086	0.0248	0.0147	0.0158	0.0309	0.0363	0.0758
47624	0.0610	0.0496	0.0260	0.0138	0.0239	0.0958	0.1425	0.0911	0.0490	0.0238	0.0531	0.0478
47626	0.2988	0.2301	0.1197	0.0657	0.0750	0.1253	0.1451	0.0947	0.0504	0.0594	0.1214	0.2389
47629	0.1375	0.1866	0.1620	0.1112	0.0551	0.0193	0.0069	0.0169	0.0351	0.0464	0.0394	0.0482
47631	0.0073	0.0178	0.0345	0.0181	0.0436	0.0487	0.0550	0.0319	0.0154	0.0101	0.0089	0.0151
47632	0.0221	0.0183	0.0063	0.0035	0.0164	0.0665	0.1210	0.0649	0.0124	0.0280	0.0394	0.0266
47636	0.0245	0.0208	0.0132	0.0103	0.0183	0.0708	0.1249	0.0610	0.0075	0.0298	0.0430	0.0304
47637	0.1138	0.0827	0.0296	0.0117	0.0134	0.0399	0.0641	0.0301	0.0109	0.0211	0.0282	0.0667
47638	0.3190	0.2599	0.1437	0.0776	0.0785	0.1411	0.2150	0.1489	0.0501	0.0377	0.0787	0.2322
47640	0.1411	0.1931	0.1827	0.1407	0.0951	0.0648	0.0632	0.0852	0.0840	0.0693	0.0639	0.0788
47641	0.2650	0.2934	0.2039	0.1125	0.0932	0.1387	0.1925	0.1663	0.0851	0.0516	0.0539	0.1283
47648	0.1219	0.1227	0.0902	0.1013	0.1128	0.0783	0.0288	0.0263	0.0430	0.0376	0.0221	0.0476
47649	0.0793	0.0813	0.0469	0.0212	0.0141	0.0249	0.0453	0.0359	0.0147	0.0163	0.0220	0.0395
47651	0.0494	0.0664	0.0464	0.0301	0.0470	0.1117	0.1754	0.1035	0.0239	0.0208	0.0227	0.0220
47653	0.0536	0.0470	0.0260	0.0181	0.0369	0.1110	0.1923	0.1045	0.0202	0.0244	0.0272	0.0363
47654	0.0341	0.0336	0.0286	0.0386	0.0871	0.1848	0.2595	0.1672	0.0387	0.0133	0.0309	0.0356
47655	0.0263	0.0365	0.0357	0.0363	0.0552	0.0942	0.1050	0.0625	0.0201	0.0150	0.0248	0.0237
47656	0.1322	0.2317	0.2711	0.2707	0.2721	0.2979	0.3294	0.2873	0.1564	0.0561	0.0314	0.0501
47657	0.2404	0.3136	0.3054	0.2392	0.1822	0.1710	0.1848	0.1662	0.1012	0.0602	0.0748	0.1368
47663	0.0882	0.1398	0.1511	0.1474	0.1593	0.1969	0.2184	0.1487	0.0518	0.0175	0.0199	0.0363

WMO code	Jan	Feb	Mar	Apr	May	Jun	Jul	Aug	Sep	Oct	Nov	Dec
47666	0.0241	0.0463	0.0560	0.0474	0.0477	0.0852	0.1257	0.1016	0.0376	0.0182	0.0325	0.0293
47668	0.0587	0.1830	0.2913	0.3173	0.3058	0.2911	0.2979	0.2836	0.1871	0.0803	0.0380	0.0326
47670	0.4493	0.5121	0.5386	0.5300	0.5148	0.4648	0.4378	0.5768	0.5874	0.5363	0.4980	0.4542
47674	0.2181	0.2158	0.1582	0.0878	0.0367	0.0202	0.0189	0.0294	0.0660	0.0827	0.1073	0.1611
47675	0.0683	0.1017	0.0981	0.0784	0.0860	0.1305	0.1635	0.1382	0.0831	0.0535	0.0445	0.0398
47678	0.0723	0.1295	0.1433	0.1246	0.1016	0.0979	0.1246	0.1359	0.0892	0.0388	0.0188	0.0258
47690	0.0718	0.0731	0.0515	0.0247	0.0092	0.0053	0.0089	0.0280	0.0436	0.0495	0.0491	0.0544
47740	0.0143	0.0208	0.0187	0.0129	0.0186	0.0427	0.0462	0.0251	0.0168	0.0084	0.0036	0.0094
47741	0.0203	0.0349	0.0328	0.0246	0.0202	0.0211	0.0330	0.0428	0.0239	0.0099	0.0121	0.0140
47742	0.0173	0.0312	0.0334	0.0295	0.0268	0.0275	0.0386	0.0451	0.0239	0.0088	0.0114	0.0142
47744	0.0194	0.0377	0.0420	0.0408	0.0399	0.0401	0.0485	0.0502	0.0272	0.0104	0.0086	0.0102
47746	0.0163	0.0293	0.0321	0.0312	0.0316	0.0322	0.0424	0.0498	0.0319	0.0171	0.0142	0.0127
47747	0.0217	0.0284	0.0289	0.0276	0.0270	0.0292	0.0384	0.0412	0.0280	0.0193	0.0184	0.0182
47750	0.0274	0.0390	0.0377	0.0331	0.0295	0.0301	0.0412	0.0436	0.0243	0.0143	0.0161	0.0180
47754	0.0378	0.0625	0.0575	0.0463	0.0413	0.0416	0.0496	0.0529	0.0305	0.0124	0.0084	0.0126
47755	0.0132	0.0244	0.0313	0.0359	0.0420	0.0485	0.0582	0.0552	0.0309	0.0139	0.0097	0.0096
47756	0.0311	0.0427	0.0305	0.0173	0.0122	0.0207	0.0393	0.0355	0.0162	0.0119	0.0104	0.0117
47759	0.0350	0.0441	0.0309	0.0177	0.0125	0.0213	0.0435	0.0399	0.0194	0.0215	0.0250	0.0217
47761	0.0318	0.0316	0.0220	0.0157	0.0167	0.0280	0.0395	0.0239	0.0088	0.0153	0.0225	0.0244
47762	0.0279	0.0294	0.0205	0.0127	0.0132	0.0241	0.0519	0.0647	0.0332	0.0174	0.0195	0.0219
47765	0.0249	0.0375	0.0275	0.0141	0.0148	0.0271	0.0314	0.0311	0.0197	0.0172	0.0213	0.0176
47766	0.0191	0.0293	0.0261	0.0190	0.0201	0.0361	0.0608	0.0523	0.0207	0.0156	0.0179	0.0142
47768	0.0215	0.0383	0.0289	0.0157	0.0126	0.0191	0.0262	0.0225	0.0117	0.0150	0.0167	0.0092
47769	0.0460	0.0630	0.0441	0.0224	0.0144	0.0232	0.0410	0.0320	0.0120	0.0183	0.0229	0.0215
47770	0.0340	0.0431	0.0295	0.0156	0.0097	0.0190	0.0451	0.0403	0.0121	0.0163	0.0258	0.0228
47772	0.0402	0.0448	0.0284	0.0146	0.0096	0.0251	0.0610	0.0491	0.0139	0.0210	0.0307	0.0282
47776	0.0254	0.0282	0.0198	0.0125	0.0110	0.0217	0.0425	0.0322	0.0087	0.0159	0.0268	0.0240
47777	0.0303	0.0764	0.0753	0.0056	0.0255	0.0493	0.0690	0.0864	0.0161	0.0123	0.0112	0.0276
47778	0.0342	0.0609	0.0720	0.0700	0.0730	0.0937	0.1120	0.0836	0.0320	0.0125	0.0187	0.0226
47780	0.0608	0.0657	0.0384	0.0177	0.0114	0.0253	0.0576	0.0504	0.0186	0.0192	0.0237	0.0303
47800	0.0170	0.0184	0.0130	0.0112	0.0194	0.0372	0.0548	0.0419	0.0167	0.0094	0.0070	0.0092
47805	0.0200	0.0365	0.0285	0.0182	0.0217	0.0372	0.0653	0.0681	0.0234	0.0045	0.0038	0.0043
47807	0.0258	0.0411	0.0363	0.0264	0.0238	0.0304	0.0489	0.0578	0.0335	0.0143	0.0089	0.0102
47809	0.0149	0.0377	0.0512	0.0087	0.0248	0.0355	0.0484	0.0400	0.0218	0.0129	0.0032	0.0227
47812	0.0284	0.0323	0.0268	0.0221	0.0263	0.0435	0.0761	0.0920	0.0429	0.0084	0.0040	0.0131

WMO code	Jan	Feb	Mar	Apr	May	Jun	Jul	Aug	Sep	Oct	Nov	Dec
47813	0.0281	0.0369	0.0270	0.0170	0.0168	0.0318	0.0624	0.0669	0.0309	0.0123	0.0089	0.0117
47814	0.0115	0.0352	0.0473	0.0053	0.0244	0.0516	0.0628	0.0493	0.0176	0.0098	0.0013	0.0072
47815	0.0614	0.0980	0.0894	0.0651	0.0480	0.0448	0.0613	0.0675	0.0308	0.0076	0.0057	0.0161
47817	0.0287	0.0333	0.0610	0.0163	0.0311	0.0416	0.0627	0.0619	0.0268	0.0131	0.0072	0.0259
47819	0.0133	0.0248	0.0473	0.0081	0.0257	0.0361	0.0441	0.0402	0.0243	0.0103	0.0044	0.0189
47821	0.0162	0.0243	0.0243	0.0245	0.0333	0.0486	0.0576	0.0419	0.0180	0.0079	0.0056	0.0075
47823	0.0316	0.0384	0.0770	0.0225	0.0407	0.0543	0.0497	0.0637	0.0295	0.0169	0.0045	0.0257
47824	0.0516	0.0663	0.0537	0.0394	0.0377	0.0474	0.0616	0.0526	0.0242	0.0100	0.0085	0.0212
47827	0.0399	0.0615	0.0547	0.0417	0.0407	0.0537	0.0763	0.0697	0.0312	0.0102	0.0058	0.0122
47829	0.0627	0.0801	0.0623	0.0570	0.0678	0.0722	0.0429	0.0326	0.0368	0.0172	0.0044	0.0193
47830	0.0540	0.0904	0.0927	0.0782	0.0653	0.0530	0.0389	0.0291	0.0194	0.0109	0.0093	0.0179
47831	0.0498	0.0730	0.0575	0.0407	0.0418	0.0506	0.0590	0.0560	0.0334	0.0133	0.0055	0.0126
47835	0.0457	0.0770	0.0799	0.0714	0.0658	0.0603	0.0484	0.0328	0.0166	0.0077	0.0066	0.0143
47836	0.0214	0.0335	0.0502	0.0668	0.0737	0.0646	0.0416	0.0181	0.0070	0.0063	0.0094	0.0140
47837	0.0293	0.0486	0.0519	0.0483	0.0482	0.0471	0.0390	0.0272	0.0144	0.0066	0.0058	0.0112
47838	0.0080	0.0270	0.0474	0.0121	0.0266	0.0362	0.0418	0.0388	0.0304	0.0087	0.0031	0.0100
47887	0.0519	0.0663	0.0441	0.0221	0.0170	0.0288	0.0548	0.0550	0.0201	0.0097	0.0118	0.0200
47890	0.0594	0.0783	0.0570	0.0342	0.0275	0.0388	0.0629	0.0559	0.0220	0.0105	0.0085	0.0192
47891	0.0881	0.1086	0.0723	0.0353	0.0215	0.0264	0.0430	0.0335	0.0086	0.0061	0.0082	0.0285
47892	0.0500	0.0724	0.0584	0.0384	0.0308	0.0353	0.0485	0.0469	0.0201	0.0084	0.0083	0.0164
47893	0.0352	0.0669	0.0724	0.0646	0.0624	0.0751	0.0920	0.0713	0.0257	0.0094	0.0111	0.0134
47895	0.0380	0.0611	0.0507	0.0341	0.0308	0.0475	0.0734	0.0580	0.0170	0.0116	0.0171	0.0157
47897	0.0405	0.0677	0.0663	0.0531	0.0481	0.0546	0.0628	0.0496	0.0205	0.0089	0.0093	0.0145
47898	0.0368	0.0506	0.0377	0.0313	0.0409	0.0622	0.0616	0.0379	0.0230	0.0100	0.0060	0.0117
47899	0.0290	0.0456	0.0423	0.0332	0.0337	0.0479	0.0663	0.0538	0.0169	0.0082	0.0163	0.0177
47909	0.0500	0.0733	0.0685	0.0652	0.0803	0.0777	0.0322	0.0086	0.0175	0.0139	0.0069	0.0173
47912	0.0082	0.0142	0.0176	0.0220	0.0253	0.0148	0.0026	0.0011	0.0039	0.0073	0.0072	0.0056
47918	0.0088	0.0122	0.0195	0.0260	0.0258	0.0137	0.0042	0.0023	0.0023	0.0098	0.0135	0.0110
47927	0.0099	0.0172	0.0251	0.0293	0.0263	0.0131	0.0021	0.0007	0.0024	0.0066	0.0078	0.0074
47929	0.0200	0.0281	0.0379	0.0454	0.0471	0.0367	0.0184	0.0087	0.0040	0.0092	0.0152	0.0173
47936	0.0327	0.0376	0.0323	0.0428	0.0591	0.0385	0.0138	0.0070	0.0150	0.0124	0.0049	0.0122
47945	0.0631	0.0921	0.0769	0.0687	0.0748	0.0511	0.0061	0.0043	0.0064	0.0108	0.0074	0.0165

Appendix #4. The values of the monthly averaged SDNC from Osaka to other 136 stations.

WMO code	Jan	Feb	Mar	Apr	May	Jun	Jul	Aug	Sep	Oct	Nov	Dec
47401	0.0484	0.0393	0.0438	0.0477	0.0357	0.0134	0.0037	0.0019	0.0127	0.0470	0.0701	0.0665
47402	0.0267	0.0205	0.0241	0.0323	0.0267	0.0094	0.0043	0.0072	0.0081	0.0318	0.0510	0.0440
47404	0.0114	0.0060	0.0279	0.0378	0.0197	0.0144	0.0080	0.0090	0.0051	0.0137	0.0488	0.0465
47405	0.0202	0.0185	0.0179	0.0220	0.0184	0.0068	0.0060	0.0144	0.0116	0.0263	0.0391	0.0317
47406	0.0073	0.0056	0.0291	0.0392	0.0229	0.0165	0.0064	0.0115	0.0157	0.0159	0.0370	0.0368
47407	0.0075	0.0176	0.0271	0.0365	0.0160	0.0044	0.0034	0.0085	0.0164	0.0266	0.0279	0.0129
47409	0.0190	0.0248	0.0249	0.0279	0.0217	0.0089	0.0053	0.0131	0.0160	0.0339	0.0409	0.0257
47411	0.0457	0.0375	0.0375	0.0362	0.0207	0.0085	0.0155	0.0164	0.0132	0.0334	0.0464	0.0499
47412	0.0232	0.0202	0.0288	0.0350	0.0229	0.0089	0.0145	0.0200	0.0156	0.0298	0.0358	0.0310
47413	0.0123	0.0148	0.0269	0.0346	0.0234	0.0078	0.0070	0.0124	0.0140	0.0256	0.0263	0.0183
47417	0.0311	0.0464	0.0346	0.0199	0.0087	0.0050	0.0111	0.0197	0.0475	0.0859	0.0724	0.0355
47418	0.0174	0.0293	0.0316	0.0229	0.0184	0.0162	0.0072	0.0084	0.0359	0.0669	0.0564	0.0268
47420	0.0123	0.0269	0.0352	0.0251	0.0085	0.0036	0.0026	0.0055	0.0248	0.0669	0.0748	0.0350
47421	0.0556	0.0404	0.0379	0.0393	0.0227	0.0069	0.0136	0.0158	0.0137	0.0324	0.0491	0.0601
47423	0.0433	0.0353	0.0376	0.0354	0.0184	0.0073	0.0205	0.0189	0.0182	0.0418	0.0550	0.0544
47424	0.0222	0.0163	0.0359	0.0357	0.0240	0.0205	0.0124	0.0081	0.0171	0.0337	0.0380	0.0370
47426	0.0194	0.0230	0.0476	0.0659	0.0461	0.0210	0.0189	0.0204	0.0272	0.0420	0.0389	0.0272
47428	0.0313	0.0242	0.0498	0.0550	0.0387	0.0248	0.0074	0.0096	0.0149	0.0210	0.0541	0.0693
47430	0.0217	0.0198	0.0352	0.0467	0.0298	0.0082	0.0112	0.0171	0.0186	0.0298	0.0329	0.0296
47433	0.0063	0.0139	0.0300	0.0367	0.0170	0.0068	0.0091	0.0231	0.0258	0.0215	0.0285	0.0207
47435	0.0258	0.0228	0.0206	0.0220	0.0178	0.0076	0.0052	0.0118	0.0117	0.0294	0.0447	0.0391
47440	0.0133	0.0152	0.0195	0.0155	0.0061	0.0047	0.0185	0.0500	0.0630	0.0544	0.0347	0.0191
47520	0.0459	0.0445	0.0677	0.0835	0.0550	0.0290	0.0195	0.0457	0.1035	0.1199	0.0904	0.0580
47570	0.1285	0.0945	0.1055	0.1214	0.0782	0.0402	0.0243	0.0522	0.1357	0.2029	0.2182	0.1771
47574	0.0184	0.0168	0.0546	0.0788	0.0577	0.0351	0.0179	0.0217	0.0357	0.0362	0.0463	0.0524
47575	0.0211	0.0224	0.0379	0.0453	0.0264	0.0090	0.0226	0.0400	0.0356	0.0342	0.0291	0.0253
47576	0.0259	0.0223	0.0340	0.0397	0.0244	0.0074	0.0093	0.0409	0.0553	0.0434	0.0286	0.0290
47581	0.0180	0.0217	0.0439	0.0513	0.0260	0.0065	0.0140	0.0519	0.0752	0.0626	0.0318	0.0199
47582	0.0105	0.0136	0.0476	0.0831	0.0805	0.0535	0.0234	0.0265	0.0528	0.0505	0.0307	0.0281
47584	0.0165	0.0269	0.0696	0.0887	0.0470	0.0161	0.0099	0.0411	0.1057	0.1211	0.0828	0.0393
47585	0.0316	0.0374	0.0744	0.0849	0.0380	0.0148	0.0183	0.0712	0.1385	0.1517	0.1188	0.0678
47587	0.0133	0.0188	0.0610	0.1055	0.0973	0.0618	0.0374	0.0519	0.0857	0.0818	0.0433	0.0284
47588	0.0233	0.0433	0.0866	0.0870	0.0288	0.0354	0.0727	0.0425	0.1243	0.2366	0.1185	0.0341
47590	0.0315	0.0564	0.1091	0.1141	0.0542	0.0177	0.0396	0.1132	0.1780	0.1730	0.1005	0.0434

WMO code	Jan	Feb	Mar	Apr	May	Jun	Jul	Aug	Sep	Oct	Nov	Dec
47592	0.0230	0.0386	0.0764	0.0893	0.0512	0.0202	0.0289	0.0763	0.1250	0.1262	0.0757	0.0324
47595	0.0940	0.0885	0.1138	0.1102	0.0536	0.0164	0.0270	0.1002	0.2197	0.2792	0.2396	0.1521
47597	0.1387	0.1512	0.1984	0.1898	0.0976	0.0253	0.0236	0.1067	0.2560	0.3294	0.2927	0.1999
47600	0.0132	0.0362	0.0989	0.1455	0.0917	0.0524	0.0440	0.0829	0.1174	0.1143	0.0671	0.0239
47602	0.0114	0.0121	0.0554	0.1043	0.0857	0.0566	0.0348	0.0428	0.0568	0.0458	0.0255	0.0276
47604	0.0184	0.0223	0.0770	0.1411	0.0925	0.0637	0.0617	0.0417	0.0636	0.1110	0.0480	0.0358
47605	0.0147	0.0161	0.0446	0.1160	0.0699	0.0805	0.0676	0.0429	0.0731	0.0511	0.0421	0.0087
47606	0.0193	0.0236	0.0901	0.1400	0.1058	0.0735	0.0751	0.0728	0.0639	0.0410	0.0166	0.0227
47607	0.0159	0.0435	0.1171	0.1653	0.0980	0.0534	0.0442	0.0774	0.1060	0.1045	0.0614	0.0207
47610	0.2208	0.2140	0.1990	0.1771	0.0756	0.0434	0.0542	0.0458	0.0386	0.1197	0.1934	0.1870
47612	0.0205	0.0461	0.1269	0.1767	0.1209	0.0688	0.0481	0.0563	0.0762	0.0807	0.0569	0.0283
47615	0.3191	0.3452	0.3574	0.2935	0.1439	0.0424	0.0435	0.1326	0.2736	0.3499	0.3404	0.3130
47616	0.0372	0.0389	0.0705	0.1678	0.1125	0.1019	0.0586	0.0425	0.1079	0.2353	0.2183	0.0176
47617	0.3904	0.2633	0.1528	0.0881	0.0471	0.0599	0.0800	0.0618	0.0565	0.1410	0.3197	0.4279
47618	0.2937	0.3508	0.2372	0.2717	0.1243	0.0540	0.1188	0.0579	0.1978	0.3308	0.4270	0.3525
47620	0.4031	0.2889	0.1803	0.2978	0.1288	0.0821	0.1216	0.0813	0.1711	0.2996	0.4838	0.4510
47624	0.3151	0.2832	0.2600	0.2813	0.0778	0.0711	0.1166	0.1163	0.3212	0.3954	0.4385	0.3319
47626	0.3481	0.3178	0.3043	0.2466	0.1407	0.0695	0.0681	0.1411	0.2879	0.4011	0.4276	0.3989
47629	0.3663	0.3742	0.3626	0.2910	0.1481	0.0452	0.0433	0.1381	0.2832	0.3635	0.3685	0.3574
47631	0.0216	0.0248	0.0969	0.2228	0.2217	0.1303	0.0603	0.0660	0.1425	0.1727	0.0930	0.0195
47632	0.1441	0.0873	0.1339	0.2151	0.1446	0.2402	0.2753	0.1415	0.2937	0.3459	0.1875	0.1451
47636	0.1714	0.1580	0.1475	0.1535	0.1794	0.2117	0.2321	0.2296	0.2092	0.1892	0.1806	0.1783
47637	0.4697	0.4530	0.3118	0.3722	0.2078	0.1102	0.2021	0.1190	0.2913	0.3932	0.5191	0.5062
47638	0.5078	0.4694	0.4592	0.4288	0.3513	0.2522	0.1830	0.2261	0.3860	0.5056	0.5420	0.5406
47640	0.3513	0.4512	0.4731	0.4633	0.2464	0.1325	0.1486	0.1648	0.3724	0.4729	0.5176	0.4735
47641	0.4261	0.3981	0.3794	0.3164	0.1961	0.0993	0.0846	0.1709	0.3409	0.4523	0.4750	0.4587
47648	0.3305	0.3229	0.2832	0.2103	0.1073	0.0435	0.0617	0.1195	0.1832	0.2434	0.2746	0.3012
47649	0.6401	0.6371	0.5689	0.4131	0.1925	0.0507	0.0298	0.0333	0.1705	0.3892	0.5192	0.5976
47651	0.5259	0.5531	0.5172	0.3972	0.3119	0.3348	0.2745	0.2355	0.3922	0.5049	0.5271	0.5090
47653	0.5511	0.4913	0.4516	0.4251	0.3923	0.3442	0.2704	0.2523	0.3852	0.5192	0.5690	0.5809
47654	0.0427	0.1046	0.3577	0.4792	0.3521	0.3127	0.3153	0.2867	0.3953	0.3923	0.1842	0.0542
47655	0.0232	0.1039	0.3148	0.4166	0.3441	0.2007	0.1154	0.1691	0.2789	0.2605	0.1047	0.0204
47656	0.4648	0.5783	0.5600	0.5148	0.3217	0.2623	0.2993	0.2023	0.4469	0.4887	0.5271	0.4893
47657	0.5071	0.5829	0.5370	0.4968	0.2849	0.1978	0.2175	0.1572	0.4215	0.4961	0.5438	0.5119
47662	0.2664	0.2566	0.2748	0.2445	0.1511	0.0806	0.0760	0.1404	0.2749	0.3747	0.3811	0.3265

WMO code	Jan	Feb	Mar	Apr	May	Jun	Jul	Aug	Sep	Oct	Nov	Dec
47663	0.4814	0.5636	0.6313	0.5777	0.3836	0.3274	0.2711	0.2641	0.4194	0.4777	0.4976	0.4813
47666	0.1719	0.2493	0.3490	0.3528	0.2323	0.1015	0.0706	0.1620	0.3148	0.3644	0.2968	0.1954
47668	0.3074	0.3341	0.3839	0.3490	0.2170	0.1184	0.1004	0.2056	0.3510	0.4181	0.4169	0.3550
47670	0.3226	0.2991	0.3091	0.2766	0.1819	0.1010	0.0834	0.1504	0.3074	0.4181	0.4298	0.3853
47674	0.3187	0.3303	0.3488	0.2959	0.1605	0.0757	0.0526	0.1227	0.2638	0.3412	0.3630	0.3398
47675	0.2632	0.2894	0.3301	0.3007	0.1815	0.0824	0.0656	0.1303	0.2717	0.3646	0.3533	0.2954
47678	0.3256	0.4109	0.4489	0.4012	0.2678	0.1282	0.0894	0.1802	0.2991	0.3312	0.3017	0.2780
47690	0.1984	0.2343	0.3459	0.3521	0.1902	0.0774	0.0732	0.1573	0.2663	0.3388	0.3633	0.2856
47740	0.0465	0.0362	0.0391	0.0578	0.0451	0.0436	0.0353	0.0339	0.0415	0.0215	0.0121	0.0375
47741	0.0694	0.0531	0.0420	0.0750	0.0561	0.0341	0.0225	0.0407	0.0600	0.0335	0.0181	0.0532
47742	0.0893	0.0573	0.0385	0.0739	0.0766	0.0462	0.0398	0.0744	0.0884	0.0475	0.0282	0.0709
47744	0.0513	0.0294	0.0673	0.1636	0.1177	0.0620	0.0658	0.1121	0.1272	0.0874	0.0313	0.0348
47746	0.0499	0.0323	0.0715	0.1538	0.1145	0.0528	0.0492	0.0947	0.1103	0.0918	0.0625	0.0511
47747	0.0540	0.0364	0.1320	0.2168	0.1426	0.0609	0.0283	0.0549	0.1067	0.1886	0.2279	0.1514
47750	0.0667	0.0787	0.1756	0.2504	0.1971	0.0861	0.0369	0.0736	0.1769	0.2283	0.1732	0.0952
47754	0.0129	0.0294	0.0816	0.1329	0.1010	0.0488	0.0346	0.0619	0.0469	0.0323	0.0179	0.0067
47755	0.0466	0.0128	0.0289	0.0908	0.0689	0.0408	0.0621	0.0325	0.0315	0.0820	0.0240	0.0375
47756	0.2205	0.2004	0.1637	0.1112	0.0584	0.0271	0.0149	0.0329	0.1154	0.2007	0.2448	0.2409
47759	0.0424	0.0388	0.0423	0.0487	0.0506	0.0444	0.0333	0.0269	0.0325	0.0452	0.0531	0.0503
47761	0.4245	0.2743	0.2190	0.1922	0.1399	0.0848	0.0493	0.0908	0.2937	0.4873	0.5488	0.5326
47762	0.0694	0.0204	0.0380	0.0251	0.0099	0.0214	0.0514	0.0231	0.0013	0.0179	0.0772	0.0873
47765	0.0330	0.0722	0.1572	0.1735	0.1241	0.0847	0.0406	0.0586	0.0705	0.0431	0.0353	0.0383
47766	0.0377	0.1228	0.2614	0.2210	0.1309	0.0825	0.0677	0.1028	0.0792	0.0783	0.0565	0.0327
47768	0.1454	0.2249	0.3690	0.3782	0.2643	0.1875	0.1710	0.1367	0.1343	0.1485	0.2153	0.2219
47769	0.0379	0.4143	0.5693	0.3848	0.2712	0.0651	0.0445	0.0959	0.0424	0.1130	0.0859	0.0737
47770	0.1190	0.0877	0.0737	0.0721	0.0514	0.0558	0.0391	0.0471	0.0621	0.1179	0.1234	0.1284
47776	0.0569	0.0469	0.2259	0.3096	0.1655	0.1089	0.0703	0.0563	0.0648	0.0314	0.0400	0.0844
47777	0.3944	0.4573	0.5650	0.5454	0.3783	0.2124	0.1545	0.2448	0.4294	0.5167	0.5389	0.4702
47778	0.0422	0.2139	0.4804	0.4816	0.2949	0.2269	0.1297	0.1276	0.3439	0.3981	0.2136	0.0335
47780	0.5938	0.5965	0.5249	0.3936	0.2393	0.1120	0.0510	0.0443	0.1498	0.3352	0.4705	0.5501
47800	0.0294	0.0317	0.0207	0.0099	0.0143	0.0294	0.0473	0.0457	0.0116	0.0053	0.0110	0.0200
47805	0.0490	0.0415	0.0261	0.0178	0.0239	0.0272	0.0360	0.0541	0.0276	0.0084	0.0252	0.0461
47807	0.0162	0.0147	0.0241	0.0392	0.0344	0.0248	0.0345	0.0512	0.0251	0.0040	0.0055	0.0151
47809	0.0389	0.0331	0.0239	0.0272	0.0425	0.0489	0.0547	0.0717	0.0663	0.0511	0.0459	0.0423
47812	0.0242	0.0349	0.0356	0.0319	0.0363	0.0406	0.0637	0.0953	0.0564	0.0143	0.0141	0.0206

WMO code	Jan	Feb	Mar	Apr	May	Jun	Jul	Aug	Sep	Oct	Nov	Dec
47813	0.0236	0.0357	0.0369	0.0250	0.0250	0.0340	0.0572	0.0899	0.0619	0.0286	0.0286	0.0268
47814	0.0432	0.0616	0.0568	0.0459	0.0458	0.0469	0.0654	0.1054	0.0892	0.0461	0.0323	0.0312
47815	0.0368	0.2321	0.4132	0.3615	0.2385	0.1315	0.1442	0.1623	0.1460	0.1596	0.1024	0.0259
47817	0.0169	0.0286	0.0387	0.0398	0.0377	0.0365	0.0575	0.0823	0.0408	0.0078	0.0076	0.0142
47819	0.0036	0.0086	0.0242	0.0204	0.0368	0.0208	0.0471	0.0516	0.0201	0.0072	0.0202	0.0059
47821	0.0214	0.0277	0.0201	0.0174	0.0288	0.0461	0.0499	0.0471	0.0426	0.0279	0.0337	0.0345
47823	0.0222	0.0433	0.0809	0.1016	0.0815	0.0578	0.0696	0.1068	0.0790	0.0327	0.0180	0.0199
47824	0.0626	0.0650	0.1130	0.0800	0.0941	0.0624	0.0629	0.0866	0.0599	0.0271	0.0160	0.0676
47827	0.0137	0.0497	0.0840	0.0894	0.0792	0.0720	0.0914	0.1121	0.0596	0.0130	0.0143	0.0140
47829	0.0565	0.0902	0.1411	0.2061	0.1751	0.0796	0.0330	0.1063	0.1445	0.0463	0.0059	0.0125
47830	0.0604	0.1465	0.2713	0.3142	0.2231	0.1012	0.0376	0.0973	0.1647	0.1000	0.0352	0.0210
47831	0.0352	0.0841	0.1146	0.1158	0.0932	0.0747	0.0820	0.1038	0.0781	0.0310	0.0117	0.0122
47835	0.0302	0.1114	0.2247	0.2665	0.1949	0.1106	0.0695	0.0989	0.1187	0.0573	0.0072	0.0062
47836	0.0244	0.0604	0.0960	0.1304	0.1236	0.0857	0.0472	0.0503	0.0627	0.0238	0.0092	0.0159
47837	0.0318	0.0618	0.0918	0.1291	0.1316	0.0852	0.0294	0.0541	0.1154	0.0629	0.0129	0.0233
47838	0.0215	0.0210	0.0250	0.0239	0.0404	0.0260	0.0600	0.0570	0.0509	0.0134	0.0426	0.0214
47887	0.0657	0.1348	0.2108	0.1974	0.1123	0.0782	0.0727	0.1105	0.1163	0.0798	0.0690	0.0529
47890	0.3642	0.3988	0.4296	0.3837	0.2486	0.1223	0.0825	0.1701	0.3564	0.4378	0.4197	0.3774
47891	0.4052	0.5315	0.5672	0.3958	0.2064	0.2089	0.0996	0.0514	0.1975	0.3951	0.4729	0.4144
47892	0.0534	0.1155	0.1813	0.1974	0.1463	0.0764	0.0499	0.0883	0.1069	0.0674	0.0350	0.0300
47893	0.0513	0.1816	0.3543	0.4028	0.2926	0.1763	0.1033	0.1863	0.2969	0.2045	0.0523	0.0254
47895	0.1039	0.3642	0.5706	0.5164	0.3379	0.2693	0.1922	0.1593	0.3261	0.4549	0.3382	0.1158
47897	0.0460	0.1232	0.2456	0.2847	0.2118	0.1133	0.0827	0.1413	0.1809	0.1210	0.0507	0.0331
47898	0.0328	0.0379	0.0761	0.1867	0.1771	0.0940	0.0558	0.1262	0.1520	0.0497	0.0212	0.0276
47899	0.0321	0.0511	0.2427	0.3404	0.2469	0.1062	0.0706	0.1707	0.2528	0.1569	0.0260	0.0304
47909	0.0313	0.0590	0.0954	0.1060	0.1259	0.0699	0.0157	0.0222	0.0491	0.0345	0.0075	0.0176
47912	0.0107	0.0086	0.0047	0.0185	0.0324	0.0093	0.0035	0.0084	0.0134	0.0055	0.0200	0.0118
47918	0.0058	0.0183	0.0084	0.0102	0.0294	0.0191	0.0104	0.0065	0.0211	0.0068	0.0201	0.0107
47927	0.0091	0.0187	0.0136	0.0158	0.0250	0.0171	0.0028	0.0049	0.0141	0.0050	0.0099	0.0116
47929	0.0057	0.0195	0.0172	0.0195	0.0632	0.0458	0.0023	0.0073	0.0224	0.0086	0.0158	0.0083
47936	0.0044	0.0227	0.0251	0.0285	0.0687	0.0321	0.0011	0.0033	0.0262	0.0124	0.0139	0.0079
47945	0.0467	0.0942	0.1302	0.1197	0.0745	0.0318	0.0080	0.0039	0.0056	0.0109	0.0149	0.0213

Appendix #5. The values of the monthly averaged SDNC from observed points at the isobaric surface to Tokyo.

(a) The 500 hpa isobaric surface.

WMO code	Jan	Feb	Mar	Apr	May	Jun	Jul	Aug	Sep	Oct	Nov	Dec
47401	0.1773	0.1807	0.1346	0.1332	0.0717	0.1282	0.1460	0.1019	0.2635	0.1798	0.2410	0.2355
47412	0.1296	0.1521	0.1036	0.0906	0.0446	0.0853	0.1668	0.0976	0.2199	0.1779	0.2753	0.2358
47420	0.0548	0.0462	0.0567	0.0382	0.0164	0.0520	0.0768	0.0304	0.0671	0.0623	0.0998	0.0827
47582	0.0662	0.0916	0.0721	0.0514	0.0392	0.0522	0.1187	0.0531	0.0613	0.1153	0.1512	0.1782
47590	0.0439	0.0329	0.0183	0.0158	0.0362	0.0528	0.0458	0.0362	0.0401	0.0500	0.0545	0.0512
47600	0.0599	0.0320	0.0175	0.0287	0.0540	0.0525	0.0349	0.0328	0.0648	0.1163	0.1320	0.1014
47646	0.0383	0.0251	0.0275	0.0441	0.0207	0.0113	0.0271	0.0151	0.0202	0.0498	0.0224	0.0400
47678	0.0493	0.0251	0.0067	0.0144	0.0139	0.0024	0.0030	0.0059	0.0039	0.0053	0.0169	0.0417
47744	0.0278	0.0326	0.0121	0.0145	0.0331	0.0209	0.0065	0.0153	0.0433	0.0661	0.0864	0.0457
47778	0.0386	0.0062	0.0084	0.0049	0.0075	0.0006	0.0034	0.0109	0.0068	0.0295	0.0338	0.0327
47807	0.0326	0.0196	0.0038	0.0080	0.0134	0.0047	0.0041	0.0102	0.0339	0.0605	0.0484	0.0361
47827	0.0264	0.0143	0.0035	0.0047	0.0035	0.0012	0.0083	0.0119	0.0131	0.0193	0.0205	0.0249
47909	0.0147	0.0035	0.0044	0.0049	0.0011	0.0038	0.0092	0.0067	0.0081	0.0098	0.0141	0.0217
47918	0.0226	0.0038	0.0014	0.0033	0.0093	0.0060	0.0243	0.0037	0.0024	0.0089	0.0241	0.0042
47936	0.0181	0.0041	0.0138	0.0082	0.0039	0.0113	0.0091	0.0036	0.0006	0.0013	0.0093	0.0156
47945	0.0123	0.0024	0.0054	0.0081	0.0043	0.0027	0.0108	0.0129	0.0064	0.0060	0.0133	0.0201
47971	0.0200	0.0105	0.0281	0.0248	0.0031	0.0038	0.0084	0.0812	0.0170	0.0022	0.0257	0.0247

(b) The 850 hpa isobaric surface.

WMO code	Jan	Feb	Mar	Apr	May	Jun	Jul	Aug	Sep	Oct	Nov	Dec
47401	0.0659	0.0909	0.1876	0.2732	0.2958	0.2561	0.1008	0.0838	0.1793	0.2292	0.1955	0.1201
47412	0.0826	0.0932	0.1975	0.2893	0.3013	0.2606	0.1542	0.1295	0.1821	0.2280	0.2316	0.1690
47420	0.0197	0.0137	0.0301	0.1078	0.2019	0.2387	0.1837	0.0861	0.0482	0.0469	0.0431	0.0306
47582	0.1031	0.0753	0.1669	0.2015	0.1885	0.1327	0.1476	0.1403	0.2594	0.3104	0.3268	0.1978
47590	0.0456	0.0662	0.1586	0.1414	0.1204	0.1187	0.2202	0.1026	0.1263	0.1395	0.2043	0.0998
47600	0.1000	0.1391	0.1862	0.2371	0.2047	0.1589	0.2508	0.1922	0.2854	0.3018	0.3207	0.2321
47646	0.1397	0.0952	0.0506	0.0168	0.0058	0.0090	0.0291	0.0448	0.0453	0.0784	0.1393	0.1685
47678	0.0578	0.0473	0.0308	0.0124	0.0022	0.0011	0.0029	0.0046	0.0047	0.0192	0.0463	0.0593
47744	0.1415	0.1939	0.2055	0.1753	0.1218	0.1883	0.1421	0.1931	0.2431	0.3104	0.3000	0.3468
47778	0.0588	0.0248	0.0157	0.0140	0.0097	0.0088	0.0128	0.0104	0.0128	0.0605	0.1620	0.1510
47807	0.1254	0.1220	0.1721	0.1001	0.0887	0.0597	0.0357	0.1003	0.1822	0.1878	0.2704	0.2777
47827	0.0830	0.0549	0.0509	0.0525	0.0434	0.0214	0.0054	0.0034	0.0326	0.1152	0.1685	0.1407
47909	0.0426	0.0175	0.0165	0.0179	0.0089	0.0031	0.0163	0.0182	0.0106	0.0777	0.1578	0.1225
47918	0.0482	0.0250	0.0137	0.0095	0.0012	0.0041	0.0029	0.0017	0.0012	0.0242	0.1217	0.1207
47936	0.0402	0.0173	0.0120	0.0144	0.0018	0.0072	0.0061	0.0040	0.0066	0.0332	0.1085	0.1000
47945	0.0425	0.0161	0.0113	0.0355	0.0118	0.0029	0.0342	0.0069	0.0022	0.0715	0.0633	0.0832
47971	0.0670	0.0450	0.0132	0.0014	0.0016	0.0033	0.0114	0.0094	0.0039	0.0046	0.0148	0.0480

Chapter 7

Concluding remarks

We investigated the seasonality in the anomaly of the (daily mean) surface air temperature. The surface air temperature has the intense seasonality and there are seasonal periodicities in not only the mean but also the variance. We have shown their seasonal periodicities and investigated the property of the residuals, this is, the anomaly, which is removed seasonal periodicities in the mean and the variance from raw time series data of the surface air temperature. For the estimation of the seasonal periodicities in the mean and the variance, the Fourier polynomials have been adopted in order to obtain the regularly seasonality under the strategy to represent clearly the yearly distinctive variablities. Then the fluctuation of the low-pass filtered anomalous data that is smoothed using the running mean weighted by the binomial filter presents the feature of the yearly distinctive variablities quantitatively and it has been suggested that the structure of the low-pass filtered anomalous data is the most important (but the most difficult) subject from the viewpoint of long-term forecasting.

The monthly changes of the power spectrum was confirmed in the analysis of the monthly selected datasets from January through December of the anomaly, and we have considered a non-stationary AR model parameterized by the coefficients assuming seasonally varying function. The model characterizes seasonally distinctive characteristic variability depending on the location of stations. The daily power spectrum transformed from the coeffients of the model has obviously indicated the seasonality. In analysys of the high-pass filtered datasets, we have discovered the fact that the seasonality in the anomalies has a certain clear effect from the Japan Current which affects the seasonally distinctive variability at the southern stations located at small islands or near coast. The result suggests that the long-term prediction of the surface air temperature might be improved by taking the effect from the Japan Current as an exogenous factor, and is also useful in terms of investigating the causal relationship between anomalies among the stations. Moreover, in applying to pricing of

weather derivatives, we have shown the difference of the prices depending upon the seasonality. The result offers that we cannot neglect the seasonality in the valuation of the weather risk in the future.

For investigating the relationship between anomalies among the stations, the non-stationary AR model has been extended to a multivariate model. We have considered that the surface air temperature is a product which various factors such as heat fluxes are intricately intertwined, and by assuming that the external factors are random variables and the mechanism of the generation of the anomalies is a linear system of the factors, we have applied the multivariate model to surface data and the upper atmosphere data in Japan. The daily noise contribution estimated from the multivariate model can quantitatively grasp the relation and causality between stations and we have confirmed the structure of the surface air temperature and upper atmosphere data in Japan. In particular, the feature in the surface is the clearly seasonal change and the propagation of the causality, and they have suggested the local teleconnection between stations. It is expected that the detailed investigation presents us the greatly useful knowledge in the viewpoint of long-term forecasting, the climatic analysis and the weather risk management. This will be investigated further in our future research.

There are, however, two problem in analysis of the multivariate model. The first is the problem of the dimension; though, for avoidance of instability due to high dimensional analysis, we used bivariate models in this paper, in order to grasp the general relation, we need to analyze all station data simultaneously and a method that analizes lots of variables stably is demanded. The second is the ploblem of the noise contributions of correlated noise sources; for weather variables such as air temperature, the correlation between variables in positional neighborhood is often recognized and their treatment and modeling are the exceedingly difficult problem. It seems that the problem of high dimension and correlated noise sources can not be solve by the framework of the ordinary least squares method, a new approach such as the Bayesian method and the state space modeling will lead to solve. This will also be studied further in our future research.

References

Adams, G.J. and Goodwin, G.C. (1995). Parameter estimation for periodically ARMA models, *Journal of Time Series Analysis*, 16, 127–145.

Akaike, H. (1968). On the use of a liner model for the identification of feedback systems. *Ann. Inst. Statist. Math. , 20*, 425-439.

Akaike, H. (1974). A new look at the statistical model identification. *IEEE Trans. Automat. Control, 19*, 716-723.

Akaike, H. (1979). On the construction of composite time series models. *Bull. Inst. Statist. Inst.*, XLVIII, Book 1, 411-422.

Akaike, H. (1980). Seasonal adjustment by a Bayesian modeling, *J. Time Ser. Anal.*, 1, 1-13.

Akaike, H. and Ishiguro, M. (1980). BAYSEA, a Bayesian seasonal adjustment program, *Comput. Sci. Monographs*, No.13, The Institute of Statistical Mathematics, Tokyo.

Anderson, P. L. , Meerschaert, M. M. and Veccia, A.V. (1999). Innovations algorithm for periodically stationary time series. *Stochastic Processes and their Applications*, 83, 149–169.

Anderson, P. L. and Vecchia, A. V. (1993). Asymptotic results for periodic autoregressive movingaverage processes, *Journal of Time Series Analysis*, 14, 1–18.

Bernanke, B. S. (1986). Alternative Explanations of the Money-Income Correlation, *Carnegie-Rochester Conference Series on Public Policy*, 25, 49-100.

Blanchard, O. J. (1989). A Traditional Interpretation of Macroeconomic Fluctuations, *American Economic Review*, 79, 1146-1164.

Caballero, R. , Jweson, S. and Brix, A. (2002). Long memory in surface air temperature detection, modeling, and application to weather derivative valuation. *Climate Research, 21*, 127-140.

Cao, M. and Wei, J. (2000). Pricing the weather, *Risk, 13(5)*, 14-22.

Chambers, J. M. and Hastie, T. J. (1991). *Statistical Models in S*, Chapman and Hall / CRC.

Cleveland,R.B.,Cleveland,W.S.,McRae,J.E. and Terpenning,I.(1990) : STL : A Seasonal-Trend Decomposition Procedure Based on Loess. *Journal of Official Statistics* **6**,3-73.

Dischel, B. (1998). Black-Scholes won't do, *Energy and Power Risk Management*, October.

Dobrovolskii, S.G. (1999). *Stochastic Climate Theory*, Springer.

Dornier, F. and Queruel, M. (2000). Caution to the wind, *Energy and Power Risk Management*, August, 30–32.

Geweke, J. (1982). Measurement of linear dependence and feedback between multiple time series, *Journal of the American Statistical Association*, 77,304-313.

Geweke, J. (1984). Measurement of conditional linear dependence and feedback between time series, *Journal of the American Statistical Association*, 79, 907-915.

Geweke, J., Messe, R., Dent, W. (1983). Comparing alternative tests of causality in temporal systems : analytic results and experimental evidence, Journal of Econometrics, 21, 161-194.

Gladyshev, E. G. (1961). Periodically correlated random sequences, *Soviet Math.*, 2, 385-388.

Gladyshev, E. G. (1963). Periodically and almost periodically correlated random processes with continuous time parameter, *Theory Prob. Appl.*, 8,173-177.

Granger, C. W. J. (1969). Investigating causal relations by econometric models and cross-spectral methods, *Econometrica*, 37(3), 424-438.

Green, P. J. and Silverman, B. W. (1994). *Nonparametric Regression and Generalized Linear Models*, CRC Press.

Harrison, M.S.J., Palmer, T.N., Richardson, D.S. and Buizza, R. (1999). Analysis and model dependencies in medium-range ensembles : Two transplant case-studies, *Quart. J. Meteorol. Soc.*, 125, 2487-2515.

Hasselmamm, K. (1976). Stochastic Climate Models. Part1. Theory , *Tellus*, 28, 473-485.

Hastie, T.J. and Tibshirani, R.J. (1990). *Generalized Additive Models*, Chapman and Hall,London.

Helmer, S. and Tiao, G. (1982). An ARIMA-based approach to seasonal adjustment, *J. Amer. Statist. Assoc.*, 77, 63-70.

Hijikata, K (2000). *Weather Derivatives*, Sigmabasecapital (in Japanese).

Imkeller, P and Storch, J. S. Von (Eds.). (2001). *Stochastic Climate Models*, Birkhauser.

Iwasaki, T. and Kuma, K. (1999). A report of the symposium on “Predictability-A Challenge to Chaos” at the 1998 spring assembly of the Meteorological Society of Japan, *Temki*, 46(3), 169-196.

Japan Meteorological Agency (1999). *For the spread of probability expression of seasonal forecasts*, The training text for seasonal forecasts of the Japan Meteorological Agency (in Japanese).

Japan Meteorological Agency (2000). *one-month forecast guidance*, Japan Meteorological Business Support Center (in Japanese).

Jones, R. H. and Brelsford, W. M. (1967). Time series with periodic structure, *Biometrika*, 54, 403-410

Jweson, S. and Caballero, R. (2003). Seasonality in the statistics of surface air temperature and the pricing of weather derivatives. *Meteorological Applications, 10*, 367-376.

Kitagawa, G. (1993). Fortran77 Programming for Time Series Analysis, Iwanami Publishing Company (in Japanese).

Kitagawa, G. and Akaike, H. (1978). A procedure for the modeling of non-stationary time series. *Ann. Inst. Statist. Math. , Vol. 30, No. 2, B*, 351-363.

Kitagawa, G. and Akaike, H. (1981). ON TIMSAC-78, *Applied Time Series Analysis II*, D.F.Findley ed., Academic Press, New York 499-547.

Kitagawa, G. and Gersch. W. (1984). A smoothness priors – state space modeling of time series with trend and seasonality, *J. Amer. Statist. Assoc.*, 79, 378-389.

Kitagawa, G. and Gersch. W. (1985a). A smoothness priors - time varying AR coefficient modeling of nonstationary covariance time series. *IEEE Trans. Automatic Control, AC-30*, 48-56.

Kitagawa, G. and Gersch. W. (1985b). A smoothness priors - long AR model method for spectral estimation. *IEEE Trans. Automatic Control, AC-30*, 57-65.

Lorenz, E. N. (1963). Deterministic nonperiodic flow. J.Atmos.Sci.,20,130-141

Moreno, M. (2000). Riding the Temp. *Weather Derivatives, FOW Special Supplement, December*.

Ogura, H. (1971). Spectral representation of a periodic nonstationary random processes, *IEEE Trans. Inform. Theory*, IT-17, 143-149.

Ogura, H. and Yoshida, Y. (1982). Time series analysis of a periodic stationary random process, *Trans. Inst. Electr. Comm. Eng. Japan*, J65-A, 22-29 (in Japanese).

Otomo,T. , Nakagawa, T. and Akaike, H. (1972). Statistical approach to computer control of cement rotary kilns, *Automatica*, 8, 35-48.

Pagano, M. (1978). On periodic and multiple autoregressions, *Ann. Statist.*, 6, 1310-1317.

Palmer, T. N. (1999). Predicting uncertainty in forecasts of weather and climate, Research Department Technical Memorandum No.294, ECMWF, 63pp.

Parzen, E. and Pagano, M. (1979). An approach to modeling seasonally stationary time series, *Journal of Econometrics*, 9, 137-153.

Parzen, E., Tanabe, K. and G. Kitagawa (Eds.). (1998). *Selected Papers of Hirotsugu Akaike*. Springer, New York.

Pierce, D. A. and Haugh, L. D. (1977). Causality in temporal systems : Characterization and a survey, *Journal of Econometrics*, 5(3), 265-293.

Shiskin, J., Young, A.H. and Musgrave, J. C. (1967). The X-11 variant of the census method Ⅱ seasonal adjustment program, Tech. Paper 15, Bureau of the Census, Washington, D. C.

Sims, C. A. (1972). Money, incocome and causality, *American Economic Review*, 62, 540-552.

Sims, C. A. (1980). Comparison of interwar and postwar business cycles, *American Economic Review*, 70, 250-257.

Sims, C. A. (1986). Are forecasting models usable for policy analysis?, *Federal Reserve Bank of Minneapolis Quarterly Review*, 3-16.

Stephenson, D.B., Pavan, V. and Bojariu, R. (2000). Is the North Atlantic Oscillation a random walk? *International Journal of Climatology*, *20*, 1-18.

Storch, H. von, Zwiers, F.W. (1999). *Statistical Analysis in Climate Research*. Cambridge University Press, Cambridge.

Tanokura,Y. (2004) Generalization of Akaike's Power Contribution, Doctoral dissertation, The Graduate University for Advanced Studies.

Tanokura,Y. and Kitagawa,G. (2004). Power contribution analysis for multivariate time series with correlated noise sources. Advances and Applications in Statistics, 4,65-95.

Tiao, G.C. and Grupe, M.R. (1980). Hidden periodic autoregressive moving average models in time series data, *Biometrika*, 67, 365-373.

Torro,H.,Meneu,V. and Valor,E. (2001). Single factor stochastic models with seasonality applied to underlying weather derivatives variables. *European Financial Management Association, Tech. Rep. 60.*

Troutman, B. M. (1979). Some results in periodic autoregression, *Biometrika*, 6, 219-228.

Vecchia, A. V. and Ballerini, R. (1991). Testing for periodic autocorrelations in seasonal time series data, *Biometrika*, 78, 53-63.

Wakaura, M. (2004). The analysis of the mean and the variance of temperature processes in Japan using generalized additive models, *Japanese Journal of Applied Statistics*, 33, 181-200 (in Japanese).

Wakaura, M. (2005). The theory and methodology of weather derivatives pricing, *JAPANESE JOURNAL of RISK and INSURANCE*, 1, 21-39 (in Japanese).

Wakaura, M. (2006). Seasonal autocorrelation structure in air temperature processes and weather derivatives, *JAPANESE JOURNAL of RISK and INSURANCE*, 2, 3-19 (in Japanese).

Wong, K. F. K. (2005), Multivariate time series analysis of Heteroscedastic data with application to neuroscience, Doctoral dissertation, The Graduate University for Advanced Studies.

Wong, K. F. K. and Ozaki, T. (2006), Akaike causality in state space part Ⅰ - instantaneous causality between visual cortex in fMRI time series, Research Memorandum No.1018, The Institute of Statistical Mathematics, Tokyo.

Zeng, L. (2000). Weather derivatives and weather insurance: concept, application and

analysis, *Bull. Am. Met. Soc*., 81, 2075–2982

Zwiers, F.W. and Storch, H. von. (1990). Regime dependent auto-regressive time series modeling of the Southern Oscillation. *Journal of Climate, 3,*1347-1363.